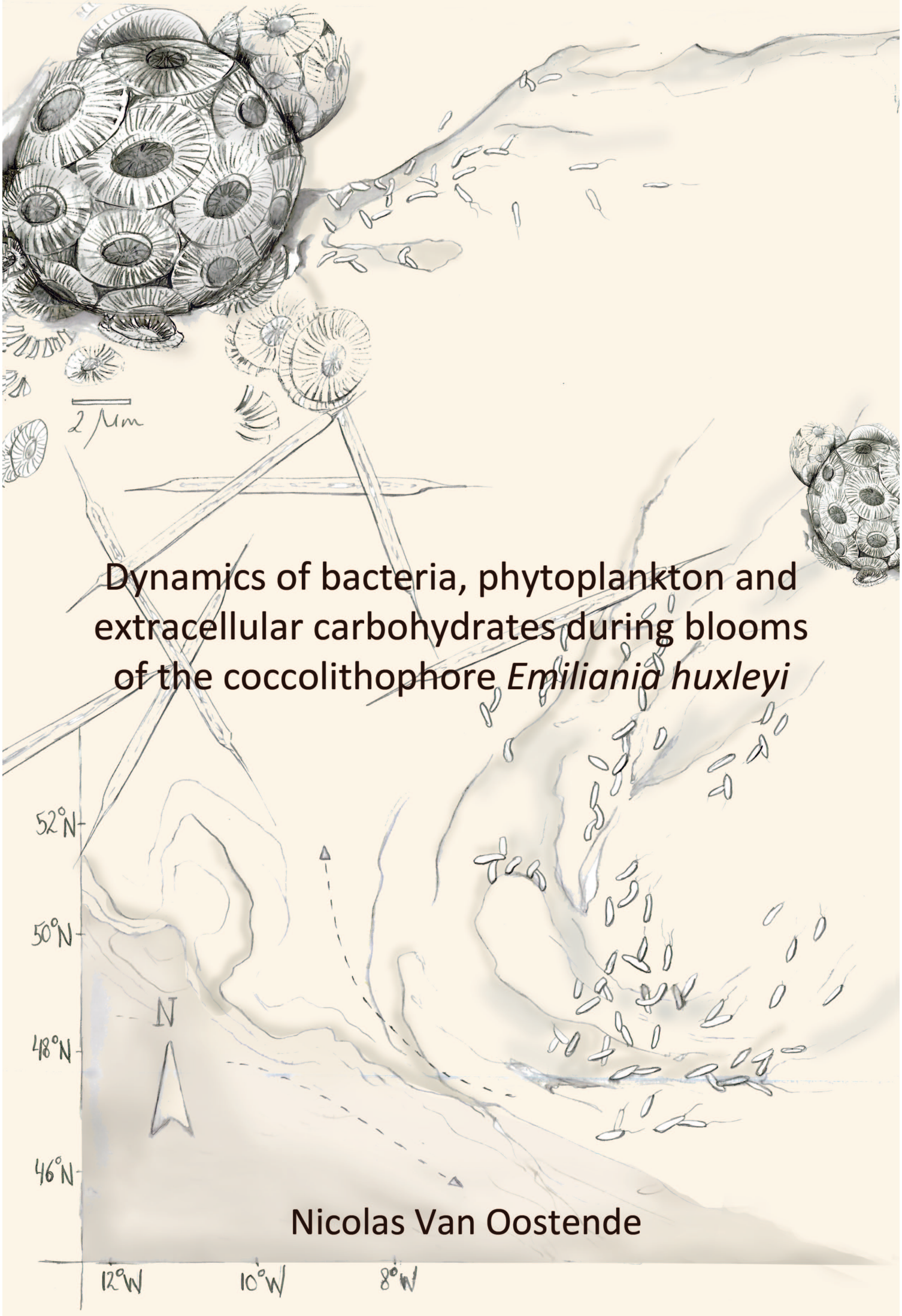

Dynamics of bacteria, phytoplankton and extracellular carbohydrates during blooms of the coccolithophore *Emiliania huxleyi*

Nicolas Van Oostende

Department of Biology
Laboratory for Protistology and Aquatic Ecology

Dynamics of bacteria, phytoplankton and extracellular carbohydrates during blooms of the coccolithophore *Emiliania huxleyi*

Nicolas Van Oostende

Promoter: Prof. Dr. Koen Sabbe
Co-Promoter: Dr. Eric Boschker
Co-Promoter: Prof. Dr. Wim Vyverman

Dissertation submitted in fulfillment of the requirements for the degree of Doctor of Philosophy in Science, Biology.
September 15th 2011

Academic year 2010 -2011

Onderzoek gefinancierd met een onderzoeksbeurs van het agentschap voor Innovatie door Wetenschap en Technologie (IWT).

This work was supported by a Ph.D. grant from the agency for Innovation by Science and Technology (IWT).

Members of the examination and reading committee

Prof. Dr. Dominique Adriaens (chairman)
Department of Biology, Ghent University

Prof. Dr. Koen Sabbe (promoter)
Department of Biology, Ghent University

Dr. Eric Boschker (co-promoter)
Department of Marine Microbiology, Center for Estuarine and Marine Ecology,
NIOO-KNAW (NL)

Prof. Dr. Wim Vyverman (co-promoter)
Department of Biology, Ghent University

Prof. Dr. Christiane Lancelot (reading committee)
Department of Biology, Université Libre de Bruxelles

Dr. Felipe Artigas (reading committee)
Maison de la Recherche en Environnements Naturels, Université du Littoral d'Opale (F)

Dr. Jérôme Harlay (reading committee)
Astrophysics, Geophysics and Oceanography Department, Université de Liège

Dr. Jan Vanaverbeke (reading committee)
Department of Biology, Ghent University

Prof. Lei Chou
Océanographie Chimique et Géochimie des Eaux, Université Libre de Bruxelles

Prof. Dr. Stephen Louwye
Department of Geology and Soil Science, Ghent University

Dr. Pieter Vanormelingen
Department of Biology, Ghent University

Acknowledgements

The work presented in this Ph.D. dissertation would not have been possible without the support, help, and work of other people, which I would like to thank formally in this dedicated section.

Here we go.

First of all, I would like to express my sincere gratitude to Koen Sabbe and Wim Vyverman for giving me the opportunity to join the Protistology and Aquatic Ecology lab at the University of Gent. It all started in 2004 when I decided that the ocean definitely offered greater perspectives than the bees and the flowers, and I applied for doing my second MSc thesis at your lab on the diversity productivity relationship in diatom communities. I was immediately hooked on the little creatures. Following an unfortunate attempt at getting an IWT scholarship for a daring diatom-meets-microtechnology project, I was offered a position to work on an oceanographic project (PEACE), which I excitedly accepted. The second attempt at an IWT scholarship was a success. This let me in charge of two complementary scientific projects with the focus on the biogeochemical role of *E. huxleyi*. Thank you Eric Boschker, from NIOO Yerseke, for letting me intrude your mainly benthic lab with my pelagic topic and introducing me to the world of fatty acids and stable isotopes. I also much appreciated the support of Jack Middelburg for permitting the collaboration with the NIOO in Yerseke (NL). At last, I would like to thank the members of the examination and reading committee for their constructive comments and discussion which certainly improved this manuscript.

Except for the last nine months or so, I spent most of my Ph.D. period surrounded by a happy bunch of helpful and interesting colleagues at the PAE lab at “de Sterre”. As I soon came to realise that experimental science has a high rate of failure, your daily support was highly valued. In particular I would like to thank: Annelies Pede, for breaking the (probably dreadful) silent mode I sometimes got into when working too long behind the desk we shared; Caroline Souffreau, Aaike De Wever, Bart Vanelslander, and Dries De Bock for joining me (or replacing me) on the RV Belgica in the Bay of Biscay to carry out the oceanographic

campaigns in sometimes difficult sea conditions; Pieter Vanormelingen for always having strong ecological convictions and valuable statistical advice; Ilse Daveloose for her commitment to the carbohydrate analyses and her good mood; Ann-Eline Debeer for CN analyses; Marie Huysman for allowing me to use the colour camera and flow cytometer at the VIB; Sofie D'hondt for introducing me to the art of DGGE at the molecular lab and for her praised advice; Tine Verstraete for having run dozens of gels and cut out hundreds of bands, I could not have done this without your work; Andy Vierstraete for his help with autoclaving large volumes; Marie Lionard for introducing me to the world of CHEMTAX; Renaat Dasseville for showing me around the HPLC and SEM; and other colleagues that I didn't mention yet: Sara, Els, Jeroen, Jeroen, Katrijn, Ana, Heroen, Klaas, Lennert, Agnieszka, Frederik, and the new crew Evelien, Wim, Dagmar, and Ines for being around when I needed you and making my day. Additionally, I would explicitly like to thank Dirk van Gansbeke and Tanja Moerdijk for sharing their time and expertise at the analytical labs at UGent and NIOO Yerseke, respectively.

One very important reason why I genuinely enjoyed the oceanographic science part of my work is the collaboration with the members of the PEACE project and the merry crew of the RV Belgica. I would like to thank Jérôme Harlay for answering my many questions and taking a genuine interest into my research. Furthermore I am happy to have been able to work with experienced marine scientists like Lei Chou, Anja Engel, and Alberto Borges. Thank you to Judith, Nicole und Corinna for showing me around at the AWI, Bremerhaven.

Finally, my gratitude goes to the incredible friends (you know who you are) and family (you too) that shared my life during those exciting last years. Particularly I would like to thank Alexandra Mein for her unconditional support, for pushing the boundaries of her patience, and for delivering the cover art work (this thesis will actually be worth some money the day she becomes famous); Thank you Maxime Willems for proofreading and Jeremy Godenir for providing advice on using the Adobe programs (sorry for your Mac). Of course this whole endeavour would not have been possible without my loving parents, who put me on this Earth in the first place and gave me the freedom and support to do exactly what I wanted to.

Merci

Nicolas

Abbreviations

ara	arabinose
AVHRR	Advanced Very High Resolution Radiometer
CCD	charge-coupled device
cf.	confer
Chla	chlorophyll *a*
CP	coccolith polysaccharide
DAPI	4',6-diamidino-2-phenylindole
DGGE	denaturing gradient gel electrophoresis
DIC	dissolved inorganic carbon
DMS	dimethyl sulfide
DMSP	dimethylsulfoniopropionate
DOC	dissolved organic carbon
DOM	dissolved organic matter
dSi	dissolved silicic acid
e.g.	example given
EDTA	ethylenediaminetetraacetic acid
fuc	fucose
gal	galactose
glc	glucose
GPA	glutamic acid-proline-alanine
HMW	high molecular weight
HR	high reflectance
i.e.	id est
LC/IRMS	liquid chromotography isotope ratio mass spectrometry
man	mannose
MCHO	dissolved mono- and oligosaccharides
MLD	mixed layer depth
NAld	neutral aldose
NOx	dissolved nitrate and nitrite
OM	organic matter
PCR	polymerase chain reaction
PIC	particulate inorganic carbon
PLFA	phospholipid-derived fatty acid
PN	particulate nitrogen
PO4	dissolved phosphate
POC	particulate organic carbon
rDNA	ribosomal deoxyribonucleic acid
rha	rhamnose
rib	ribose
rRNA	ribosomal ribonucleic acid

RS	remote sensing
SeaWiFS	Sea-viewing Wide field-of-view Sensor
SEM	scanning electron microscopy
sp.	species (singular)
spp.	species (plural)
TA	total alkalinity
TCHO	dissolved total carbohydrates
TE	Tris and EDTA
TEA	TE and acetic acid
TEP	transparant exopolymer particles
TFF	tangential flow ultrafiltration
Tris	tris(hydroxymethyl)aminomethane
UML	upper mixed layer
UV	ultra violet
xyl	xylose

Contents

Aims

This dissertation focuses on the dynamics and the biogeochemical role of blooms of the coccolithophore *E. huxleyi* and bacterial communities in the Bay of Biscay (NE Atlantic). The composition of bacterial and phytoplankton communities during phytoplankton blooms, and their interactions, are important properties of the microbial food web, which can potentially have a strong impact on the fate of organic matter and hence carbon cycling in the world's oceans (see further in introductory section). Because each functional group, size class, or microbial species can potentially influence specific biogeochemical cycles in their own way, their abundance and activities will shape the world we live in. Moreover, rapidly changing global conditions of ocean temperature and acidity will probably affect these functional microbial groups in a species-specific way, prompting investigation in the contemporary environmental factors that control their distribution. Therefore, one of the main aims of this thesis is to contribute to a better knowledge of the composition and dynamics of bacterial and phytoplankton assemblages in relation to the abiotic and biotic environment during blooms of coccolithophores, a key biogeochemical phytoplankton group. Besides physicochemical factors, biotic interactions such as viral infection or microzooplankton herbivory can exert a tight, sometimes species-specific control onto the phytoplanktonic biomass accumulation. This so-called top-down control can effectively divert elemental fluxes up (grazing) or down (cell lysis) the trophic ladder, influencing the fate of the primary produced carbon (be it in organic form such as DMSP, or inorganic form such as calcite). We therefore quantified the importance of cell lysis and microzooplankton grazing to assess the fate of phytoplankton groups during blooms. Finally, in nutrient-depleted environments part of the primary production can be released extracellularly in the dissolved form and can therefore potentially escape export to the seabed in the absence of water column mixing. However, particle formation by the assembly of dissolved polysaccharides can form an important pathway to convert dissolved OM into particulate OM such as TEP during phytoplankton blooms. Recently, bacterial interactions have been shown to promote the formation TEP in algal cultures, emphasizing the importance the role of bacteria-phytoplankton interactions in the carbon cycle. Furthermore, coccolith production may

constitute a potential source of TEP precursors, as acidic polysaccharides are produced by the cell to precipitate Ca^{2+} into calcite. We therefore investigated the role *E. huxleyi* and bacteria in the production of TEP and its potential contribution to carbon export.

We studied the composition and dynamics of phytoplankton and bacterioplankton communities in late spring phytoplankton blooms along the North East Atlantic continental margin in the northern Bay of Biscay, and complemented these field studies with laboratory culturing experiments to study the role of bacteria and the coccolithophore *E. huxleyi* in HMW carbohydrates and TEP production. **Chapter 1** provides the reader with an introduction to important concepts and terms dealt with in this thesis. In **chapter 2** we describe the distribution patterns of phytoplankton groups during three oceanographic campaigns (2006-2008) in relation to the prevailing environmental conditions. This allowed us to quantify the chlorophyll *a* standing stocks of coccolithophores, diatoms, and other phytoplankton groups and to characterise the conditions associated with the occurrence and/or dominance of these groups, and the production of TEP. Because bacteria are the main consumers of organic matter produced by phytoplankton, in **chapter 3** we assessed the distribution and diversity of bacterial communities associated with these phytoplankton blooms. One of the aims in this chapter was to investigate the composition of these bacterial communities and their temporal and spatial variability. Once this was established, we used an indirect approach to link bacterial diversity to their potential function in **chapter 4**, by assessing how changes in physical and environmental variables, and phytoplankton, related to bacterial community structure, and which bacterial species were associated with particular conditions. Having described the biomass distribution of phytoplankton groups and the bacterial community structure we went on to study loss processes regulating these blooms. In **chapter 5** we quantified the rates of cell lysis and microzooplankton grazing mortality to which phytoplankton blooms were subjected. These processes influence the biological carbon pump, but also constitute a pathway to the cycling of the climate-active volatile compound DMS. This was investigated by relating cell lysis rates to the formation of dissolved DMSP, an important DMS precursor. In **chapter 6**, we performed culturing experiments, using an *E. huxleyi* strain and natural bacterial communities isolated during our campaigns, in order to investigate the influence of bacteria on the release and composition of carbohydrates by *E. huxleyi* and the formation of TEP. In cultures of non-axenic calcifying

E. huxleyi we used a stable isotope labelling approach coupled to compound-specific isotope analysis to track the fate of extracellularly released carbohydrates by *E. huxleyi* cells. In **chapter 7**, we discuss and integrate our results in the general framework of increasing water column stratification and bloom development scenario along the continental margin, and present some thoughts on future avenues of research. Finally, **chapter 8** provides a summary of this work.

All chapters excluding the introduction, discussion, and summary (chapters 1, 7 and 8) are manuscripts in preparation. The first author performed the experiments, processed the samples, analysed the data, and wrote the chapters, except when stated otherwise. Chapter 5 was a joint effort with Caroline De Bodt (ULB), who performed the cell lysis rate measurements and contributed to writing the manuscript.

Part of this thesis (chapters 2 to 5) has been carried out in the framework of the PEACE project (role of **PE**lagic c**A**lcification and export of **C**arbonat**E** production in climate change), supported by funding from the Belgian Federal Science Policy Office (SD/CS/03). The overall objective of PEACE is to assess the role of pelagic calcification and export of $CaCO_3$ production in climate regulation. Specific objectives are: (1) to study of the net ecosystem dynamics during coccolithophorid blooms, (2) to unravel the link between the microbial community, grazing, TEP dynamics, carbon export and DMS cycling during coccolithophorid blooms, (3) to assess the effects of ocean acidification on coccolithophorid metabolism and TEP production, and (4) to model coccolithophorid dynamics and their impact on ocean dissolved inorganic carbon (DIC) chemistry. Three oceanographic campaigns were carried out in the northern Bay of Biscay as part of a multidisciplinary project integrating the biological and biogeochemical aspects of calcification in phytoplankton blooms.

The remainder of this work has been supported by a Ph.D. grant from the agency for Innovation by Science and Technology (IWT Flanders grant n° 63370).

1

Introduction

This introductory section provides the reader with information on elementary concepts relating to the biogeochemical role of coccolithophores and the ecosystem functioning of the ocean in general, and at the continental margin in the northern Bay of Biscay in particular. Additionally, it introduces specific issues concerning the relationship between the community structures of phytoplankton and bacterioplankton and environmental constraints, the fate of phytoplankton in terms of cell lysis and microzooplankton grazing, and the role of the coccolithophore *Emiliania huxleyi* and bacteria in the production of transparent exopolymer particles and their potential influence on carbon export in the ocean.

The biological carbon pump

Most life on Earth directly or indirectly relies on primary production, the synthesis of organic compounds and oxygen from carbon dioxide in the process of photosynthesis (1).

$$2n\ CO_2 + 2n\ H_2O \xrightarrow{light} 2(CH_2O)_n + 2n\ O_2 \qquad (1)$$

Marine phytoplankton, i.e. the autotrophic component of the plankton (from the Greek terms “phyton” or plant and “planktos” or wanderer) obtain energy through photosynthesis. Most phytoplankton species are microscopic unicellular organisms with a size ranging between 0.4 and 200 µm (Simon *et al.*, 2009). Phytoplankton are the main primary producers in aquatic ecosystems. Despite their low contribution (1%-2%) to the global photosynthetic biomass due to their high turnover rates, they account for about 45% of the global primary production (Field *et al.*, 1998; Falkowski *et al.*, 2004). Phytoplankton production in the surface ocean drives the so-called biological organic carbon pump (fig. 1). This process creates chemical gradients in the oceans by stripping nutrients and carbon from the surface waters to form organic compounds, and exporting this organic matter to the deeper water layers where most of it is remineralised, and by delivering the remainder to the ocean floor sediments where part of it is ultimately buried (Sarmiento and Gruber, 2006). Shelf seas such as the Celtic Sea generally have higher biological activity than adjacent ocean and the shelf margin is potentially a region of significant sedimentation of organic

matter from the surface mixed layer (Joint *et al.*, 2001). The efficiency of the carbon pump depends on the fraction of the total amount of carbon produced through photosynthesis that is exported from the surface to the ocean sediments. Several biotic (e.g. grazing by zooplankton and cell lysis of phytoplankton blooms) and abiotic (e.g. particle aggregation, mixing) processes can modulate the efficiency of the biological carbon pump, by influencing how rapidly dissolved organic matter (DOM) or particulate organic matter (POM) is exported, thereby escaping remineralisation by bacteria (see fig. 1 and below).

Another important component of biogenic carbon fixation and the biological pump is calcification, a process involving the precipitation of dissolved ions (Ca^{2+} and HCO_3^-) into solid calcium carbonate or calcite ($CaCO_3$) and gaseous CO_2 (2).

$$Ca^{2+} + 2\ HCO_3^- \longrightarrow CaCO_3 + CO_2 + H_2O \qquad (2)$$

Coccolithophores, foraminifers, and pteropods are important marine calcifying organisms (Hay, 2004). Because calcification both fixes carbon into $CaCO_3$ and releases CO_2 it counteracts the organic carbon pump. The ratio of particulate organic carbon (POC) to particulate inorganic carbon (PIC), such as calcite, is about 1:1 for sinking particles at 1000 m depth (Honjo, 1996; Honjo *et al.*, 1999). Surface calcification thus fuels a significant fraction of the total carbon flux to the deep sea. One of the mechanisms enhancing organic matter export is the biomineral (e.g. $CaCO_3$, biogenic silica) ballasting of organic particle aggregates such as so-called marine snow (De La Rocha and Passow, 2007; Iversen and Ploug, 2010). Moreover, when the particulate matter reaches the deep-sea floor, most organic matter is remineralised, whereas calcium carbonate is at about six times more likely to be sequestered in burial (Westbroek *et al.*, 1993; Suykens, 2010). As a result, the balance between calcification and primary production, and the PIC content of exported matter influences the efficiency of the biological pump.

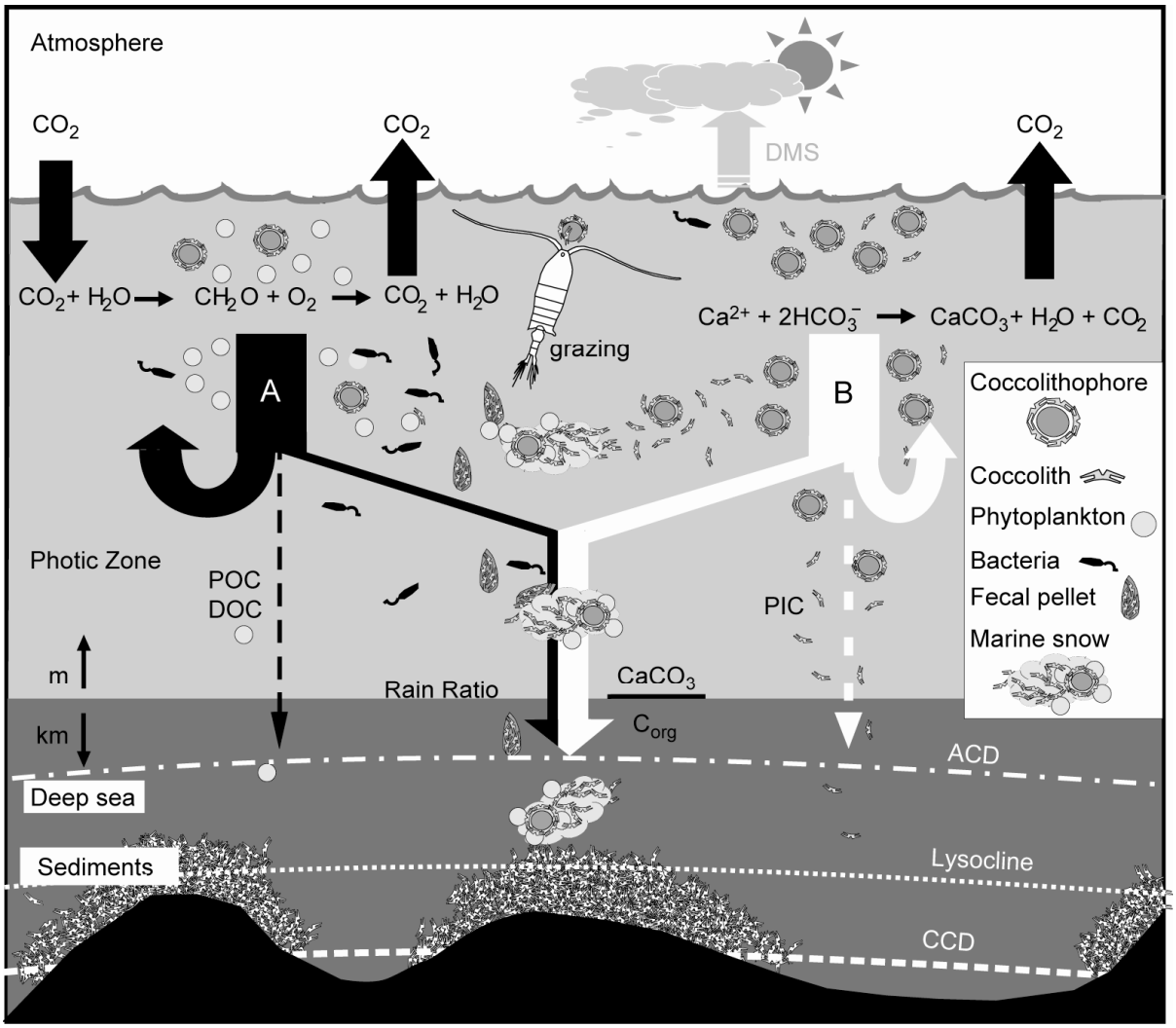

Fig. 1. Diagram representing the fluxes of atmospheric gases such as carbon dioxide (CO_2) fixed by phytoplankton in the surface ocean and their transfer to deeper water (i.e. below the mixed layer) (not to scale). Coccolithophores actively participate in gas exchange (CO_2, DMS) between seawater and the atmosphere and to the export of organic matter and calcium carbonate to the deep-sea sediment. They are the main actors of the *carbonate counter-pump* (**B**), which, through the calcification reaction, is a short-term source of atmospheric CO_2. Via the ballasting effect of their coccoliths on marine snow, coccolithophores are also one of the main drivers of the *organic carbon pump* (**A**), which removes CO_2 from the atmosphere. Abbreviations as in text. Text and image modified from De Vargas *et al.* (2007).

Phytoplankton

Although only about 5000 phytoplankton species have been formally described, phytoplankton is phylogenetically extremely diverse spread over several low taxonomical levels (fig. 2). In comparison, the wide diversity at the species level of plants and animals is two orders of magnitude higher, but all their members are included in the Opisthokonta group. Diatoms, dinoflagellates and to a lesser extent haptophytes (such as coccolithophores) and green algae (such as prasinophytes) are the most diversified groups (with respectively, approximately, 40%, 40%, 10% and 6% of the described phytoplanktonic eukaryote species) (Simon *et al.*, 2009). Diatoms (one of the major lineages within the stramenopiles), the dinoflagellates and the haptophytes (fig. 2) appear to dominate phytoplankton communities on continental shelves and are responsible for seasonal blooms in temperate and polar waters. They are more generally the main marine planktonic primary producers within the nano- and microplanktonic size classes (respectively 2–20 and 20–200 µm). However, recent studies conducted in the field of phytoplankton systematics, ecology, physiology and genomics unveiled a vast unsuspected diversity, in particular in the picoplanktonic size fraction and at the infraspecific level (Simon *et al.*, 2009).

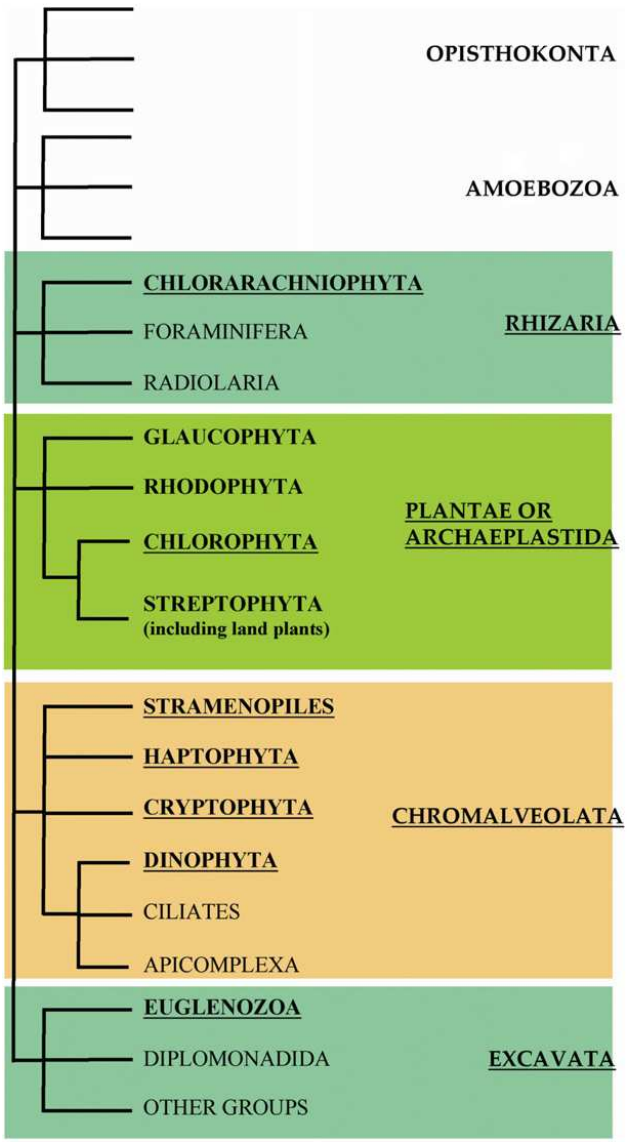

Fig. **2**. Schematic tree of the 6 eukaryotic super-groups as described by Adl *et al.* (2005) showing the distribution of the major lineages that acquired a plastid through endosymbiosis (bold) and those of these lineages that include marine phytoplanktonic representatives (bold, underlined). Animals (metazoan) and fungi lineages are included in the Opisthokonta group. Image from Simon *et al.* (2009).

The spatial and temporal distribution of phytoplankton species is important because each has particular functional characteristics which more or less determine the biogeochemical cycling of particular elements (e.g. Si, C, N, P, S, Fe) (Boyd *et al.*, 2010). Furthermore, this biological and metabolic diversity may be essential in maintaining ecosystem functioning in a global change context. From a practical point of view it makes sense to capture this diversity by grouping organisms sharing similar metabolic pathways into functional groups or biogeochemical guilds (cf. Iglesias-Rodriguez *et al.*, 2002b; Hood *et al.*, 2006). Coccolithophores, for example, precipitate calcite ($CaCO_3$), diatoms and silicoflagellates produce biogenic silica or opal (SiO_2), while some cyanobacteria fix gaseous nitrogen (N_2) (Westberry and Siegel, 2006). *Phaeocystis* spp. and coccolithophores are important players in the sulphur cycle (see below) (Stefels, 2000; Archer *et al.*, 2002). Another way through which the distribution of different phytoplankton species can impact the biogeochemical cycles is through the ecological role played by cell size. It is thought that larger, heavier phytoplankton such as diatoms are more efficiently exported to the seabed through the formation of large particles that sink rapidly, while smaller organisms (such as cyanobacteria) are generally more efficiently recycled within the euphotic zone (but see (Richardson and Jackson, 2007)). Smaller cells also have larger cell surface-to-volume ratios, allowing faster diffusion-limited exchanges of products through their cell surface and thus making their metabolism per unit biomass more efficient. However, being small means that the consumers of smaller phytoplankton cells, mostly heterotrophic protists or microzooplankton, are also small and typically have high growth rates themselves. This allows them to exert strong control on the population sizes of smaller phytoplankton species. In contrast larger phytoplankton cells can sometimes escape predation because their grazers cannot track their comparatively high growth rates (Kiørboe, 1993). The competitive advantages of smaller phytoplankton cells are therefore somewhat relaxed in nutrient-rich, more turbulent environments, where larger cells such as those of diatoms can form episodic blooms.

Despite the important implications of the abundance of these phytoplankton groups for global biogeochemical cycles, the environmental bottom-up (such as temperature and nutrient regimens), and ecological top-down control (such as microzooplankton grazing and viral lysis) for the abundance of most of these groups is still poorly understood (Boyd *et al.*,

2010). One way to approach this problem is by using conceptual frameworks or models to simplify the complexity of interactions and assess the response of certain phytoplankton groups to their environment. Ramon Margalef envisaged the succession of different phytoplankton groups to be a function of water turbulence and nutrient supply through his famous niche space 'mandala' (Margalef, 1978) (fig. 3).

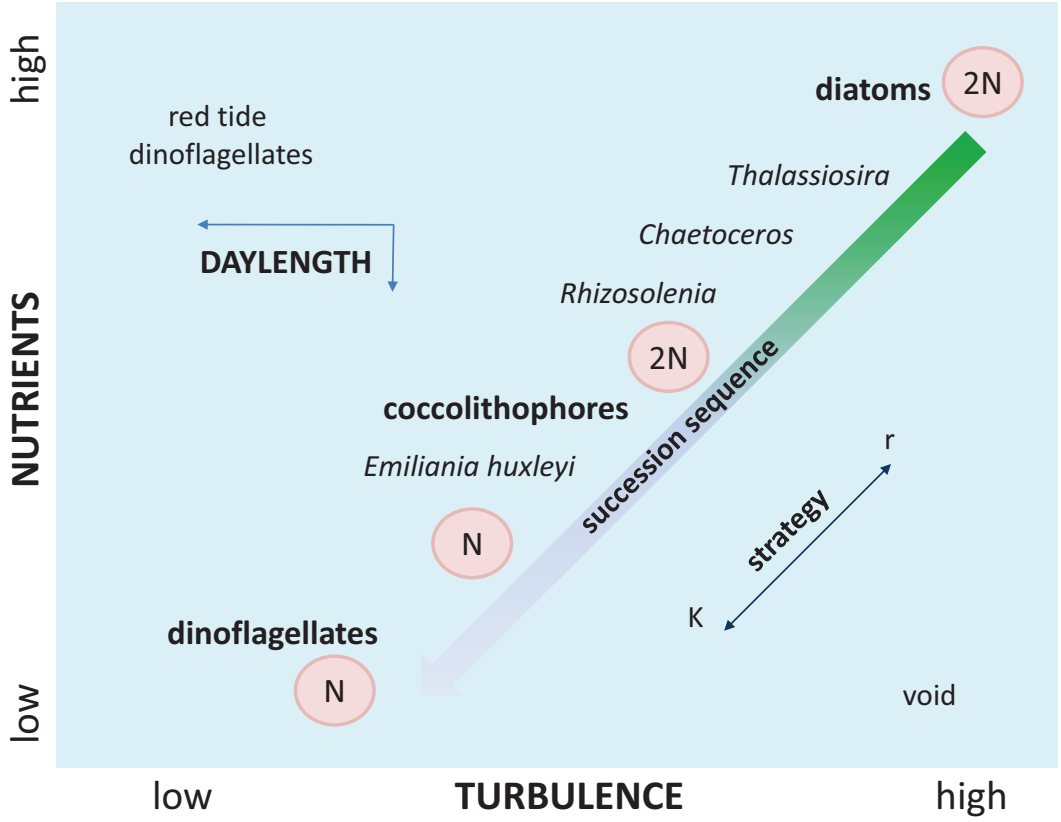

Fig. 3. Modified version of Margalef's two-dimensional niche space model (Margalef, 1978) with an additional daylength dimension (Balch, 2004), and integrating the life cycle stages of coccolithophores (2N: diploid stage; N: haploid stage) (Houdan *et al.,* 2006).

From his niche space model we can deduce that thermal stratification of the water column (i.e. reduced turbulence and thus reduced nutrient re-injection from deeper water layers) plays an important role in the succession of phytoplankton species during the latitudinal progression of spring and summer temperature and light conditions. Diatoms are typically associated with turbulent conditions while coccolithophores are recognized as a group often associated with transition zones between different environmental conditions (Uitz *et al.*, 2010) and references therein). Day length or irradiance could be added as another factor controlling the distribution of phytoplankton groups (Balch, 2004), as the coccolithophore *E.*

huxleyi has a low susceptibility to photo inactivation, conferring them a competitive advantage under high-light conditions (Loebl *et al.*, 2010). A recent study by Cermeño *et al.* (2011) using a diatom and a coccolithophore species of equal cell size demonstrated that dynamical nutrient supply allows co-existence of two primary producers competing for a single limiting nutrient. These kinds of studies together with knowledge about the physiology of phytoplankton species and about the physical dynamics of marine systems can help us to understand phytoplankton succession in the ocean.

Coccolithophores and Emiliania huxleyi

As mentioned above, coccolithophores (literally translated: "stone-carrying-berries") are important players in the global cycles of carbon and sulphur. They contribute on average to about 10- 15% to global oceanic phytoplankton biomass (Sarmiento and Gruber, 2006) and up to 60% of the bulk pelagic calcite deposited on the ocean floors (Honjo, 1996). Coccolithophores are important producers of DMSP, the precursor of DMS, a climate active volatile compound contributing 50% to 60% of the natural sulphur emissions to the atmosphere (Stefels *et al.*, 2007) (fig. 1). Because each molecule of DMSP contains five atoms of carbon, DMSP synthesis is also important in the carbon cycle; its production is estimated to account for 3–10% of the global marine primary production of carbon (Kiene *et al.*, 2000), and its degradation supplies about 3–10% of the carbon requirements of heterotrophic bacteria in surface waters (Simó *et al.*, 2002; Sievert *et al.*, 2007). However, despite the importance of coccolithophores in biogeochemical cycles relatively little is still known about their biology and ecology (Westbroek *et al.*, 1993; Billard and Inouye, 2004).

One of the most abundant, cosmopolitan, bloom-forming coccolithophore species is *Emiliania huxleyi* (Lohmann) Hay and Mohler (fig. 4). This unicellular marine golden-brown algal species (phylum *Haptophyta*, class *Prymnesiophyceae*) is covered by calcite platelets, called coccoliths, which can be produced in superfluous amounts and shed into the surrounding water. The latter typically occurs when cell proliferation becomes decoupled from coccolith production upon nutrient limitation (Shiraiwa, 2003). It has been hypothesized that the increased production of coccoliths in nutrient limited condition (particularly phosphorus), is caused by an overflow mechanism which diverts photosynthetic energy flow to the production of carbon-rich molecules such as calcium precipitating polysaccharides (see also further) (Harlay, 2009). However, the functions of calcification in

relation to photosynthesis and nutrient acquisition are still debated (Brownlee and Taylor, 2004). Accumulation of these coccoliths in the water column increases the water leaving radiance properties (i.e. reflectance) and even the water temperature of such patches (Holligan and Groom, 1986; Robertson *et al.*, 1994) allowing their observation through remote sensing (Holligan *et al.*, 1993) (fig. 5). These visible patches however usually only represent the dissipative/decaying phase of the bloom (Westbroek *et al.*, 1993), leaving the *in situ* dynamics of these blooms scarcely documented (Garcia-Soto *et al.*, 1995; Fileman *et al.*, 2002; Lampert *et al.*, 2002).

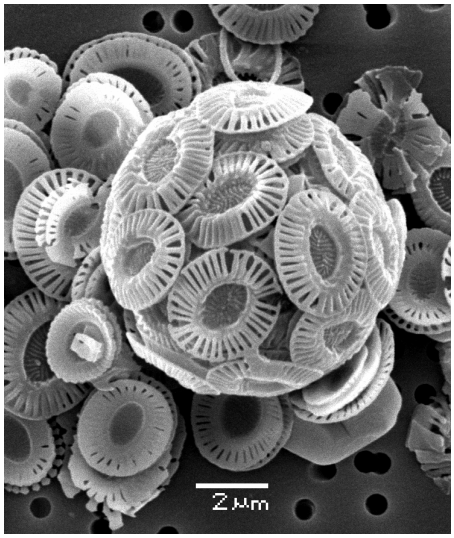

Fig. 4. SEM image of *E. huxleyi* (C-cell) shedding its coccoliths.

The life cycle of coccolithophores is haplo-diploid, with both the 1N and 2N phase capable of asexual reproduction (fig. 6). Often these phases have distinct patterns of scale ornamentation characteristic for each ploidy state (Billard and Inouye, 2004; Houdan *et al.*, 2004). This biphasic life cycle differs from that of two other important marine phytoplankton groups, diatoms and dinoflagellates, which have a diploid and respectively haploid life cycle (Houdan *et al.*, 2004) (fig. 3). In *E. huxleyi*, several types of cells have been reported of which the three most important are: a non-motile, calcifying, diploid cell (C-cell), a motile, non-calcifying, haploid cell (S-cell), and a non-calcifying, non-motile, diploid cell (N-cell) (fig. 6).

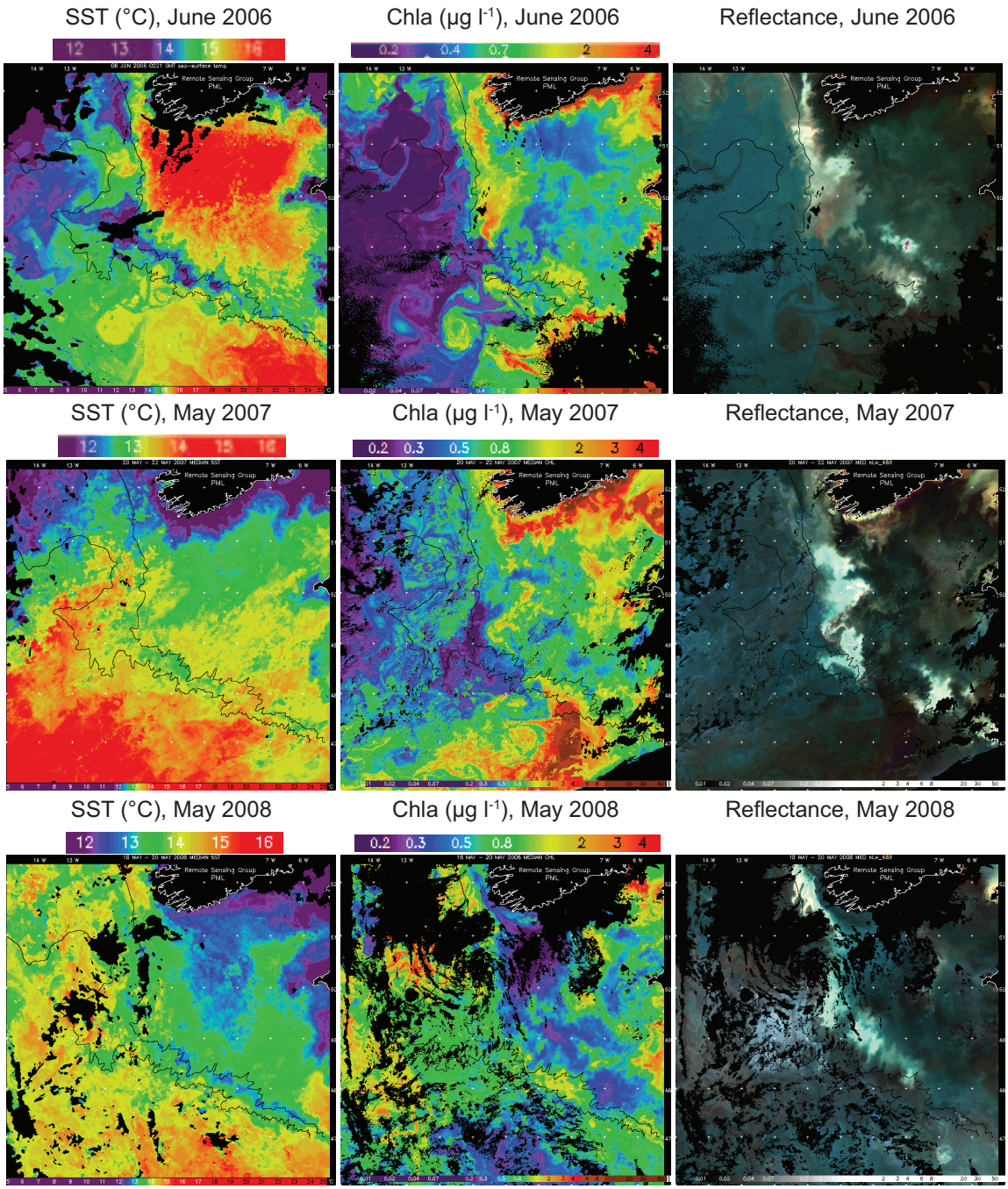

Fig. 5. Remote sensing images of sea surface temperature (SST) (Advanced Very High Resolution Radiometer), chlorophyll *a* concentration (Chl-a) (Sea-viewing Wide Field-of-view Sensor), and reflectance (unitless, false-colour (443, 490 and 555 nm bands), SeaWiFS) contemporary to the May 2006, June 2007 and 2008 campaigns in the Bay of Biscay (6th of June 2006; composite 20 to 22nd of May 2007; composite 18th of May 2008) [courtesy of S. Groom, Remote Sensing Group of the Plymouth Marine Laboratory], and bathymetry (black lines represent the 200 m and 2000 m isobaths). Image modified from Suykens *et al.* (2010).

The C-cell is the form most reported in natural conditions because it is the dominant form during blooms (Paasche, 2002). N-cells present the same morphological features as C-cells but are unable to form coccoliths and are considered to be mutants only described from laboratory cultures (de Jong *et al.*, 1979; Paasche, 2002). S-cells possess two flagella and are covered with organic scales (hence the S for scaly). The occurrence and timing of sexuality in the life cycle of *E. huxleyi* remains unknown to date (Houdan *et al.*, 2004). The few studies that investigated the ecophysiology (Houdan *et al.*, 2004; Houdan *et al.*, 2005; Houdan *et al.*, 2006), and recently the transcriptome of the haploid stage of *E. huxleyi* (von Dassow *et al.*, 2009) demonstrated that this stage could play a role in the widening of the ecological niche of *E. huxleyi* (fig. 3). Because of the greater transcriptome richness in diploid cells they may be more versatile for exploiting a diversity of rich environments compared to haploid cell which have an intrinsically more streamlined transcriptome, offering them a competitive edge in oligotrophic conditions (von Dassow *et al.*, 2009).

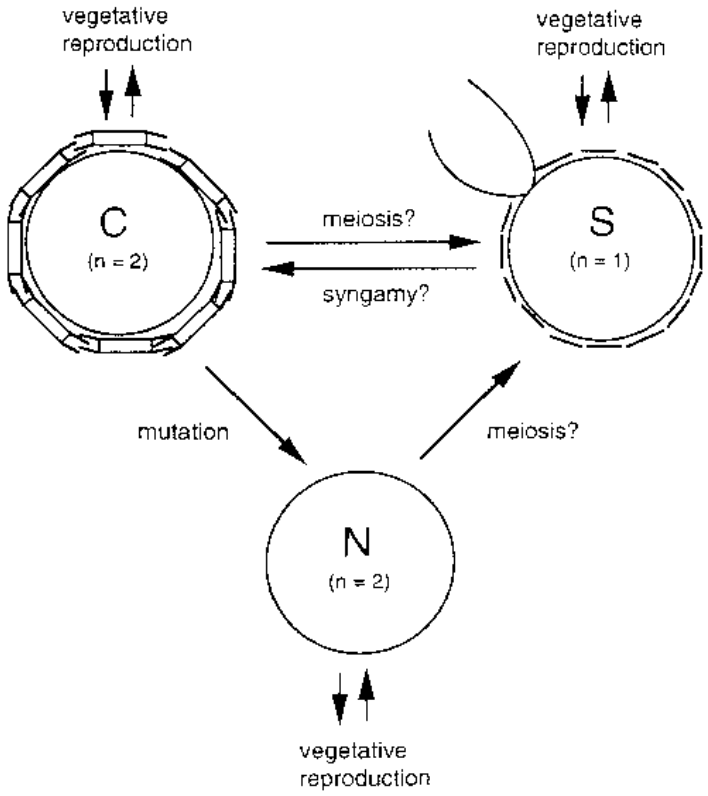

Fig. 6. Life cycle of *E. huxleyi*. The diploid C-cell carries coccoliths while the haploid S-cell is flagellated and scaly. The naked N-cells are only described from laboratory cultures and assumed to be mutants. Image from Paasche (2002).

Bacteria and the microbial food web

Heterotrophic bacteria, which together with phytoplankton and heterotrophic protists are the protagonists of the microbial food web, are central to the decomposition of particulate and dissolved organic matter (POM and DOM) and the regeneration of inorganic nutrients in the ocean. The microbial loop is the pathway by which DOM, which would otherwise be lost for consumption, is returned to higher trophic levels through incorporation into bacterial biomass (Pomeroy, 1974; Azam *et al.*, 1983). This pathway is further coupled to the classic food chain formed by phytoplankton and microzooplankton, mesozooplankton, and nekton by herbivory and predation (fig. 7). Because of their sheer numbers and biomass, and their elevated and diverse metabolic capacity, bacteria effectively respire most of the organic matter that sinks into the ocean's depths (Aristegui *et al.*, 2009), hereby countering the biological carbon pump through carbon dioxide production (fig. 1). However, the bacterial transformation of organic matter is dependent on its composition or bioavailability, the latter being a function of the metabolic and uptake capabilities of the bacterial community members at a particular time and place (Arnosti, 2004).

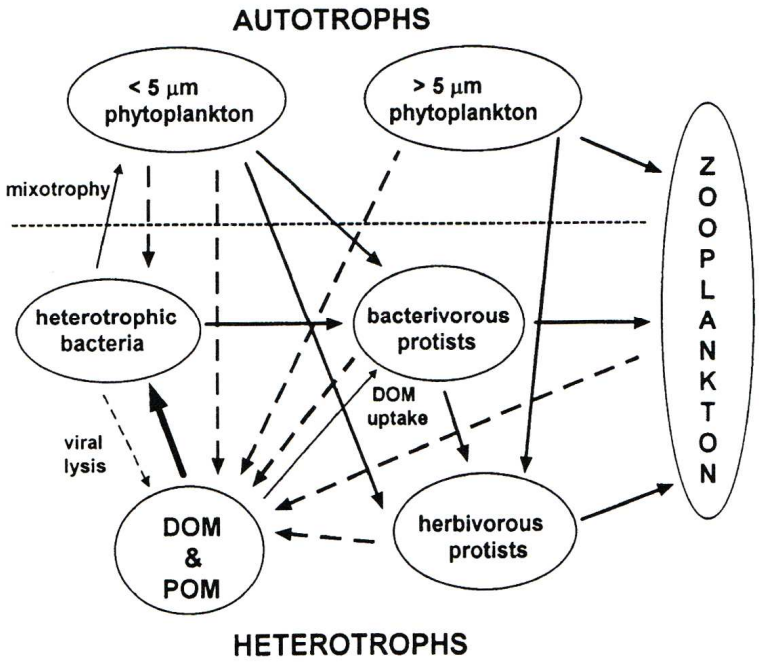

Fig. 7. Conceptual diagram of the microbial food web according to Sherr and Sherr (2000). Solid arrows show pathways of consumption of organic matter; dashed arrows show pathways by which dissolved and particulate organic matter (DOM and POM) is released from living organisms. The microbial food web is divided between autotrophic and heterotrophic microbes. Image from Sherr and Sherr (2000).

Since the advent of genetic molecular techniques in aquatic microbiology (Olsen *et al.*, 1986; Pace *et al.*, 1986), bacterial cells are no longer just little dots in the microscope but can actually be identified on the basis of molecular biomarkers such as the 16S rRNA gene or functional genes, without the need to culture them (Rappe and Giovannoni, 2003). We now know that marine bacterial communities can be hugely diverse (>20000 taxa) (Sogin *et al.*, 2006), and that they are not homogenously distributed in time and space, but show distinct seasonal and latitudinal gradients in composition (Fuhrman *et al.*, 2006; Pommier *et al.*, 2007). Apart from a relatively small number of common species in a particular environment there is generally a large number of very rare species, dubbed the rare biosphere (Sogin *et al.*, 2006). Typically, 16S rRNA gene clone libraries or pyrosequencing studies of bacterioplankton reveal few dominant species (<50) (Gilbert *et al.*, 2010), which could indicate competition for a narrow range of available substrates (Fuhrman and Hagström, 2008). Building evidence supports the existence of functional groups and ecological niche divergence for bacteria (Gasol *et al.*, 2008 and references therein) and *Archaea* (Varela *et al.*, 2008). For example, succession of bacterial communities has been observed during algal blooms (Pinhassi *et al.*, 2004; Lamy *et al.*, 2009), and certain taxonomic clusters have distinct ecological niches e.g. *Bacteroidetes*, are metabolically well-adapted to decompose polymeric organic matter (Bauer *et al.*, 2006), while others e.g. *Roseobacter* and *Gammaproteobacteria* typically occur during blooms of DMSP-producing algae (Gonzalez *et al.*, 2000; Vila *et al.*, 2004). In addition to bottom-up and top-down control (such as viral lysis), positive or negative interactions between bacteria can affect bacterial community structure (Mayali and Azam, 2004). Of particular interest are the close interactions between phytoplankton and bacteria, as bacteria can, for example, directly modulate aggregation processes by influencing algal exudation (Gärdes *et al.*, 2010; Bruckner *et al.*, 2011). Although coccolithophorid blooms are biogeochemically important, the bacterial communities during these blooms have only been studied on a few occasions (Gonzalez *et al.*, 2000; Zubkov *et al.*, 2001b; Riemann and Middelboe, 2002; Stoica and Herndl, 2007; Neufeld *et al.*, 2008).

Extracellular release and the organic matter size continuum

Although traditionally DOM and POM are treated as separate fractions, they are actually part of an OM size continuum where active exchanges between pools spanning several orders of magnitude occur (fig. 8) (Verdugo *et al.*, 2004). DOM is operationally defined as the

OM that passes through a glass fibre (GF/F) or a 0.2 µm pore-size membrane filter. The global DOC pool is estimated to be 685 Gt C (Hansell and Carlson, 1998), a value comparable to the mass of inorganic carbon in the atmosphere (Fasham *et al.*, 2001). In addition, about 17% (1.2 Gt C yr^{-1}) of the global new production of DOM escapes direct bacterial reminalisation due to its more refractory nature (i.e. semi-labile DOM, turnover time between months and years) and is available for export to the ocean's interior (Hansell and Carlson, 1998). Thus factors that control the production, removal, and accumulation of DOM in the surface ocean have both ecological and biogeochemical significance (figs. 1 and 7) (Carlson, 2002).

As mentioned before, the primary source of OM in the ocean is primary production by phytoplankton. Several mechanisms are responsible for the production of DOM including extracellular release (ER) by phytoplankton cells, grazer mediated release and excretion, release via viral cell lysis, solubilisation of organic particles, and bacterial transformation and release (Carlson, 2002). Extracellular release of DOM by phytoplankton is thought to proceed in two ways: passive diffusion of low molecular weight (LMW) OM (< 1 kDa) through the cell membrane caused by the maintenance of a concentration gradient across the cell membrane (Bjørnsen, 1988), or/and by the overflow of a cell's photosynthate when sufficient light and limiting levels of inorganic nutrients constrain cellular incorporation of the photosynthate and growth (Wood and Van Valen, 1990). According to the overflow model extracellularly released DOM should consist of both LMW and high molecular weight (HMW) material (fig. 8) because of simultaneous leakage of LMW DOM and exudation of HMW DOM.

Because DOM produced by exudation is expected to contain minimal amounts of limiting nutrients (N and P) and because one of the first products of photosynthesis is glyceraldehyde-3-phosphate, a monosaccharide formed during the Calvin-cycle (Bassham *et al.*, 1950), the carbon-rich carbohydrates make up an important share (13% - 46%) of DOC in the ocean (Pakulski and Benner, 1994). Furthermore, polysaccharides make up an even higher fraction (25% - 50%) of the HMW colloidal fraction of marine DOM (Benner *et al.*, 1992; Biddanda and Benner, 1997). Some of these colloidal compounds contain acidic sugars that facilitate polysaccharide aggregation into particles known as transparant exopolymer particles (TEP) (figs. 8 and 9) (Alldredge *et al.*, 1993). TEP, operationally defined as particles

retained on a 0.4 µm pore-size membrane filter stained by alcian blue, typically occur in phytoplankton blooms, especially when nutrients become limiting (Passow, 2002b). Moreover, coccolithophores have been shown to produce considerable amounts of TEP, probably through the extracellular release of acidic polysaccharides by calcifying cells (Nanninga *et al.*, 1996). Coccoliths can be scavengend by sticky TEP and aggregated into larger, less porous particles with a much higher density (Engel *et al.*, 2009). TEP are thus important biogeochemical agents in particle-mediated processes such as marine snow formation and sinking and therefore have the potential to account for deep export of carbon on shorter time scales than DOM, which relies on convective mixing processes (Engel *et al.*, 2004a).

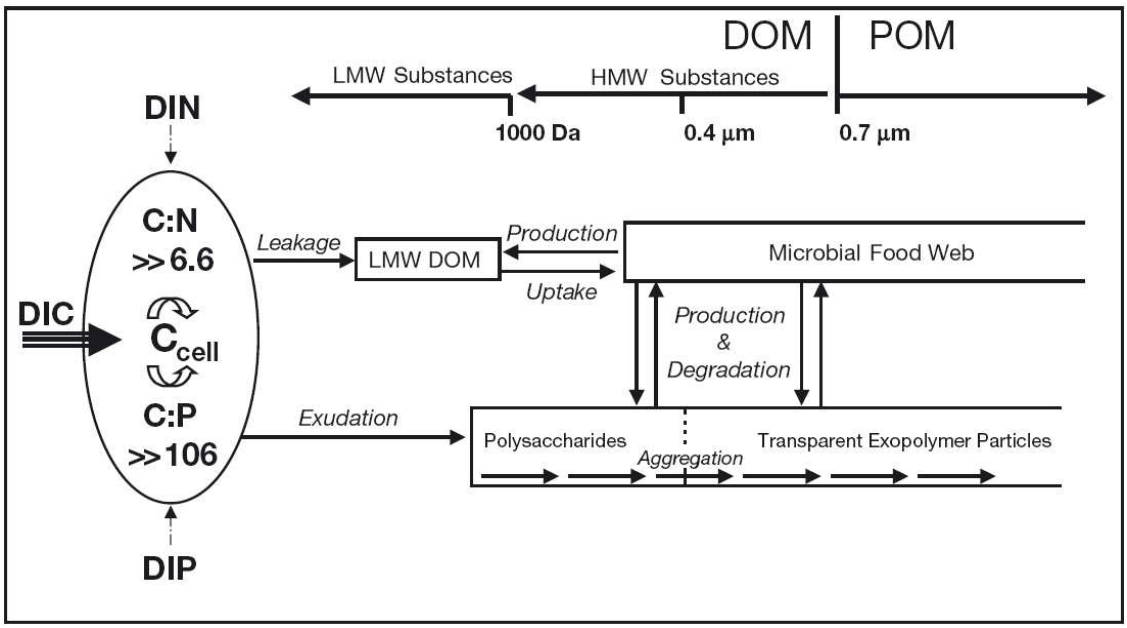

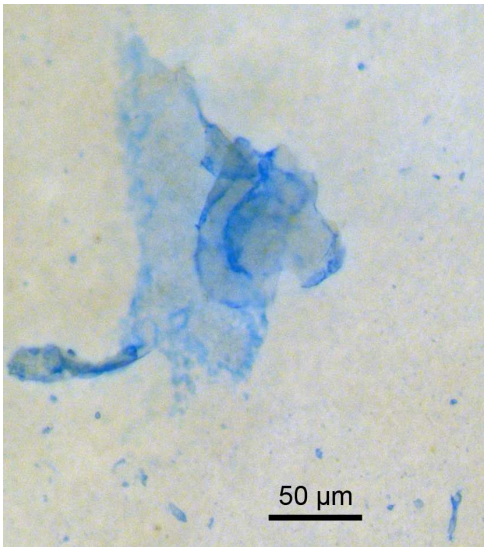

Fig. 8. (above) Conceptual model showing potential pathways of organic matter releases by a phytoplankton cell. Under the assumption that assimilation of dissolved inorganic carbon (DIC) greatly exceeds uptake of dissolved inorganic nitrogen (DIN) or phosphorus (DIP), a fraction of the organic carbon accumulating intracellularly is released from the cell by leakage and exudation. Depending on its quality, extracellular organic carbon can enter the microbial food web or aggregate into particles, such as transparent exopolymer particles. Text and image from Engel *et al.* (2004b).

Fig. 9. Transparant exopolymer (TEP) particle stained by alcian blue.

Coagulation of dissolved polymeric precursors and TEP formation are abiotic transformations of OM, which are not influenced by biological availability but rather are dependent on their composition and concentration. In contrast, bacterial degradation of OM, and interactions and associations between bacteria and phytoplankton, which can be highly specific, are thought to modulate the production and formation of dissolved carbohydrates and TEP through yet unknown mechanisms (Grossart *et al.*, 2005; Gärdes *et al.*, 2010). TEP can also act as substrate or microhabitat for bacteria (Passow and Alldredge, 1994; Mari and Kiorboe, 1996; Pedrotti *et al.*, 2009), potentially shaping bacterial community structure by differentiating the "free-living" (FL) from the "particle-associated" (PA) bacterial community members (Simon *et al.*, 2002; Hodges *et al.*, 2005). Moreover, these differences in bacterial community composition are further reflected in the expression of different ectoenzymes and higher metabolic activities of the PA communities (Martinez *et al.*, 1996; Grossart *et al.*, 2007a). These biological interactions with TEP can potentially further influence the efficiency of the biological carbon pump, but are as yet poorly studied.

Phytoplankton bloom formation in the Bay of Biscay

The continental margin bordering the northern Bay of Biscay was chosen as an area of study based on the regular occurrence of coccolithophorid blooms and its well-studied physical and biogeochemical characteristics (Holligan *et al.*, 1993; Pingree and New, 1995; Huthnance *et al.*, 2001; Joint *et al.*, 2001; Wollast and Chou, 2001; Sharples *et al.*, 2009). The Bay of Biscay extends northwards from Cape Ortegal in NW Spain to the Island of Ouessant in the northwest, off the coast of Brittany (F) (fig. 10). In the northern part of the Bay of Biscay, the Celtic Sea occupies a great part of the continental shelf (< 200 m depth) off Ireland, Great Britain and Brittany. The shelf break is characterized by a marked topographic discontinuity which is particularly pronounced in the northern Bay of Biscay, where the continental slope is steep and heavily indented with canyons and extends further offshore to 4000 m depth.

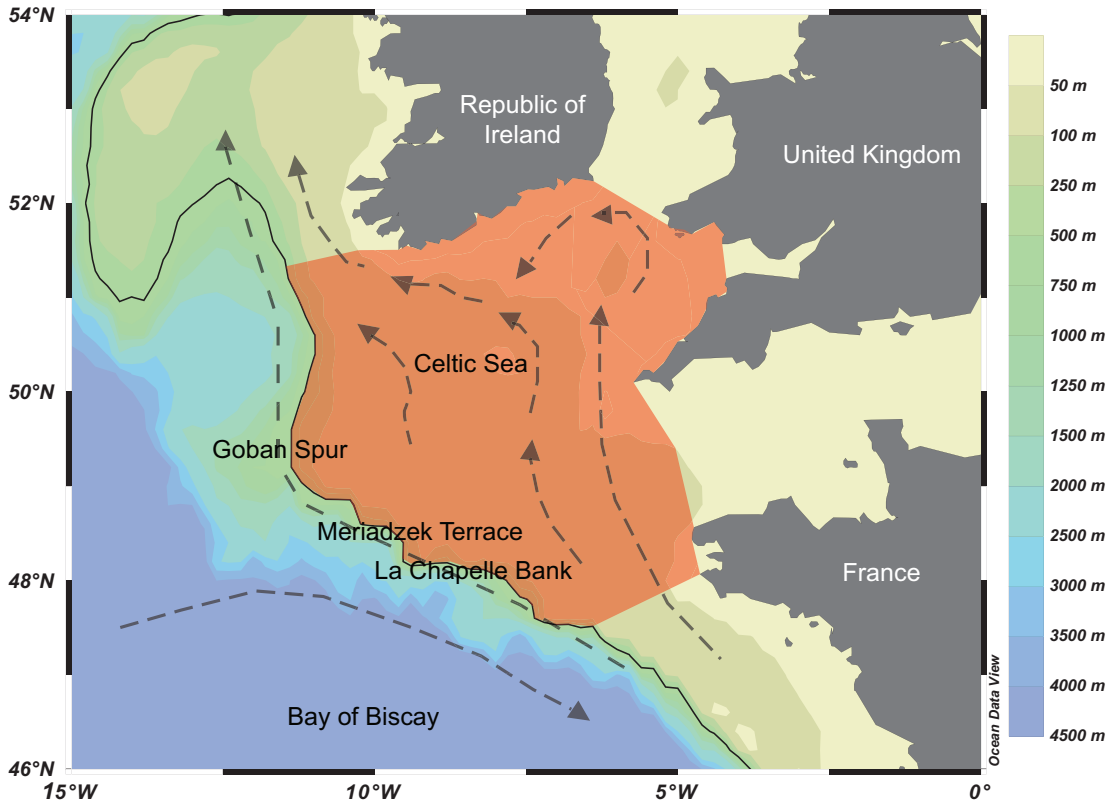

Fig. 10. Bathymetric map showing the location of the Celtic Sea (red) in the study area along the continental margin of the northern Bay of Biscay (delimiting the Celtic Sea to the West). The full black line represents the 200 m isobath, delineating the shelf edge. The dotted lines and arrows indicate the surface circulation in this region.

Seasonal warming of the sea surface is generally accompanied by the formation of a thermocline in the upper 100 m of the water column. Temperature gradients appear in April and rapidly increase in May with a shoaling of the mixed layer depth throughout summertime. Intense storms occurring in spring and summer can be responsible for the local deepening of the thermocline, reintroducing nutrients to the surface layer and relaunching primary production (Harlay *et al.*, 2010). Furthermore, semi-diurnal tidal currents across the steep continental slope, inducing vertical water displacement and internal waves at the continental slope, lead to to enhanced vertical mixing and thus injection of inorganic nutrients to the surface waters (Holligan and Groom, 1986; Lampert *et al.*, 2002; Sharples *et al.*, 2007; Harlay *et al.*, 2010). This phenomenon is visible in figure 5 and appears as an irregular ribbon of colder (by 1-2°C) water on satellite sea surface temperature images. Along the continental margin of the Bay of Biscay, phytoplankton growth, and

coccolithophorid blooms in particular, have been shown to be triggered and/or sustained by this internal tidal wave formation (fig. 5) (Holligan and Groom, 1986; Lampert *et al.*, 2002; Harlay *et al.*, 2010). Phytoplankton blooms are often patchy, reflecting the local hydrodynamics and their response to nutrient inputs and biological and physical loss processes (e.g. cell lysis, grazing, and mixing) (fig. 5).

A general scenario of bloom formation and development along the continental margin has been proposed recently by Harlay (2009). Following the diatom-dominated main spring phytoplankton bloom event in mid-April, succession of less intense, often coccolithophore-dominated blooms have been observed in the area of study (Huthnance *et al.*, 2001; Harlay *et al.*, 2010). Depleted dissolved silica concentrations, an essential nutrient for diatom growth, and increased irradiance levels provide suitable circumstances for coccolithophores to bloom (see also fig. 3). In this scenario, early phases of the coccolithophorid bloom are often encountered over the continental slope, where biological activity is triggered by vertical mixing (Harlay, 2009). The development of the bloom proceeds as the patches are advected over the continental shelf, following surface circulation patterns in the northeast direction. Patches of high reflectance, caused by the suspension of coccoliths in the surface water, follow the same pattern and intensify as thermal stratification increased (fig. 5). Finally, blooms collapse and aggregation causes these coccolith-rich patches to sink to the continental shelf floor.

2

Phytoplankton dynamics during late spring coccolithophore blooms at the continental margin of the northern Bay of Biscay (North East Atlantic, 2006-2008)

Nicolas Van Oostende[1], Jérôme Harlay[2], Caroline De Bodt[2], Lei Chou[2], Wim Vyverman[1], Koen Sabbe[1]

[1] Laboratory for Protistology and Aquatic Ecology, Biology Department, Ghent University, Krijgslaan 281 – S8, B-9000 Gent, Belgium.

[2] Laboratoire d'Océanography Chimique et Géochimie des Eaux, Université Libre de Bruxelles, Campus de la Plaine, CP208, boulevard du Triomphe, B-1050 Brussels, Belgium.

Authors' contributions

NVO, JH, LC and KS conceived and designed the study. CDB and LC performed the nutrient, particulate matter and TEP concentration measurements. NVO performed the pigment analyses. NVO analysed the data and wrote the manuscript. KS, JH, WV, and LC revised the manuscript.

Abstract

We determined the spatial and temporal dynamics of major phytoplankton groups in relation to biogeochemical and physical variables during the late spring coccolithophore blooms (May-June) along and across the continental margin of the northern Bay of Biscay (2006-2008). Photosynthetic biomass (Chla) of the dominant plankton groups was determined by CHEMTAX analysis of HPLC pigment signatures; uni- and multivariate statistics were used to identify the main physical and biogeochemical variables underlying the variation in phytoplankton biomass and community structure.

Phytoplankton standing stock biomass varied substantially between and during the campaigns (areal Chla (mg Chla m^{-2}) in June 2006: 63.8 ± 26.5, May 2007: 27.9 ± 8.4, and May 2008: 41.3 ± 21.8), reflecting the different prevailing weather, irradiance, and sea surface temperature conditions between the campaigns. Coccolithophores, represented mainly by *Emiliania huxleyi*, and diatoms were the dominant phytoplankton groups, with a maximal contribution of, respectively, 72% and 89% of the total Chla. Prasinophytes, dinoflagellates, and chrysophytes often co-occurred during coccolithophorid blooms, while diatoms dominated the phytoplankton biomass independently of the abundance of other groups. The location of the stations on the shelf or on the slope side of the continental margin did not influence the biomass and the composition of the phytoplankton community despite significantly stronger water column stratification and lower nutrient concentrations on the shelf. The alternation between diatom and coccolithophorid blooms of similar biomass, following the mostly diatom-dominated main spring bloom, was partly driven by changes in nutrient stoichiometry (N:P and dSi:N). High concentrations of transparent exopolymer particles (TEP) were associated with stratified, coccolithophore-rich water masses, which probably originated from the slope of the continental margin and warmed during advection onto the shelf. Although we did not determine the proportion of export production attributed to phytoplankton groups, the abundance of coccolithophores, TEP, and coccoliths may affect the carbon export efficiency through increased sinking rates of particles formed by aggregation of TEP and coccoliths.

Introduction

Continental shelves and margins are areas of high primary productivity and carbon export and as such play a key role in global biogeochemical cycles and fisheries (Joint *et al.*, 2001; Sharples *et al.*, 2009). Spring phytoplankton blooms are a prominent seasonal feature of the North East Atlantic Ocean (NE Atlantic) (Henson *et al.*, 2006) and are characterized by an intense diatom bloom followed by nanoplankton (a.o. prymnesiophytes, prasinophytes and cyanobacteria) when first dissolved silicate and then other nutrients become depleted, and increasing water column stratification hinders nutrient replenishment to the euphotic zone (Joint *et al.*, 1986; Lochte *et al.*, 1993; Rees *et al.*, 1999; Raitsos *et al.*, 2006; Leblanc *et al.*, 2009). Especially coccolithophores are a prominent feature of the late spring bloom, and this has been attributed to their tolerance for high irradiances, lower nutrient requirements and/or ability to utilize organic nitrogen or phosphorus sources (Leblanc et al. 2009 and references therein). Bloom termination follows when nutrient depletion depresses primary productivity and grazing and viral control catch up with algal growth (Brussaard, 2004; Calbet and Landry, 2004; Behrenfeld, 2010). In reality, this general NE Atlantic spring bloom scenario can be more or less scrambled due to local weather conditions and physical phenomena (Ji *et al.*, 2010), both in the open ocean, where movements of eddies and other water masses can reset succession events (Smythe-Wright *et al.*, 2010) and along continental margins, where vertical mixing resulting from internal tides can bring nutrient-rich deeper water into the euphotic zone (Sharples *et al.*, 2007). Along the continental margin of the Bay of Biscay, phytoplankton growth, and coccolithophorid blooms in particular, have been shown to be triggered and/or sustained by internal tidal wave formation at the shelf break leading to enhanced vertical mixing and the injection of inorganic nutrients to the surface waters (Holligan and Groom, 1986; Lampert *et al.*, 2002; Sharples *et al.*, 2009; Harlay *et al.*, 2010).

A general scenario of late spring bloom evolution at the continental margin of the northern Bay of Biscay is proposed by Harlay *et al.* (2010): when the main diatom spring bloom (mid April) has depleted dissolved silicate (dSi) to levels below 2 µmol l^{-1}, vertical inputs of nutrients along the shelf break trigger mixed blooms mainly dominated by coccolithophores. These blooms further exhaust nutrients as the water column stratifies and the water mass is advected over the continental shelf, following the general residual circulation in the area

(Pingree and Lecann, 1989; Huthnance *et al.*, 2001; Suykens *et al.*, 2010), while dinoflagellates, chrysophytes, prasinophytes and cryptophytes become increasingly more important. This succession leads to the appearance of high reflectance (HR) patches which are associated with the dissipative stage of coccolithophorid blooms (of *Emiliania huxleyi* in particular), when coccoliths are shed into the water column, affecting the albedo of the surface water (Westbroek *et al.*, 1993; Harlay *et al.*, 2010). This bloom succession considerably alters the biogeochemical characteristics of their environment through biogenic calcification and the release of transparent exopolymer particles (TEP), which affect carbon export through mineral ballasting and aggregation (Armstrong *et al.*, 2002; Engel *et al.*, 2004b; De La Rocha and Passow, 2007), and dimethylsulphide (DMS) production, which introduces sulphur into the atmosphere (Burkill *et al.*, 2002; Stefels *et al.*, 2007; Seymour *et al.*, 2010). However, additional evidence is still needed to ascertain the phytoplankton bloom succession along the continental margin following the main spring bloom.

While the annual occurrence of extensive coccolithophore blooms in late spring in the NE Atlantic is well documented (Leblanc 2009 and references therein), there is no consensus on the factors triggering coccolithophorid blooms and modulating the turnover time of the calcite they produce (Lessard *et al.*, 2005; Poulton *et al.*, 2007; Boyd *et al.*, 2010; Poulton *et al.*, 2010). Changes in environmental control factors such as light intensity, water column stability, temperature, CO_2 concentration, nitrate and phosphate levels and their ratio, and the concentration trace metals (e.g. Fe, Zn, and Mn) have been shown to influence coccolithophore physiology and control phytoplankton community assemblage to various extent (Nanninga and Tyrrell, 1996; Zondervan, 2007; Boyd *et al.*, 2010, and references therein). Moreover, only few studies have described the structure and the spatial and temporal dynamics of phytoplankton during these blooms along the western European continental margin (Head *et al.*, 1998; Joint *et al.*, 2001; Fileman *et al.*, 2002; Lampert *et al.*, 2002). This information is needed, as the importance of the phytoplankton community structure to the biological pump is still poorly understood (Smythe-Wright *et al.*, 2010, and references therein). Changes in the community composition are expected to impact primary and export production, and as such food web structure and dynamics, as well the biogeochemical cycling of carbon and other bio-limiting elements in the sea (Guidi *et al.*, 2009; Finkel *et al.*, 2010).

As part of the oceanographic research project PEACE ("role of PElagic cAlcification and export of CarbonatE production in climate change"), we investigated the dynamics of the main phytoplankton groups during three campaigns (2006-2008) in late spring (May-June, i.e. after the main diatom bloom in April), along and across the continental margin of the northern Bay of Biscay. More specifically, we investigated if (1) water column properties such as stratification, nutrient levels and the ratios differed between the shelf and the slope side of the continental margin, (2) how changes in such physical and biogeochemical variables influence the phytoplankton community structure and biomass, and (3) how phytoplankton biomass and community structure is related to the standing stocks of particulate organic carbon (POC), particulate inorganic carbon (PIC – calcite), and especially TEP. Phytoplankton community structure was assessed using a chemotaxonomic (pigment-based) approach and its dynamics and relation to biogeochemical variables analysed using multivariate non-parametric analyses.

Materials & Methods

Study area and general set-up of the campaigns

The study area along the continental margin of the northern Bay of Biscay and on the shelf of the Celtic Sea included three different areas: La Chapelle Bank (LC), Meriadzek Terrace (M) and the Goban Spur (GS) area (fig. 1 and table 1). Three campaigns were carried out from the 31st May to the 9th of June 2006, from the 10th to the 24th of May 2007, and from the 7th to the 23rd of May 2008, onboard RV *Belgica*. All campaigns took place after the main diatom spring bloom which took place in April (fig. 2). Most stations were located in the vicinity of the La Chapelle Bank (47°N, 8°W) while 8 stations were located over the shallow part (<200 m depth) of the Goban Spur (50°N, 10°W) (fig. 1). Eight deeper stations (from 450 to 1400 m depth) were located over the continental slope at the Meriadzek Terrace (48°N, 9°W) and the La Chapelle Bank. A list of all sampling stations, their geographic location and their main physical characteristics is provided in table 1. Each campaign consisted of two legs allowing some stations to be revisited with a 1-2 week interval. Revisited stations are denoted with a "b" following their numeral identifier. Due to shorter ship-time, sampling during the June 2006 campaign was limited to the area around the La Chapelle Bank, while during the two following campaigns sampling was carried in the whole

area outlined above (see fig. 1 and table 1). Near real-time MODIS Aqua remote sensing images were used to track phytoplankton community dynamics through phases of emergence and disintegration of coccolithophorid blooms during the campaigns, (Suykens *et al.*, 2010) (see chapter 1, fig. 5).

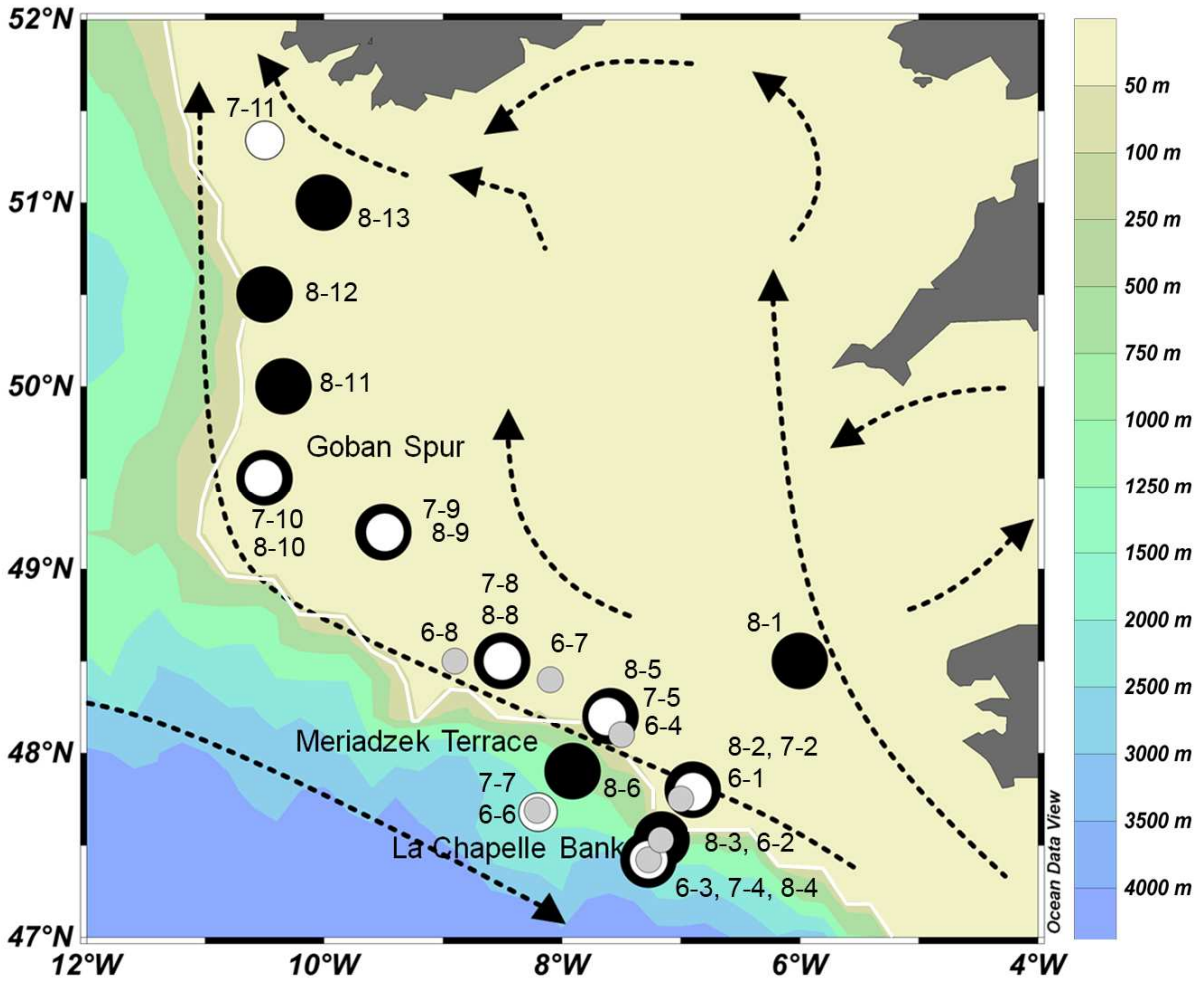

Fig. 1. Bathymetric map showing the location of the stations sampled along the continental shelf break. The brown and green shades represents the continental slope, the full white line follows the 200 m isobath, delineating the shelf edge. The stations visited during June 2006, May 2007, and May 2008 are represented by grey, white, and black dots, respectively. Exact position and label of stations can be found in table 1. Dotted lines represent the main residual surface circulation (adapted from Suykens *et al.* 2010). Topographical information was obtained using ODV software (Schlitzer, R., Ocean Data View, http://odv.awi.de, 2011).

Table 1. Overview of physical variables characterising the stations visited during the three campaigns. The first numeral of the station code denotes the last digit of the year of the respective campaign (2006, 2007, 2008), followed by the station number during each campaign. Station codes followed by a "b" indicate the station was revisited during the second leg of the campaign. Stations located at the slope of the continental margin are denoted by an asterisk. Latitude (lat.), longitude (lon.), sea surface temperature (SST), stratification degree (strat. deg.), mixed layer depth (MLD).

date	station	area	lat. (°N)	lon. (°W)	bottom depth (m)	SST (°C)	surface salinity (psu)	strat. deg. (kg m^{-3})	MLD (m)
31/05/2006	6-1	La Chapelle	47.75	7.00	157	13.03	35.61	0.31	32
1/06/2006	6-2*	La Chapelle	47.53	7.17	558	12.99	35.63	0.21	40
1/06/2006	6-3*	La Chapelle	47.42	7.27	1400	13.95	35.67	0.42	21
2/06/2006	6-4	Meriadzek	48.10	7.50	163	13.28	35.60	0.39	34
6/06/2006	6-8	Meriadzek	48.50	8.90	178	14.47	35.54	0.73	19
7/06/2006	6-6*	Meriadzek	47.69	8.21	1100	14.85	35.65	0.60	16
7/06/2006	6-7	Meriadzek	48.40	8.10	164	14.51	35.57	0.69	20
8/06/2006	6-4b	Meriadzek	48.10	7.50	159	14.32	35.61	0.62	23
9/06/2006	6-1b	La Chapelle	47.75	7.00	158	14.32	35.62	0.56	22
10/05/2007	7-2	La Chapelle	47.79	6.90	165	13.41	35.57	0.27	42
12/05/2007	7-5	Meriadzek	48.20	7.62	172	12.97	35.53	0.24	39
13/05/2007	7-8	Meriadzek	48.50	8.50	158	13.21	35.56	0.27	39
14/05/2007	7-9	Goban Spur	49.20	9.49	154	12.98	35.49	0.33	43
15/05/2007	7-10	Goban Spur	49.50	10.51	139	12.73	35.45	0.32	36
16/05/2007	7-11	Goban Spur	51.34	10.50	150	12.30	35.31	0.39	39
21/05/2007	7-8b	Meriadzek	48.50	8.50	158	13.27	35.52	0.29	43
22/05/2007	7-5b	Meriadzek	48.22	7.59	172	13.30	35.52	0.31	36
23/05/2007	7-4*	La Chapelle	47.42	7.27	1200	13.38	35.63	0.11	54
23/05/2007	7-7*	Meriadzek	47.68	8.20	1100	13.49	35.59	0.24	36
24/05/2007	7-2b	La Chapelle	47.80	6.89	165	13.40	35.56	0.22	28
7/05/2008	8-1	Armorican	48.50	6.00	122	12.42	35.39	0.30	13
7/05/2008	8-3*	La Chapelle	47.53	7.16	567	12.72	35.60	0.17	40
8/05/2008	8-2	La Chapelle	47.80	6.90	167	12.75	35.48	0.25	15
9/05/2008	8-6*	Meriadzek	47.90	7.91	479	12.25	35.59	0.04	100
10/05/2008	8-5	Meriadzek	48.20	7.59	174	12.91	35.51	0.27	25
11/05/2008	8-8	Meriadzek	48.50	8.50	150	12.95	35.50	0.31	18
12/05/2008	8-9	Goban Spur	49.20	9.50	154	12.91	35.47	0.38	15
13/05/2008	8-10	Goban Spur	49.50	10.50	138	13.13	35.54	0.43	22
14/05/2008	8-11	Goban Spur	50.50	10.50	159	12.70	35.58	0.31	14
19/05/2008	8-12	Goban Spur	51.00	10.00	121	13.61	35.54	0.60	19
20/05/2008	8-13	Goban Spur	50.00	10.34	129	13.42	35.58	0.46	34
21/05/2008	8-9b	Goban Spur	49.20	9.50	154	13.62	35.52	0.48	23
22/05/2008	8-5b	Meriadzek	48.20	7.60	174	13.53	35.56	0.37	39
23/05/2008	8-4*	La Chapelle	47.42	7.27	1200	14.30	35.61	0.48	20

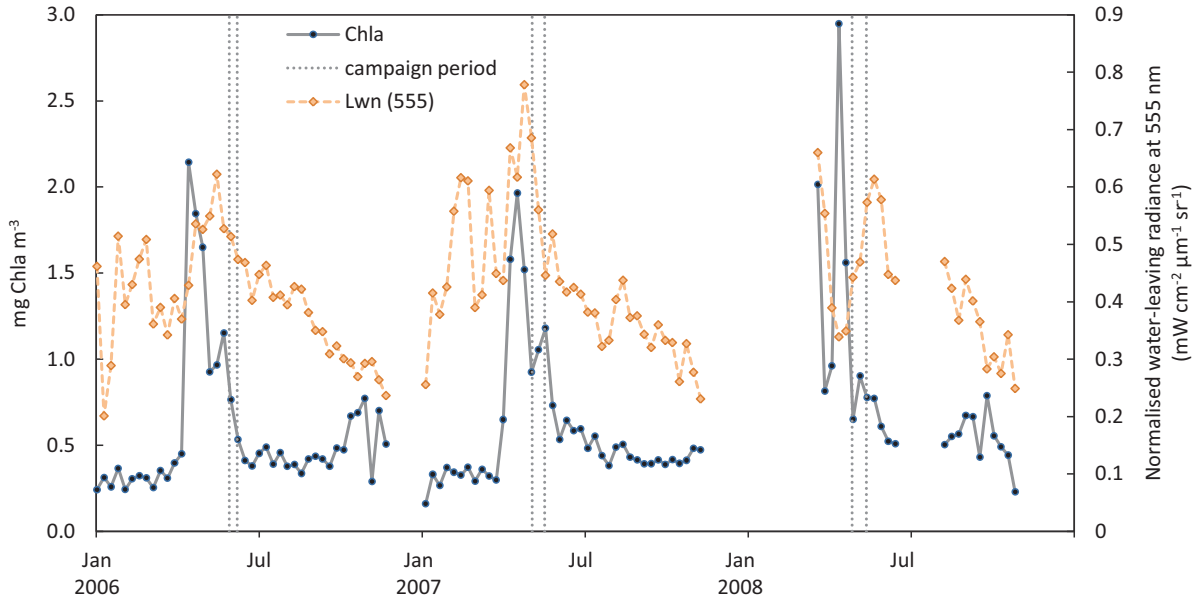

Fig. 2. Monthly time series of 8-day composite SeaWiFS Chla concentration (black full line) and normalized water-leaving radiance at 555 nm (yellow dashed line) at La Chapelle Bank (values averaged over area: 47-49 N° latitude by 6-9 W° longitude, 0.083° resolution). The vertical dotted lines delineate the time period during which the campaigns took place. Data generated from NASA's Giovanni (giovanni.gsfc.nasa.gov) on January 6th 2011. Note that normalized water-leaving radiance at 555 nm from January to March can be biased due to cloud coverage (Steve Groom, personal communication).

Sample collection and analyses

Physical parameters

Water samples were collected using a rosette of 12 Niskin bottles (10 l) coupled to a conductivity and temperature-pressure probe (CTD) (Seabird SBE21). CTD casts covered surface waters, thermocline, and deeper waters down to 80 m depth. The reported values of sea surface temperature (SST) have been measured at 10 m depth to avoid influence from diurnal changes. The degree of stratification of the water column was calculated as the difference in seawater density (σ_θ) at 100 m and at 10 m depth. These depths were chosen to make sure that the upper value was within the mixed layer (where density was homogeneous), and that the bottom value was below the base of the thermocline (table 1; Suykens et al 2010). The upper mixed layer depth (MLD) was operationally defined as the depth where σ_θ increased by ≥ 0.1 kg m^{-3} compared to the water density at 10 m depth. Nutrient data (collected every 10 m, see below) were used to compute the depth of the

nitracline, a proxy of nutrient supply to the upper mixed layer of the ocean, which was operationally defined as the shallowest depth at which nitrate+nitrite concentration (NOx) exceeds 1.00 µmol l^{-1} (Cermeño *et al.*, 2008; Landry *et al.*, 2009). Since density gradients were driven principally by temperature rather than salinity (Suykens et al. 2010) the term thermocline is used here to describe the intermediate layer between the upper mixed layer and deeper mixed layer.

Dissolved nutrients

Samples for the measurement of dissolved phosphate (PO_4), nitrate and nitrite (NOx) – further referred to as nitrate-, and dissolved silicate (dSi) were filtered through 0.4 µm pore size Nuclepore filters (∅=47 mm). PO_4 and dSi samples were stored at 4 °C until onboard analysis by spectrophotometry, using the molybdate/ascorbic acid method (Grasshoff *et al.*, 1983); NOx samples were stored at -20 °C until analysis and their concentration was determined spectrophotometrically using a Skalar Autoanalyzer system (Grasshoff *et al.*, 1983). The detection limit was 0.01 µmol l^{-1} for PO_4 and 0.05 µmol l^{-1} for NOx and dSi.

Particulate matter

Particulate organic and inorganic carbon samples (POC and PIC) were collected by filtration of 0.2 – 2.0 l seawater through pre-combusted (4h at 500 °C) GF/F filters. The filter samples were stored at -20 °C until analysis (within three months after the cruise) and dried overnight at 50 °C prior to analysis. POC was determined using a Fisons NA-1500 elemental analyzer after carbonate removal from the filters by overnight HCl fuming. Total particulate carbon content was determined using unacidified filters. PIC content was derived from the difference between total particulate carbon content and POC content. Four to five standards of certified reference stream sediment (STSD-2) from the Geological Survey of Canada, together with three to four blank filters, were used for calibration. Particulate nitrogen (PN) was determined from untreated filters in the same way as particulate carbon.

Transparent exopolymer particles (TEP) were measured spectrophotometrically after alcian blue staining and hydrolysis (Alldredge *et al.*, 1993; Harlay *et al.*, 2009). TEP concentration determined this way reflects the density of stainable moieties in particulate matter, such as

acidic and sulphated sugars, and should thus be considered as a semi-quantitative measure of TEP concentration expressed in µg xanthan gum equivalents per litre (µg X eq. l^{-1}).

Microscopic identification

Microscopic screening of phytoplankton diversity in water samples (100 ml) from the upper mixed layer of stations from each campaign was performed by the Utermöhl sedimentation method (Utermöhl, 1958) using a Zeiss inverted microscope. These samples were preserved using a mixture of alkaline Lugol's iodine solution (0.1 % v/v) and borate-buffered formaldehyde solution (0.9% v/v, all final concentrations) (Sherr and Sherr, 1993). The microscopic screening was performed to verify the presence of the dominant phytoplankton groups using specific pigment biomarkers (Havskum *et al.*, 2004; Irigoien *et al.*, 2004). Sea surface water samples (1.0 l) for scanning electron microscopy (SEM) were filtered through polycarbonate membrane filters (0.8 µm pore size, Ø 47 mm, Millipore), dried onboard for 12h at 50°C and stored dry before being mounted onto microscope slides and coated with gold (Bollmann *et al.*, 2002). Coccolithophores were identified by scanning electron microscopy (SEM) using a Jeol JSM 5600 LV at a minimum magnification of 600 times. Taxonomic identification was performed according to Hasle and Syvertsen (1996).

Photosynthetic pigments and chlorophyll a partitioning

For pigment analysis, 0.5 to 3.5 l of seawater was filtered through glass fibre filters (Whatman GF/F, Ø47 mm) using a low vacuum pressure (< 200 mbar). The filters were stored in liquid nitrogen until analysis. Extraction of the pigments was performed in a 90% acetone aqueous solution, spiked with an internal standard (trans-β-apo-8'-carotenal), while cell disruption was further facilitated by sonification for 30 s with 50 W pulses (Bidigare *et al.*, 2005). The extracts were cleared from debris by filtration through a 0.2 µm Teflon syringe filter after centrifugation for 4 minutes at 700 x g (at -5 °C). Pigment extracts were analysed by high pressure liquid chromatography (HPLC) according to the method of Wright *et al.* (Wright *et al.*, 1991; Wright and Jeffrey, 1997) using an Agilent 1100 series HPLC system equipped with an Machery-Nagel reverse-phase C_{18} column (Nucleodur C_{18} pyramid, pore size 100 Å, particle size 5 µm). Deionised water (Milli-Q) was added to extracts to avoid peak distortion of early eluting peaks (Zapata and Garrido, 1991), preventing the loss of non-polar

pigments prior to injection. Pigments were identified by comparison of retention times and absorption spectra and quantified by calculating response factors using pure pigment standards (supplied by DHI Lab, Denmark). We measured the concentration of the following pigments: chlorophyll *c3*, chlorophyll *c1+c2*, peridinin, 19'-butanoyloxyfucoxanthin, fucoxanthin, 19'-hexanoyloxyfucoxanthin, pasinoxanthin, violaxanthin, diadinoxanthin, alloxanthin, zeaxanthin, chlorophyll *b*, and chlorophyll *a*. Abbreviations of the pigments are given in table 2.

Table 2. Chemotaxonomic relationships used in this study. Species in bold emphasize the value of the associated pigment as a major taxonomic biomarker.

Pigment	Abbreviation	Occurrence
alloxanthin	Allo	**cryptophytes**
19'-butanoyloxyfucoxanthin	But	**chrysophytes**
chlorophyll *a*	Chla	total algal biomass (including *Synechococcus*)
chrolophyll *b*	Chlb	**prasinophytes**
chlorophyll c_3	$Chlc_3$	prymnesiophytes, chrysophytes, diatoms
fucoxanthin	Fuc	**diatoms**, prymnesiophytes, **chrysophytes**
19'-hexanoyloxyfucoxanthin	Hex	**prymnesiophytes (coccolithophores)**
peridinin	Per	**dinoflagellates**
violaxanthin	Viol	**prasinophytes**
prasinoxanthin	Pras	**prasinophytes**
zeaxanthin	Zea	***Synechococcus***, prasinophytes

Quantification of the dominant phytoplankton groups was performed by means of a CHEMTAX routine using multiple runs (n=64) and depth bins (n=6) per year (Mackey *et al.*, 1996; Latasa, 2007). Chla was partitioned between the main phytoplankton groups identified by microscopic screening of samples from the Chla maximum depth and based on pigment biomarker ratios from relevant literature (Johnsen and Sakshaug, 1993; Mackey *et al.*, 1996; Liu *et al.*, 1999; Llewellyn and Gibb, 2000; Schluter *et al.*, 2000; Gibb *et al.*, 2001; Latasa *et al.*, 2004; Six *et al.*, 2004; Zapata *et al.*, 2004) (see tables 2, SP1, SP2 and SP3). In our study, the pigment butanoyloxyfucoxanthin was mainly associated with the chrysophyte group s.l., i.e. chrysophytes and pelagophytes (Andersen *et al.*, 1996; Rodriguez *et al.*, 2003). Because *Rhizosolenia* spp. were part of the diatom community, part of the pigment $chlc_3$ was attributed to the diatom group (Richardson *et al.*, 1996). Having low taxonomic specificity, diadinoxanthin was omitted from the CHEMTAX analysis (Gibb *et al.*, 2001).

Initial pigment ratios used for each phytoplankton group (table SP1) were multiplied by a random value between 0.65 and 1.35 for each CHEMTAX run to overcome the sensitivity of the routine to initial seed values. We used the mean of the five best results from the 64 runs, having the lowest residual square means, as an estimate of phytoplankton group abundances. Table SP2 shows the average pigment ratios of the best results after performing the CHEMTAX routine for the May 2008 campaign using the 20 m depth bin.

Areal values of Chla concentration were calculated by trapezoidal integration of volumetric values from 0 to 80 m depth.

Statistical treatment of data

Averages are reported as their arithmetic mean followed by their standard deviation. We used Spearman rank correlations to assess the degree and significance of linear relationships between two variables. To test the difference in areal Chla concentration between campaign years a non-parametric permutational analysis of variance (PERMANOVA) was performed using the PRIMER v6 and PERMANOVA+ add-on software (PRIMER-E Ltd., Plymouth, U.K.) (Clarke and Gorley, 2006; Anderson *et al.*, 2008). To test the difference in environmental variables between campaign years and areas (La Chapelle Bank and Meriadzek Terrace versus Goban Spur) or shelf/slope position of stations and campaign years, PERMANOVA's with a fully crossed two-factor design were performed using type III (partial) sums of squares. The interaction term informs about the difference in environmental variables among campaign years. A Euclidean distance-based resemblance matrix was used and probability values were obtained by permutation ($n=10^4$). Nutrient concentrations were log transformed to approach normal distribution.

Unconstrained multivariate analyses of phytoplankton group biomass were performed using principal coordinates analysis (PCO) to investigate differences between stations and years in terms of phytoplankton community structure. Phytoplankton group biomasses were square root transformed to reduce the contribution of highly abundant groups in relation to less abundant ones in the calculation of the Bray-Curtis measure. The significance of the relation of environmental variables (plotted as supplementary variables) to the PCA and PCO axes of the phytoplankton community were plotted was tested using Spearman rank correlations

(PRIMER-E Ltd., Plymouth, U.K.). We adopted a probability threshold of $p<0.05$ for all analyses, unless stated otherwise.

Results

Thermal stratification and nutrient levels

Sea surface temperature (SST) was on average higher in June 2006 (13.84 °C ± 0.76) than in May 2007 (13.25 °C ± 0.16) and May 2008 (13.04 °C ± 0.66) (table SP1 and pairwise tests: p(2007)=0.042 and p(2008)=0.023), however SST did not significantly differ between shelf and slope stations (table 1, 6, SP1, and fig. 4). Most slope stations, except 6-6 and 8-4, lacked a distinct thermocline and were significantly less stratified (LC&M: 0.28 ± 0.19 kg m^{-3}) than the shelf stations (LC&M: 0.38 ± 0.17 kg m^{-3}; GS: 0.41 ± 0.09 kg m^{-3}) (fig. SP1, table 1 and 3), while the water column over the shelf was significantly more stratified in 2006 (0.55 ± 0.17 kg m^{-3}) than in 2007 (0.27 ± 0.03 kg m^{-3}) and 2008 (0.30 ± 0.05 kg m^{-3}) (tables 1 and SP4) (pairwise tests: p(2007)=0.002 and p(2008)=0.035). We also found a low but significant negative relationship between bottom depth - which can be used as proxy for the difference between slope and shelf stations - and the stratification degree. Differences in MLD were significant between shelf and slope stations (tables 1 and 3) yet inter-annual differences were not significant (table SP4) (LC&M: 2006: 25 ± 8 m; 2007: 40 ± 6 m; 2008: 30 ± 22 m). Nutrients in the upper mixed layer of the shelf stations were usually depleted during the three campaigns, as indicated by the low maximum values measured in the upper mixed layer (NOx < 1.47 µmol l^{-1}; PO_4 < 0.10 µmol l^{-1}; dSi < 1.95 µmol l^{-1}). In contrast, most slope stations had higher nutrient levels (maximum values of slope stations: NOx < 2.45 µmol l^{-1}; PO4 < 0.26 µmol l^{-1}; dSi < 1.40 µmol l^{-1}) (except station 8-4 which also had depleted levels). In all years, the slope stations had significantly higher NOx and PO_4 concentrations than the shelf stations (tables 3, 6, and SP4). In contrast, dSi was not significantly higher at the slope stations (table SP4). Neither N:P, nor dSi:N ratios were significantly higher on the slope than on the shelf (table SP4). The depth profiles of PO_4, NOx, and dSi concentration are inversely correlated to the temperature profiles (Pearson r = -0.69, -0.68 and -0.51, $p<0.01$, respectively). Consequently, the depth of the nitracline was also very variable and estimated to be between surface and 38 m in 2006, between surface and 43 m in 2007, and between surface and 48 m in 2008) (fig. SP1).

Table 3. Mean values and standard deviations (SD) of environmental variables and phytoplankton group biomass (µg Chla l^{-1}) in the upper mixed layer of the stations in the different sampling areas during 2006-2008. Sea surface temperature (SST), water column stratification degree (strat. deg.), mixed layer depth (MLD), nitracline depth (nitracline), nitrate+nitrite (NOx), phosphate (PO_4), dissolved silicic acid (dSi), ratio of NOx to PO_4 (N:P), ratio of dSi to NOx (dSi:N), transparent exopolymer particles (TEP), chlorophyll *a* (Chla).

	June 2006				May 2007						May 2008					
	La Chapelle & Meriadzek				La Chapelle & Meriadzek				Goban spur		La Chapelle & Meriadzek				Goban spur	
	slope		shelf		slope		shelf		shelf		slope		shelf		shelf	
	mean	SD	mean	SD	mean	SD	mean	SD	mean	SD	mean	SD	mean	SD	mean	SD
SST (°C)	13.85	1.07	13.94	0.68	13.34	0.07	13.22	0.16	12.65	0.34	13.03	1.07	13.04	0.33	13.26	0.36
strat. deg. (kg m^{-3})	0.41	0.19	0.55	0.17	0.18	0.09	0.27	0.03	0.35	0.04	0.23	0.23	0.30	0.05	0.44	0.10
MLD (m)	26	13	25	7	45	13	38	5	39	3	53	42	24	11	21	7
nitracline (m)	4	6	30	5	13	19	18	16	26	23	9	16	24	7	33	13
NOx (µmol l^{-1})	1.53	0.86	0.26	0.27	1.35	1.19	0.87	0.41	0.79	0.37	2.32	2.00	0.58	0.74	0.22	0.04
PO_4 (µmol l^{-1})	0.12	0.06	0.04	0.07	0.12	0.04	0.08	0.02	0.07	0.01	0.20	0.12	0.08	0.04	0.03	0.01
dSi (µmol l^{-1})	1.01	0.61	0.73	0.51	0.69	0.72	0.63	0.76	0.48	0.29	0.80	0.67	0.46	0.33	0.12	0.09
N:P	12.36	1.84	6.05	5.12	10.10	6.77	12.09	7.39	11.42	4.35	9.69	5.40	5.48	4.42	10.42	10.16
dSi:N	0.70	0.21	6.36	5.39	0.45	0.14	0.57	0.47	0.81	0.70	0.30	0.13	1.70	2.22	0.56	0.41
TEP (µg X eq. l^{-1})	1101	597	520	538	138	158	23	15	22	11	38	33	49	21	67	26
Chla (µg l^{-1})	1.44	0.46	0.90	0.34	0.59	0.00	0.46	0.10	0.57	0.37	0.39	0.14	0.68	0.60	0.68	0.41
diatom	0.11	0.12	0.39	0.25	0.05	0.06	0.22	0.13	0.05	0.07	0.12	0.03	0.08	0.08	0.13	0.14
dinoflagellate	0.15	0.07	0.04	0.03	0.03	0.01	0.04	0.04	0.03	0.02	0.04	0.01	0.08	0.04	0.07	0.08
coccolithophore	0.86	0.34	0.17	0.17	0.24	0.12	0.07	0.11	0.20	0.08	0.13	0.11	0.25	0.31	0.27	0.29
chrysophyte	0.10	0.02	0.07	0.03	0.07	0.05	0.02	0.01	0.03	0.03	0.02	0.00	0.05	0.04	0.06	0.05
prasinophyte	0.14	0.09	0.15	0.07	0.05	0.02	0.03	0.05	0.15	0.08	0.02	0.01	0.09	0.09	0.05	0.05
cryptophyte	0.03	0.02	0.10	0.08	0.09	0.11	0.05	0.08	0.07	0.09	0.04	0.02	0.13	0.08	0.08	0.06
Synechococcus	0.03	0.01	0.01	0.00	0.07	0.01	0.03	0.03	0.04	0.03	0.01	0.01	0.01	0.00	0.01	0.00

Nitracline depth was significantly negatively related to bottom depth (table 6). In general, there was a sharpening of the thermocline of stations revisited during the second leg (fig. SP1). The increase in stratification for stations 6-1 and 6-4 when revisited one week later is very pronounced, as is the increase in nutrient levels in station 8-5 (fig. SP1). Stations visited in 2007 were much more homogeneous in terms of nutrient levels and stratification degree than those visited in 2006 and 2008 (fig. SP1).

Phytoplankton community composition and standing stocks

Chla depth maxima occurred around the nitracline or at the surface in stations having a deeper mixed layer (fig. SP1). Most Chla was always present in the upper 40 m (0.72 ± 0.49 µg l^{-1}), with negligible Chla levels measured at 80 m (0.16 ± 0.19 µg l^{-1}). Areal Chla concentrations for each station showed significant inter-annual variation but no relation with the location of the stations on the shelf or the slope of the continental margin (fig. 3 and table SP4). Average areal Chla values per year were significantly higher in June 2006 (63.8 ± 26.5 mg Chla m^{-2}) than in May 2007 (27.9 ± 8.4 mg Chla m^{-2}) and May 2008 (41.3 ± 21.8 mg Chla m^{-2}) (pairwise tests: p(2007)=0.044 and p(2008)<0.001) (table SP5).

Coccolithophores and diatoms were on average the most dominant groups throughout the study period and could constitute up to 72% respectively 89% of total phytoplankton biomass (Chla) (table 4). Pigment concentrations at the depth of Chla maximum are provided in table SP3. Microscopic observations by SEM confirmed that coccolithophores were mainly represented by the coccolithophore *Emiliania huxleyi* (fig. 3).

Table 4. Mean values and standard deviations of the relative and absolute (Chla) abundance of phytoplankton groups at the depth of Chla maximum as estimated by the CHEMTAX routine.

phytoplankton group	relative abundance			abundance (µg Chla l^{-1})		
	max	mean	SD	max	mean	SD
diatoms	0.89	0.29	0.27	1.08	0.30	0.31
dinoflagellates	0.69	0.09	0.09	0.36	0.07	0.07
coccolithophores	0.72	0.30	0.20	1.57	0.32	0.37
chrysophytes	0.20	0.07	0.04	0.18	0.07	0.05
prasinophytes	0.46	0.11	0.09	0.38	0.11	0.10
cryptophytes	0.60	0.12	0.12	0.72	0.10	0.14
Synechococcus	0.32	0.03	0.05	0.16	0.03	0.05

Fig. 3. SEM micrographs of *Emiliania huxleyi* coccospheres and coccoliths in surface waters of station (a) 8-5, (b) 8-5b, (c) 8-9b, (d) 8-12, illustrating the coccolithphorid bloom development.

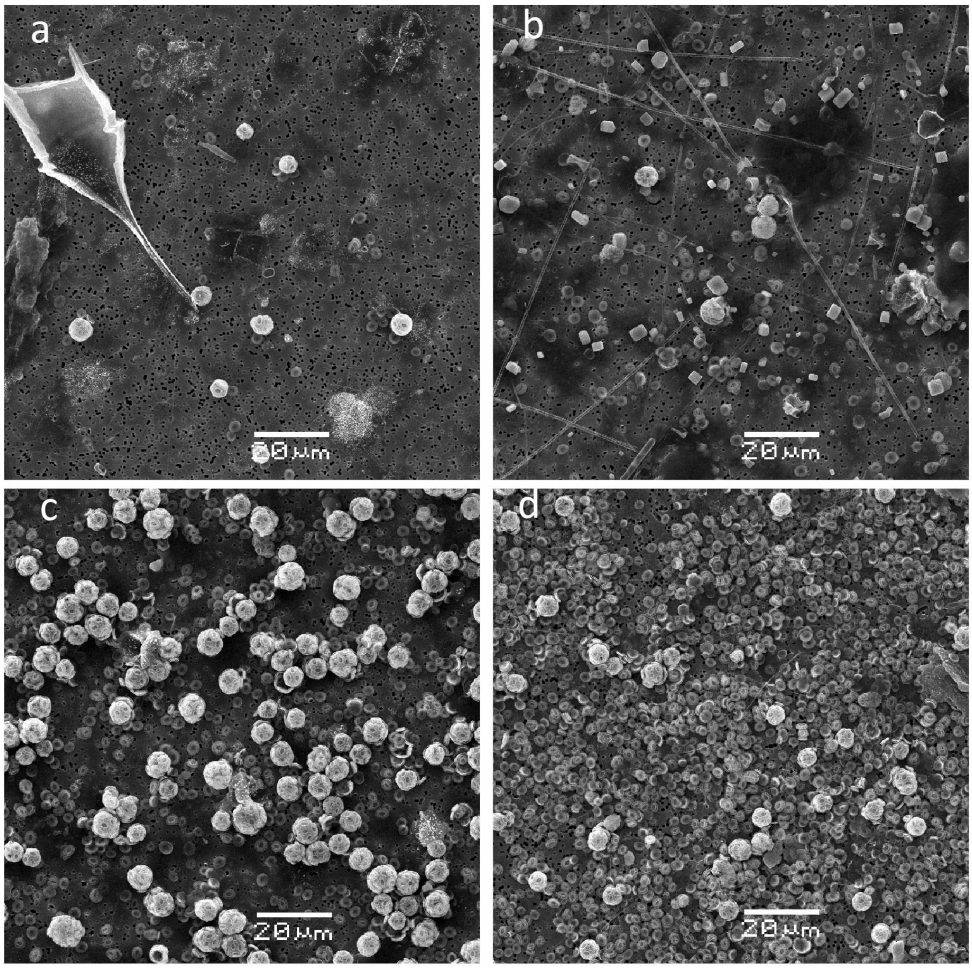

In June 2006, Chla concentrations ≥ 1.32 µg l-1 were measured at the Chla maximum depth, except at stations 8 and 1b where lower maximal Chla concentrations were measured (< 0.85 µg l-1). The range of maximal Chla concentrations and areal Chla concentrations per station was quite wide (0.61 – 2.31 µg l-1 and 35.2 – 114.0 mg Chla m-2). Stations 1, 2, 3, and 6 had the highest areal Chla levels and coccolithophore biomass compared to stations 4, 7, and 4b where the areal Chla levels were lower and diatoms were dominant (fig. 4a).

In May 2007, Chla concentrations ≤ 0.92 µg l^{-1} were measured at the Chla maximum depth, except at station 11 (1.36 µg l^{-1}). The range of maximal Chla concentrations per station was limited (0.36 – 1.36 µg l^{-1}); areal Chla concentrations were generally low (17.2 – 38.6 mg Chla m^{-2}). Stations 5, 8, 5b, and 8b were dominated by diatoms, while at stations 2, 4, 7 and 9 coccolithophores were dominant. Station 2b was dominated by dinoflagellates, while

stations 10, and 11 were populated by a mix of coccolithophores, prasinophytes and cryptophytes (fig. 4b).

Fig. 3. Areal Chla concentrations (upper 80 m of the water column) partitioned by CHEMTAX among the dominant phytoplankton groups identified for the stations visited in (a) June 2006, (b) May 2007, and (c) May 2008. The Chla concentration at the depth of maximum Chla concentration at each station is indicated by a cross. Stations are ordered chronologically and asterisks denote those located at the slope of the continental shelf.

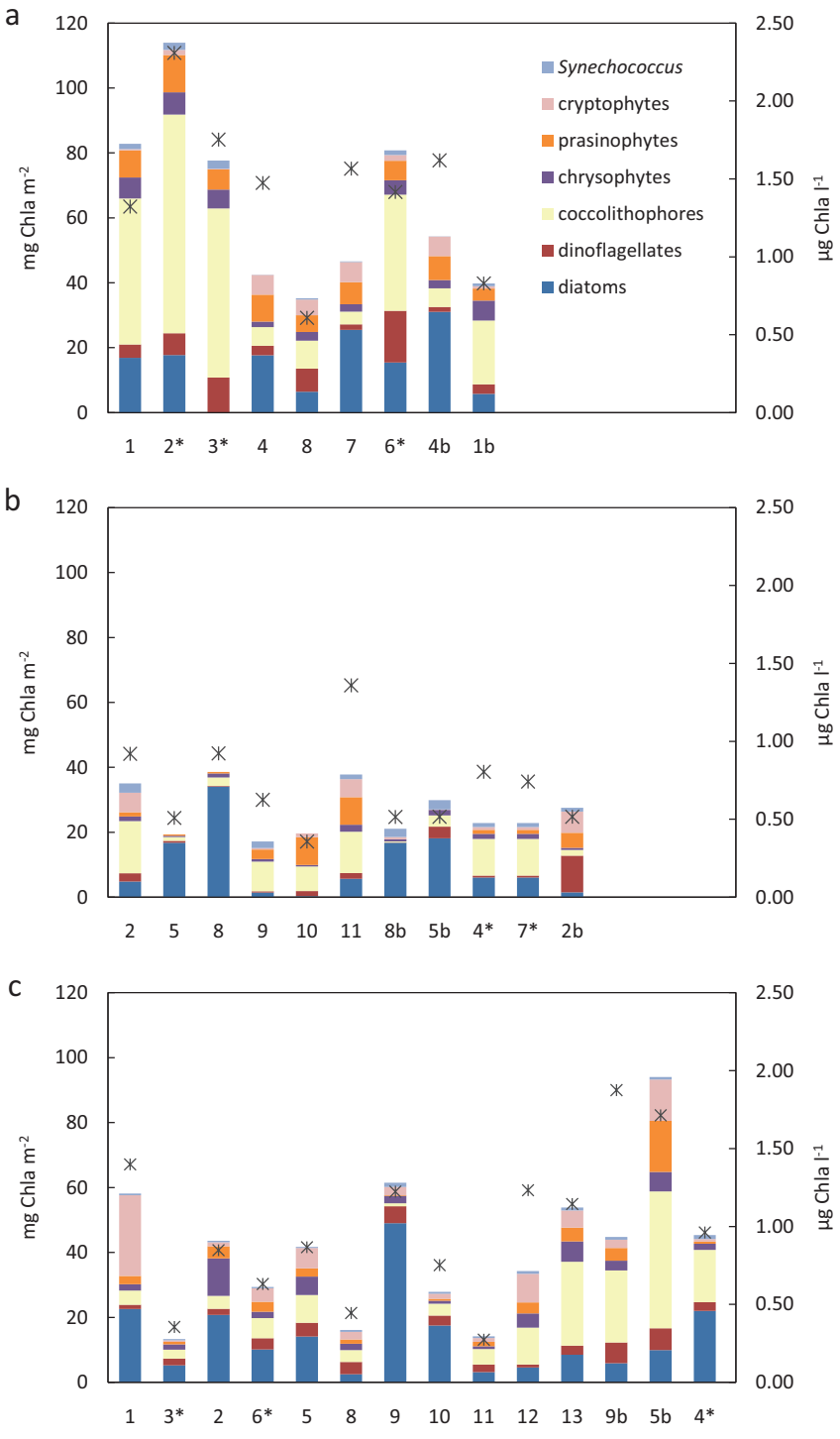

In May 2008, a wide range of maximal Chla concentrations was measured (0.27 – 1.88 µg l^{-1}), with stations 9b, 5b, 1, 12, 9, 13, and 4 having the highest concentrations (≥ 0.96 µg l^{-1}). Likewise, the areal Chla concentration per station varied greatly (range: 13.3 – 94.0 mg Chla m^{-2}). The phytoplankton community at stations 2, 4, 9 and 10 was dominated by diatoms while at stations 12, 13, 9b and 5b coccolithophores were dominant. Stations 3, 5, 6, 8 and 11 had lower areal Chla concentrations and a more heterogeneous community composition, while station 1 had a high prevalence of cryptophytes and diatoms (fig. 4c).

Phytoplankton community and environmental variables

PCO of the phytoplankton biomass data (only upper mixed layer samples, including the depth of the Chla maximum, n=93) captured 67 % of the total variation in the phytoplankton community along the first two axes (fig. 5). The first principal coordinate axis represents a gradient from low to high biomass of all phytoplankton groups. Diatom biomass varies independently from the other phytoplankton groups (except for a significant negative correlation with *Synechococcus*, data not shown) along the second PCO axis. Samples from the 2006 campaign, and to a lesser degree those of the 2008 campaign, are characterized by higher Chla values, while most 2007 samples (with low biomass values) are located in the lower left part of the diagram (see also fig. 4b). Only Chla and (to a lesser degree) TEP concentrations are positively correlated to both axes. Nutrient concentrations (NOx, PO_4, dSi) and the ratios of dSi:N and N:P are not correlated to the first two axes (table 5). Note that stratification degree of the water column, the depth of the nitracline, MLD and bottom depth (reflecting the slope versus shelf divide) are not correlated to these PCO axes, nor to any of the phytoplankton groups (except a slightly negative correlation between dinoflagellates and nitracline depth, table 5). TEP concentration, on the other hand, was positively correlated to Chla and the biomass of coccolithophores, chrysophytes, prasinophytes and dinoflagellates, (but not to diatom biomass) and to the stratification degree of the water column (tables 5 and 6). Diatom abundance was negatively correlated to concentration of NOx and the N:P ratio (table 5).

Table 5. Spearman rank correlation coefficients between the absolute biomass of the phytoplankton groups, the first two principal coordinates axes (fig. 9), and environmental variables for all samples of the upper mixed layer. Only significant correlation coefficients are shown; those > |0.40| are highlighted in bold; '-' denotes non-significant.

	PCA1	PCA2	SST	MLD	strat. deg.	nitracline depth	bottom depth	PO4	NOx	dSi	N:P	dSi:N	Chla	TEP	PIC	POC	PN	PIC:POC	POC:PN
PCA1			-	-	-	-	-	-	-	-	-	-	**0.55**	0.32					
PCA2			-	-	-	-	-	-	-	-	-	-	**0.71**	0.26					
Diatoms	**-0.64**	**0.73**	-	-	-	-	-	-	-0.23	-	-0.20	-	**0.41**	-	-	0.24	-	-	0.24
Dinoflagellates	**0.54**	-	-	-	-	-0.21	-	-	-	-	-	-	**0.41**	0.32	-	-	-	-	-
Coccolithophores	**0.75**	0.34	-	-	-	-	-	-	-	-	-	-	**0.64**	0.36	-	-	-	-	-
Chrysophytes	**0.58**	**0.59**	-	-	-	-	-	-	-	0.25	-	0.28	**0.77**	**0.50**	-	0.27	0.24	-	-
Prasinophytes	**0.58**	**0.44**	-	-	-	-	-	-	-	0.39	-	**0.40**	**0.65**	**0.43**	-	-	-	-	-
Cryptophytes	**0.48**	-	-	-	-	-	-	-	-	0.28	-	0.38	**0.44**	-	-	-	-	-	-
Synechococcus	**0.41**	-	-	-	-	-	-	0.21	0.24	-	-	-	0.28	-	-	-	-	-	-
n samples	93	93	93	93	93	93	93	93	93	93	93	93	93	93	76	76	76	76	76

Table 6. Spearman rank correlation coefficients between the environmental variables (fig. 8) for all samples of the upper mixed layer. Only significant correlation coefficients are shown; those > |0.40| are highlighted in bold; '-' denotes non-significant.

	SST	MLD	strat. deg.	nitracline depth	bottom depth	PO4	NOx	dSi	N:P	dSi:N	chla	TEP	PIC	POC	PN	PIC:POC
MLD	-															
strat. deg.	**0.55**	-0.33														
nitracline depth	-	-0.20	**0.57**													
bottom depth	-	-	-0.26	**-0.50**												
PO4	**-0.51**	0.26	**-0.44**	**-0.49**	**0.49**											
NOx	**-0.51**	**0.42**	**-0.47**	**-0.62**	**0.41**	**0.83**										
dSi	-	0.26	-0.28	**-0.46**	0.39	0.31	**0.40**									
N:P	-0.26	0.39	-0.30	**-0.59**	0.22	0.35	**0.77**	0.29								
dSi:N	0.27	-	-	-	-	**-0.51**	**-0.55**	**0.47**	**-0.42**							
Chla	-	-	-	-	-	-	-	0.23	-	0.21						
TEP	**0.48**	-0.33	0.39	-	0.23	-0.28	-0.30	-	-	0.35	**0.42**					
PIC	-	-	-	-	-	-	-	-	-	-	-	-				
POC	0.34	0.26	-	-	-	-	-	-	-	-	0.34	-	-0.37	-		
PN	-	0.26	-	-	-	-	-	-	-	-	-	-	-	**0.68**		
PIC:POC	-	-	-	-	-	-	-	-	-	-	-	-	**0.96**	**-0.55**	-0.30	
POC:PN	-	-	-	-	-	-0.25	-	0.26	-	**0.49**	-	-	-	-	**-0.57**	-

In order to assess the relation between selected environmental variables and blooms of specific phytoplankton groups in the study we used the proportions of phytoplankton groups biomass values of upper mixed layer samples, having Chla concentrations above the median Chla concentration (n=44, > 0.66 µg Chla l^{-1}). Higher N:P ratios were associated with coccolithophore blooms, while higher dSi:N ratios were typical for the diatom-dominated samples (table 7).

Table 7. Spearman rank correlations between the relative biomass values of phytoplankton groups and ratios of dissolved nutrient concentrations and particulate material concentrations for all samples with an above-median Chla concentration. Only significant correlation coefficients are shown; those > |0.40| are highlighted in bold; '-' denotes non-significant.

	N:P	dSi:N	PIC:POC	POC:PN
Diatoms	-0.31	**0.48**	-	**0.55**
Dinoflagellates	0.31	**-0.60**	-	**-0.57**
Coccolithophores	0.38	**-0.50**	-	-0.40
Chrysophytes	-	-	-	-
Prasinophytes	-	**0.59**	-	0.36
Cryptophytes	-	0.34	-0.39	-
Synechococcus	**0.48**	**-0.44**	-	-
n samples	44	44	32	32

Particulate matter distribution

Particulate organic carbon (POC) and particulate nitrogen (PN) showed higher concentrations above the thermocline than at 80 m depth (fig. SP2). In the upper 80 m of the water column POC concentrations varied from 1.1 to 24.6 µmol l^{-1} in 2006, from 1.8 to 22.9 µmol l^{-1} in 2007, and from 0.7 to 17.9 µmol l^{-1} in 2008. PN concentrations varied from 0.2 to 1.8 µmol l^{-1} in 2006, from 0.1 to 3.8 µmol l^{-1} in 2007, and from 0.2 to 3.4 µmol l^{-1} in 2008. POC and PN were significantly correlated during each campaign (2006: r=0.83, n=38; 2007: r=0.78, n=40; 2008: r=0.82, n=67, all at $p<0.05$), with the average C:N molar ratio either being above the Redfield ratio (C:N=6.6) in 2006 (9.21) and 2007 (7.01) or slightly below this ratio during the 2008 campaign (5.21), implying particulate organic matter was enriched in carbon in 2006 (cf. Harlay *et al.* 2009).

Fig. 8. PCO plot of phytoplankton biomass data for the samples from the upper mixed layer (2006: red dots, 2007: blue dots, 2008: green dots). The size of each dot is relative to the Chla concentration. Environmental variables which are significantly correlated with at least one of the PCO axes are shown in the lower left part of the diagram; the other variables are shown in grey. Percentages refer to the percentage variance explained in the species data by the PCO axes.

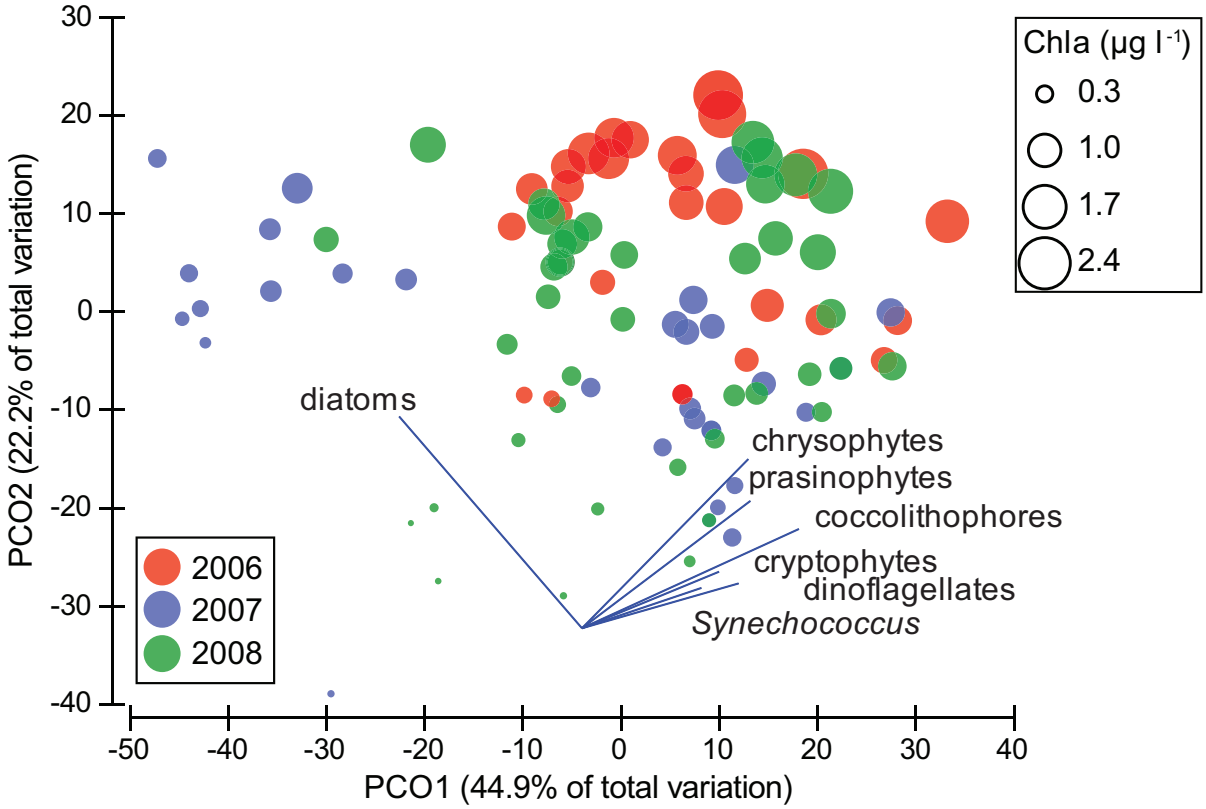

In contrast to POC, PIC concentrations were not always higher at surface. PIC concentrations varied from 0.3 to 10.6 µmol l^{-1} in 2006, from 0.2 to 16.1 µmol l^{-1} in 2007, and from undetectable to 12.4 µmol l^{-1} in 2008 (fig. SP2). Interestingly, PIC had accumulated below the thermocline at certain stations (6-4, 6-4b, 6-7, 6-8, 7-2b, 7-4, 7-5, 8-9, 8-10), indicative of prior coccolithophorid calcification (figs. SP1 and SP2). PIC and POC were not correlated to each other within campaigns, and the average PIC:POC ratio was similar during each campaign (2006: 0.63; 2007: 0.56; 2008: 0.60).

TEP concentration generally decreased with increasing depth (upper mixed layer: 231 ± 425 µg X eq. l^{-1}; 80 m: 52 ± 62 µg X eq. l^{-1}) (see also Harlay 2009). Maximum TEP concentrations at each station ranged from 414 (station 1) to 3199 µg X eq. l^{-1} (station 2) during the June

2006 campaign, from 14 (station 2) to 269 µg X eq. l^{-1} (station 7) in 2007, and from 19 (station 1) to 132 µg X eq. l^{-1} (station 9) in 2008. TEP concentrations were higher at the LC and M shelf stations during 2006 than during 2007 and 2008 (table 3).

Discussion

We studied the dynamics of phytoplankton standing stocks and community structure during late spring coccolithophore blooms at the continental margin of the northern Bay of Biscay over a period of 3 years (2006-2008). We related the spatial and temporal development of these blooms to a suite of physical, geochemical and biological variables in order to identify the main environmental conditions driving the wax and wane of these blooms, and to discuss the potential importance of phytoplankton community composition on the carbon balance and export in this area.

Environmental setting of the blooms and phytoplankton standing stocks during late spring

Our data show that late spring nutrient concentrations in the study area are indeed largely depleted and that surface Chla concentrations are typically lower than those reported during the main diatom spring bloom event (e.g. for the La Chapelle area: SeaWiFS weekly averaged Chla concentration 2006-2008: 15 April – 1 May: 1.80 ± 0.54 µg Chla l^{-1}; SeaWiFS campaign periods: 0.89 ± 0.17 µg Chla l^{-1}). The observed range in surface Chla (0.27 – 2.31 µg Chla l^{-1} at Chla maximum) is within the ranges reported in other studies of the NE Atlantic (Gibb *et al.*, 2001; Leblanc *et al.*, 2009; Painter *et al.*, 2010a) or the Bay of Biscay and the Celtic Sea for a similar period as our campaigns (Joint 1986; Rees 1999; Joint 2001; Lampert 2002). There was considerable variation in phytoplankton areal biomass between campaigns (fig. 4). Chla levels were generally distinctly lower in 2007 than in 2006 and 2008. The first leg of the 2007 campaign was characterized by storms with high wind speeds; this resulted in a pronounced deepening of the upper mixed layer (40 ± 6 m vs < 10 m in April, see (Thyssen *et al.*, 2009)) and thus partial dilution of the plankton biomass in waters which were already largely depleted of nutrients after the April blooms. Chla levels were also lower in many stations during the 2008 campaigns, most probably owing to overcast skies during the first two weeks of the campaigns, which may have slowed down bloom development. The higher phytoplankton biomass (Chla) in June 2006 compared to the 2007 and 2008 campaigns may have been produced thanks to partial replenishment of depleted nutrient stocks due to a

mixing event prior to the campaign, while phytoplankton growth would probably have been favoured by prevailing high irradiance levels and SST during the 2006 campaign. This mixing event is apparent from the deepening of the MLD and a drop in SST as described by Harlay *et al.* (2011) using modelled data by Met Office National Centre for Ocean Forecasting for the North-East Atlantic.

We observed pronounced spatial and temporal variation in areal Chla levels during each campaign, which can not readily be explained by linear relations with measured environmental variables (cf. fig. SP2, table 6). Given the enhanced vertical mixing and associated nutrient fluxes associated with the shelf edge, an increase in areal Chla biomass associated with this specific area could be expected. However, despite a significantly shallower nitracline, and significantly higher inorganic N and P levels in the UML of the slope stations (fig. SP1, tables 3 and 6), we did not find differences in areal Chla between the shelf and the slope stations (cf. Sharples *et al.*, 2009). This is most probably due to complex interplay between the dynamics of internal tidal mixing and hence vertical nutrient fluxes, mixed layer shoaling (which is significantly higher on the shelf than the slope, table 6), meteorological conditions, together with other loss factors, such as herbivory, viral lysis, enhanced export through aggregation, which determine the wax and wane of phytoplankton blooms but which were not quantified for most stations during our campaigns (but see chapter 5 (Van Oostende *et al.*, *in prep. b*)). In addition, changes in water circulation patterns and seasonal convective mixing intensity, influenced by meteorological conditions (Follows and Dutkiewicz, 2002; Henson *et al.*, 2006), will also impact on horizontal heterogeneity in phytoplankton standing stocks.

Phytoplankton community structure

During the study period, phytoplankton communities in the study area were dominated by diatoms and/or coccolithophores, with prasinophytes, cryptophytes and dinoflagellates as codominants. In 2006, the diatom community was mainly represented by the genera *Rhizosolenia*, *Bacteriastrum*, *Thalassiosira*, *Thalassionema*, *Chaetoceros* and *Pseudo-nitzschia*. Some of these diatom genera have been reported to make up the spring phytoplankton bloom community at the Goban Spur area in April (Rees 1999). *E. huxleyi* was the most dominant coccolithophore (fig. 3), but other taxa were observed as well (*Syracosphaera* spp. and *Gephyrocapsa oceanica*). The genera *Protoperidinium*, *Dinophysis*,

Ceratium, *Gymnodinium* and *Gyrodinium* were common dinoflagellate representatives. Molecular data (see chapter 4, (Van Oostende *et al.*, *in prep. c*)) showed that *Micromonas pusilla* was an abundant member of the prasinophytes. Chrysophytes and *Synechoccocus* were never dominant during the study period.

Our observations agree with the general scenario for phytoplankton bloom development in the NE Atlantic outlined by Leblanc *et al.* (2009, and references therein), with early spring diatom blooms being replaced by dominance of coccolithophores, most probably as a result of mixed layer shoaling and depleted dSi levels (Boyd *et al.*, 2010). They also confirm previous reports (Barlow *et al.*, 1993; Gibb *et al.*, 2001; Joint *et al.*, 2001; Barlow *et al.*, 2002; Dandonneau *et al.*, 2006; Leblanc *et al.*, 2009) which show that the late spring blooms in the NE Atlantic are composed of mixed assemblages, dominated by diatoms and coccolithophores, but also with important contributions of prasinophytes, dinoflagellates and chrysophytes (such as silicoflagellates, cf. Lampert *et al.* (2002)). The average diatom and coccolithophore biomass concentration in the UML for all the stations did not differ much (table 4), showing that despite the low dSi levels, diatoms can be important components of the late spring blooms. This is in agreement with Barlow *et al.* (Barlow *et al.*, 1993) who found that diatoms could constitute between 23-70% of the Chla biomass in early May at 47°N in the NE Atlantic, yet when dSi concentrations were still 2 µmol l^{-1}, higher than the maximum in the UML in our study. In general, the location of the station on the slope or the shelf side did not affect the composition of phytoplankton blooms or their magnitude, as indicated by the lack of correlation between the principal coordinates axes and the bottom depth, a proxy for shelf-slope separation (fig. 5 and table 5).

Ordination and correlation analyses (fig. SP2, tables 5 and 6) show that during the study period blooms (defined here as above median Chla values) can be associated with both high diatom and high coccolithophore biomass, and that bloom development in these groups is independent of each other, in other words there is no negative correlation between diatom and coccolithophore biomass. The occurrence of the other, sometimes co-dominant phytoplankton groups is always significantly associated with coccolithophore blooms, never with diatoms. An anti-correlation between the biomass of phytoplankton groups would be expected when competitive exclusion takes place in a stable environment where the level or the stoichiometry of limiting resources such as nutrients favours the physiologically more

adapted group. In a steady-state scenario where nutrient levels are low coccolithophore would be favoured by virtue of their lower half-saturation constants for nutrient uptake and small intracellular quotas (Tozzi *et al.*, 2004). While the relative importance of coccolithophores and associated taxa versus diatoms during blooms is significantly related to nutrient ratios (higher N:P and low dSi:N values for coccolithophores, dinoflagellates and *Synechococcus*, and the opposite for diatoms, table 7), the N:P ratio *per se* does not seem to determine absolute biomass development, and hence the magnitude of the blooms (cf. also above). Our results are in general agreement with other studies investigating the conditions conducive to coccolithophore bloom development, such as a low dSi:N ratio, shallow mixed layer depth, and increased irradiances (Brown and Yoder, 1994; Painter *et al.*, 2010b). An increasing proportion of coccolithophore biomass was associated to higher N:P ratios, even though these ratios were not very high (table 3). The support for phosphate limitation (high inorganic N:P ratios) for allowing coccolithophores to blooms is not equivocal as discussed by Lessard *et al.* (2005), who demonstrated that this was not a necessary condition (but compare with e.g. Tyrrell and Taylor (1996)). Although *E. huxleyi* may be well-adapted to grow in low nutrient conditions, as it has been shown to have very high affinity for phosphate, the ability to use organic nitrogen sources such as amino acids, purines, amines, and urea, and can access dissolved organic phosphorus as well, using alkaline phosphatase (Palenik and Henson, 1997; Riegman *et al.*, 2000; Benner and Passow, 2010). It is not unlikely that conflicting results regarding the necessary nutrient conditions may have been related to the high physiological and genetic variability between *E. huxleyi* strains, as has been shown for e.g. nitrogen use (Strom and Bright, 2009).

The occurrence of diatom blooms during the campaigns is more surprising. The low levels of dSi encountered during the campaigns (from 0.03 µmol l^{-1} to 1.95 µmol l^{-1}) were probably the result of prior consumption by diatoms and thus did not favour further diatom growth to earlier spring bloom levels (Egge and Aksnes, 1992). While this may have led to the competitive advantage of coccolithophores and nanoplanktonic flagellates, it does appear to allow more lightly silicified diatoms such as *Rhizosolenia* spp. to grow. Furthermore, the low surface NOx levels at many stations may have actually favoured the appearance of diatom species which harbour diazotrophic symbionts, such as *Rhizosolenia* spp. and *Chaetoceros* spp. (Gomez *et al.*, 2005; Bar Zeev *et al.*, 2008). In that case their growth would have been

limited by low PO_4 and dSi concentrations rather than NOx, or possibly the availability of trace metals such as iron (Boyd *et al.*, 2010), for which coccolithophores, on the other hand, were shown to have low requirements and high affinity (Sunda and Huntsman, 1995; Muggli and Harrison, 1996b). However, diatoms have been shown to outcompete e.g. coccolithophores in a situation where intermittent nutrient pulses are provided, such as is the case at the shelf break, thanks to their higher maximum nutrient uptake rates and storage capabilities potentially allowing them to sustain higher growth rates for several generations (Litchman *et al.*, 2007; Cermeño *et al.*, 2011). Our data also show that the generally accepted diatom-to-coccolithophore succession scenario (Joint et al 1986; Leblanc et al. 2009) is not universal, and that diatom and coccolithophore growth can alternate in the same area and during the same period. This is further corroborated by the presence of surface diatom-dominated blooms at stations where PIC had accumulated below the thermocline, reminiscent of prior coccolithophorid calcification (figs. 4, SP1 and SP2).

Thermal stratification of the water column and bloom progression

As outlined above, stratification of the water column was not linearly related to biomass of any of the phytoplankton groups during the sampling period. However, figure 9 shows that this is largely due to the fact that biomass of total phytoplankton and the two most dominant groups, coccolithophores and diatoms, displays a unimodal-like relationship with stratification: highest biomass values are encountered at intermediate stratification (± 0.4 kg m^{-3}), although variation here can be high. Our data generally confirm the conceptual frame for phytoplankton bloom development and decline at the continental margin of the northern Bay of Biscay proposed by Harlay et al. (2011) on the basis of the 2006 data. Enhanced vertical mixing along the shelf edge (most probably as a result of internal tides) lead to elevated inorganic nutrient levels (N, P, dSi) and lower nitracline depth trigger mixed phytoplankton blooms, dominated by coccolithophores and/or diatoms. As the water masses are advected over the shelf, they become more stratified and as a result of phytoplankton growth, nutrients are depleted (table 6).

Implications of phytoplankton community structure for carbon export

Phytoplankton community structure has been shown to have an important impact on the fate of carbon in the ocean. Larger and heavier cells (> 10 µm) like diatoms sink faster and may enhance the vertical transport of carbon (Michaels and Silver, 1988; Guidi *et al.*, 2009),

while they are also more efficiently grazed upon by larger zooplankton, such as copepods. Nanoplankton cells, such as coccolithophores, are thought to be more likely recycled in the microbial food web in the UML and contribute less to vertical carbon export by sinking. However, as pointed out by Richardson and Jackson (2007), export efficiency of small plankton cells is likely greater than thought and can be enhanced by aggregation processes which could act as trophic elevators. Moreover, recent experiments comparing the effect of incorporation of biogenic minerals from different sources into marine aggregates on their decomposition and sinking velocities have shown that ballasting by carbonate increased sinking velocities and reduced respiration rate compared to aggregates ballasted by opal (Iversen and Ploug, 2010). Leblanc *et al.* (2009) suggested sedimentation of diatoms in the form of aggregates based on the correspondence between TEP and biogenic silica at depth, while they also observed TEP associated to prymnesiophytes in the surface layer. They concluded that the relative contribution of diatoms and coccolithophores to carbon export in the North East Atlantic was still unresolved.

During our study, TEP concentrations appeared to be significantly correlated with coccolithophore and total phytoplankton biomass but not with diatoms (fig. 5 and tables 5 and 6). TEP levels were highest when water column stratification was highest and nutrients depleted (fig. 7 and table 6). This was typically the case in June 2006 when we investigated the coccolithophorid blooms during their transition between growth and decline (Harlay *et al.*, 2009), even though negative correlations between water column stratification and TEP concentration, determined using microscopy, within individual campaigns may reflect processes such as aggregation or other loss processes (Harlay *et al.*, 2011). Piontek et al. (submitted) found significantly higher dissolved polysaccharide concentrations during the June 2006 campaign compared to May 2007, possibly pointing to their accumulation in surface waters due to exudation by phytoplankton and slow degradation by bacteria when nutrients are depleted. Coccolithophores and *E. huxleyi* in particular have been shown to potentially produce large amounts of TEP (Engel *et al.*, 2004b; Harlay *et al.*, 2009) as have diatoms in diatom-dominated communities (Passow *et al.*, 2001; Passow, 2002a). The release of TEP precursors has been shown to occur in conditions of unbalanced growth of phytoplankton, when the cells excrete carbon rich material such as polysaccharides into the surrounding water due to lack of nutrients necessary for cell growth (Wood and Van Valen,

1990; Myklestad, 1995; Schartau *et al.*, 2007). Accumulation of these precursors and their subsequent aggregation are responsible for the formation of TEP (Zhou *et al.*, 1998; Passow, 2002b). The production of coccoliths in itself may constitute a direct source of TEP, as discussed in chapter 6 (Van Oostende *et al.*, *in prep. e*).

Fig. 7. Scatter plots showing the relationship between the degree of water column stratification and average Chla concentration of the total phytoplankton community, the diatoms, and the coccolithophores, and the log-transformed concentration of TEP in the upper mixed-layer. The symbols of the year during which the sample were taken are colour-coded (2006: red, 2007: blue, 2008: green). Full and empty symbols represent samples taken, respectively, at the shelf and slope side of the continental margin.

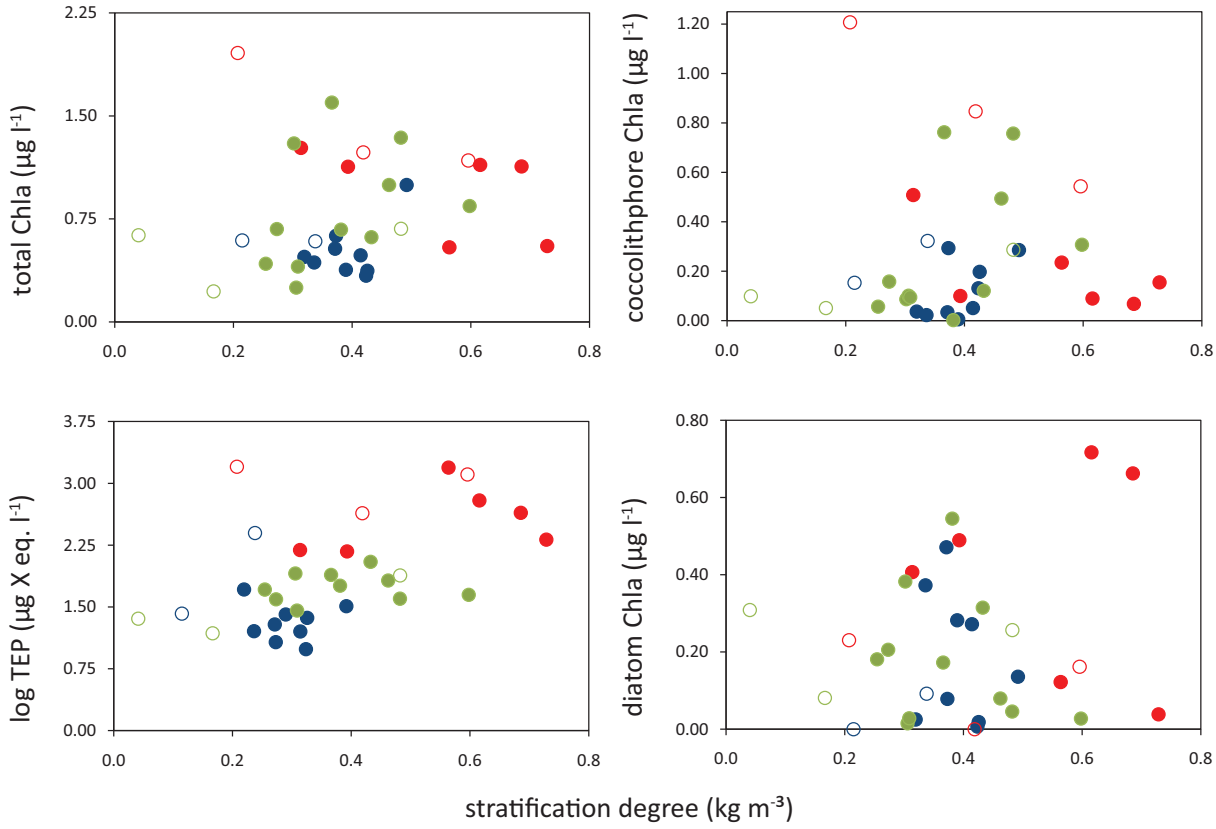

The presence of coccolithophore biomass was always associated to at least some PIC, minimizing the presence of haploid non-calcifying *E. huxleyi* cells or other non-calcifiying prymnesiophytes such as *Phaeocystis* sp. in our study. Even though we observed good congruence between high reflectance patches from remote sensing images and coccolithophore biomass (fig. 2, 3, and 4, chapter 1, fig. 5) (Harlay *et al.*, 2009; Suykens *et*

al., 2010), the lack of correlation between PIC and coccolithophore Chla biomass (table 5) emphasizes the temporal and spatial (vertical) decoupling between the accumulation of biomass and the accumulation of coccoliths associated with cells or shed during the calcification phase of the bloom (fig. 3 and chapter 1, fig. 5) (Beaufort and Heussner, 1999). Therefore, as reported before (Leblanc *et al.*, 2009), PIC concentration is probably not a good indicator of *in situ* coccolithphore biomass but rather is an accumulative signal of prior calcification activity on short temporal time scale (much like total alkalinity anomaly compared to conservative mixing, but in the particulate form). This temporal decoupling is further complicated by TEP-mediated aggregation of coccoliths or their incorporation into faecal pellets after grazing, promoting the rapid disappearance of high reflectance remote sensing patches and potentially enhancing carbon export efficiency due to increased sinking velocity (De La Rocha and Passow, 2007; Harlay *et al.*, 2009; Iversen and Ploug, 2010).

Conclusions

Variation in bloom magnitude during and between our campaigns is ascribed to different conditions of temperature, irradiance, and wind-driven mixing of the surface layer during or preceding the campaigns. However, the high (sub-) mesoscale heterogeneity in phytoplankton bloom stage and composition during each campaign was probably caused by the interplay of enhanced vertical mixing caused by internal tide at the slope of the continental margin and the thermal stratification of the water masses during advection away from the continental slope.

The recurrent scenario emerging from previous studies is that diatoms dominate the main spring bloom event, sometimes co-occurring with prymnesiophytes or dinoflagellates, and tend to be outcompeted by prymnesiophytes during later stages of the spring bloom due to changing light and nutrient availability and possibly grazer control (Leblanc *et al.*, 2009; Painter *et al.*, 2010b). In this study high reflectance patches detected by remote sensing (chapter 1, fig. 5), phytoplankton pigment signatures (fig. 4 and table SP3), PIC levels (fig. SP2), and microscopic detection of coccospheres and coccoliths (fig. 3) confirm the importance and the recurrent nature of coccolithophorid blooms along the continental shelf break of the northern Bay of Biscay after the main spring bloom. These blooms were not monospecific even though coccolithophores could constitute more than two thirds of the

total phytoplankton biomass. The alternation between diatom and coccolithophorid blooms of magnitude following the main spring bloom was partly driven by changes in nutrient stoichiometry (N:P and dSi:N). However, selective loss processes such as grazing and viral lysis might also play a role in shaping the phytoplankton community but were not included in this study (see chapter 5, (Van Oostende *et al.*, *in prep. b*)). The location of the stations on the shelf or on the slope side of the continental margin did not influence the biomass and the composition of the phytoplankton community despite significantly stronger water column stratification and lower nutrient concentrations on the shelf. Furthermore, high TEP concentrations associated with nutrient-depleted, coccolithophore-rich water masses could facilitate the disappearance of the bloom and enhance the production export through aggregation and ballasting mechanisms. Thus, phytoplankton community structure and composition would not only affect the cell size distribution but also the carbon export efficiency. Further studies combining *in situ* measurements with high-resolution remote sensing images to differentiate phytoplankton groups (e.g. PHYSAT, see Alvain *et al.* (2008)) and the use of altimetry-derived Lagrangian diagnostics of the surface transport (d'Ovidio *et al.*, 2010) could greatly improve our understanding of phytoplankton bloom dynamics and its potential control on the biological carbon pump at areas of important biogeochemical cycling such as the continental margins.

Acknowledgments

The authors sincerely thank the officers and crew members of the R.V. Belgica for their logistic support during the campaigns. J. Backers, J.-P. De Blauw, and G. Deschepper of the Unit of the North Sea Mathematical Models (Brussels/Ostend, Belgium) are acknowledged for their support in data acquisition during the field campaigns. S. Groom is acknowledged for providing remote sensing images. We are grateful to C. Souffreau, A. De Wever, B. Vanelslander and D. De Bock for their assistance during sample collection and to F. Steen and N. Breine for performing the optical microscopy analyses. We thank I. Daveloose and R. Dasseville for help with the HPLC analyses, and N. Roevros for performing nutrient analyses. Finally, we are grateful to all members of the PEACE network for their support during the campaigns. This study was financed by Belgian Federal Science Policy Office in the framework of the PEACE project (contract numbers SD/CS/03A and SD/CS/03B). C. De Bodt was supported by a PhD grant from the EU FP6 IP CarboOcean project (contract no. 511176–2). N. Van Oostende received a PhD grant from the agency for Innovation by Science and Technology (IWT-Flanders).

Supplementary tables

Table SP1. Initial pigment ratios per taxonomic group used to partition Chla by CHEMTAX analysis.

Group/Pigment	$Chlc_3$	Per	But	Fuc	Hex	Pras	Viol	Allo	Zea	Chlb
diatoms	0.04	0	0	0.25	0	0	0	0	0	0
dinoflagellates	0	0.75	0	0	0	0	0	0	0	0
coccolithophores	0.18	0	0	0.21	0.74	0	0	0	0	0
chrysophytes	0.12	0	0.56	0.63	0	0	0	0	0	0
prasinophytes	0	0	0	0	0	0.2	0.08	0	0.07	0.67
cryptophytes	0	0	0	0	0	0	0	0.23	0	0
Synechococcus	0	0	0	0	0	0	0	0	0.78	0

Table SP2. Final average pigment ratios per taxonomic group used to partition chla by CHEMTAX analysis.

Group/Pigment	$Chlc_3$	Per	But	Fuc	Hex	Pras	Viol	Allo	Zea	Chlb
diatoms	0.06	0	0	0.35	0	0	0	0	0	0
dinoflagellates	0	0.42	0	0	0	0	0	0	0	0
coccolithophores	0.13	0	0	0.08	0.34	0	0	0	0	0
chrysophytes	0.05	0	0.23	0.30	0	0	0	0	0	0
prasinophytes	0	0	0	0	0	0.09	0.05	0	0.04	0.31
cryptophytes	0	0	0	0	0	0	0	0.14	0	0
Synechococcus	0	0	0	0	0	0	0	0	0.48	0

Table SP3. Pigment concentrations at the depth of Chla maximum in µg l^{-1}. Abbreviations of pigments as in table 2, chlorophyll *c1* and *c2* ($Chlc_{1+2}$), diadinoxanthin (Diad).

date	station	depth	$Chlc_3$	$Chlc_{1+2}$	Per	But	Fuc	Hex	Diad	Pras	Viol	Allo	Zea	Chlb	Chla
31/05/2006	6-1	3	0.02	0.02	0.02	0.06	0.22	0.45	0.08	0.01	0.00	0.00	0.02	0.12	1.32
1/06/2006	6-2	10	0.28	0.18	0.07	0.07	0.31	1.05	0.14	0.01	0.01	0.01	0.04	0.30	2.31
1/06/2006	6-3	20	0.25	0.15	0.21	0.09	0.19	0.89	0.08	0.01	0.01	0.00	0.05	0.16	1.75
2/06/2006	6-4	10	0.05	0.06	0.05	0.03	0.39	0.14	0.09	0.05	0.03	0.07	0.02	0.29	1.47
6/06/2006	6-8	20	0.03	0.04	0.16	0.03	0.08	0.16	0.03	0.02	0.01	0.02	0.01	0.07	0.61
7/06/2006	6-7	20	0.05	0.04	0.04	0.04	0.52	0.11	0.12	0.04	0.03	0.03	0.02	0.20	1.57
7/06/2006	6-6	40	0.16	0.14	0.31	0.05	0.37	0.62	0.11	0.01	0.01	0.01	0.03	0.18	1.42
8/06/2006	6-4b	20	0.10	0.09	0.06	0.04	0.68	0.11	0.09	0.03	0.02	0.03	0.01	0.27	1.62
9/06/2006	6-1b	40	0.07	0.04	0.04	0.11	0.13	0.41	0.03	0.00	0.00	0.00	0.02	0.10	0.83
11/05/2007	7-2	20	0.16	0.17	0.07	0.03	0.24	0.52	0.09	0.00	0.00	0.06	0.09	0.04	0.92
12/05/2007	7-5	5	0.09	0.13	0.03	0.01	0.40	0.04	0.07	0.00	0.01	0.00	0.00	0.02	0.51
13/05/2007	7-8	40	0.22	0.24	0.01	0.02	0.84	0.08	0.08	0.00	0.00	0.00	0.00	0.03	0.92
14/05/2007	7-9	5	0.12	0.14	0.02	0.02	0.14	0.42	0.15	0.04	0.02	0.01	0.14	0.10	0.63
15/05/2007	7-10	20	0.04	0.05	0.03	0.01	0.04	0.17	0.03	0.03	0.03	0.01	0.00	0.14	0.36
16/05/2007	7-11	5	0.15	0.31	0.07	0.07	0.35	0.50	0.11	0.08	0.05	0.10	0.12	0.34	1.36
21/05/2007	7-8b	5	0.12	0.14	0.02	0.02	0.55	0.04	0.19	0.00	0.00	0.00	0.34	0.00	0.51
22/05/2007	7-5b	5	0.09	0.11	0.08	0.03	0.31	0.08	0.14	0.00	0.00	0.00	0.21	0.00	0.52
23/05/2007	7-4	5	0.13	0.22	0.06	0.12	0.20	0.38	0.10	0.02	0.01	0.09	0.18	0.09	0.80
23/05/2007	7-7	5	0.22	0.27	0.03	0.03	0.34	0.53	0.28	0.01	0.01	0.01	0.19	0.04	0.74
24/05/2007	7-2b	5	0.04	0.09	0.06	0.01	0.10	0.07	0.06	0.05	0.04	0.09	0.00	0.13	0.52

Table SP3. continued

date	station	depth	$Chlc_3$	$Chlc_{1+2}$	Per	But	Fuc	Hex	Diad	Pras	Viol	Allo	Zea	Chlb	Chla
7/05/2008	8-1	20	0.09	0.19	0.02	0.02	0.35	0.05	0.05	0.01	0.00	0.12	0.01	0.03	1.40
7/05/2008	8-3	3	0.04	0.04	0.02	0.01	0.08	0.06	0.03	0.01	0.00	0.01	0.01	0.01	0.36
8/05/2008	8-2	20	0.13	0.09	0.04	0.05	0.39	0.08	0.04	0.03	0.01	0.01	0.02	0.09	0.85
9/05/2008	8-6	3	0.04	0.07	0.03	0.01	0.17	0.07	0.04	0.01	0.01	0.02	0.01	0.03	0.63
10/05/2008	8-5	40	0.09	0.08	0.05	0.02	0.28	0.07	0.02	0.00	0.00	0.02	0.00	0.02	0.87
11/05/2008	8-8	10	0.03	0.05	0.08	0.01	0.03	0.08	0.03	0.00	0.01	0.02	0.01	0.04	0.44
12/05/2008	8-9	20	0.13	0.16	0.07	0.02	0.75	0.02	0.09	0.00	0.01	0.01	0.05	0.00	1.22
13/05/2008	8-10	20	0.10	0.10	0.06	0.02	0.30	0.12	0.05	0.00	0.00	0.01	0.01	0.02	0.75
14/05/2008	8-11	30	0.02	0.03	0.04	0.01	0.03	0.08	0.02	0.02	0.01	0.01	0.01	0.04	0.27
19/05/2008	8-12b	20	0.16	0.17	0.02	0.09	0.24	0.37	0.06	0.02	0.01	0.05	0.01	0.08	1.23
20/05/2008	8-13b	20	0.16	0.16	0.04	0.07	0.21	0.39	0.09	0.01	0.01	0.02	0.01	0.06	1.14
21/05/2008	8-9b	20	0.29	0.25	0.24	0.08	0.32	0.72	0.08	0.04	0.01	0.02	0.01	0.10	1.88
22/05/2008	8-5b	40	0.28	0.22	0.06	0.06	0.38	0.64	0.08	0.05	0.02	0.05	0.02	0.16	1.71
23/05/2008	8-4b	30	0.17	0.14	0.04	0.01	0.33	0.22	0.03	0.00	0.00	0.00	0.01	0.02	0.96

Table SP4. Results from two-way crossed PERMANOVA analyses for the difference in SST, strat. deg., MLD, the average concentration in the upper mixed layer of NOx, PO_4, and dSi, and their ratios, and areal Chla concentrations at each station between campaign years (2006, 2007, 2008) and location of stations on the shelf or and the slope of the continental margin.

Factors		**SST**	**strat. deg.**	**MLD**	**NOx**	**PO_4**	**dSi**	**N:P**	**dSi:N**	**areal Chla**
shelf-slope	df	1	1	1	1	1	1	1	1	1
	MS	0.00	0.11	952.54	1.71	0.04	0.19	0.64	1.42	120.94
	pseudo-F	0.01	6.77	5.21	16.59	23.61	2.20	1.62	3.07	0.87
	p	0.915	0.014	0.036	0.001	0.000	0.149	0.215	0.086	0.359
year	df	2	2	2	2	2	2	2	2	2
	MS	1.53	0.12	544.04	0.04	0.00	0.11	0.14	0.06	1634.00
	pseudo-F	4.59	7.06	2.97	0.42	1.86	1.23	0.36	0.13	11.72
	p	0.021	0.004	0.083	0.661	0.183	0.307	0.705	0.881	0.00
shelf-slope	df	2	2	2	2	2	2	2	2	2
x year	MS	0.11	0.00	547.80	0.17	0.00	0.03	0.52	0.27	698.21
	pseudo-F	0.33	0.04	2.99	1.63	2.19	0.38	1.32	0.58	5.01
	p	0.723	0.955	0.096	0.210	0.141	0.696	0.290	0.556	0.02
Res	df	27	27	27	27	27	27	27	27	27.00
	MS	0.33	0.02	182.94	0.10	0.00	0.09	0.39	0.46	139.48

Table SP5. Results from one-way PERMANOVA analysis for the differences in areal Chla concentration between campaign years (2006, 2007, 2008).

Factor		**areal Chla**
year	df	2
	MS	1379.20
	pseudo-F	7.78
	p	0.002
Res	df	31
	MS	177.16

Supplementary figures

Fig. SP1. Water column profiles of seawater temperature (line), NOx (empty circles), and chlorophyll a (black dots) concentration. Stations located on the slope of the continental margin are marked with “slope” in the upper left corner of the plots.

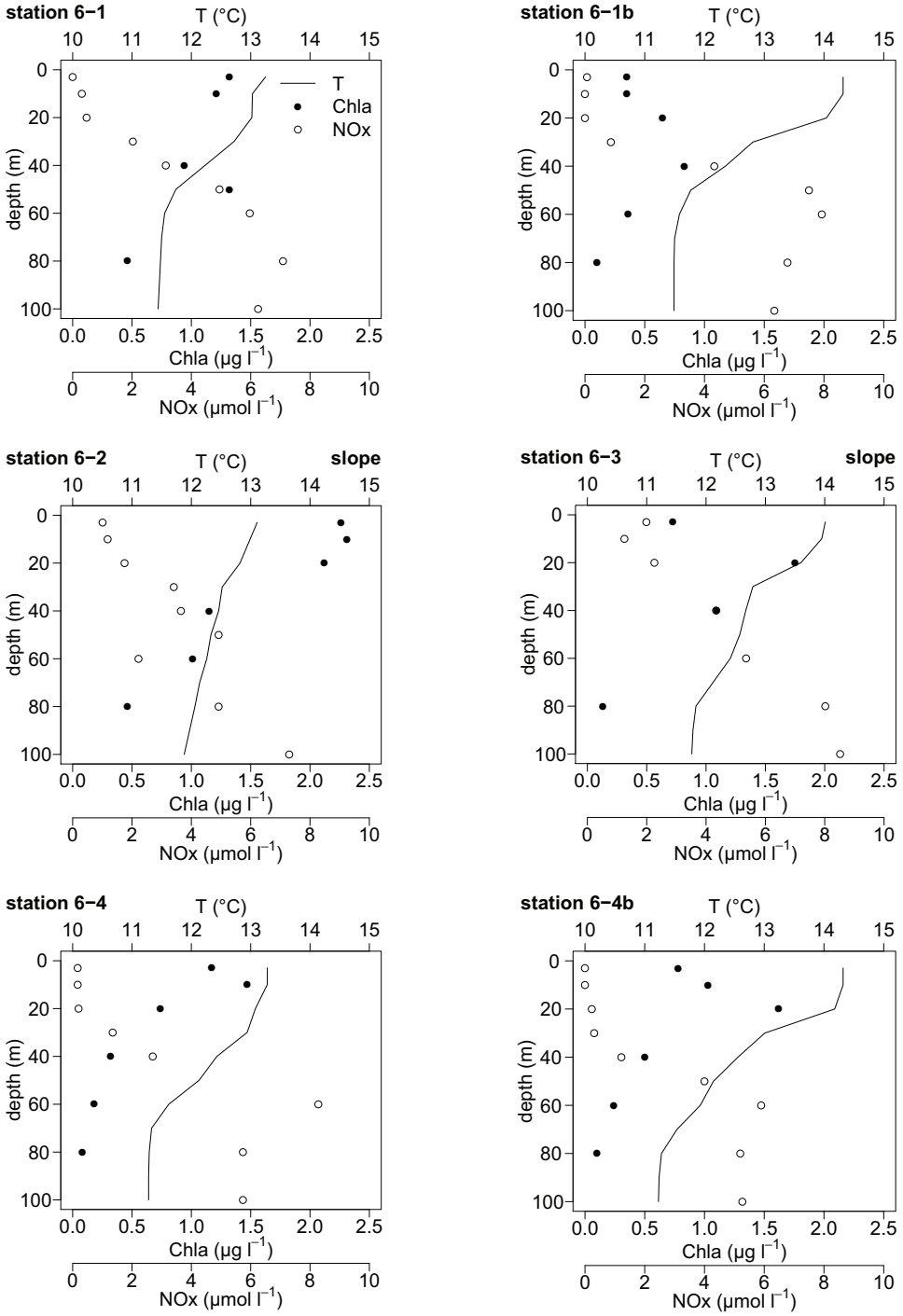

Fig. SP1. Continued

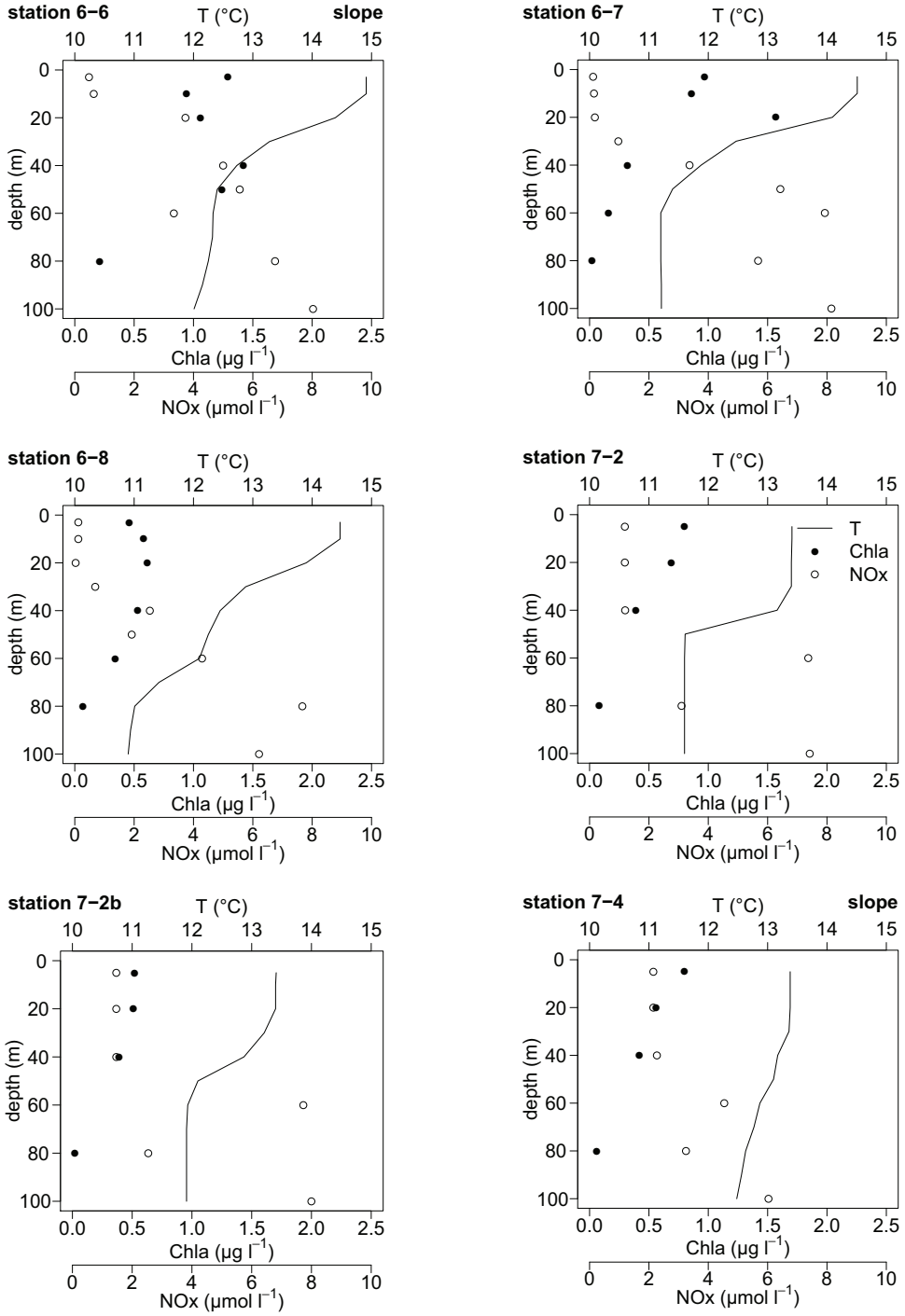

Fig. SP1. Continued

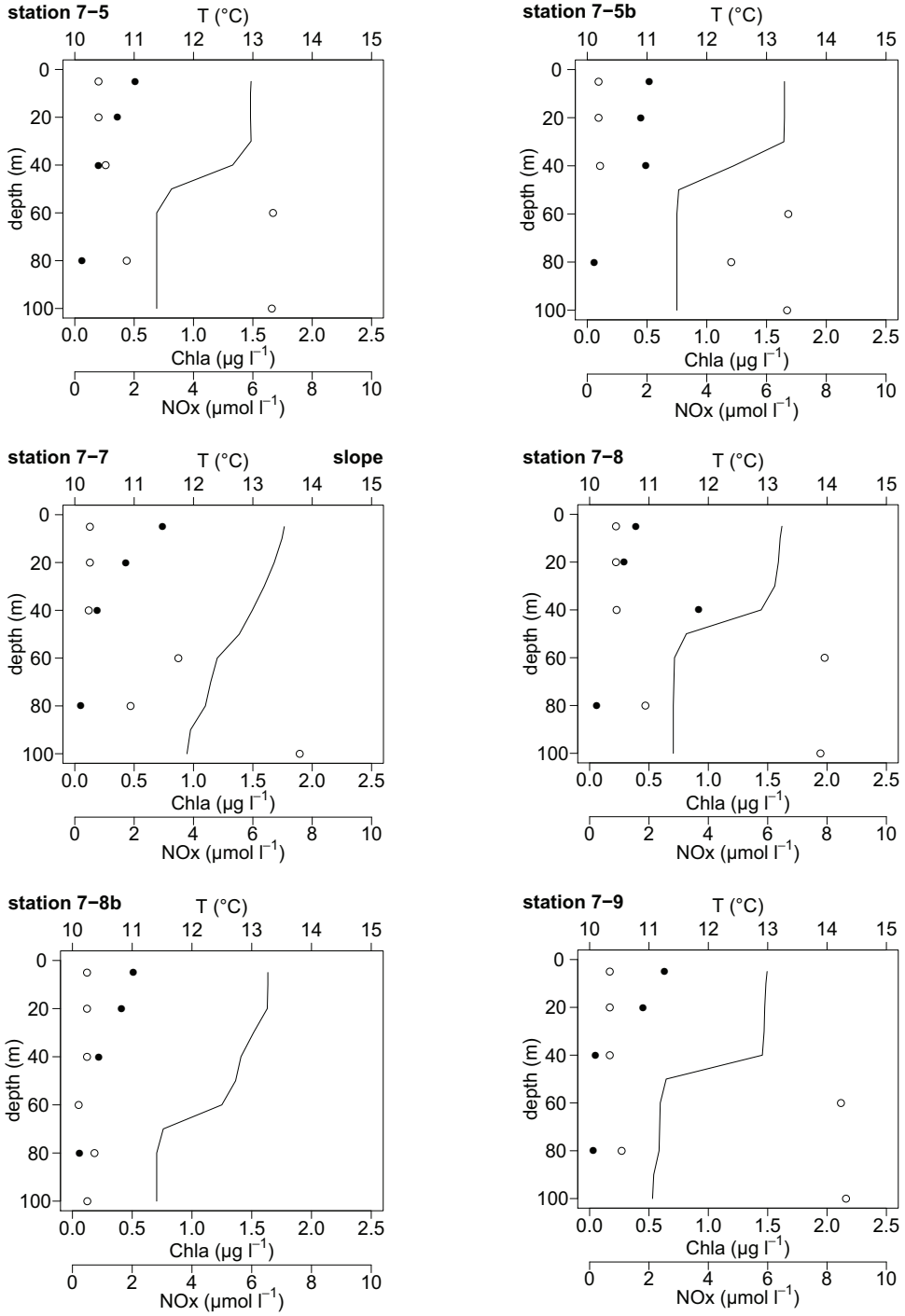

Fig. SP1. Continued

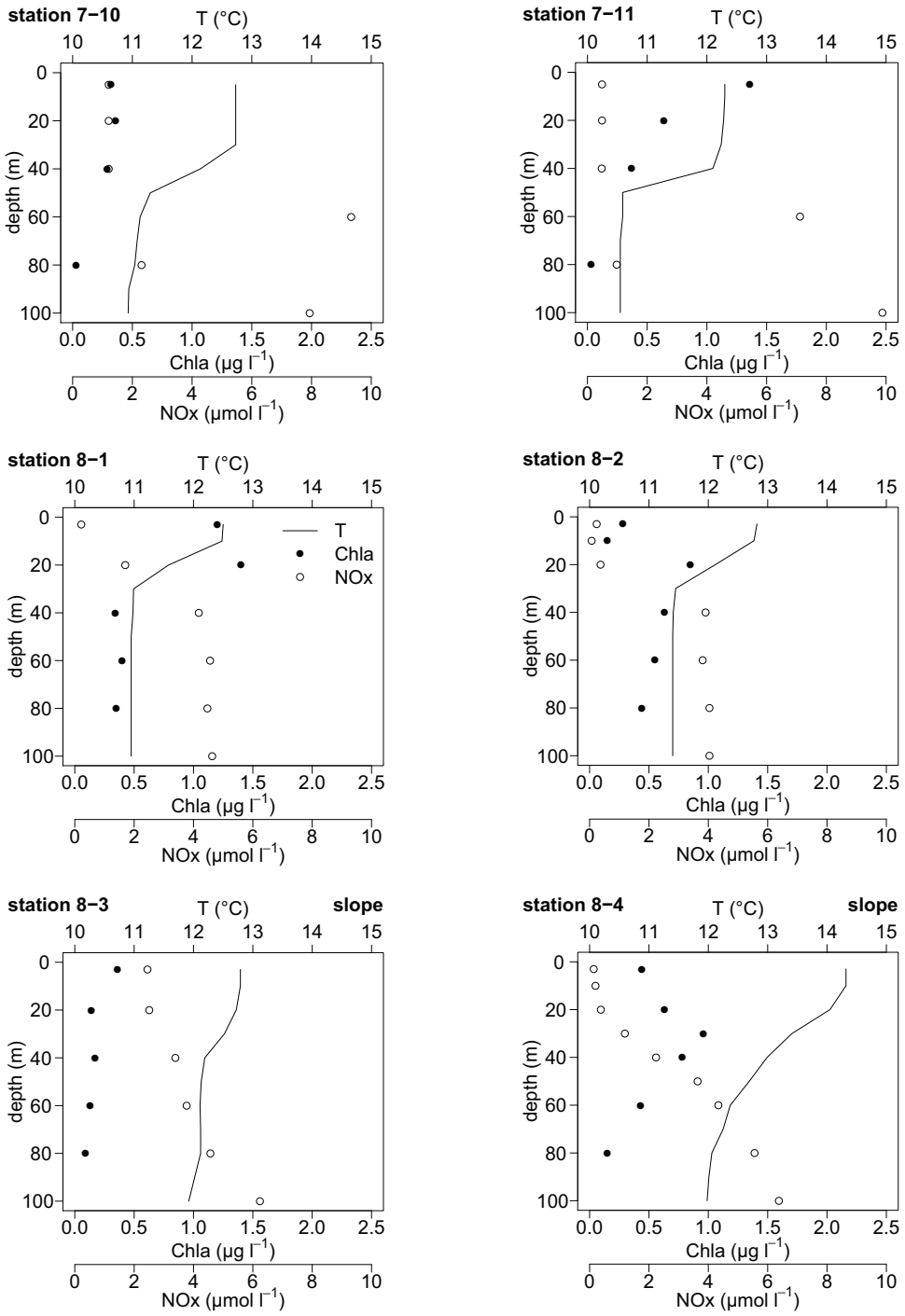

Fig. SP1. Continued

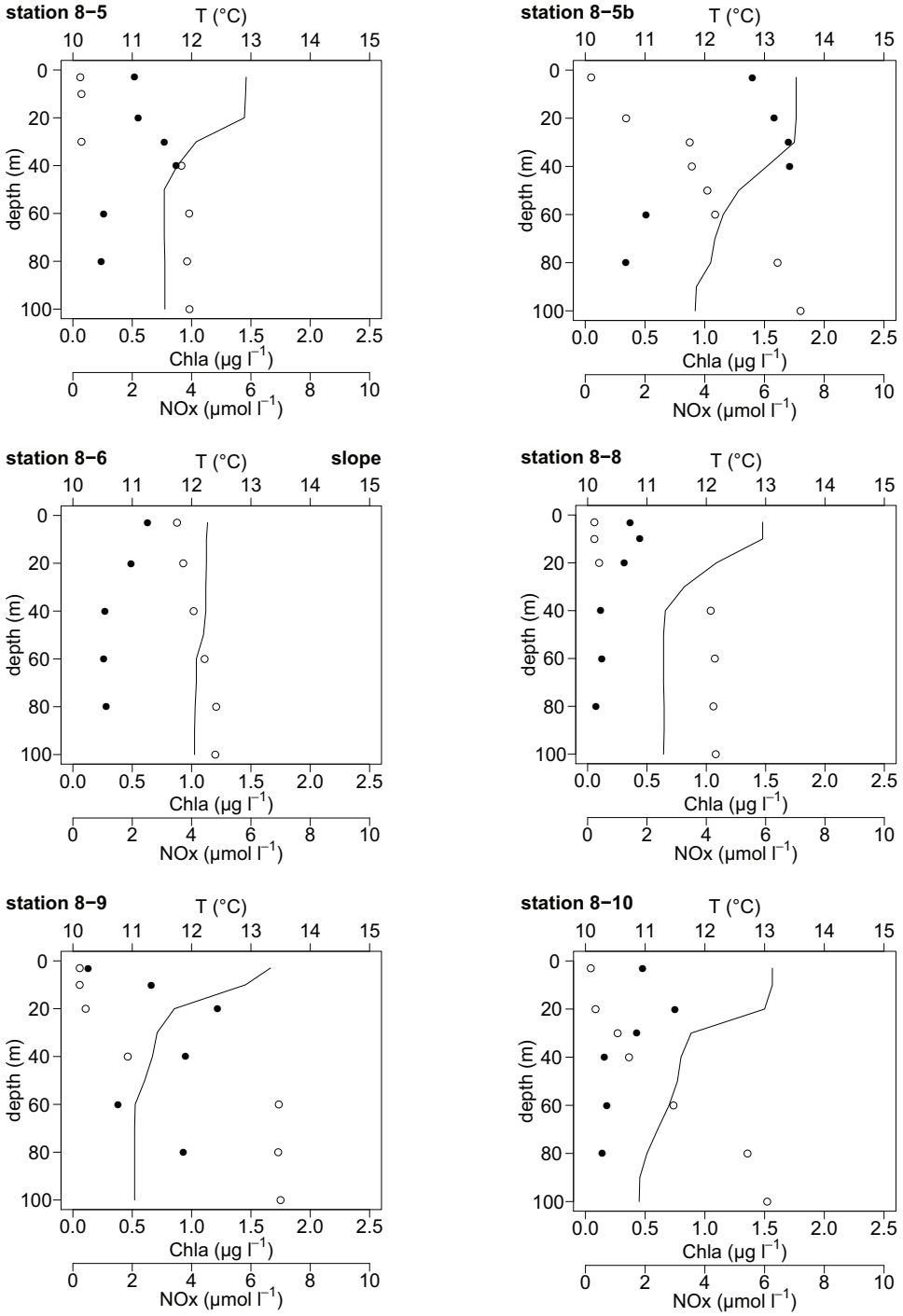

Fig. SP1. Continued

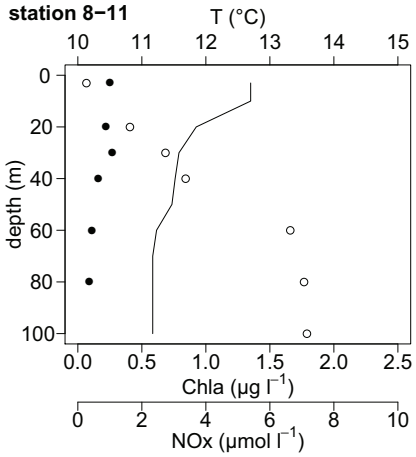

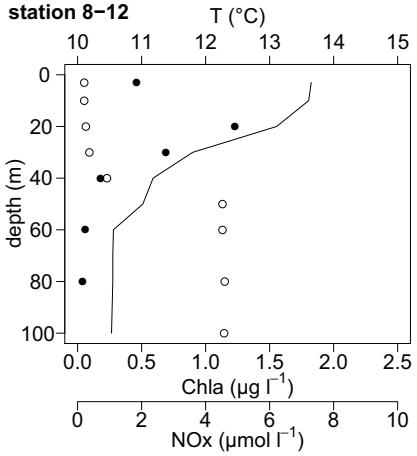

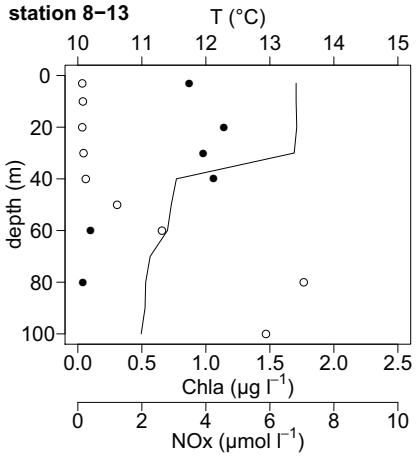

Fig. SP2. Water column profiles of POC (black dots), PIC (empty circles), and PN (grey dots) concentration. Stations located on the slope of the continental margin are marked with "slope" in the upper left corner of the plots.

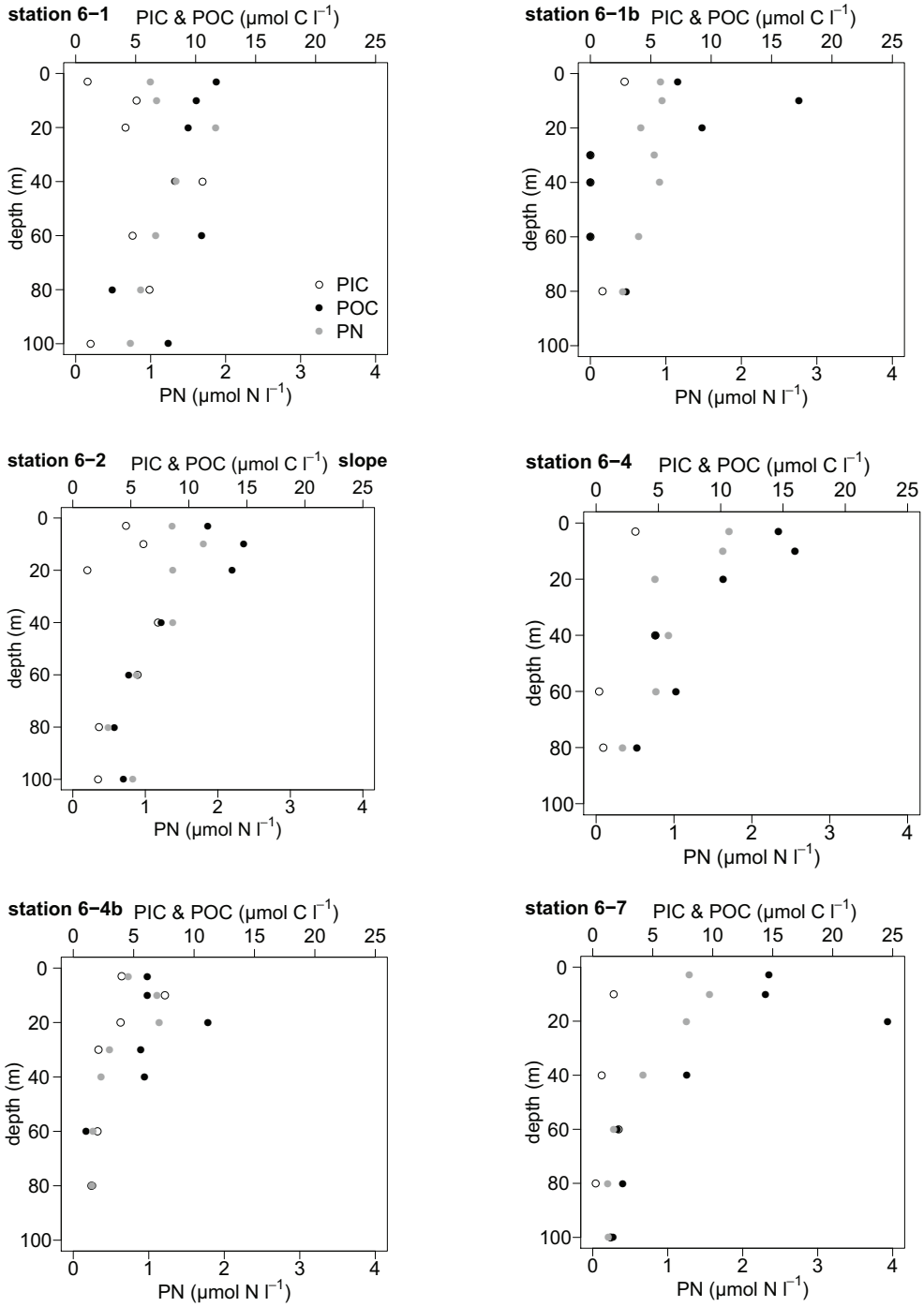

Fig. SP2. Continued

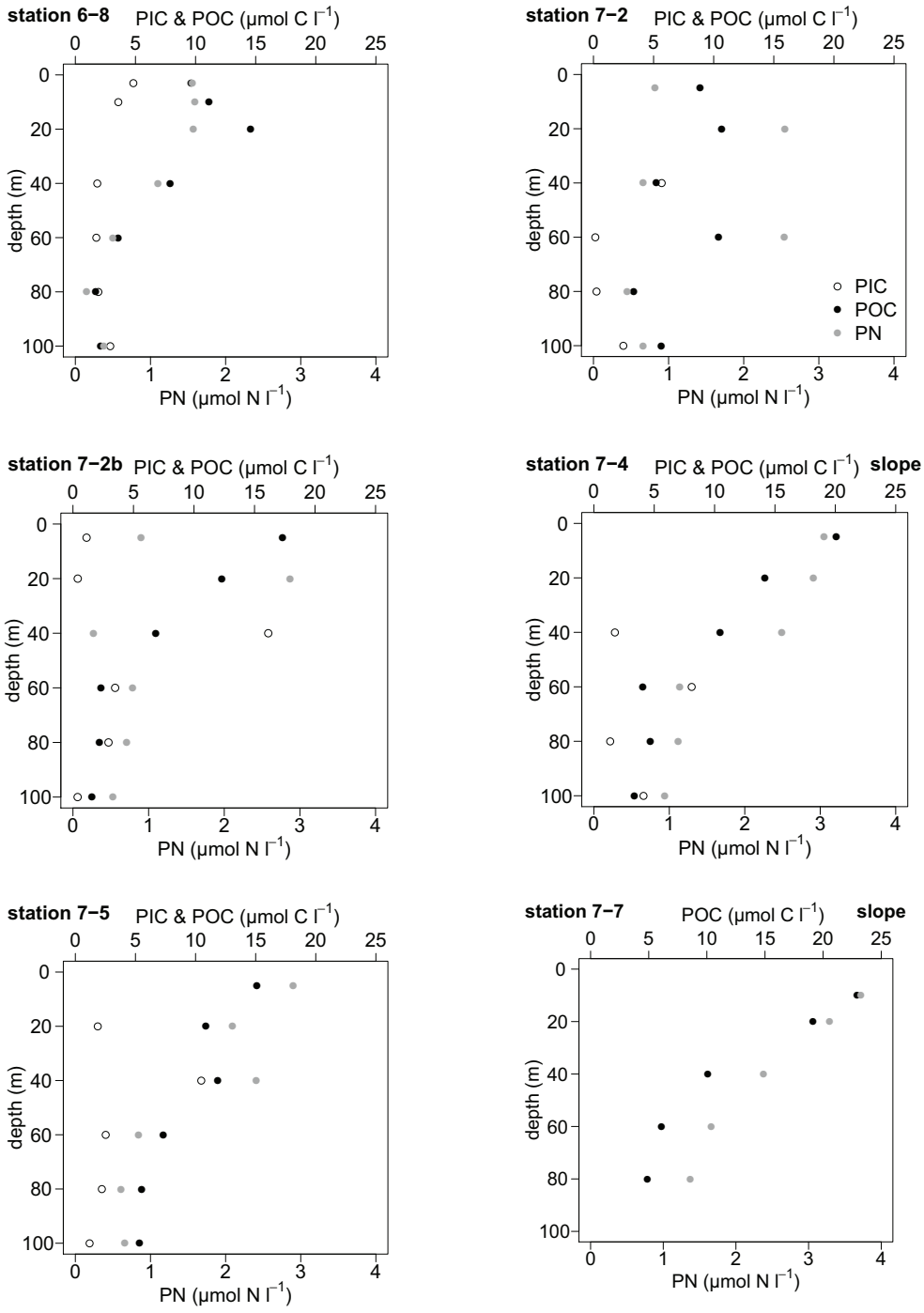

Fig. SP2. Continued

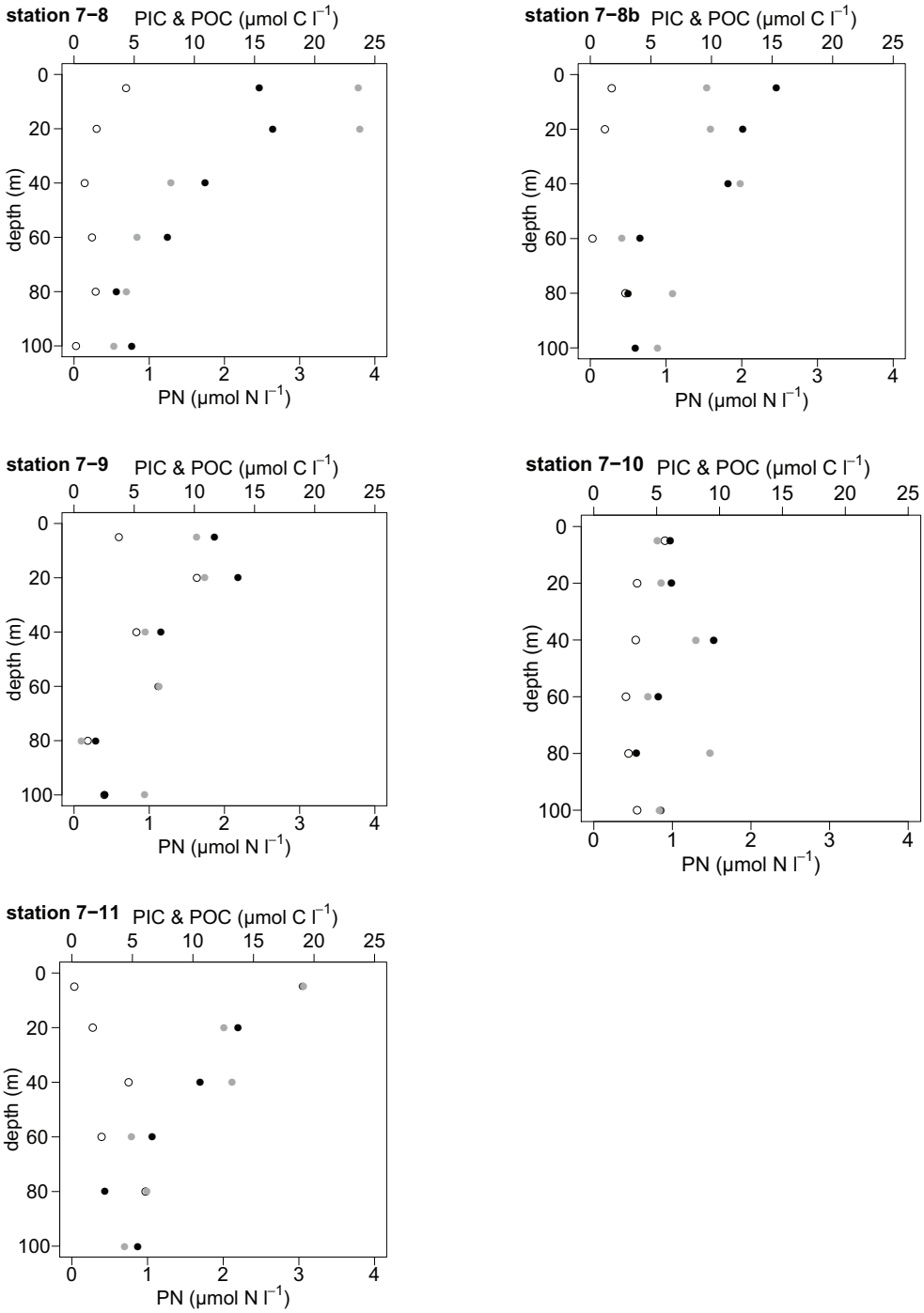

Fig. SP2. Continued

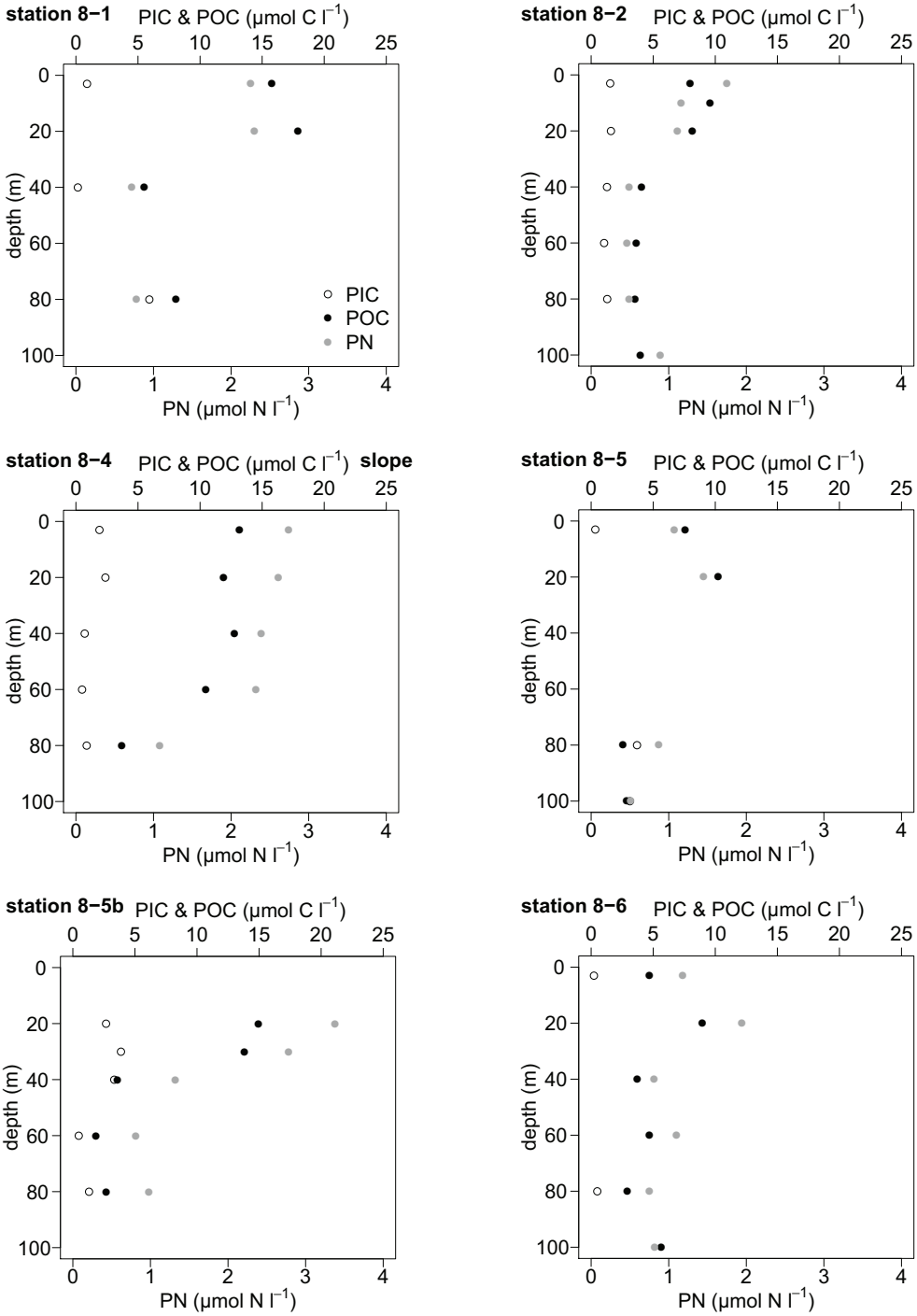

Fig. SP2. Continued

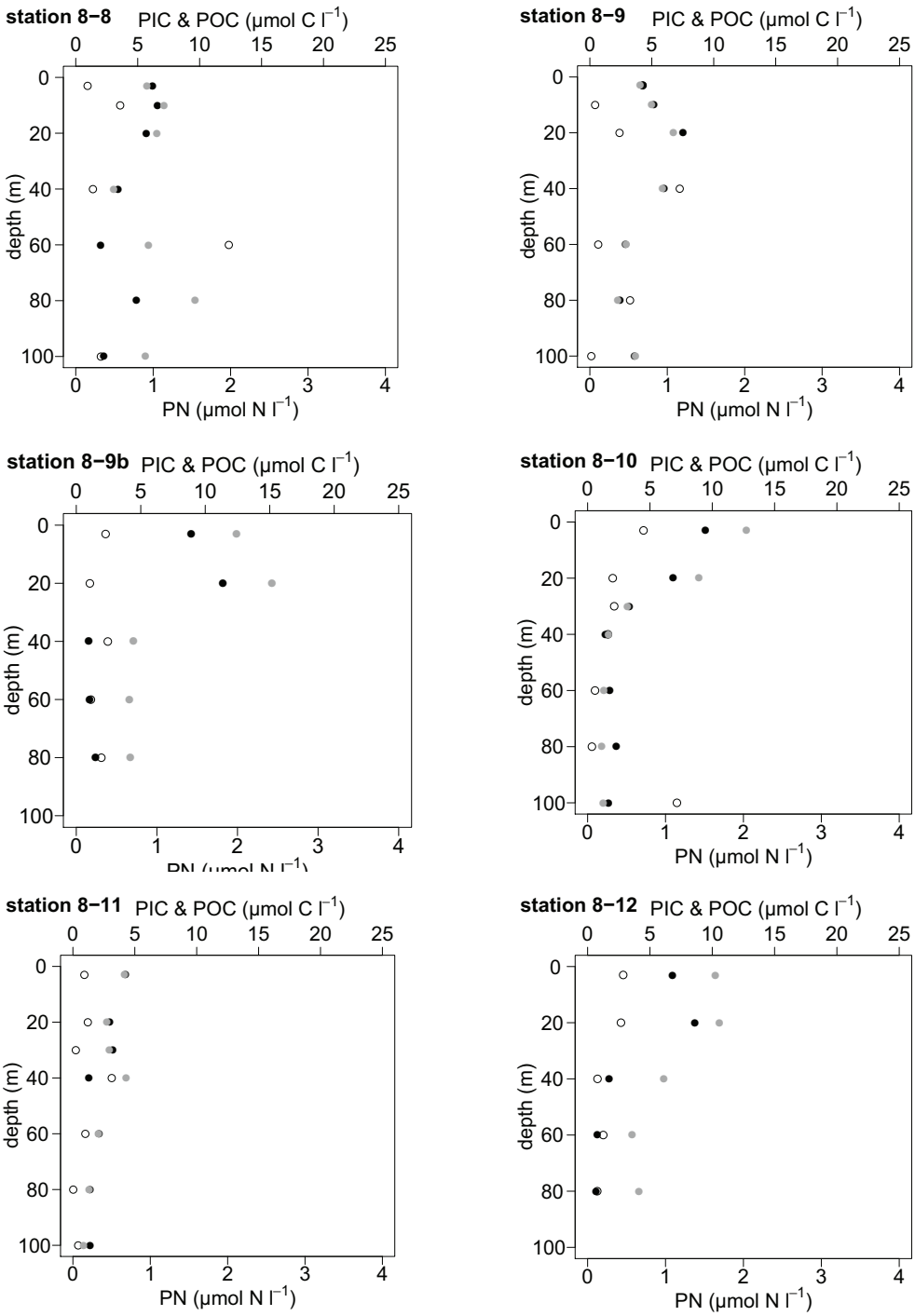

Fig. SP2. Continued

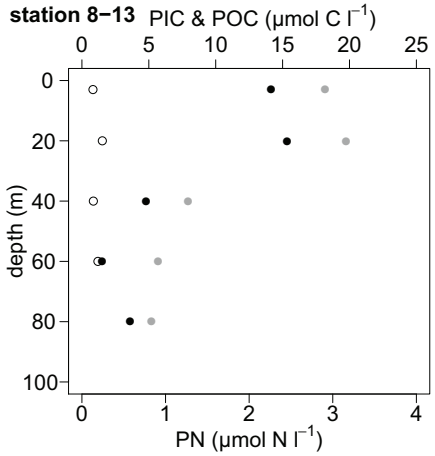

3

Community composition of free-living and particle-associated bacterial assemblages in late spring phytoplankton blooms along the North East Atlantic continental shelf break (northern Bay of Biscay, 2006-2008)

Nicolas Van Oostende[1], Lei Chou[2], Wim Vyverman[1], Koen Sabbe[1]

[1] Laboratory for Protistology and Aquatic Ecology, Biology Department, Ghent University, Krijgslaan 281 – S8, B-9000 Gent, Belgium.

[2] Laboratoire d'Océanography Chimique et Géochimie des Eaux, Université Libre de Bruxelles, Campus de la Plaine, CP208, boulevard du Triomphe, B-1050 Brussels, Belgium.

Authors' contributions

NVO, LC and KS conceived and designed the study. NVO performed the DGGE analyses. NVO analysed the data and wrote the manuscript. KS, WV, and LC revised the manuscript.

Abstract

The continental margin of the Bay of Biscay is characterised by often extensive phytoplankton blooms, mainly consisting of coccolithophores and diatoms. Despite important functional role in biogeochemical cycling and carbon export, very little is known about the composition and dynamics of bacterial communities associated with these blooms. We performed detailed PCR-based DGGE fingerprinting analyses of free-living (FL) and particle-associated (PA) bacterial communities in the upper 150 m of the water column during late spring blooms along the shelf break between 2006 and 2008. Bacterial phylotypes were identified by sequencing of partial 16S rDNA (DGGE bands) and near complete 16S rDNA (clone libraries). Bacterial communities were dominated by *Gammaproteobacteria* and *Bacteroidetes*, and by *Alphaproteobacteria*. Members of the *Flavobacteriaceae*, *Polaribacter* sp., and *Pseudoalteromonas* sp. were typical representatives of the PA communities, while phylotypes belonging to the *Rhodobacteriaceae*, the SAR11 group and the *Gammaproteobacteria* characterized the FL community. Nevertheless, ordination and non-parametric permutational analyses revealed a considerable overlap in the composition of both communities, suggesting frequent exchanges. Furthermore, the similarity between FL and PA community structures varied according to the campaign year. Interestingly, the same bacterial phylotypes were present each year even though bacterial community structure was variable between different sampling areas along the shelf break. Overall, the community structure of FL bacteria was more homogeneous than that of the PA bacteria which showed greater variability (within life mode similarity of 46% and 32%, respectively). Although we observed only a moderate but significant depth gradient in community structure, the PA bacterial communities showed a more pronounced depth gradient (surface - 150 m) compared to the FL communities, suggesting changes in particle composition with depth. Finally, turbulent mixing at the stations located on the slope of the continental margin favoured a stronger exchange between FL bacterial communities from the deeper and the surface water layers compared to stations located over the shelf.

Introduction

Due to their immense taxonomical and functional diversity and their high cumulative biomass, bacterial communities are central to the way marine ecosystems function (Whitman *et al.*, 1998; Sogin *et al.*, 2006; Fuhrman, 2009). Variation and changes in community structure help us to understand the factors that control communities and as such allow making predictions about how future environmental change will affect these communities. A recent study showed that seasonal changes in bacterial community structure could accurately be predicted on the basis of temperature, nutrients and phytoplankton concentrations (Fuhrman *et al.*, 2006), suggesting a certain degree of determinism in community assembly. Additionally, significant change at timescales on the order of days to weeks has been observed during Langrangian field studies and mesocosm experiments (Pinhassi *et al.*, 2004; Fandino *et al.*, 2005; Hewson *et al.*, 2006). Spatial patchiness of coherent communities tends to be on the scale of kilometres or tens of kilometres (Hewson *et al.*, 2006; Fuhrman, 2009), while change with depth can be significant at the scale of tens of metres (Fuhrman and Hagström, 2008; Treusch *et al.*, 2009).

Bacterial communities are often differentiated on the basis of their free-living (FL, planktonic) or particle-associated (PA, sessile) lifestyle, which can have distinct compositions (Delong *et al.*, 1993; Simon *et al.*, 2002; Hodges *et al.*, 2005). These differences in composition are also reflected in the production of different ectoenzymes and the higher activity of PA communities compared with FL ones (Martinez *et al.*, 1996; Fandino *et al.*, 2001; Grossart *et al.*, 2007a), which can affect the efficiency of the microbial loop and export production. However, other studies did not observe differences in community composition (Hollibaugh *et al.*, 2000; Ghiglione *et al.*, 2009), suggesting a continuum in life styles or transitions between them (Malfatti and Azam, 2009; Slightom and Buchan, 2009). To our knowledge, there are to date no studies reporting multi-annual vertical patterns in community structure of FL and PA bacterial communities in marine systems.

Continental shelves and margins are areas of high primary productivity and carbon export playing a key role in global biogeochemical cycles and in sustaining fisheries (Joint *et al.*, 2001; Sharples *et al.*, 2009). In the northern Bay of Biscay, primary production along the

shelf edge is driven by intermittent mixing of the water column due to internal wave formation (Huthnance *et al.*, 2001; Sharples *et al.*, 2007). Only few studies have documented bacterial dynamics in the Bay of Biscay, reporting on patterns of bacterial production and biomass (Artigas, 1998; Barquero *et al.*, 1998; Morán *et al.*, 2010) or activity of specific bacterial groups (Zubkov *et al.*, 2001a). To our knowledge, no studies have investigated bacterial community structure along the continental margin and the shelf to slope transition in the northern Bay of Biscay. In the present study, we document spatial and temporal variation patterns in the composition of FL and PA bacterial communities associated with late spring phytoplankton blooms along the shelf edge in this area. Bacterial community composition is described on the basis of a community fingerprinting technique (Denaturing Gradient Gel Electrophoresis, DGGE) and clone libraries based on 16S rDNA. We specifically focus on differences between the FL and PA fractions, between the slope and the shelf, between depths (surface-150 m depth) and between years (2006-2008). In the next chapter, we will only treat the bacterial community samples from the upper mixed layer to investigate their relationship with phytoplankton and environmental variables into more detail.

Materials and Methods

Description of the study area and its hydrography

The continental margin of the northern Bay of Biscay (NE Atlantic Ocean) is characterised by a wide continental shelf (the Celtic Sea) which is bordered in the West and South by a steep slope down to 4000 m depth (fig. 1). At the shelf edge, large semi-diurnal tidal currents cause internal tides which induce vertical mixing of the water column (Pingree and New, 1995). In total, 34 stations were sampled in 2006 (from the 31st of May to the 9th of June), in 2007 (from the 10th to the 24th of May), and in 2008 (from the 7th to the 23rd of May), including 7 stations which were revisited 6 to 14 days later during the second legs of the campaigns (chapter 2, table 1). Most stations were located in the vicinity of the La Chapelle Bank (47°N, 8°W) while 8 stations were located over the shallow part (<200 m depth) of the Goban Spur (50°N, 10°W) (fig. 1). Eight deeper stations (from 450 to 1400 m depth) were located over the continental slope at the Meriadzek Terrace (48°N, 9°W) and the La Chapelle Bank.

Fig. 1. (a) Bathymetric map showing the location of the stations in the Celtic Sea along the continental shelf break. The yellow shade represents the continental shelf, while the white line represents the 200 m depth isobaths bordering the shelf break. The stations visited during June 2006, May 2007, and May 2008 are represented by grey, white, and black circles respectively. Station numbers can be found in Chapter 2, table 1. Dotted lines represent the main residual circulation (adapted from Suykens *et al*., 2010).

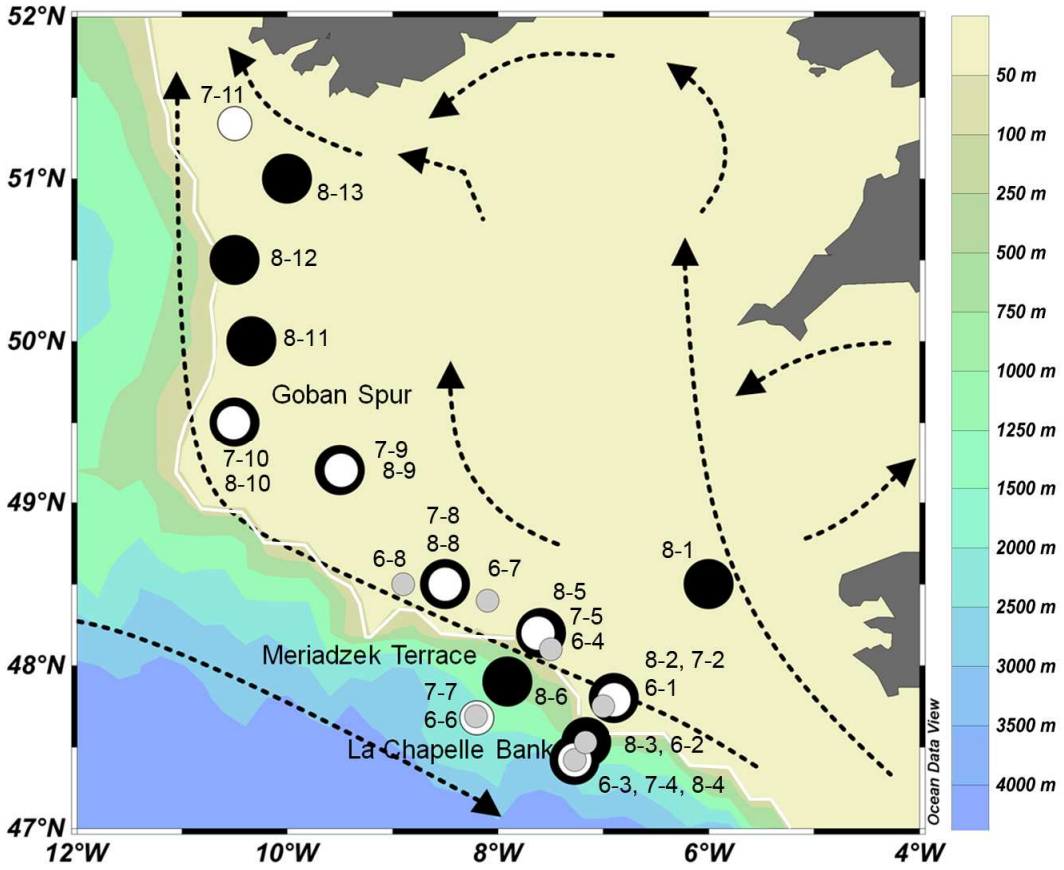

Fig. 1. (b) Advanced Very High Resolution Radiometer remote sensing image of sea-surface temperature on June 5th 2006, showing injection of deep, cold water to the surface along the continental shelf break (courtesy of Steve Groom, Plymouth Marine Laboratory).

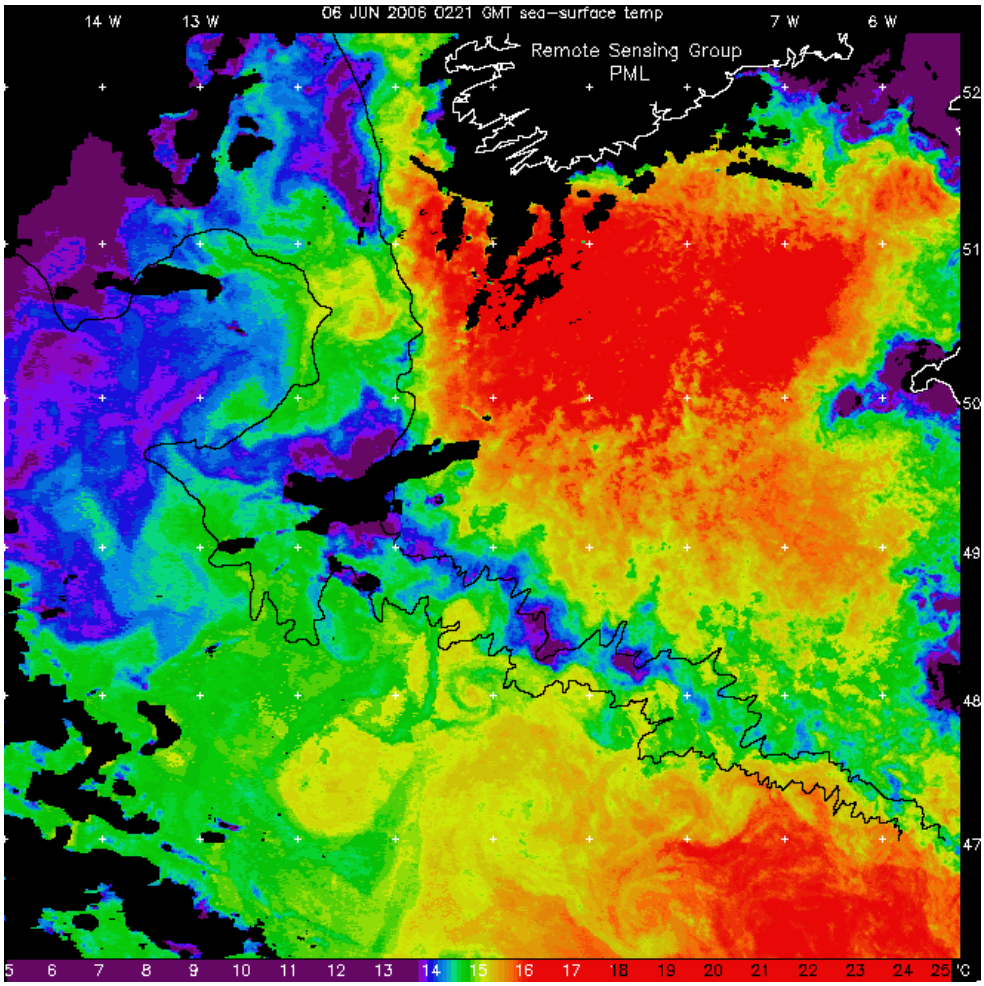

Sample collection and nucleic acid extraction

Seawater samples were collected using a rosette of 12 Niskin bottles (10 l) coupled to a conductivity, temperature-pressure probe (CTD) (Seabird SBE21). The degree of stratification of the water column (strat. deg.) was calculated as the difference in seawater density (σ_θ) at 100 m and at 10 m depth (chapter 2, table 1); these depths were selected to avoid diurnal changes in water density occurring at the surface and to include water from below the thermocline (when present). The surface mixed layer depth (MLD) was operationally defined as the depth where water density increased by 0.1 kg m^{-3} compared to the density of the surface layer (10 m). Sampling depths covered the surface waters, the thermocline region, and deeper waters (down to 150 m depth, but always at least 10 m above bottom).

Seawater samples for bacterial DNA isolation (50 - 200 ml) were filtered sequentially through cellulose mixed-ester membranes (Millipore) with nominal pore size of 3.0 µm and 0.22 µm. These bacterial populations were operationally defined as the "particle-associated" (PA) (> 3.0 µm) and the "free-living" (FL) (3.0 - 0.22 µm) fractions, respectively. These filters were stored in sterile cryovials containing 1 ml TES buffer solution (50 mM Tris-HCl, pH 8.3; 40 mM EDTA; 0.75 M sucrose) (Pinhassi *et al.*, 2004) and stored at -70°C until processing. DNA was extracted as described by Boström *et al.* (2004). Cells were lysed by treating the filters with sodium dodecyl sulphate (0.9% final concentration) and beat-beating (Zwart *et al.*, 1998). DNA was extracted and precipitated with isopropanol (100%), sodium acetate (3 M, pH 5.2), and yeast tRNA (Roche Applied Sciences) as a co-precipitant. Following extraction, the DNA was purified with a Wizard DNA clean-up system (Promega, Madison, Wisconsin) as specified by the manufacturer.

Fingerprinting and cloning

For the denaturing gradient gel electrophoresis (DGGE) analysis, the purified DNA extract were amplified by PCR with the bacteria-specific primers 357F with GC-clamp (5'-CGCCCGCCGCGCCCCGCGCCCGGCCCGCCGCCCCCGCCCCCCTACGGGAGGCAGCAG-3') and 518R (5'-ATTACCGCGGCTGCTGG-3'). PCR was carried out in a temperature cycler (Biometra, Westburg) according to Van der Gucht *et al.* (2005). The quality of the purified PCR products was assessed by electrophoresis of an aliquot of the PCR product on a 1.5% (w/v) agarose gel, staining with ethidium bromide, and comparison with a molecular weight marker (Smartladder, Eurogentec) using the software package Bionumerics 4.61 (Applied Maths BVBA, Kortrijk, Belgium). The DNA concentration of the purified and concentrated PCR products were measured spectrophotometrically using a NanoDrop device (Thermo Scientific).

DGGE was performed using a D-Code system from Bio-Rad Laboratories. Amplicon concentrations were normalised (500 ng) per lane to allow comparison of banding patterns and intensities between samples. Electrophoresis was performed on 8% (w/v) 1 mm thick polyacrylamide gels, containing a 35 to 60% gradient of denaturant (100% corresponded to 7 M urea and 40% (v/v) formamide), in a 1x TAE buffer solution, under constant voltage (75 V) for 16 h. Temperature was set at 60 °C. Following electrophoresis, the DGGE gels were stained with SYBR Gold and photographed with a CCD camera using UV transillumination

(Bio-Rad Laboratories, GelDoc XR). Representative bands in each gel were excised for sequence analysis (see further). In each gel, three marker lanes were included for alignment of the different gels using the software package Bionumerics 4.61. These markers consisted of a mixture of DNA from nine clones obtained from a clone library of the 16S rRNA genes as described by Van der Gucht *et al.* (2001). Band intensities of the selected band classes were standardized per sample in order to calculate relative band intensities per sample (Muylaert *et al.*, 2002). Band intensities measured in DGGE gels represent the number of 16S rRNA gene copies amplified by PCR. Thus, analyses of the bacterial community structure are at least semi-quantitative and the relative abundance data obtained this way in this study were used with this limitation in mind (Ferrari and Hollibaugh, 1999; Riemann *et al.*, 1999).

Excised bands from the gels were eluted overnight in TE buffer at 4 °C and PCR products of these bands were run in parallel with original samples to confirm their original migration position. In total, 404 bands were excised, 235 of which were successfully sequenced. Binning of bands at the same location into a single band class was based on the comparison of bands with identical sequences at the same position in the gels. Representative band sequences of the different phylotypes are available from GenBank (http://www.ncbi.nlm.nih.gov) under accession numbers HQ686085 to HQ686139.

In order to obtain near full-length 16S rRNA gene sequences to compare with the shorter DGGE band sequences, a clone library (n=141) was constructed from two pooled samples from each bacterial size-fraction (FL: station 6-7 at 10 m depth and station 6-4b at 50 m depth; and PA: station 6-8 at 40 m depth and station 6-1b at 10 m depth). Small subunit 16S rDNA was amplified using the bacteria-specific primers 27F (5'-AGAGTTTGATCMTGGCTCAG-3') and 1492R (5'-GRTACCTTGTTACGACTT-3') (Höfle *et al.*, 2005). Construction of the clone library was performed as described by De Wever *et al.* (De Wever *et al.*, 2008). Clones were screened using DGGE to allow comparison of band positions and the clones' insert sequence with the representative phylotypes from the community analyses. Identification of the DGGE phylotypes was performed by aligning them with our own 16S rDNA clone sequence library and by assigning 16S rRNA gene sequences to the new phylogenetically consistent higher-order bacterial taxonomy using the Classifier tool of the Ribosomal Database Project (10.22) (Cole *et al.*, 2009). A bootstrap confidence threshold of 80% and 95% was used to classify the

sequences of the bands and clones, respectively. Clone library nucleotide sequences are available from GenBank under accession numbers EU394538 to EU394678.

Data treatment and statistical analyses

Averages are reported as their arithmetic mean ± standard deviation. Ambiguous band classes (i.e. band classes for which replicate sequences – obtained from different lanes – gave different closest matches, see tables 2 and SP1) and band classes of eukaryotic origin (including plastids, see table SP1), were excluded from the analyses. We then selected only band classes which were represented in at least 5% of all the samples to discard the underrepresented ones, resulting in a final data set of 35 band classes which were used in the analyses outlined below.

The SIMPER routine was used to identify the phylotypes which contribute most to the similarities within each bacterial life form group (PA and FL), campaign month (June in 2006 and May in 2007 and 2008) and depth (surface: ≤ 20 m and deeper: 80 – 150 m) and to obtain the overall percentage contribution each phylotype makes to the average dissimilarity between groups (i.e. the total average dissimilarity) (Clark and Gorley 2006). Phylotypes are displayed in order of decreasing contribution (Av.Diss.%) to the total between-group dissimilarity. SIMPER also returns the ratio (Diss/SD) of the average phylotype contribution (Av.Diss.%) divided by the total standard deviation (SD) of those contributions across all pairs of samples. Phylotypes with higher dissimilarity to standard deviation ratios (Diss/SD) are better between-group discriminators because they contribute relatively consistently to that distinction.

To test the difference in bacterial community structures between life form group (FL and PA) and campaign years (2006, 2007, 2008) a two-way crossed non-parametric permutational analysis of variance (PERMANOVA) was performed using a resemblance matrix based on Bray-Curtis similarities of square root-transformed standardised band intensities (Clarke and Gorley, 2006; Anderson *et al.*, 2008). Probability values were obtained by permutation ($n=10^4$). The effect of sampling area (the shelf and slope stations at La Chapelle Bank and Meriadzek Terrace (LC&M) versus station at Goban Spur (GS)) and campaign years on both the FL and PA bacterial communities was tested by PERMANOVA's with a fully crossed two-factor design using type III (partial) sums of squares. Finally, three-way crossed

PERMANOVA's were used to assess the influence of campaign year, the shelf or slope location of the community sample, and the water layer (surface: ≤ 20 m and deeper: 80 – 150 m) on the structure of FL and PA communities from the La Chapelle and Meriadzek area (LC&M). Homogeneity of dispersion was tested by PERMDISP analyses for any of the tested terms in each PERMANOVA, checking that patterns found were not confounded by artefacts due to variable's dispersions.

Principal coordinates analysis (PCO) was used to assess variation patterns in species composition between bacterial community samples. Bray-Curtis similarity of square root-transformed standardised band intensities were used for the calculation of the PCO axes. Spearman rank correlations were used to assess change in community composition (represented by the PCO axes) in relation with supplementary variables: bottom depth (as a proxy for the slope to shelf divide), area (La Chapelle, Meriadzek, Goban Spur), longitude and latitude, sample depth, seawater temperature and year (2006-2008). Qualitative variables (e.g. year) were introduced as categorical variables.

The PCO, PERMANOVA and SIMPER analyses were performed using the PRIMER v6 and PERMANOVA+ add-on software (PRIMER-E Ltd., Plymouth, U.K.) (Clarke and Gorley, 2006; Anderson *et al.*, 2008). Permutation tests consisted of 10^4 iterations and the significance level was set at 0.05 unless stated otherwise.

Results

Community composition of the free-living and particle-associated bacterial communities

In total, 68 distinct band classes (i.e. phylotypes) could be distinguished in 301 bacterial community fingerprints (151 FL, 150 PA). We obtained sequences for 44 band classes, including 10 belonging to eukaryotes (mainly plastids) and 5 ambiguous ones. A list of all band sequences and their phylogenetic affiliations can be found in tables 1 and SP1, while table 2 lists the corresponding clones from our libraries.

Table 1. Relatedness of phylotypes to known organisms. Phylogenetic affiliation of SSU rRNA gene sequences from excised DGGE bands representative for each bandclass (phylotype). Phylotypes were used in the statistical community analyses and designate band classes where a single sequence type was found after excision and sequencing of multiple representative bands. The remaining phylotypes (see table SP1) were of eukaryotic origin or could not unambiguously be assigned to a single band class. Sequence similarity is given next to the accession number of the Genbank relatives in the right-hand column.

Phylotype	GenBank acc. no.	Phylogenetic affiliation	Relative in GenBank and sequence similarity
Alpha_1	HQ686115	*Proteobacteria*	Uncultured marine bacterium clone MOLA_MAY07-5m-134; GU204773 (100%)
Rhodo	HQ686135	*Alphaproteobacteria*	Uncultured *alpha proteobacterium* EB080_L11F12; GU474937 (100%)
Alpha_4	HQ686138	*Alphaproteobacteria*	*Ruegeria* sp. HD-28; GU057915 (93%)
Pelagi	HQ686137	*Pelagibacter*	Uncultured SAR11 cluster bacterium HF0010_09O16; GU474904 (100%)
Bact_1	HQ686085	*Bacteroidetes*	Uncultured *Bacteroidetes* bacterium clone 1_C1; EU600573 (100%)
Flavo_1	HQ686092	*Flavobacteriaceae*	Uncultured *Flavobacteria* bacterium clone NorSea54; AM279200 (100%)
Flavo_2	HQ686098	*Flavobacteriaceae*	Uncultured *Flavobacteria* bacterium clone NorSea81; AM279179 (99%)
Flavo_3	HQ686100	*Flavobacteriaceae*	Uncultured *Flavobacteria* bacterium clone Vis_St6_1; FN433465 (100%)
Flavo_4	HQ686118	*Flavobacteriaceae*	Uncultured *Flavobacteria* bacterium clone Vis_St3_34; FN433446 (100%)
Flavo_5	HQ686119	*Flavobacteriaceae*	*Polaribacter* sp. J15-9; HM010402 (100%)
Gam_2	HQ686099	*Gammaproteobacteria*	Uncultured *gamma proteobacterium* clone plankton_C03; FJ664795 (100%)
Gam_3	HQ686101	*Gammaproteobacteria*	Uncultured *gamma proteobacterium* clone SHAB566; GQ348664 (100%)
Gam_4	HQ686102	*Gammaproteobacteria*	Uncultured *gamma proteobacterium* clone CB0565b.34; GQ337124 (100%)
Gam_6	HQ686110	*Alcanivorax*	*Alcanivorax* sp. EM484; GU223378 (100%)
Gam_7	HQ686112	*Gammaproteobacteria*	Uncultured marine bacterium clone MOLA_JUN08-5m-151; GU204632 (98%)
Gam_9	HQ686134	*Proteobacteria*	Uncultured *gamma proteobacterium* clone C13W_84; HM057682 (100%)
Gam_10	HQ686097	*Proteobacteria*	Uncultured bacterium clone 1C227523; EU799860 (95%)
PsAlt_2	HQ686125	*Pseudoalteromonas*	*Pseudoalteromonadaceae* bacterium; HQ164448 (100%)
PsAlt_3	HQ686130	*Alteromonadales*	*Pseudoalteromonas* sp. BCw012; FJ889600 (97%)
SAR86_3	HQ686090	*Bacteria*	Uncultured marine bacterium clone MOLA_JAN08-5m-133; GU204457 (100%)
SAR86_4	HQ686091	*Gammaproteobacteria*	Uncultured SAR86 cluster *gamma proteobacterium* clone 3_C4; EU600487 (100%)

Table 2. Relatedness of clones to known organisms and associations between clones from our clone library and affiliated phylotypes (% similarity).

GenBank acc. no. of clone	Phylogenetic affiliation	Phylotype	GenBank acc. no. of band	% similarity
EU394547	*Alphaproteobacteria*	**Alpha_1**	HQ686115	100
EU394601	*Rhodobacteraceae*	**Rhodo**	HQ686135	100
EU394591	*Pelagibacter*	**Pelagi**	HQ686137	99
EU394563	*Cryomorphaceae*	Cryo	HQ686093	99
EU394567	*Saprospiraceae*	Diat_2	HQ686127	98
EU394611	*Flavobacteriaceae*	Diat_2	HQ686128	100
EU394574	*Flavobacteriaceae*	**Flavo_4**	HQ686118	100
EU394573	*Polaribacter*	**Flavo_5**	HQ686119	100
EU394620	*Flavobacteriaceae*	SAR86_1	HQ686088	93
EU394613	*Gammaproteobacteria*	Gam_1	HQ686095	97
EU394576	*Haliea*	**Gam_2**	HQ686099	100
EU394541	*Gammaproteobacteria*	**Gam_4**	HQ686102	100
EU394672	*Gammaproteobacteria*	Pras_1	HQ686106	100
EU394552	*Gammaproteobacteria*	SAR86_1	HQ686087	100
EU394540	*Gammaproteobacteria*	SAR86_2	HQ686089	99
EU394555	*Gammaproteobacteria*	**SAR86_3**	HQ686090	100
EU394540	*Gammaproteobacteria*	**SAR86_4**	HQ686091	100
EU394659	*Cyanobacteria*	Crypt_1	HQ686117	99
EU394564	*Cryptomonadaceae*	Crypt_2	HQ686123	100
EU394579	*Bacillariophyta*	Diat_2	HQ686126	99
EU394562	*Chloroplast*	Ehux	HQ686111	100
EU394571	*Chlorophyta*	Pras_1	HQ686105	100
EU394578	*GpIIa*	Syncoc	HQ686121	100

On average, the number of bands in the FL and PA communities was similar (FL: 14.5 ± 3.7, 7 - 25; PA: 14.4 ± 3.7, 4 - 22). The majority of the identified bacterial phylotypes were related to the *Gammaproteobacteria* (39%) or *Bacteroidetes* (24%), the remainder were of alphaproteobacterial (11%), plastid (17%) or uncertain (9%) origin. Cumulatively, the identified bands of bacterial origin made up a high proportion of total intensity of all bands within each sample, indicating that we identified the most prominent members of the bacterial community (FL: 88.3% and PA: 87.1% of all the selected unambiguous band classes) (table 3). *Alphaproteobacteria* was on average the most prominent group in the FL population, while the *Bacteroidetes* group was most dominant in the PA bacterial

community (based on relative band intensities). In general, members of the *Bacteroidetes* group and *Alphaproteobacteria* were more abundant in the surface mixed layer, while *Gammaproteobacteria* were more abundant in deeper parts of the water column (table 3) (see also further). The high standard deviations associated to the relative abundance of these phylogenetic groups suggest that the response of bacterial communities to different environments is apparent, even at the phylogenetic class level.

Table 3. Total relative band intensities (mean ± SD) of the three main phylogenetic groups in the upper mixed layer (upper ML) and the whole water column (all) during 2006-2008.

water layer	**bacterial community**	**phylogenetic affiliation**			
		Alpha-proteobacteria	*Gamma-proteobacteria*	*Bacteroidetes*	total
upper ML	FL (n=74)	46 ± 14	22 ± 14	22 ± 17	90 ± 10
all	FL (n=151)	39 ± 16	31 ± 18	18 ± 15	88 ± 10
upper ML	PA (n=73)	24 ± 16	26 ± 19	40 ± 20	90 ± 12
all	PA (n=150)	21 ± 15	31 ± 21	35 ± 19	87 ± 14

Similarity between free-living and particle-associated bacterial community structure

The structure of the FL and PA communities spanning the entire depth range (surface – 150 m) differed significantly from each other over all the campaign years and within each year (table SP2; pairwise tests within each year: all $p<0.0001$). However, the difference between FL and PA communities was smallest in 2006 (49.5% dissimilarity) compared to 2007 and 2008 (58.9% and 73.5% dissimilarity, respectively) indicating a significant interaction effect of the campaign year on the partition between the structure of both communities. Moreover, a significant dispersion effect (FL/PA x year: $F=33.28$, $df1=5$, $df2=295$, $p<0.0001$) influenced the statistical division of both communities as visualised by the high overlap in composition between the FL and PA communities in the PCO diagram (fig. 2). The average dissimilarity between all pairs of samples from the FL and PA fractions (69.0%) can mainly be attributed to differences in the relative abundance of ten species only, which account for three-quarters of the average dissimilarity of both communities (table 4). The FL bacterial communities were on average more similar to each other than the PA ones (average similarity 46.3% and 31.5%, respectively). The structure of both bacterial communities is shaped by the phylotypes with the highest relative abundance, which they also share (table

4). PsAlt_2, Gam_4, Flavo_1, Flavo_4, Rhodo, Pelagi and SAR86_3 are good discriminators between the FL and PA bacterial communities (highest Diss/SD values) (table 4). Specific phylotypes identified as *Flavobacteria*ceae (Flavo_4: 14% ± 15% and Flavo_5: 7% ± 11%) and a *Pseudoalteromonas* sp. (PsAlt_2: 14% ± 18%) were relatively more abundant in the PA community, while a *Gammaproteobacterium* (Gam_4: 16% ± 12%), a *Rhodobacteraceae* (Rhodo: 21% ± 10%), and a SAR11 bacterium (Pelagi: 16% ± 11%) were prominent in the FL community (table 4, see also fig. 2).

Table 4. Results of the SIMPER routine for all stations and depths sampled during the campaigns (n=301), showing the average abundance of the phylotypes (Av. Abund.) which can best discriminate between the FL and PA communities. The total average dissimilarity of the phylotypes differentiating the communities was 69.0%.

Phylotype	FL Av. Abund.	PA Av. Abund.	Av.Diss. %	Diss/SD	Cum. Contrib. %
PsAlt_2	0.06	0.14	7.56	0.87	10.95
Gam_4	0.16	0.04	6.86	1.20	20.89
Flavo_4	0.05	0.14	6.67	0.96	30.56
Rhodo	0.21	0.11	6.46	1.28	39.92
Pelagi	0.16	0.08	6.31	1.34	49.07
Flavo_5	0.04	0.07	3.95	0.80	54.79
Flavo_1	0.05	0.06	2.98	1.00	59.11
Flavo_2	0.03	0.04	2.56	0.69	62.82
47.2	0.05	0.01	2.49	0.82	66.43
SAR86_3	0.04	0.02	2.31	1.05	69.77
Flavo_3	0.01	0.04	2.16	0.66	72.90
Gam_3	0.01	0.03	1.68	0.67	75.33

Fig. 2. (next page) Principal coordinates analysis (PCO) diagram showing the variation in bacterial community structure of free-living (empty symbols) and particle-associated (filled symbols) populations during each campaign (2006: red, 2007: blue, 2008: green) along the first two PCO axes (PCO1 and PCO2). The amount of variation captured by each PCO axis is shown. Triangles denote deeper samples while the circles represent the samples above 80 m depth. The diagram to the right shows the direction of steepest increase of the relative abundance of the phylotypes which discriminate best between the FL and PA populations, based on SIMPER analysis (table 4).

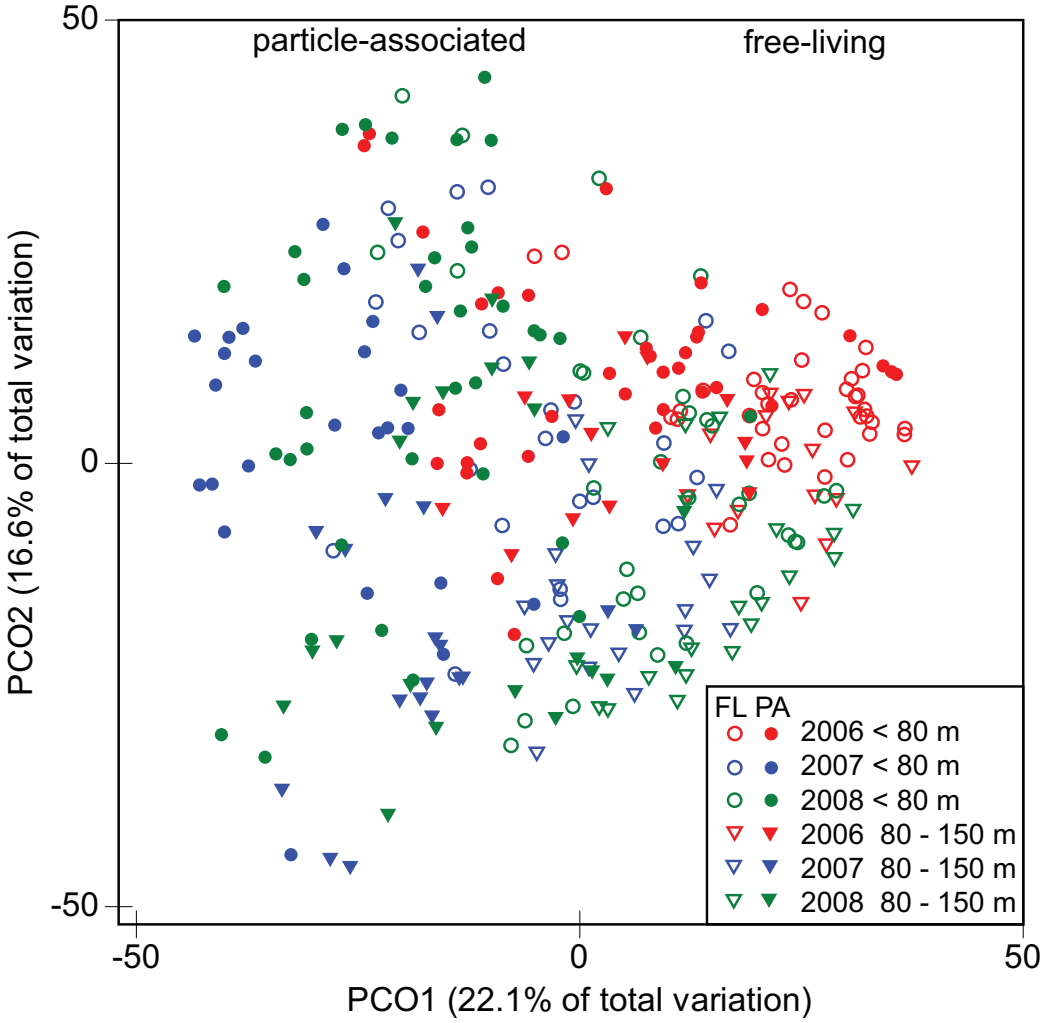
particle-associated
free-living
50
0
-50
-50
0
50
PCO2 (16.6% of total variation)
PCO1 (22.1% of total variation)
FL PA
2006 < 80 m
2007 < 80 m
2008 < 80 m
2006 80 - 150 m
2007 80 - 150 m
2008 80 - 150 m

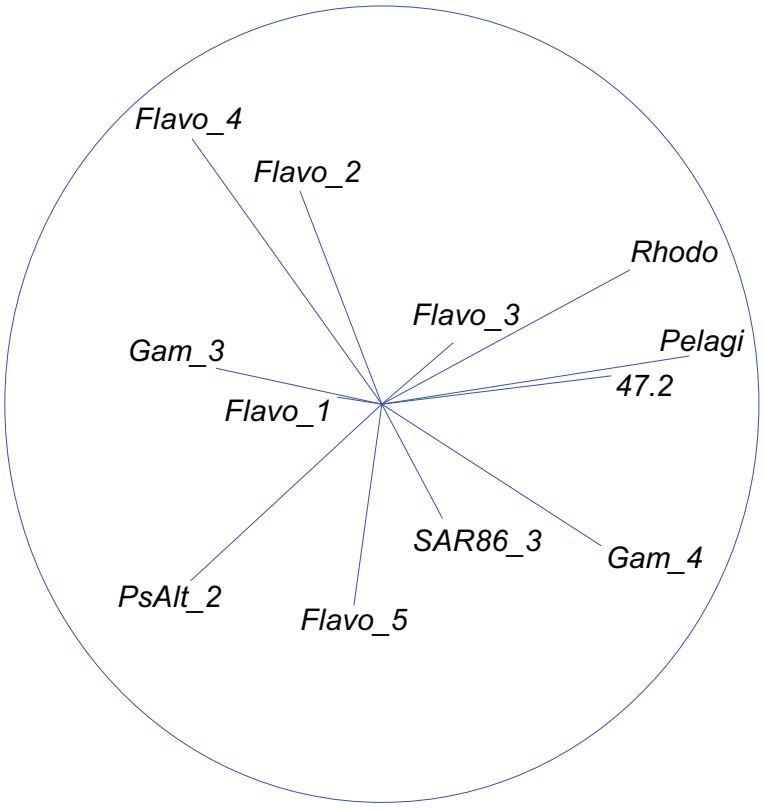
Flavo_4
Flavo_2
Rhodo
Flavo_3
Pelagi
Gam_3
47.2
Flavo_1
SAR86_3
Gam_4
PsAlt_2
Flavo_5

Spatial and temporal variation in bacterial community structure

The community structure within the FL bacterial communities depended on the area where it was sampled (i.e. on the shelf or slope of LC&M or on the shelf of GS) and on the campaign year or the associated environmental conditions (table SP3; pairwise tests between areas within each year were all significant at $p \leq 0.01$). Moreover, the difference between areas in 2006 (36.5% dissimilarity between FL communities of shelf and slope of LC&M) was smaller than the difference of the same areas in 2007 and 2008 (49.0% and 41.2%), indicating a significant interaction effect of the campaign year on the division between the structure of communities sampled in different areas. The differences in bacterial community structure between years and their different dispersion are also evident in separate PCO analyses of the FL bacterial communities in figure 3a.

The community structure within the PA bacterial communities depended on the area where it was sampled (i.e. on the shelf or slope of LC&M or on the shelf of GS) and during which campaign (table SP3; pairwise tests between areas within each year were all significant at $p \leq 0.04$). Moreover, the difference between areas in 2006 (48.6% dissimilarity between FL communities of shelf and slope of LC&M) was smaller than the difference of the same areas in 2007 and 2008 (52.8% and 61.8%), indicating a significant interaction effect of the campaign year on the division between the structure of communities sampled in different areas. The differences in bacterial community structure between years and their different dispersion are also evident in separate PCO analyses of the PA bacterial communities in figure 3b.

In both communities, the first axis is mainly related to the gradient in community structure between years, especially 2006 and 2007. The second axis in the PCO diagrams is related to sampling depth, which is negatively correlated with water temperature (fig. 3). There was no significant correlation with region, latitude or longitude, or bottom depth with the two main gradients in community structure in both the PCO of FL and PA communities (fig. 3). Some phylotypes had a higher relative abundance in June 2006 than in May 2007 and 2008 (fig. 3). In the FL community of June 2006 Pelagi, 47.2, and SAR86_4 had higher average relative abundances while Rhodo, Pelagi, and Flavo_3 had higher average relative abundances in the 2006 PA community compared to the 2007 and 2008 bacterial communities. These

phylotypes are therefore good discriminators between the June 2006 and the other campaigns, (table 5).

Table 5. Results of the SIMPER routine for all stations and depths (≤80 m) sampled during the campaigns, except stations 8-1, to determine the average abundance of the phylotypes (Av. Abund.) which were typical for the June 2006 campaign compared to the May 2007 and 2008 campaigns. The total average dissimilarity of the phylotypes differentiating the 2006 from the 2007 and 2008 campaign was 55.4% for the FL bacterial communities (a) and 71.3% for the PA bacterial communities (b).

(a)

Phylotype	2006 Av. Abund.	2007 & 2008 Av. Abund.	Av.Diss. %	Diss/SD	Cum. Contrib. %
Pelagi	0.25	0.10	8.12	1.72	14.66
Gam_4	0.13	0.18	6.65	1.25	26.67
Rhodo	0.22	0.22	5.35	1.35	36.34
PsAlt_2	0.01	0.08	4.10	0.63	43.74
47.2	0.09	0.03	3.90	1.25	50.78
Flavo_4	0.02	0.06	2.98	0.78	56.16
SAR86_3	0.05	0.04	2.65	1.19	60.94
Flavo_1	0.03	0.07	2.62	1.08	65.67
Flavo_5	0.02	0.05	2.50	0.72	70.19
Flavo_2	0.03	0.03	2.20	0.76	74.16
SAR86_4	0.04	0.00	2.15	0.75	78.04

(b)

Phylotype	2006 Av. Abund.	2007 & 2008 Av. Abund.	Av.Diss. %	Diss/SD	Cum. Contrib. %
PsAlt_2	0.09	0.16	8.79	0.98	12.33
Flavo_4	0.09	0.17	7.56	1.09	22.93
Pelagi	0.15	0.04	6.28	1.37	31.74
Rhodo	0.17	0.08	5.33	1.56	39.22
Flavo_5	0.02	0.09	4.40	0.77	45.39
Flavo_3	0.07	0.02	3.88	0.91	50.84
Gam_4	0.08	0.03	3.69	1.37	56.02
Flavo_1	0.02	0.07	3.14	0.98	60.42
Flavo_2	0.04	0.03	2.88	0.77	64.46
Gam_3	0.03	0.03	2.39	0.84	67.81
Gam_7	0.03	0.02	2.00	0.37	70.63
53.4	0.02	0.03	1.73	0.67	73.05
47.2	0.03	0.01	1.57	0.57	75.25

At the La Chapelle and Meriadzek area the structure of both FL and PA communities at surface (≤ 20 m depth) was significantly different from that of the deeper communities (80 – 150 m) in all campaign years (table SP3). This depth gradient was more pronounced in the PA communities than in the FL communities (dissimilarity surface-deep FL and PA: 51.2% and 75.3%). In the FL bacterial community the relative abundance of certain phylotypes was either positively (Gam_4, SAR86_3, 61.6) or negatively correlated (Rhodo and Flavo_2) with increasing water depth (fig. 3), while in the PA bacterial community the relative abundance of the Flavo_5, Flavo_2 and Flavo_4 displayed respectively, a positive and negative correlation with depth (fig. 3). Based on the relative band intensities in samples of the upper mixed-layer of the water column, Rhodo (26% ± 10%), Pelagi (18% ± 12%), and Gam_4 (10% ± 10%) were proportionally more abundant in the FL fraction, while in the PA fraction Flavo_4 (19% ± 17%), Rhodo (12% ± 7%), PsAlt_2 (10% ± 14%), and Pelagi (9% ± 10%) made up the highest share of the community. In deeper samples (80 – 150 m), the dominant phylotypes in the bacterial communities were Gam_4 (25% ± 10%), Rhodo (13% ± 5%), Pelagi (12% ± 8%), and PsAlt_2 (9% ± 14%) for the FL bacteria, and PSAlt_2 (18% ± 22%), Flavo_5 (11% ± 10%), and Flavo_1 (8% ± 9%) for the PA bacteria.

Fig. 3. (next two pages) PCO diagrams summarising the variation in bacterial community structure along the first two ordination axes for all stations (a) free-living bacterial community, (b) particle-associated bacterial community (2006: red, 2007: blue, 2008: green). In the upper diagrams, only phylotypes that had a higher than 40% fit along one of the axes are shown to avoid cluttering of the diagrams. Spatial and temporal variables are added as supplementary variables in the lower diagrams. Those which correlate significantly ($p<0.05$) to one of the PCO axes are printed in black, others are in grey.

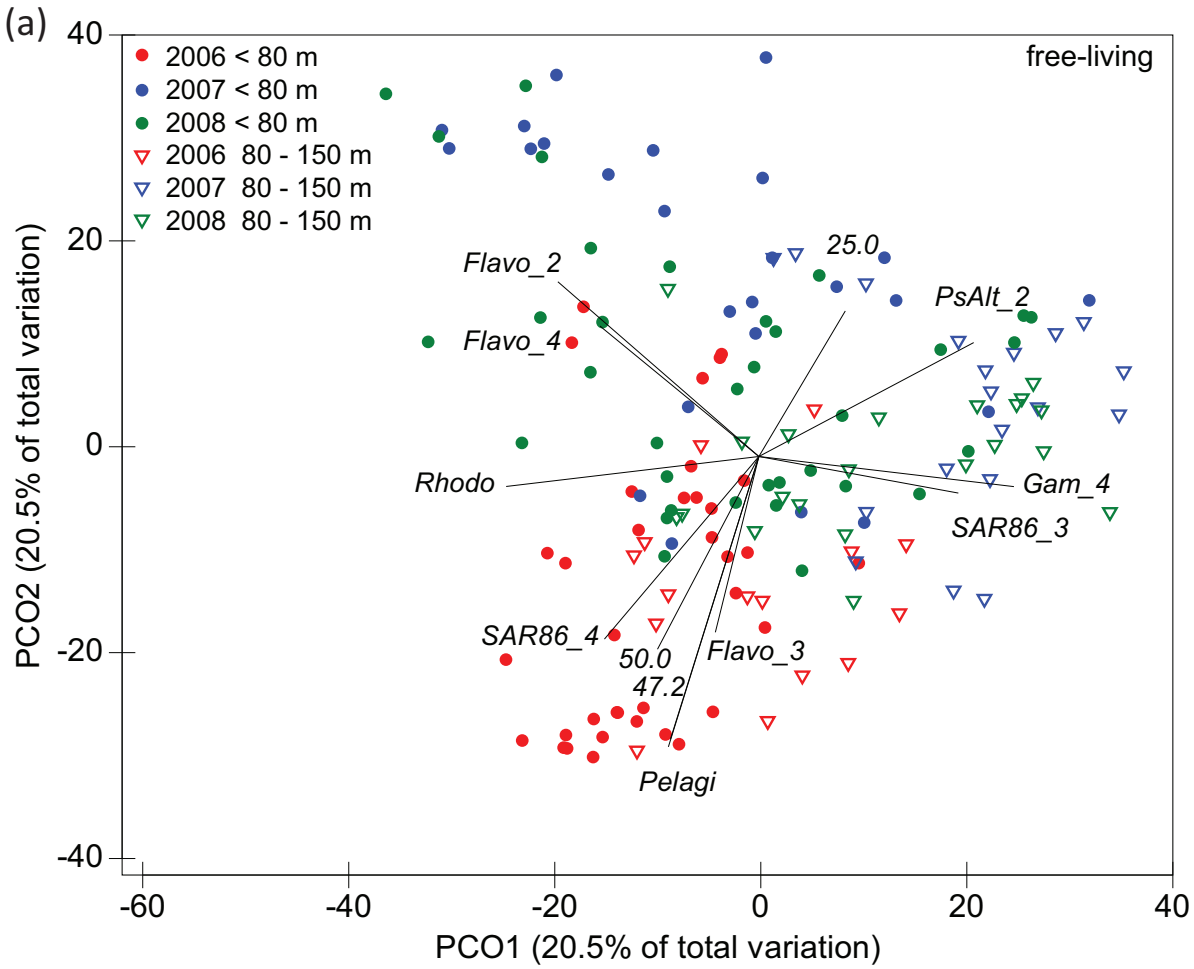
(a)
free-living
2006 < 80 m
2007 < 80 m
2008 < 80 m
2006 80 - 150 m
2007 80 - 150 m
2008 80 - 150 m
Flavo_2
Flavo_4
25.0
PsAlt_2
Rhodo
Gam_4
SAR86_3
SAR86_4
50.0
47.2
Flavo_3
Pelagi
PCO2 (20.5% of total variation)
PCO1 (20.5% of total variation)
40
20
0
-20
-40
-60
-40
-20
0
20
40

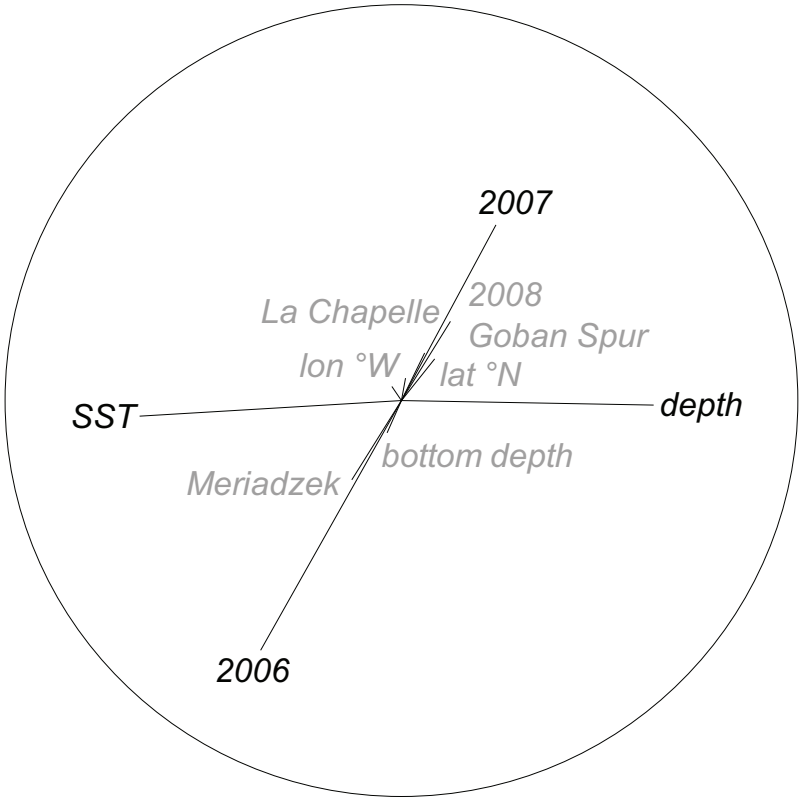
2007
2008
La Chapelle
Goban Spur
lon °W
lat °N
SST
depth
bottom depth
Meriadzek
2006

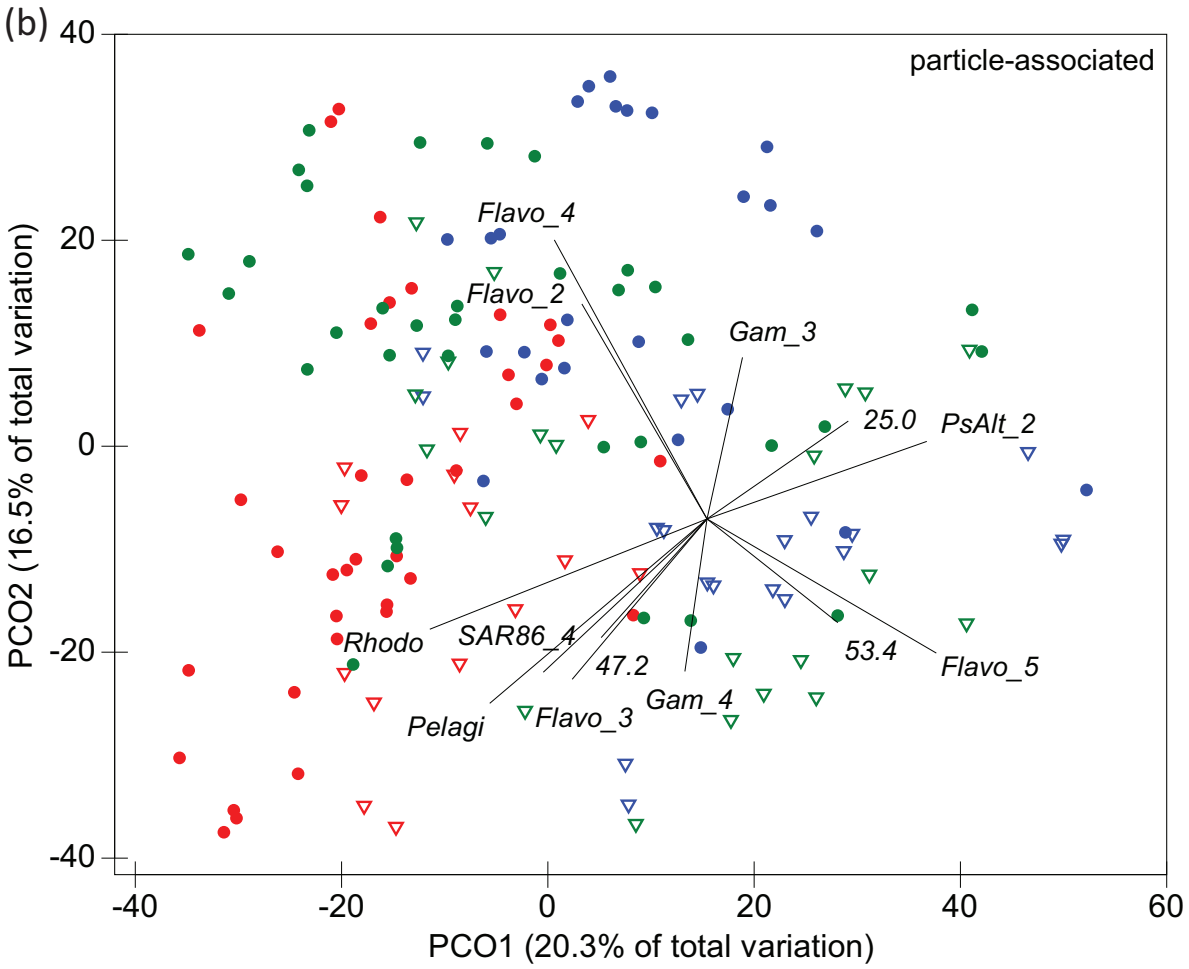
(b)
particle-associated
PCO2 (16.5% of total variation)
PCO1 (20.3% of total variation)
40
20
0
-20
-40
-40
-20
0
20
40
60
Flavo_4
Flavo_2
Gam_3
25.0
PsAlt_2
Rhodo
SAR86_4
47.2
53.4
Flavo_5
Pelagi
Flavo_3
Gam_4

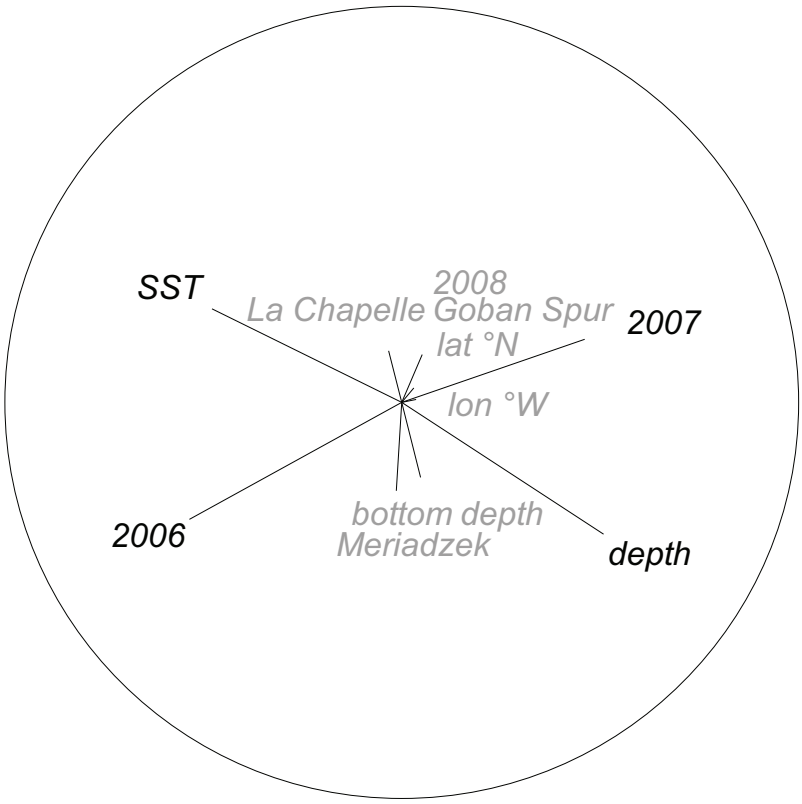
SST
2008
La Chapelle Goban Spur
2007
lat °N
lon °W
2006
bottom depth
Meriadzek
depth

During our campaigns, the water column of the stations on the slope of the continental margin was generally less stratified than those on the shelf (median stratification degree at shelf stations = 0.32 kg m^{-3}; slope stations = 0.22 kg m^{-3}) (see chapter 2, (Van Oostende et al. *in prep. a*)). The difference in community structure between the FL bacterial communities on the shelf and the slope of the La Chapelle and Meriadzek area were significant except in 2006 (pairwise tests: p(2006)= 0.056, p(2007)=0.009, p(2008)=0.048), however we did not find significant differences between the structure of the PA bacterial communities of stations on the slope and the shelf of the continental margin (table SP3). Furthermore, the FL communities at surface and from deeper samples resembled each other significantly more on the slope than on the shelf (pairwise comparisons: 53.4% and 47.8% similarity, respectively), indicating stronger connectivity between surface and deeper communities at the slope.

Discussion

Community composition of bacterioplankton in the northern Bay of Biscay

The importance of the three main marine phylogenetic classes, *Alphaproteobacteria*, *Gammaproteobacteria*, and the *Bacteroidetes*, has also been observed in other coastal and oceanic environments (Fuhrman and Hagström, 2008; Gilbert *et al.*, 2009; Wietz *et al.*, 2010) (tables 3 and 4, 1 and 2). The most dominant phylotypes in the *Alphaproteobacteria* class were affiliated to the SAR11 cluster and the *Rhodobacteraceae* (including the *Roseobacter* clade) (table 1 and 2). The SAR11 cluster is a diverse lineage which constitutes about 33% of many euphotic zone communities (Morris *et al.*, 2002; Acinas *et al.*, 2004), while members of the *Roseobacter* clade typically constitute about 15% in mixed layer ocean communities (Zubkov *et al.*, 2001b; Buchan *et al.*, 2005). In a multi-annual study on the seasonal and vertical structure of microbial communities in the north-western Sargasso Sea, Treuch *et al.* (Treusch *et al.*, 2009) found that the relative abundance of RFLP fragments affiliated to SAR11 (19%) overshadowed that of other organisms. This observation is analogous to the often high relative abundance of SAR11 affiliated phylotype Pelagi in our results (18% ± 12%). The prevalence of the Rhodo phylotype affiliated to the *Rhodobacteraceae* in our study is probably due to occurrence of phytoplankton, and more specifically coccolithophorid blooms in 2006 (fig. 3 and table 5). Members of the *Roseobacter* clade,

which are *Rhodobacteraceae*, have indeed been reported to be associated with blooms of phytoplankton and more specifically coccolithophores (Gonzalez *et al.*, 2000; Vila *et al.*, 2004; Rink *et al.*, 2007), which formed blooms during our studies (see chapter 2).

About 40% of the identified phylotypes belonged to the *Gammaproteobacteria* (table 1 and 3), several of which were well-represented throughout the dataset (e.g. SAR86_3, Gam_4 and PsAlt_2). However, the majority of other gammaproteobacterial phylotypes were less common. As in our study, members of the SAR86 and *Pseudoalteromonas* clade have previously been shown to be important constituents of the bacterioplankton during phytoplankton blooms (Gonzalez *et al.*, 2000; Alonso-Gutierrez *et al.*, 2009; Wietz *et al.*, 2010). This may be explained by their rapid potential growth rates, well-suited for a feast-and-famine life-style. In this respect, the competitive growth advantage in environments experiencing nutrient pulses (Pernthaler *et al.*, 2001) and the capability for rapid chemotactic response of *Pseudoalteromonas* strains (Stocker *et al.*, 2008) may explain its high relative abundance in our study area, where phytoplankton blooms are triggered by intermittent nutrient injection at the shelf edge (Joint *et al.*, 2001; Sharples *et al.*, 2009; Harlay *et al.*, 2010). The gammaproteobacterial SAR86 clade is one of the most common groups observed in clone libraries constructed from surface water samples, especially when stratification is high; they were absent from water below 100 m depth, except after convective overturn (Treusch *et al.*, 2009). In our study, the relative abundance of the SAR86_3 phylotype increased with depth, suggesting it has a different niche than the SAR86 phylotypes reported by (Treusch *et al.*, 2009) (see also chapter 5 (Van Oostende et al. *in prep. d*)).

Bacteria belonging to the *Bacteroidetes* are highly diverse, having been found in a wide range of habitats, and may account for as much as half of all bacterioplankton cells potentially detected in a seawater sample by fluorescent *in situ* hybridisation (Cottrell and Kirchman, 2000). We found several phylotypes affiliated to the *Flavobacteria* class, a member of the *Bacteroidetes* and one of the most abundant bacterioplankton classes, which displayed a high similarity with sequenced clones from previous studies from diverse habitats (Alonso *et al.*, 2007; Alonso-Gutierrez *et al.*, 2009; Gomez-Pereira *et al.*, 2010) (table 1 and 2). The phylotype Flavo_5 is related to the *Polaribacter* genus, an abundant member of the *Flavobacteria* clade, which has been especially associated with colder water masses of

the North Atlantic Ocean and has been detected in the phycosphere of nanophytoplankton cells (Gomez-Pereira *et al.*, 2010).

Variable dynamic exchange between FL and PA community members

Compositional distinctiveness of the FL and PA bacterial populations in our studies was not absolute but rather constituted a gradient of similarity in community structure varying with the environmental conditions associated with each campaign. Such a varying degree of overlap in community composition has also been reported in other studies (Hollibaugh *et al.*, 2000; Moeseneder *et al.*, 2001; Ghiglione *et al.*, 2009) and indicates exchange between both populations. However, other authors reported pronounced differences between FL and PA bacteria in respectively coastal, off-shore, and estuarine environments (Delong *et al.*, 1993; Acinas *et al.*, 1999; Crump *et al.*, 1999). These discrepancies may result from methodological artefacts such as different fractionation procedures or molecular techniques. An underestimation of the differences in community structure can result from the imperfect separation of both size fractions during the collection procedure. Free-living bacteria can be retained in the PA sample due to clogging of the pre-filter and PA bacteria may be dislodged during the filtration process. However, no clogging of the pre-filters was observed during the filtration procedure. On the other hand, differences in particle load, trophic status, and phytoplankton bloom type have been shown to influence the partition between FL and PA communities (Fandino *et al.*, 2005; Zhang *et al.*, 2007; Ghiglione *et al.*, 2009). In this respect, we noted that the similarity between the structure of FL and PA communities varied from year to year (fig. 2). The later period of sampling during 2006, allowing more time for the surface water layer to warm up (chapter 2, table 1), could provide an explanation for this observation although nutrient concentration and phytoplankton bloom dynamics have been shown to influence bacterial communities as well. The relation between environmental and phytoplankton variables is further explored in chapter 5 ((Van Oostende et al. *in prep. d*).

Members of the *Flavobacteria*ceae, *Polaribacter* sp., and a *Pseudoalteromonas* sp. were typically more dominant in the PA fraction, while *Rhodobacteriaceae*, the SAR11 group and the *Gammaproteobacteria* were typically found in the FL community (table 4). These results are consistent with the mostly reported life mode of most of these genera. Commonly, *Bacteroidetes* are thought to be taking part in organic matter degradation by having developed adaptations to the degradation of polymeric organic carbon substances and a

distinct capability for surface adhesion (Bauer *et al.*, 2006), which may explain their prominence in the PA community. This has been demonstrated for *Polaribacter* sp. strain MED152, which contains a substantial number of genes for attachment to surfaces or particles, gliding motility, and polymer degradation (Gonzalez *et al.*, 2008). Although the *Pseudoalteromonas* phylotype PsAlt_2 was also present in the FL community, surface-associated life mode adaptations revealed by genome analysis (Thomas *et al.*, 2008) may explain its prevalence in the PA communities in our study. Furthermore, members of the *Pseudoalteromonas* clade may play a similar role to *Bacteroidetes* as particle colonizers, as suggested by the large share of hydrolytic enzymes detected in its protein secretome, potentially making it an efficient degrader of complex organic matter (Thomas *et al.*, 2008). The Rhodo phylotype, probably affiliated to the *Roseobacter* clade based on the associated clone sequence identity (Macián *et al.*, 2005), was proportionally more abundant in FL than in PA communities in our study. However, their abundance is often highest near phytoplankton blooms or in association with organic particles, suggesting that cell-surface interactions are a defining feature of lineage members (Slightom and Buchan, 2009). Nonetheless, the same authors concluded that diversity of members of the *Roseobacter* lineage was probably related to transition between sessile and planktonic life mode, by e.g. loss of chemotaxis genes, which would reflect the versatility necessary for clade members to predominate in disparate and varied environments (Slightom and Buchan, 2009).

Thus, operational distinction between PA and FL bacteria may rather reflect a continuum in life strategies, ranging from particle specialists to generalists, which are influenced by specific circumstances, such as quorum-sensing, grazing pressure, or the formation of bacterial and colloidal networks (Grossart *et al.*, 2006b; Malfatti and Azam, 2009).

Vertical community patterns and the influence of mixing at the shelf slope

In general, the PA bacterial community showed a more pronounced depth gradient (surface - 150 m) compared to the FL community (fig. 3). This is in contrast to the conclusions of Moeseneder *et al.* (2001), who found a stronger depth gradient in the FL than the PA communities and hypothesized that the sedimentation of particles would transfer the newly colonizing bacteria to greater depth, ultimately leading to a more uniform PA community over the water column. In an environment of low turbulence Ghiglione *et al.* (2007) reported a similar depth gradient in the community structure of both FL and PA bacteria, and

suggested that the bacterial exchanges between both FL and PA communities occurred as a strategy to adapt to trophic and physical changes with depth. Our results suggest a change in particle composition with increasing depth. Although some phylotypes were shown to display a depth-related distribution, the gradient in community structure from surface to 150 m depth was all by all modest, suggesting regular mixing events occur in our area of study. In this respect, internal tides have been shown to cause turbulent mixing at the shelf edge in the study area (Pingree and New, 1995; Sharples *et al.*, 2007). These mixing events are modulated by the spring-neap tide transition and their intensity is irregular along the shelf break of the Bay of Biscay but highest at the La Chapelle Bank (Huthnance *et al.*, 2001; Sharples *et al.*, 2007). This is in agreement with our observation that stations located over the shelf display a more pronounced depth gradient in FL community structure than the slope stations.

Conclusions

Here we presented the first comprehensive, multi-annual account of the community composition of pelagic bacterial communities along the continental shelf break of the northern Bay of Biscay (NE Atlantic Ocean) using a combination of DGGE and clone libraries. Despite significant inter-annual differences in community structure probably reflecting the different bloom conditions, the high degree of compositional overlap between years supports the notion of predictability of bacterial assemblages (Fuhrman et al. 2006). Likewise, despite differences between the structure of FL and PA bacterial communities there was a substantial overlap in composition between both, with most differences related to differences in relative abundance of phylotypes rather than presence-absence. While there were significant differences in community structure between the different sampling areas along the shelf break, we also observed a significant albeit modest depth gradient in community structure in the upper 150 m of the water column. Turbulent mixing at the slope stations probably caused a stronger exchange between FL bacterial communities from the deeper and the surface water layers compared to stations located over the shelf, while this exchange was not influenced by the station's location for the PA communities.

Acknowledgements

The authors sincerely thank the officers and crew members of the R.V. Belgica for their logistic support during the campaigns. J. Backers, J.-P. De Blauw, and G. Deschepper of the Unit of the North Sea Mathematical Models (Brussels/Ostend, Belgium) are acknowledged for their support in data acquisition during the field campaigns. S. Groom is acknowledged for providing remote sensing images. We are grateful to C. Souffreau, A. De Wever, B. Vanelslander, and D. De Bock for their assistance during sample collection. We thank T. Verstraete and S. D'Hondt for performing most of the molecular analyses, and J. Goris at Applied Maths for database building support. Finally, we are grateful to all members of the PEACE network for their support during the campaigns. This study was financed by Belgian Federal Science Policy Office in the framework of the PEACE project (contract numbers SD/CS/03A and SD/CS/03B). N. Van Oostende received a PhD grant from the agency for Innovation by Science and Technology (IWT-Flanders).

Supplementary tables

Table SP1. Relatedness of phylotypes to known organisms. Phylogenetic affiliation of SSU rRNA gene sequences from excised DGGE bands representative for each bandclass (phylotype). Phylotypes of eukaryotic origin or where more than one sequence type was found after excision, and hence could not unambiguously be assigned to a single band class. Sequence similarity is given next to the accession number of the Genbank relatives in the right-hand column.

Phylotype	GenBank acc. no.	Phylogenetic affiliation	Relative in GenBank and sequence similarity
Cnid_1	HQ686086	*unclassified*	*Diadumene cincta* 18S ribosomal RNA gene; EU190856 (100%)
SAR86_1	HQ686087	*Gammaproteobacteria*	Uncultured *gamma proteobacterium* clone 4810-27F; FR648221 (100%)
SAR86_1	HQ686088	*Bacteroidetes*	Uncultured *Flavobacteria* bacterium clone Vis_St6_22; FN433457 (92%)
SAR86_2	HQ686089	*Gammaproteobacteria*	Uncultured *gamma proteobacterium* NAC11-11; AF245636 (99%)
Cryo	HQ686093	*Flavobacteriales*	Uncultured *Bacteroidetes* bacterium clone SHBC947; GQ350657 (100%)
Cnid_2	HQ686094	*unclassified*	*Resomia* sp. SHDH-2008a 18S ribosomal RNA gene; EU880275 (99%)
Gam_1	HQ686095	*Gammaproteobacteria*	Uncultured *gamma proteobacterium* clone 23; AM748198 (97%)
Gam_1	HQ686096	*Bacteroidetes*	Uncultured CFB group bacterium clone 51; AM748226 (97%)
Gam_5	HQ686103	*Bacteria*	uncultured marine bacterium clone LibG_C09; FR686191 (100%)
Gam_5	HQ686104	*Flavobacteriaceae*	Uncultured *Bacteroidetes* bacterium clone Flo-11; AY684355 (100%)
Pras_1	HQ686105	*Chlorophyta*	Uncultured *Micromonas* clone 1_F1; EU600587 (100%)
Pras_1	HQ686106	*Gammaproteobacteria*	Uncultured *gamma proteobacterium* clone C13W_124; HM057690 (100%)
Pras_1	HQ686107	*Pseudomonas*	*Pseudomonas fluorescens* strain d3; HQ166099 (95%)
PsAlt_1	HQ686108	*Pseudoalteromonas*	*Pseudoalteromonas mariniglutinosa* strain: Do-80; AB257337 (100%)
PsAlt_1	HQ686109	*Gammaproteobacteria*	*Gamma proteobacterium* HTCC6370; EF182733 (100%)
Ehux	HQ686111	*Cyanobacteria*	Uncultured prymnesiophyte C8704; HM565911 (100%)
Gam_8	HQ686113	*Gammaproteobacteria*	Uncultured *gamma proteobacterium* clone C13W_103; HM057685 (100%)
Bact_2	HQ686114	*Flavobacteriaceae*	Uncultured *Flavobacteria* bacterium clone Vis_St6_90; FN433396 (100%)

Table SP1. Continued.

Phylotype	GenBank acc. no.	Phylogenetic affiliation	Relative in GenBank and sequence similarity
Crypt_1	HQ686116	*Bacteria*	Uncultured *Cryptomonadaceae* clone JML-4; FN423911 (96%)
Crypt_1	HQ686117	*Cyanobacteria*	Uncultured bacterium clone SHWN_night2_16S_634; FJ745122 (100%)
Altero_1	HQ686120	*Alteromonas*	Uncultured *Alteromonas* sp. clone DOM16; HQ012277 (100%)
Syncoc	HQ686121	*GpIIa*	Uncultured cyanobacterium clone 4820-27F; FR648231 (100%)
Diat_1	HQ686122	*Bacillariophyta*	Uncultured phototrophic eukaryote clone CBM02C12; EF395719 (100%)
Crypt_2	HQ686123	*Cryptomonadaceae*	*Teleaulax amphioxeia*; AB471793 (100%)
Crypt_2	HQ686124	*Bacillariophyta*	*Chaetoceros socialis* strain NOZ; FJ159135 (100%)
Diat_2	HQ686126	*Bacillariophyta*	Uncultured cyanobacterium clone A_1_ControlD35_A5; GQ242972 (98%)
Diat_2	HQ686127	*Bacteria*	Uncultured marine bacterium clone MOLA_MAY07-5m-51; GU204863 (98%)
Diat_2	HQ686128	*Flavobacteriaceae*	Uncultured *Flavobacteria* bacterium clone Vis_St6_1272; FN433347 (100%)
Copepod	HQ686129	*unclassified*	*Canuella perplexa* strain C16 18S ribosomal RNA gene; EU370432 (100%)
Pras_2	HQ686131	*Chlorophyta*	*Micromonas pusilla* plastid strain CCMP 489; FN563098 (100%)
Alpha_2	HQ686132	*Pelagibacter*	Uncultured SAR11 cluster bacterium HF0770_37D02; GU474927 (100%)
Alpha_2	HQ686133	*Pelagibacter*	uncultured marine bacterium clone LibI_A08; FR686232 (100%)
Pelagi_2	HQ686136	*Pelagibacter*	Uncultured *alpha proteobacterium*; GQ337224 (97%)
UnBa_2	HQ686139	*Bacteria*	Uncultured Gram-positive bacterium clone 71; AM748246 (100%)

Table SP2. Results from two-way crossed PERMANOVA analyses assessing the differences in community structure between FL and PA bacteria and the effect of campaign year for the entire dataset (n=301) of bacterial community (BC) (a), and analyses assessing the effect of sampling area (locality) and campaign year on the structure of either the FL or PA BC (b).

(a) Factors		**total BC**
FL-PA	df	1
	MS	47719
	pseudo-F	34.64
	p	0.0001
year	df	2
	MS	36152
	pseudo-F	26.24
	p	0.0001
FL-PA x year	df	2
	MS	5193
	pseudo-F	3.77
	p	0.0001
Res	df	295
	MS	1378

(b) Factors		**FL BC**	**PA BC**
locality	df	2	2
	MS	5023	5211
	pseudo-F	5.47	3.29
	p	0.0001	0.0002
year	df	2	2
	MS	18290	20904
	pseudo-F	19.93	13.21
	p	0.0001	0.0001
	df	3	3
locality x year	MS	3505	5027
	pseudo-F	3.82	3.18
	p	0.0001	0.0001
Res	df	139	138
	MS	918	1583

Table SP3. Results from three-way crossed PERMANOVA analyses assessing the effect of campaign year and location of the sampling stations on the shelf or the slope of the continental margin, and at surface (≤ 20 m) or deeper (80 m -150 m) on the community structure of FL (a) and PA (b) bacteria in the La Chapelle and Meriadzek area.

(a)	**FL BC LC&M surface-deep**			
Factors	df	MS	pseudo-F	p
shelf-slope	1	1907	2.51	0.0152
surface-deep	1	7381	9.73	0.0001
year	2	9816	12.94	0.0001
shelf-slope x surface-deep	1	507	0.67	0.7003
shelf-slope x year	2	2144	2.83	0.0010
surface-deep x year	2	1053	1.39	0.1557
shelf-slope x surface-deep x year	2	145	0.19	0.9976
Res	67	759		

(b)	**PA BC LC&M surface-deep**			
Factors	df	MS	pseudo-F	p
shelf-slope	1	2662	1.86	0.0798
surface-deep	1	7508	5.25	0.0003
year	2	11962	8.36	0.0001
shelf-slope x surface-deep	1	2038	1.43	0.1959
shelf-slope x year	2	2535	1.77	0.0481
surface-deep x year	2	2102	1.47	0.1166
shelf-slope x surface-deep x year	2	629	0.44	0.9492
Res	66	1430		

4

Influence of phytoplankton bloom composition and water column stratification on the bacterial community structure during coccolithophorid blooms in the northern Bay of Biscay (2006-2008)

Nicolas Van Oostende[1], Jérôme Harlay[2], Caroline De Bodt[2], Alberto Vieira Borges[3], Kim Suykens[3], Lei Chou[2], Wim Vyverman[1], Koen Sabbe[1]

[1] Laboratory for Protistology and Aquatic Ecology, Biology Department, Ghent University, Krijgslaan 281 – S8, B-9000 Gent, Belgium.

[2] Laboratoire d'Océanography Chimique et Géochimie des Eaux, Université Libre de Bruxelles, Campus de la Plaine, CP208, boulevard du Triomphe, B-1050 Brussels, Belgium.

[3] Chemical Oceanography Unit, Université de Liège, Institut de Physique (B5), B-4000 Sart Tilman, Belgium.

Authors' contributions

NVO, JH, LC and KS conceived and designed the study. CDB, JH and LC performed the nutrient, particulate matter and TEP concentration measurements. LC measured the DMS and DMSP concentration. KS measured the total alkalinity. NVO performed the pigment and DGGE analyses. NVO analysed the data and wrote the manuscript. KS, JH, AVB, WV, and LC revised the manuscript.

Abstract

We analysed the community structure of free-living (FL) and particle-associated (PA) bacteria in the upper mixed layer of the water column on 34 occasions in late spring along the NE Atlantic continental margin (2006-2008, Bay of Biscay). We used ordination methods and variation partitioning to relate the bacterial community structure and composition to changes in physical (e.g. water column stratification), biogeochemical (e.g. nutrients and transparent exopolymer particles (TEP), anomaly of total alkalinity), and phytoplankton composition (chemotaxonomic groups).

Variation in the FL and PA community structure during the three campaigns was generally related to the same set of spatial, temporal, environmental, and phytoplankton variables which together explained, 43.8% and 37.7% of the total variation in the FL and PA data sets respectively, but showed significant overlap between one another (16.8% and 13.5%, respectively). We observed significant correlations between the occurrence of dominant phylotypes, affiliated to the SAR86, *Rhodobacteraceae*, SAR11, and *Flavobacteria*, with environmental variables (e.g. stratification degree, TEP, nutrients, dissolved dimethylsulphoniopropionate (DMSPd)) and the biomass of phytoplankton groups. The proportion of explained variation in community structure during each campaign was consistently lower for the PA compared with the FL communities and differed more than threefold between years. This suggests that different factors regulate both communities and that bacterial community structure within each year could be shaped by unaccounted factors or showed non-linear responses to environmental conditions. The structure of the multi-annual communities was significantly correlated to the abundance of phytoplankton groups (diatoms, coccolithophores, prasinophytes, dinoflagellates, and cryptophytes), which uniquely explained 4.3% and 7.4% of the total variation in the FL and PA community structure. Finally, we found that water column stratification had a profound direct and/or indirect influence on shaping succession in the pelagic bacterial communities in our study area, suggesting a significant degree of determinism in bacterial community assembly similar to that of phytoplankton communities.

Introduction

Seasonal changes in water column thermal stratification and mixing are known to be important factors regulating changes in marine phytoplankton and bacterial community structure (Morris *et al.*, 2005; Fuhrman *et al.*, 2006; Henson *et al.*, 2006; Alonso-Gutierrez *et al.*, 2009; Carlson *et al.*, 2009; Treusch *et al.*, 2009; Behrenfeld, 2010) (see also chapter 2, (Van Oostende *et al.*, *in prep. a*)). Pelagic bacterial community structure can be successfully predicted on the basis of temporal patterns of environmental variables, such as temperature, oxygen, chlorophyll *a*, and macronutrient concentrations, over seasonal and multi-annual scales (Fuhrman *et al.*, 2006). Recurrent temporal patterns in the occurrence of different bacterial groups also suggest that there is only a low level of redundancy within marine bacterial communities (Fuhrman *et al.*, 2006). Nonetheless, bacterial communities are probably shaped by a complex network of interactions among its members, phytoplankton, heterotrophic protist, viri, and the physical environment Fuhrman and Steele (2008)

Several studies have described changes in composition and structure of bacterial communities during phytoplankton blooms (Riemann *et al.*, 2000; Fandino *et al.*, 2001; Pinhassi *et al.*, 2004; Rink *et al.*, 2007; Sapp *et al.*, 2007a; Jones *et al.*, 2010), which may be pivotal to the cycling of the phytoplankton-derived dissolved organic matter (DOM) (Frette *et al.*, 2010; McCarren *et al.*, 2010). These changes can on the one hand be attributed to the environmental conditions and on the other hand to biotic interactions (such as grazing and lysis, see chapter 5, (Van Oostende *et al.*, *in prep. b*)), which also drive the development and composition of the phytoplankton blooms. Moreover, evidence is building that close interactions between specific bacterial species with particular phytoplankton species and their organic matter production exist (Grossart *et al.*, 2005; Hasegawa *et al.*, 2007; Sapp *et al.*, 2007b; Amin *et al.*, 2009; Sarmento and Gasol, subm.). Because physicochemical factors such as temperature and nutrient regime structuring the bacterioplankton community often correlate with those that shape the phytoplankton assemblage (Sapp *et al.*, 2007a; Teira *et al.*, 2008), it is difficult to separate and quantify the effect of phytoplankton on the bacterial community structure. Although the use of multivariate statistics and ordination techniques in microbial ecology is increasing (Ramette, 2007), few studies accounted for the inter-

correlation between environment and phytoplankton to untangle and quantify the unique effect of changes in environmental conditions and phytoplankton community composition on bacterial community structure (but see: Muylaert *et al.*, 2002; Van der Gucht *et al.*, 2007; Lear *et al.*, 2008)).

Spring phytoplankton blooms along the continental margin of the Bay of Biscay (NE Atlantic) are characterized by the alternation of diatom and coccolithophore-dominated communities (Lampert *et al.*, 2002; Harlay *et al.*, 2010), which is believed to be controlled by the depletion of nutrients (notably silicic acid) following phytoplankton growth and increases in water column stratification during spring and summer, and the northward advection of water masses over the continental shelf ((Leblanc *et al.*, 2009) and references therein) (see also chapter 2, (Van Oostende *et al.*, *in prep. b*)). However, wind-induced mixing and turbulent tidal mixing at the shelf edge can partly reset this phytoplankton bloom succession and will probably influence the bacterioplankton assemblage as well. While there was a large degree of overlap in the general composition of late spring particle-associated (PA) and free-living (FL) bacterial communities in this area between consecutive years (chapter 3, (Van Oostende *et al.*, *in prep. c*)), significant inter-annual differences in community structure probably reflected the different environmental and bloom conditions The general composition of late spring FL and PA bacterial communities in the top 150 m of the water column along the continental margin of the Bay of Biscay in the period 2006-2008 is described in chapter 3 (Van Oostende et al. *in prep. c*).

Here, we describe the variation in the structure of these communities in relation to environmental conditions and phytoplankton composition and development in the upper mixed layer of the water column. We hypothesize that water column stratification and nutrient depletion, as well as phytoplankton composition will impact bacterial community structure, and that the effect of the latter factor would be greater on the community structure of PA compared with the FL bacteria. In order to assess these multivariate relations we performed principal coordinates and correlation analyses on bacterial community fingerprints obtained by denaturing gradient gel electrophoresis (DGGE), complemented with clone libraries. To quantify the unique contribution of spatial, temporal, environmental, and phytoplankton variables to explaining the variation in bacterial community structure we performed variation partitioning using distance-based redundancy analyses.

Methods and Materials

Description of the study area and its hydrography

The continental margin in the northern Bay of Biscay (NE Atlantic Ocean) is characterised by a broad continental shelf (the Celtic Sea) and delimited westwards by a steep slope down to 4000 m depth (chapter 3, fig. 1). At the shelf edge of the Celtic Sea, large semi-diurnal tidal currents cause large internal tides which induce vertical displacement of the water column (Pingree and New, 1995). In total, 34 stations were sampled in 2006 (from the 31st of May to the 9th of June), 2007 (from the 10th to the 24th of May), and 2008 (from the 7th to the 23rd of May), of which 7 stations were revisited 6 to 14 days later (table SP1). Most of the stations were located in the vicinity of the La Chapelle Bank while 8 stations were located over the shallow part (<200 m depth) of the Goban Spur, towards the Irish coast (chapter 3, fig. 1). Eight deeper stations (from 450 to 1400 m depth) were located over the continental slope at the Meriadzek Terrace and the La Chapelle Bank.

Sample collection

Seawater samples were collected using a rosette of 12 Niskin bottles (10 l) coupled to a conductivity, temperature-pressure probe (Seabird SBE21). The degree of stratification of the water column (strat. deg.) was calculated as the difference in seawater density at 100 m and at 10 m depth (table SP1); these depths were selected to avoid diurnal changes in water density occurring at the surface and to include water from below the thermocline (when present). The upper mixed layer depth (MLD) was operationally defined as the depth where water density increased by 0.1 kg m^{-3} compared to the density of the surface layer (10 m). The depth of the nitracline, a proxy of nutrient supply to the upper mixed layer of the ocean, was operationally defined as the depth at which nitrate+nitrite concentration was 1.00 µmol l^{-1}. The steepness of the pycnocline was estimated by using the slope of linear regression between water depth and water density along the pycnocline. Sampling depths covered the surface waters and the thermocline region, and deeper waters (down to 150 m depth).

For the bacterial community analyses we only used samples from the upper mixed layer and including the depth at which chlorophyll *a* (Chla) was maximal. At station 8-6, which lacked a thermocline, only bacterial community samples of the upper 20 m which included the depth of Chla maximum were used in the analyses.

Analytical methods for biogeochemical variables

Photosynthetic pigments were extracted from glass fibre filters and quantified by HPLC as described in chapter 2 (Van Oostende *et al.*, *in prep. a*). Chlorophyll *a* concentration (Chla) was used as a proxy for photosynthetic biomass and was partitioned among phytoplankton groups using CHEMTAX routine based on plankton group-specific marker pigments (Mackey *et al.*, 1996; Latasa, 2007). Dissolved nutrient concentrations (NOx: nitrate and nitrite, PO_4: orthophosphate, dSi: silicic acid) were determined as described in Harlay *et al.* (2010).

Bacterial abundance was determined by epifluorescence microscopy where at least 600 cells were counted in at least 25 fields of view. Samples were preserved with paraformaldehyde (filtered through a 0.2 µm pore-size filter) (final concentration, 2% [wt/vol]), stained with a final concentration of 5 µg of 4',6-diamidino-2-phenylindole (DAPI) ml^{-1} for 15 min and filtered onto black 0.2 µm pore-size polycarbonate filters at a pressure of 100 to 200 mm Hg (Porter and Feig, 1980). The microscopic slides supporting the filters were stored frozen (-20°C) until analysis two months later.

Particulate organic carbon samples (POC) were collected by filtration of seawater (0.2 – 2 l) through pre-combusted (4h at 500 °C) glass fibre filters (GF/F, Whatman). The filter samples were stored at -20 °C until analysis, within three months after the cruise, and dried overnight at 50 °C prior to analysis. POC was determined using a Fisons NA-2000 elemental analyzer after carbonate removal from the filters by overnight HCl fuming. Particulate nitrogen (PN) concentrations were determined from unacidified filters. Four to five standards of certified reference stream sediment (STSD-2) from the Geological Survey of Canada, together with three to four blank filters, were used for calibration.

Transparent exopolymeric particles (TEP) were measured spectrophotometrically according to the dye-binding assay of Alldredge *et al.* (1993). TEP concentration determined after alcian blue staining and hydrolysis using this method reflects the density of stainable moieties, such as acidic and sulphated sugars, in particulate matter and should thus be considered as a semi-quantitative measure of TEP concentration.

Total alkalinity (TA) was measured by titration using HCl 0.1 M as titrant, and using the Gran method to determine the end-point as described by Suykens *et al.* (2010). The anomaly of TA (TA anomaly) with respect to conservative mixing of water mass was calculated as in Suykens

et al. (2010) to represent $CaCO_3$ production/dissolution and corrected for nutrient uptake/release to exclude the effect of organic matter production/degradation. Oxygen concentration (O_2) was measured with the Winkler technique using a potentiometric end-point determination. Oxygen saturation level ($\%O_2$) was computed from the O_2 saturation using the algorithm of Benson and Krause (1984) as described in Suykens *et al.* (2010).

Dissolved dimethylsulfoniopropionate (DMSPd) concentration was determined from the filtrates of seawater samples (GF/F, Whatman) using a TRACE gas chromatography device (INTERSCIENCE) equipped with a Flame Photometric Detector, as described in chapter 5 (Van Oostende *et al.*, *in prep. b*).

Nucleic acid extraction

Seawater samples for bacterial DNA isolation (50 - 200 ml) were filtered sequentially through cellulose mixed-ester membranes (Millipore) with nominal pore size of 3.0 µm and 0.22 µm, respectively. These bacterial populations were operationally defined as the "particle-associated" (PA) (> 3.0 µm) and the "free-living" (FL) (3.0 - 0.22 µm) fractions respectively. These filters were stored deep-frozen at -70°C until processing as described in chapter 3 (Van Oostende *et al.*, *in prep. c*). DNA was extracted as described by Boström *et al.* (2004). Following extraction, the DNA was purified with a Wizard DNA clean-up system (Promega, Madison, Wisconsin) as specified by the manufacturer.

Fingerprinting and cloning

The purified DNA extract were amplified by PCR with the bacteria-specific primers 357F with GC-clamp and 518R for the denaturing gradient gel electrophoresis (DGGE) analysis. PCR was carried out in a temperature cycler (Biometra, Westburg) according to Van der Gucht et al. (2005). The quality of the purified PCR products was assessed by electrophoresis of an aliquot of the PCR product on a 1.5% (w/v) agarose gel, staining with ethidium bromide, and comparison with a molecular weight marker (Smartladder, Eurogentec) using the software package Bionumerics 4.61 (Applied Maths BVBA, Kortrijk, Belgium). The DNA concentration of the purified and concentrated PCR products were measured spectrophotometrically using a NanoDrop device (Thermo Scientific).

DGGE was performed as described in chapter 3 using a D-Code system from Bio-Rad Laboratories. Following electrophoresis, the DGGE gels were stained with SYBR Gold and

photographed with a CCD camera using UV transillumination (Bio-Rad Laboratories, GelDoc XR). Representative bands in each gel were excised for sequence analysis (see further). In each gel, three marker lanes were included for alignment of the different gels using the software package Bionumerics 4.61. These markers consisted of a mixture of DNA from nine clones obtained from a clone library of the 16S rRNA genes as described by Van der Gucht *et al.* (2001). Band intensities of the selected band classes were standardized per sample in order to calculate relative band intensities per sample (Muylaert *et al.*, 2002).

Excised bands from the gels were eluted overnight in TE buffer at 4°C and amplified using the same primers as above but without GC-clamp. Bands with identical sequence data and position in the gels were used to validate the binning of other bands at the same relative location into a single band class. Representative sequences of the different phylotypes are available from GenBank (http://www.ncbi.nlm.nih.gov) under accession numbers HQ686085 to HQ686139. A complementary clone library was constructed to compare the shorter DGGE band sequences with the near complete 16S rRNA gene sequences obtained this way. Clone library nucleotide sequences are available from GenBank under accession numbers EU394538 to EU394678. Identification of the DGGE phylotypes (see also chapter 3) was performed by aligning them with our own 16S rDNA clone sequence library and by the Sequence Match tool of the Ribosomal Database Project (10.22) (Cole *et al.*, 2009).

We used upper mixed layer community structure data from 147 bacterial community fingerprints, of which 74 in the FL fraction and 73 in the PA fraction. In total, 68 distinct band classes (phylotypes) were identified by DGGE. Eleven of these were of eukaryotic origin, including 8 chloroplast sequences (see chapter 3, tables 1, SP1 and 2). The latter band classes were not included in analyses, as were band classes with ambiguous sequence data (i.e. sequences of multiple origins). In a next step, only band classes that were present in at least 5% of all the samples were used in further analyses (n=35).

Data treatment and statistical analyses

To test the difference in bacterial community structures between life form group (FL and PA) and campaign years (2006, 2007, 2008) a two-way crossed non-parametric permutational analysis of variance (PERMANOVA) was performed using a resemblance matrix based on Bray-Curtis similarities of square root-transformed standardised band intensities (Clarke and

Gorley, 2006; Anderson *et al.*, 2008). Probability values were obtained by permutation ($n=10^4$). Homogeneity of dispersion was tested by PERMDISP analyses for any of the tested terms in each PERMANOVA, checking that patterns found were not confounded by artefacts due to variable's dispersions.

Principal coordinates analysis (PCO) was used as an unconstrained ordination method to assess variation patterns in species composition and relative abundance between bacterial community samples. Bray-Curtis similarity of square root-transformed standardised band intensities were used for the calculation of the PCO axes. Correlations between gradients in community structure and species composition (represented by the PCO axes), environmental variables and relative band intensities (hereafter referred to as relative abundance) of bacterial phylotypes were calculated using the Spearman rank correlation coefficient.

Partitioning of the variation in bacterial community structure related to spatial, temporal, and environmental variables and phytoplankton groups was performed using distance-based redundancy analysis (McArdle and Anderson, 2001) as implemented in the DISTLM routine (Anderson *et al.*, 2008). We used a Bray-Curtis similarity matrix of bacterial community composition data and permutation tests (10^4 iterations) to test the null hypothesis of no relationship between the bacterial community and transformed predictor variables or sets of variables. This allowed us to assess how much variation in the BCC can be explained by sets of predictor variables and to elucidate the unique contribution of each predictor set to the variation in bacterial community structure. Predictor variables were grouped into spatial, temporal, environmental, and phytoplankton predictor sets to test the relative contribution of each set to the total explained variation in bacterial community structure. We distinguished 7 phytoplankton groups based on chemotaxonomic-partitioning of the pigment composition data (see also chapter 2, (Van Oostende et al. *in prep. a*)). In the analyses we introduced 12 environmental variables (strat. deg., MLD, pycnocline steepness, nitracline depth, water temperature, Chla, $\%O_2$, NOx, PO_4, dSi, TA anomaly and TEP concentrations), 8 spatial variables (latitude, longitude, shelf/slope, region (La Chapelle Bank, Meriadzek Terrace or Goban Spur) and distance to the slope (distance of the stations to the 200 m isobath, where slope stations have negative values)), and 3 temporal variables (Julian day, and a nominal variable for each campaign year). Given that the global test for the predictor variables included in each set was significant ($p<0.001$), predictor variables were

included in the appropriate set using a step-wise selection procedure. We used the Bonferroni corrected p-value as an inclusion threshold for variables, to account for these multiple comparisons (initial p-value set at 0.05). As such, the initial value of the probability threshold (p) is divided by the total number of simultaneous independent comparisons (Legendre and Legendre, 1998). Furthermore, we used the parsimonious "adjusted R^2" (R^2 adj.) coefficient as a measure of the proportion of explained variation by the model, which takes the number of samples and variables used in the redundancy analyses into account, and hence allows comparison of the sizes of portions explained by different sets of predictor variables with different numbers of variables (Peres-Neto *et al.*, 2006).

Averages of the data are reported as their arithmetic mean. Square root-transformed standardised band intensities were used in all analyses. The PCO, PERMANOVA and DISTLM analyses were performed using the PRIMER v6 and PERMANOVA+ add-on software (PRIMER-E Ltd., Plymouth, U.K.) (Clarke and Gorley, 2006; Anderson *et al.*, 2008). Permutation tests consisted of 10^4 iterations and the probability threshold was set at 0.05 unless stated otherwise.

Results

Environmental setting and phytoplankton blooms

Weather conditions during the sampling campaigns and the location of the stations on the shelf or the slope of the continental margin influenced the sea surface temperature (SST) distribution and the density structure of the water column (table SP1) (see chapter 2, fig. 1). SST was on average higher during the June 2006 campaign, when weather conditions were particularly sunny and calm. In May 2007, a severe storm during the first leg (from 10 to 16 May) succeeded to a calm and sunny period (from 21 to 24 May), that resulted in a deeper mixed layer and often displayed a sharp thermocline. In May 2008, the weather was overcast during much of the campaign. This led to significant differences in stratification degree of the water column on the shelf between years (table SP1) (chapter 2, (Van Oostende *et al.*, *in prep. a*)). Nutrients in surface waters were often depleted during the three campaigns, with the exception of most slope stations (table SP2). For the distribution of nutrients and POC and PN within the water column of the different stations we refer to chapter 2 (Van Oostende *et al.*, *in prep. a*). A wide range in TA anomalies was observed (from

2 to -28 µmol kg^{-1}, cf. Suykens *et al.,* 2010). Average TEP concentrations in the upper mixed layer were highest in 2006 (ranging from 149 to 1587 µg X eq. l^{-1}), while they were lower in 2007 and 2008 (from 2 to 249 µg X eq. l^{-1}) (table SP2) (Harlay *et al.*, 2009). The concentrations of DMSPd in the upper mixed layer were only determined for a few stations (6-2, 6-7, 6-8, 8-5, 8-5b, 8-9, 8-9b, 8-12) and ranged from 3 µmol l^{-1} at the surface (station 6-7) to 58 µmol l^{-1} at station 8-5b. The distribution of DMSPd within the water column of each station is described in chapter 5 (Van Oostende *et al.*, *in prep. b*).

Bacterial abundances were determined for the 2006 and 2008 campaign (the 2007 samples were lost due to preservation issues). In 2006, bacterial cell densities ranged from 0.60 10^9 to 2.57 10^9 cells l^{-1} at surface, and from 0.38 10^9 to 1.61 10^9 cells l^{-1} at a depth of 80 m. Stations 6-4, 6-6 and 6-7 showed the highest overall cell densities. In 2008, cell densities ranged from 0.45 10^9 cells l^{-1} to 2.51 10^9 cells l^{-1} at surface (at stations 8-5 and 8-10, respectively). In general, bacterial cell numbers decreased with increasing depth.

A wide range in phytoplankton biomass concentration and community composition was observed (table SP3) (see also chapter 2) (Van Oostende et al. in prep. a). Average Chla concentrations in the upper mixed layer ranged from 0.21 to 1.96 µg l^{-1}, and were on average higher during 2006 (table SP3) (chapter 2). Most phytoplankton communities were dominated by diatoms or coccolithophores, but intermediate community types (e.g. coccolithophores with prasinophytes, cryptophytes or dinoflagellates as co-dominants) were also observed (table SP3). Throughout the study, coccolithophores were predominantly represented by *Emiliania huxleyi*, which formed remotely-sensed high reflectance patches at the declining stage of their blooms, when surface waters were characterized by high concentrations of suspended coccoliths (Suykens *et al.*, 2010) (see also chapter 1, fig. 5).

Unconstrained ordination of bacterial communities

In a PCO analysis of the FL bacterial communities (fig. 1), the first two principal components captured 45.3% of the variation in FL community structure. These axes are mainly related to nutrient concentrations, the concentration of TEP, $\%O_2$ and biomass of most phytoplankton groups (except diatoms, coccolithophores and *Synechocccus*) (fig. 1 and table SP2). The main gradient of variation in the PA bacterial community structure is generally related to the same variables as the FL community, except for NOx and PO_4 concentration, while the

second principal component was only significantly related to TA anomaly (fig. 1 and table SP2). These first two principal components together captured 37.7% of the variation in PA community structure. Several physical (e.g. water temperature, the degree of water column stratification, MLD) and the distance of the stations from the shelf edge display significant correlations with the PCO axes of both communities as well (fig. 1 and table 1). The lack of significant correlation between the PCO axes and depth of sampling indicate the lack of community gradient in the upper mixed layer.

The structure of FL and PA bacterial communities from the upper mixed layer in each campaign year differed from each other, yet with a consistent overlap in community composition between each year and life mode (table SP4). The significant interaction between bacterial life mode and year (pairwise tests FL-PA: p(2006), p(2007), p(2008), all $p<0.0005$) is evident from the varying degree of similarity between the structure of FL and PA communities with year (FL-PA similarity in 2006: 51.5%, 2007: 42.8%, 2008: 38.9%). As apparent from the PCO diagrams of the FL and PA bacterial communities (fig. 1) and confirmed by PERMDISP analyses, the 2006 community samples clustered more than the 2007 and 2008 samples which were more dispersed, sometimes confounding the between year differences assessed by PERMANOVA (table SP4). Nonetheless, the 2006 bacterial community samples clustered more in the direction of stronger stratification and higher TEP concentrations than those of 2007 and 2008, when less pronounced water column stratification and lower TEP levels were encountered (table SP4).

Fig. 1. (next pages) PCO diagrams summarising variation in bacterial community structure for all stations and samples above the thermocline and including the Chla maximum depth along the first two ordination axes. The size of the bubbles is proportional to the coccolithophorid biomass (µg Chla l^{-1}). Only phylotypes that had a higher than 40% fit along one of the axes are shown to avoid cluttering of the diagrams. Phylotypes driving the variation in the bacterial communities are indicated by their alias next to the arrows indicating the direction of steepest increase of their relative abundance. Projection of phytoplankton groups, physical and biogeochemical variables (added as supplementary variables) significantly correlated to one of the axes are shown below the PCO diagrams (see table 1 for abbreviations of the variables' name and the Spearman rank correlation coefficients).

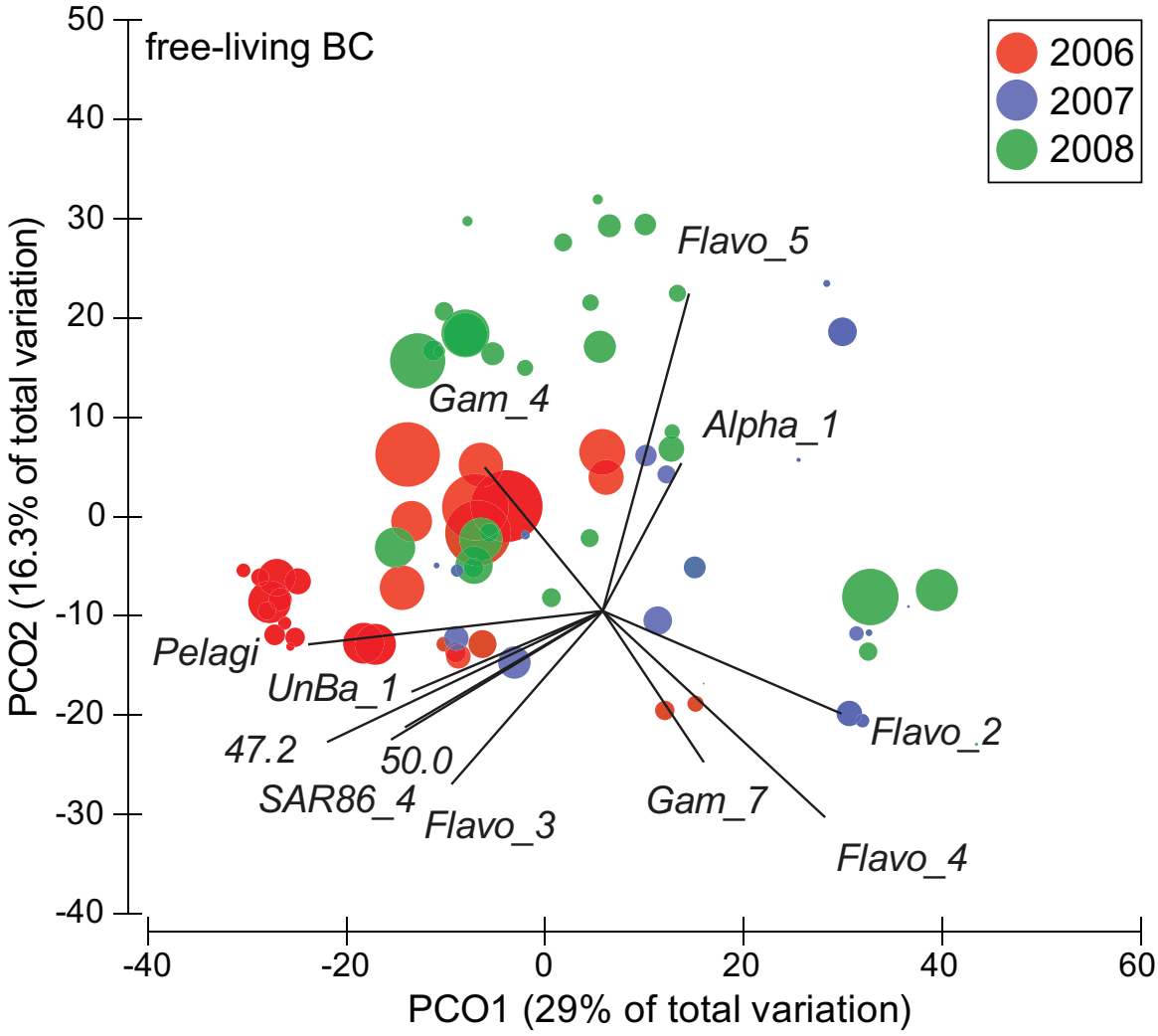
free-living BC
2006
2007
2008
PCO2 (16.3% of total variation)
PCO1 (29% of total variation)
50
40
30
20
10
0
-10
-20
-30
-40
-40
-20
0
20
40
60
Flavo_5
Gam_4
Alpha_1
Pelagi
UnBa_1
47.2
50.0
SAR86_4
Flavo_3
Gam_7
Flavo_2
Flavo_4

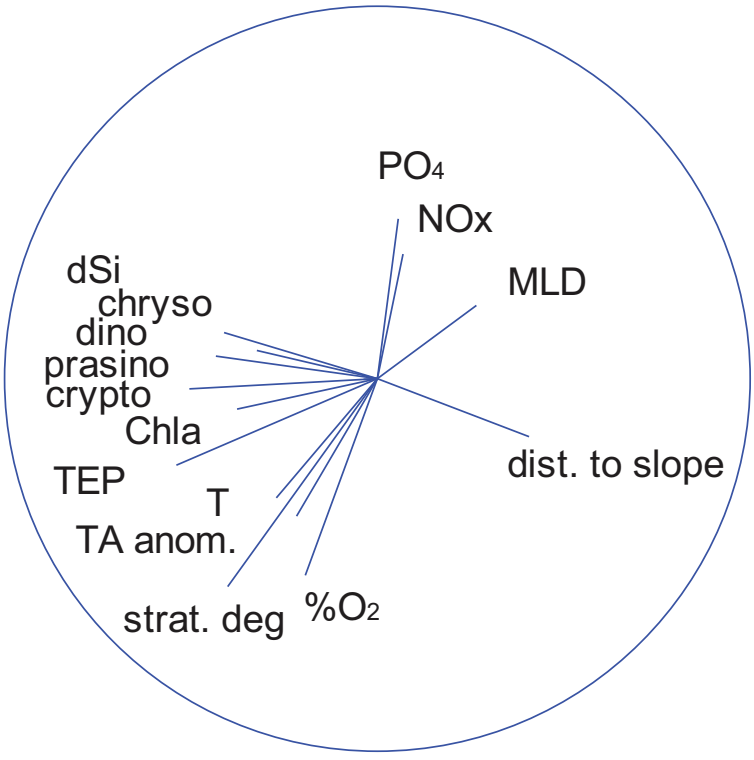
PO4
NOx
MLD
dSi
chryso
dino
prasino
crypto
Chla
TEP
T
TA anom.
strat. deg
%O2
dist. to slope

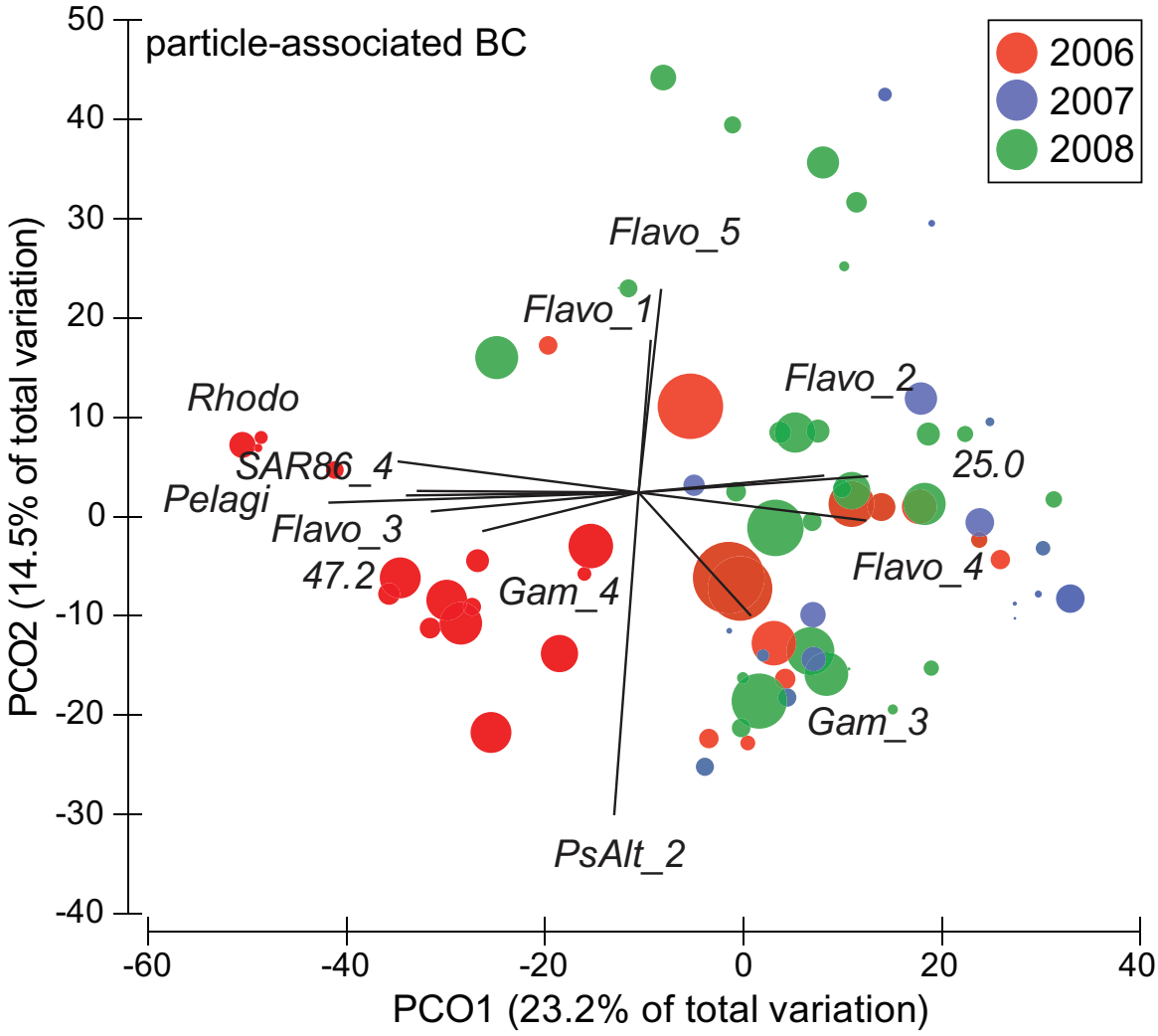
particle-associated BC
2006
2007
2008
Flavo_5
Flavo_1
Flavo_2
Rhodo
SAR86_4
Pelagi
Flavo_3
47.2
Gam_4
25.0
Flavo_4
Gam_3
PsAlt_2
PCO2 (14.5% of total variation)
PCO1 (23.2% of total variation)
50
40
30
20
10
0
-10
-20
-30
-40
-60
-40
-20
0
20
40

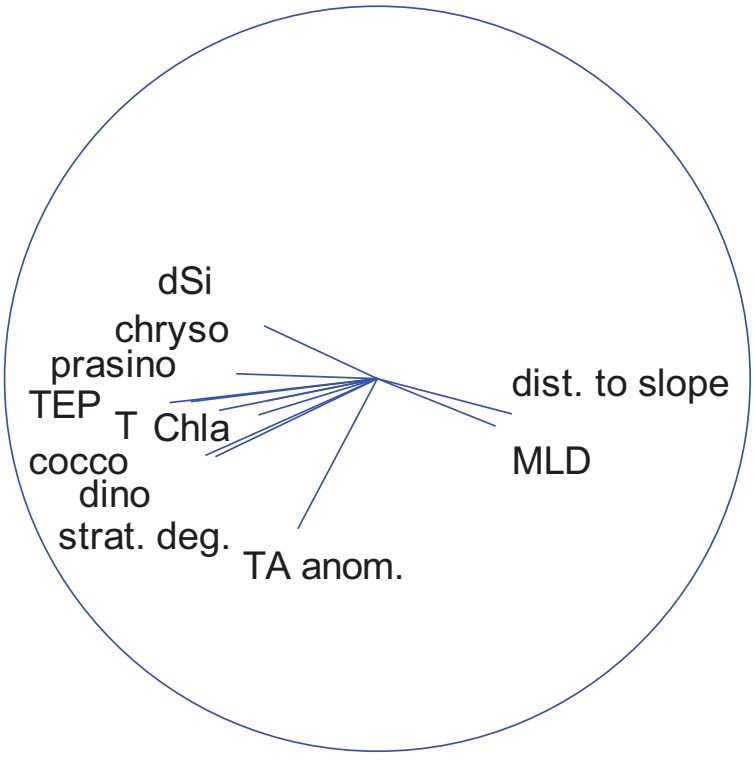
dSi
chryso
prasino
TEP
T
Chla
cocco
dino
strat. deg.
TA anom.
dist. to slope
MLD

Table 1. Spearman rank correlation, significant at the p=0.05 level, between the principal coordinate axes (PCO1 and PCO2) of the ordination of the free-living (FL) and the particle-associated (PA) bacterial community structure, and physical and biogeochemical variables, and phytoplankton groups (figure 1).

bacterial community	**FL**		**PA**	
ordination axis	PCO1	PCO2	PCO1	PCO2
depth	*ns*	*ns*	*ns*	*ns*
distance to slope	0.41	*ns*	0.36	*ns*
temperature	-0.27	-0.32	-0.30	*ns*
MLD	0.27	*ns*	0.32	*ns*
stratification degree	-0.40	-0.56	-0.46	*ns*
PO_4	*ns*	0.43	*ns*	*ns*
NO_x	*ns*	0.33	*ns*	*ns*
dSi	-0.41	*ns*	-0.30	*ns*
TEP	-0.54	-0.23	-0.56	*ns*
TA anomaly	*ns*	-0.37	*ns*	-0.40
$\%O_2$	*ns*	-0.53	*ns*	*ns*
chlorophyll *a*	-0.38	*ns*	-0.42	*ns*
diatom	*ns*	*ns*	*ns*	*ns*
dinoflagellate	-0.32	*ns*	-0.42	*ns*
coccolithophore	*ns*	*ns*	-0.31	*ns*
chrysophyte	-0.43	*ns*	-0.37	*ns*
prasinophyte	-0.50	*ns*	-0.49	*ns*
cryptophyte	-0.30	*ns*	*ns*	*ns*
Synechococcus	*ns*	*ns*	*ns*	*ns*

Phylotypes in both the FL and PA populations that were typically encountered in more stratified waters were Pelagi, SAR86_4, Flavo_3, and 47.2, while Flavo_5 was characteristic for less stratified conditions (tables 2 and 3). The variation in FL bacterial community structure was also related to nutrient levels (PO_4, NOx, and dSi), which are influenced by the bloom development and MLD. In this respect, Flavo_5 was associated with higher PO_4 and NOx concentrations, while Rhodo and SAR86_4 were typically relatively more abundant in more nutrient depleted conditions (table 2). Furthermore, the FL community had a different structure when the biomass of flagellated phytoplankton groups was higher, with samples characterized by high flagellated phytoplankton biomass clustering close together (fig. 1); especially the relative abundance of the SAR11 phylotype Pelagi appears to be strongly related to high biomass of these phytoplankton groups including coccolithophores (table 2).

Table 2. Spearman rank correlation between the relative band intensities of phylotypes in the FL bacterial community (BC) in figure 1 and environmental variables (significance level <0.05; *ns*= not significant). Correlation values higher than |0.40| are highlighted in bold. GenBank accession numbers in the table must be preceded by HQ686 to be complete.

free-living BC		Alpha_1	Pelagi	SAR86_4	Gam_4	Gam_7	Gam_10	Flavo_2	Flavo_3	Flavo_4	Flavo_5	47.2	50.0
GenBank accession n°	n	115	137	091	102	112	097	098	100	118	119		
temperature	74	*ns*	0.34	**0.40**	-0.29	*ns*	0.28	*ns*	*ns*	*ns*	-0.32	0.38	**0.42**
strat. deg.	74	-0.35	0.33	**0.51**	-0.36	*ns*	**0.54**	*ns*	**0.48**	*ns*	**-0.54**	**0.58**	**0.56**
MLD	74	*ns*	*ns*	-0.30	0.33	*ns*	*ns*	0.24	*ns*	*ns*	*ns*	-0.28	**-0.42**
PO_4	74	*ns*	*ns*	-0.39	0.23	-0.26	-0.28	*ns*	*ns*	*ns*	**0.45**	*ns*	*ns*
NOx	74	*ns*	*ns*	**-0.44**	0.23	-0.29	-0.39	*ns*	*ns*	*ns*	0.34	*ns*	*ns*
dSi	74	*ns*	0.31	*ns*	0.39	*ns*	*ns*	*ns*	0.24	-0.27	*ns*	*ns*	*ns*
TA anomaly	74	*ns*	*ns*	**0.48**	*ns*	*ns*	0.39	*ns*	*ns*	*ns*	**-0.43**	0.39	0.29
TEP	74	-0.34	**0.58**	**0.45**	*ns*	*ns*	0.28	*ns*	*ns*	-0.27	*ns*	**0.54**	0.38
POC	62	*ns*	*ns*	*ns*	*ns*	*ns*	*ns*	0.27	*ns*	*ns*	*ns*	*ns*	0.25
PN	62	*ns*	*ns*	*ns*	*ns*	-0.34	*ns*	*ns*	*ns*	*ns*	*ns*	*ns*	*ns*
DMSPd	22	*ns*	*ns*	**-0.62**	**0.48**	*ns*	*ns*	*ns*	**-0.48**	*ns*	**0.47**	*ns*	**-0.51**
$\%O_2$	74	**-0.51**	*ns*	**0.44**	*ns*	0.26	0.29	0.31	0.28	*ns*	-0.41	0.37	0.39
Chla	74	*ns*	**0.49**	*ns*	*ns*	-0.27	*ns*	*ns*	*ns*	*ns*	*ns*	0.27	*ns*
diatom	74	*ns*	*ns*	0.33	*ns*	*ns*	*ns*	*ns*	*ns*	*ns*	*ns*	*ns*	*ns*
dinoflagellate	74	*ns*	0.35	*ns*	*ns*	*ns*	*ns*	-0.32	0.25	-0.27	*ns*	0.36	0.28
coccolithophore	74	*ns*	**0.46**	*ns*	*ns*	*ns*	*ns*	*ns*	*ns*	*ns*	*ns*	*ns*	*ns*
chrysophyte	74	*ns*	**0.57**	*ns*	0.27	*ns*	*ns*	*ns*	*ns*	-0.23	*ns*	0.24	*ns*
prasinophyte	74	*ns*	**0.52**	0.35	0.29	-0.26	0.27	*ns*	*ns*	-0.26	*ns*	0.29	*ns*
cryptophyte	74	*ns*	0.31	0.30	*ns*	-0.27	*ns*	-0.35	*ns*	*ns*	*ns*	0.23	*ns*
Synechoccocus	74	*ns*	*ns*	-0.36	*ns*	*ns*	-0.33	*ns*	0.34	*ns*	*ns*	*ns*	*ns*

Table 3. Spearman rank correlation between the relative band intensities of phylotypes in the PA bacterial community (BC) in figure 1 and environmental variables (significance level <0.05; *ns*= not significant). Correlation values higher than |0.40| are highlighted in bold. GenBank accession numbers in the table must be preceded by HQ686 to be complete.

particle-associated BC		Rhodo	Pelagi	SAR86_4	PsAlt_2	Flavo_2	Flavo_3	Flavo_4	Flavo_5	25.0	47.2
GenBank accession n°	n	135	137	091	125	098	100	118	119		
temperature	73	**0.46**	0.33	**0.51**	*ns*	*ns*	0.32	*ns*	*ns*	*ns*	0.35
strat. deg.	73	**0.52**	**0.48**	**0.60**	*ns*	*ns*	**0.43**	-0.28	**-0.53**	*ns*	**0.54**
MLD	73	-0.35	-0.27	-0.36	0.25	*ns*	-0.34	*ns*	0.28	**0.40**	**-0.45**
PO_4	73	-0.26	*ns*	-0.28	*ns*	*ns*	*ns*	*ns*	**0.44**	*ns*	*ns*
NOx	73	-0.31	*ns*	-0.34	*ns*	*ns*	*ns*	*ns*	0.37	*ns*	*ns*
dSi	73	*ns*	0.24	*ns*	*ns*	*ns*	*ns*	-0.37	0.32	-0.26	*ns*
TA anomaly	73	*ns*	*ns*	0.37	0.36	*ns*	*ns*	-0.33	*ns*	*ns*	0.25
TEP	73	**0.67**	**0.58**	**0.45**	*ns*	*ns*	0.31	-0.28	*ns*	-0.23	**0.41**
POC	61	*ns*	*ns*	*ns*	*ns*	0.25	*ns*	*ns*	*ns*	*ns*	*ns*
PN	61	*ns*	*ns*	*ns*	*ns*	*ns*	*ns*	*ns*	0.31	*ns*	*ns*
DMSPd	21	*ns*	*ns*	**-0.59**	*ns*	*ns*	*ns*	*ns*	**0.69**	*ns*	**-0.59**
$\%O_2$	73	0.29	*ns*	**0.44**	*ns*	**0.43**	*ns*	-0.29	*ns*	*ns*	**0.41**
Chla	73	**0.41**	**0.43**	*ns*	*ns*	*ns*	0.24	*ns*	*ns*	-0.32	*ns*
diatom	73	*ns*	*ns*	*ns*	*ns*	*ns*	*ns*	*ns*	*ns*	*ns*	*ns*
dinoflagellate	73	0.36	0.36	*ns*	0.24	-0.34	0.34	*ns*	*ns*	**-0.43**	0.32
coccolithophore	73	**0.41**	**0.44**	*ns*	*ns*	*ns*	*ns*	*ns*	*ns*	*ns*	*ns*
chrysophyte	73	**0.47**	**0.46**	*ns*	*ns*	*ns*	*ns*	*ns*	*ns*	*ns*	*ns*
prasinophyte	73	**0.42**	**0.48**	0.28	*ns*	*ns*	*ns*	-0.36	*ns*	-0.35	*ns*
cryptophyte	73	*ns*	*ns*	*ns*	*ns*	-0.24	0.30	*ns*	*ns*	-0.41	*ns*
Synechoccocus	73	*ns*	*ns*	*ns*	*ns*	*ns*	*ns*	0.27	*ns*	*ns*	*ns*

In the PCO diagram of the PA community, coccolithophore biomass shows a low but significant relationship with the first PCO axis (fig. 1 and table 1). The ordination was driven by the relative abundances of phylotypes associated with more stratified conditions (see above) and by the relative abundance of a *Pseudoalteromonas* phylotype (PsAlt_2) and a flavobacterial phylotype (Flavo_5). The relative abundance of the former was related to increasing TA anomaly, while the latter was more abundant when DMSPd levels were high (table 3).

Partitioning of the variation in bacterial community structure

Variation partitioning was used to assess the unique contribution of predictor sets to the total explained variation in bacterial community structure to determine their relative importance. Together, selected spatial, temporal, and environmental variables and phytoplankton groups significantly explained 43.8% and 37.7% of the total variation in FL and PA bacterial populations, respectively (fig. 2 and table 4); respectively 16.8% and 13.5% concerned inter-correlation of the different predictor sets.

Fig. 2. Portions variation of the community structure of FL and PA bacteria in all the campaign years, in 2006, in 2007, and in 2008, that could be explained by spatial, temporal, environmental, and phytoplankton variables. The unique contribution of each variable group to the explained variation is shown together with their overlap (see table).

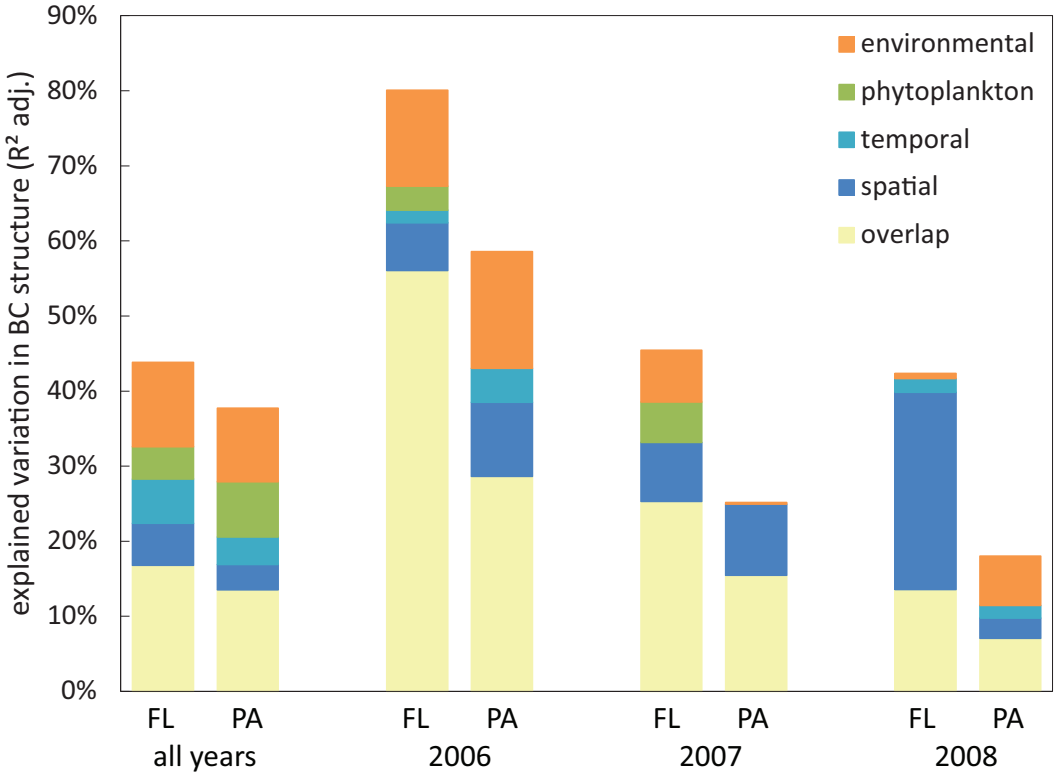

The unique contribution of each set of spatial and temporal variables and phytoplankton groups explained a similar proportion of the variation in multi-annual FL bacterial community (5.6%, 5.9%, and 4.3%, respectively). The largest share of explained variation was attributed to environmental variables which had a unique contribution of 11.2%. Similar portions of total variation in PA community structure (3.4% and 3.7%, respectively) were attributed to the unique contribution of selected sets of spatial and temporal variables. Variation in PA community structure could mainly be explained by environmental variables and phytoplankton groups which had unique contributions of 9.8% and 7.4%, respectively.

The selected predictor variables of the phytoplankton group set, which explained a significant part of the variation in both data sets, always included the prasinophytes, dinoflagellates and coccolithophores, and additionally diatoms and cryptophytes for the FL and PA bacterial community respectively (table 4). Inter-annual differences in bacterial community structure were significant in both the FL and PA assemblages, contributing respectively 17.9% and 16.5% to their variation, but were mainly related to environmental and phytoplankton variables, as indicated by the overlap of explained variation between temporal, and environmental and phytoplankton variables (FL: 9.8%; PA: 8.2%, results not shown).

When performing the variation partitioning for each campaign year separately, we found large differences in terms of the amount of explained variation, both between years and between bacterial community fractions (fig. 2 and table 4). As a general pattern, a greater proportion of variation could be explained in the FL than in the PA bacterial communities, as was already apparent in the variation partitioning of the three years together. While the different sets of predictors explained most of the variation of the bacterial community structure in 2006 (FL: 80.1%, PA: 58.6%), less than half of the variation in FL bacterial community structure could be explained for the 2007 and 2008 campaigns (2007: 45.4%, 2008: 42.4%). The patterns in PA community structure of the 2007 and 2008 campaigns were least amenable to explanation by the selected variables (2007: 25.2%, 2008: 18.0%). Moreover, there are significant differences in the unique contributions of the predictor variables, with environmental variables being most important in 2006, and negligible in the PA fraction in 2007 and the FL fraction in 2008, and spatial variables being most important in the latter fraction.

Table 4. Portions of variation (R^2 adj) in bacterial community structure explained by selected variables (+) in spatial, temporal, environmental, and phytoplankton predictor sets for yearly and multi-annual community datasets. Values in bold indicate the unique contribution of a particular predictor set to the total variance explained. Values in italics indicate the portion of explained variation before partitioning. The R^2 adj. coefficient of the 'global' predictor encompasses the unique contribution of all four sets of predictors and their overlap in explaining the bacterial communities' variation (cf. fig. 2).

campaign year	**all years**		**2006**		**2007**		**2008**	
bacterial community	**FL**	**PA**	**FL**	**PA**	**FL**	**PA**	**FL**	**PA**
n samples	74	73	28	27	17	17	29	29
predictor sets and selected variables								
spatial	**5.6**	**3.4**	**6.4**	**9.9**	**7.9**	**9.5**	**26.3**	**2.7**
unpartitioned	*8.7*	*3.9*	*55.7*	*35.9*	*32.2*	*25.0*	*38.7*	*9.0*
La Chapelle	+							
Meriadzek		+	+	+				
Goban Spur							+	
distance to slope	+					+	+	
latitude			+		+		+	+
longitude			+	+			+	
temporal	**5.9**	**3.7**	**1.7**	**4.5**	ns	ns	**1.8**	**1.7**
unpartitioned	*17.9*	*16.5*	*11.1*	*9.5*	ns	ns	*4.5*	*5.7*
2006	+							
2007	+	+						
Julian day		+	+	+			+	+
environmental	**11.2**	**9.8**	**12.8**	**15.6**	**6.9**	**0.2**	**0.7**	**6.6**
unpartitioned	*27.8*	*24.0*	*57.6*	*49.2*	*19.1*	*17.7*	*14.5*	*13.8*
strat. deg.	+	+	+					
pycnocline	+						+	+
MLD				+				
nitracline depth			+					
dSi	+	+			+	+		
TEP	+	+						
Chl a				+				
$\%O_2$	+	+						
TA anomaly		+	+	+				
phytoplankton groups	**4.3**	**7.4**	**3.2**	ns	**5.4**	ns	ns	ns
unpartitioned	*14.5*	*14.9*	*48.0*	ns	*18.4*	ns	ns	ns
diatoms	+				+			
coccolithophores	+	+	+					
prasinophytes	+	+						
dinoflagellates	+	+	+					
cryptophytes		+	+					
overlap	**16.8**	**13.5**	**56.1**	**28.6**	**25.3**	**15.5**	**13.6**	**7.1**
global	**43.8**	**37.7**	**80.1**	**58.6**	**45.4**	**25.2**	**42.4**	**18.0**

Discussion

Seasonal sea surface warming and thermocline development have been shown to impact both the phytoplankton bloom succession and the bacterial community composition, while close interactions between phytoplankton and bacterial species are also known to influence the bacterial community composition (Alonso-Saez *et al.*, 2007; Teira *et al.*, 2008; Amin *et al.*, 2009; Teira *et al.*, 2010; Sarmento and Gasol, subm.). However, bacteria-phytoplankton associations in the field are often difficult to disentangle. In this study we demonstrated a close relation between the structure of FL and PA bacterial communities and both environmental conditions and bloom composition during diatom and coccolithophore-dominated phytoplankton blooms in late spring.

Variation in the structure of FL and PA bacterial communities

In this study we found that spatial, temporal, environmental, and phytoplankton variables explained 43.8% and 37.7% of the variation in multi-annual FL and PA bacterial community structure, respectively. These values are in the same range than those reported by Lami *et al.* (2009), who found that 48.7% and 27% of the variation in the FL bacterial community during a seasonal cycle at a coastal Mediterranean site could be explained by bottom-up environmental and temporal variables, respectively. The structure of the FL and PA bacterial communities in our study is largely influenced by the same variables (table 1), yet a consistently lower portion of explained variation in PA compared to FL bacterial communities suggests that other predictor variables not included in the analyses were shaping this particular community, or that other, stochastic processes were important. Surprisingly, variables relating to the quantity and quality of particulate matter, such as POC, PN, TEP, and their respective ratios did not add explanatory power to the selected sets of predictors using a reduced dataset (not shown). This is in contrast with the study of Weinbauer *et al.* (2010) where it was found that water particle concentration probably shaped the difference in community composition in total and free-living bacterial community.

In the present study, we compared bacterial communities from different stations, during different years and during only one season and thus along a shorter gradient in bacterial community succession, which may explain the slightly lower proportions of explained

variance compared to Lami *et al.* (2009). Furthermore, our values of explained variation in bacterial community structure were slightly lower owing partly to the more stringent selection procedure used for the predictor variables and because we reported the portions of explained variation using the more parsimonious adjusted R^2 coefficient (Peres-Neto *et al.*, 2006). However, a substantial part of the variation in bacterial community structure in our study remains unexplained. This could be related to the importance of "top-down" controls such as mortality due to microzooplankton grazing and viral lysis in shaping bacterial communities (Yokokawa and Nagata, 2005; Longnecker *et al.*, 2010). The relation between DMSPd concentration, released through phytoplankton cell lysis, and the occurrence of specific phylotypes in our study suggests this was also the case here (see below).

Distribution of phylotypes and their relation to environmental conditions

The general composition of the FL and PA bacterial communities is described in chapter 3 (Van Oostende *et al.*, *in prep. c*). Below, the association of the dominant phylotypes with particular environmental factors is discussed in more detail. The phylotypes that contributed most to the variation in bacterial community structure, represented in the PCO diagrams in figure 1, were usually also the most abundant ones (based on the relative band intensities) (cf. chapter 3). In general, if these phylotypes were represented in both the FL and PA communities, they displayed similar relationships to specific environmental or phytoplankton bloom conditions in each community (tables 2 and 3).

In the FL bacterial community, various phylotypes affiliated to the *Gammaproteobacteria* shaped variation in community structure (fig. 1). The Gam_4 phylotype was negatively related with increased stratification and higher inorganic nutrient concentrations, in contrast with SAR86_4, Gam_7, and Gam_10, which were associated with more stratified and nutrient depleted conditions. The occurrence of *Gammaproteobacteria* is often associated with phytoplankton blooms due to their typical feast–and-famine life-style (Fuhrman and Hagström, 2008; Lauro *et al.*, 2009). However, our data show that except for Gam_7 these gammaproteobacterial phylotypes were not associated with higher phytoplankton biomass, except prasinophytes (table 2). The relative abundance of the alphaproteobacterial phylotype Pelagi, affiliated to the SAR11 clade (see chapter 3), on the other hand, showed a significant positive correlation with Chla and coccolithophores, prasinophytes, chrysophytes,

and cryptophytes and was prevalent when the water column was more stratified. Members of the dominant heterotroph SAR11 clade are generally believed to be oligotrophs occurring in more stratified conditions (Alonso-Gutierrez *et al.*, 2009; Carlson *et al.*, 2009; Lauro *et al.*, 2009), so their association to phytoplankton blooms in more stratified conditions is not so surprising and has been observed before (Gonzalez *et al.*, 2000).

The multi-annual variation in FL (but also the PA) bacterial community structure was driven by changes in the relative band intensities of several phylotypes affiliated to the *Flavobacteria* of the *Bacteroidetes* phylum (fig. 1 and tables 2 and 3). Members of the *Flavobacteria* are typically associated with later stages of phytoplankton blooms, when polymeric organic matter on which they thrive has accumulated in the water column (Pinhassi *et al.*, 2004; Grossart *et al.*, 2005; Bauer *et al.*, 2006). However, we did not find any significant correlations between their relative abundance and POC, PN, or TEP. Only Flavo_3 was positively correlated to dinoflagellate abundance (tables 2 and 3). As was the case for some of the FL gammabacterial phylotypes, Flavo_3 and Flavo_5 displayed an antagonistic response towards water column stratification, suggesting they have a different ecological niche (table 3). The phylotype Flavo_5, which was less abundant in stratified waters, is affiliated to the *Polaribacter* genus, an abundant member of the *Flavobacteria*, which has been especially associated with colder water masses of the North Atlantic Ocean and has been detected in the phycosphere of nanophytoplankton cells (Gomez-Pereira *et al.*, 2010). However, we did not find any significant correlation between Flavo_5 and phytoplankton groups' biomass.

The PA bacterial community structure (table 1 and fig. 1) was significantly related to the changes in bloom development (as evidenced by Chla and TA anomaly resulting from calcification), inorganic nutrient depletion, and TEP accumulation. The relative abundance of several phylotypes affiliated to the *Rhodobacteraceae* (Rhodo), the SAR11 (Pelagi) and the SAR86 cluster (SAR86_4), and to the *Flavobacteriaceae* (Flavo_3), were positively related to the concentration of TEP (table 3). High TEP concentrations were measured during the 2006 campaign (table SP2), when important *E. huxleyi* blooms were observed (Harlay *et al.*, 2009) (see also chapter 2). Significant amounts of TEP are produced during *E. huxleyi* blooms (Engel *et al.*, 2004b) and the release of TEP precursors is probably linked to the production of coccoliths and carbon overconsumption during unbalanced growth (Schartau *et al.*, 2007;

Godoi *et al.*, 2009) (see also chapter 6). It is unclear if these specific phylotypes are consumers or producers of TEP, or if they facilitated the formation of TEP by interacting with the coccolithophores, as observed for planktonic diatoms (Gärdes *et al.*, 2010). Nonetheless, the strength of the relation between TEP concentration and the bacterial community structure of each separate campaign was subordinate to that of other environmental conditions, as this variable was not selected during our redundancy analyses (table 4). PsAlt_2 (*Pseudoalteromonas*), together with Flavo_5 also played an important role in shaping the variation in PA bacterial community structure (fig. 1). *Pseudoalteromonas* is often found in association with eukaryotic hosts, and many *Pseudoalteromonas* species produce biologically active and even algicidal compounds (Skerratt *et al.*, 2002; Skovhus *et al.*, 2007). In our study we found a modest significant correlation only between PsAlt_2 and the abundance of dinoflagellates and TA anomaly, suggesting PsAlt_2 was more abundant in water masses where calcification had occurred and that had not recently been mixed, characteristic for the declining stage of blooms.

Finally, specific phylotypes in the FL and the PA community showed a positive (Gam_4 and Flavo_5) or a negative correlation (SAR86_4 and Flavo_3) with the concentration of DMSPd, the precursor of atmospheric active dimethyl sulphide (DMS) released by phytoplankton through cell lysis or herbivory (Stefels *et al.*, 2007) (tables 2 and 3). This suggests that these phylotypes might be involved in the cycling of DMSP. Studies investigating the relationship and function of bacteria with sulphur cycling in phytoplankton blooms identified members of the SAR11, *Roseobacter*, SAR86, *Methylophaga*, and *Bacteroidetes* group to be present during blooms of *E. huxleyi*, a major DMSP producer (Gonzalez *et al.*, 2000; Neufeld *et al.*, 2008).

Influence of phytoplankton on bacterial community structure

The patterns of variation in bacterial community structure obtained by principal coordinates analyses were significantly related to the biomass of phytoplankton groups such as prasinophytes, coccolithophores, chrysophytes, dinoflagellates, and cryptophytes (fig. 1 and table 1). Nonetheless, this relation may be indirect, as environmental variables structuring bacterioplankton communities often correlate with those affecting phytoplankton species (e.g. nutrient availability and temperature). Although several studies have investigated the relation between changes in bacterioplankton and natural phytoplankton blooms (Fandino

et al., 2001; Rink *et al.*, 2007; Sapp *et al.*, 2007a; Jones *et al.*, 2010), none accounted for the inter-correlation between environmental variables and phytoplankton composition. Results from variation partitioning analyses showed that the unique contribution of phytoplankton to explaining the variation in bacterial community structure (i.e. once the variation explained by spatial, temporal, and environmental variables had been accounted for) was less than half (FL) or comparable (PA) to the unique contribution of the environmental variables (fig. 2 and table 4). The higher amount of unique variation explained by phytoplankton in PA compared to FL bacterial communities suggests PA bacteria can be associated to the phycosphere itself (cf. Jasti *et al.*, 2005; Sapp *et al.*, 2007b; Gärdes *et al.*, 2010). This relationship between bacterial community structure and phytoplankton groups for the separate years however was only significant for the FL communities in 2006 and 2007, suggesting that within campaigns, unaccounted factors may obscure this relation or that the finer association patterns present during the campaigns were not resolved due to under-sampling. Moreover, the measure of abundance of phytoplankton groups used here is based on the chemotaxonomic partitioning of the Chla concentration, and thus has a low phylogenetic resolution. Although we detected a moderate influence of the abundance of particular phytoplankton groups on the bacterial community structure, we believe the many layers of environmental factors, water mass biogeochemical history, and trophic interactions may confound tight bacteria-phytoplankton species associations compared to those detected in experimental settings (Grossart *et al.*, 2005; Amin *et al.*, 2009). In this respect, Pinhassi *et al.* (2004) suggested that variation in substrate supply to bacteria due to differences in phytoplankton community composition, which was induced by different turbulence regime, could have been further amplified by different grazing intensity and assemblages, differentially impacting nutrient cycling. Additionally, close bacteria-phytoplankton associations in the field may be further obscured by the generalist (yet diverse) life strategy adopted by many bacterial phylogenetic groups (Mou *et al.*, 2008; Lauro *et al.*, 2009; Sarmento and Gasol, subm.).

Thermal stratification of the water column and bacterial community change

Thermal stratification and mixing of the water column is a key determinant of transitions of microbial community structure on seasonal time scales (Morris *et al.*, 2005; Sapp *et al.*, 2007a; Treusch *et al.*, 2009), but also on the timescale of weeks as shown here and in other (mostly lacustrine) studies (Hollibaugh *et al.*, 2001; De Wever *et al.*, 2005). Unconstrained

ordination analyses highlight the prominent role stratification of the water column in shaping the turnover of bacterial assemblages (fig. 1 and table SP2). This is further illustrated in figure 3 where the main gradient in community structure (i.e. PCO axes) of FL and PA bacteria is plotted along the stratification gradient.

Fig. 3. Relationship between the change in FL (upper plot) and PA (lower plot) bacterial community structure (as the sample scores along, respectively, the second and the first PCO axis, as in fig. 1) and the stratification degree of the water column. Bacterial community samples from the upper mixed layer including Chla maximum depth in 2006 (red dots), 2007 (blue dots), and 2008 (green dots). Trendlines represent significant linear regressions ($p<0.01$), where $r^2 = 0.33$ and 0.39 for FL and PA communities, respectively.

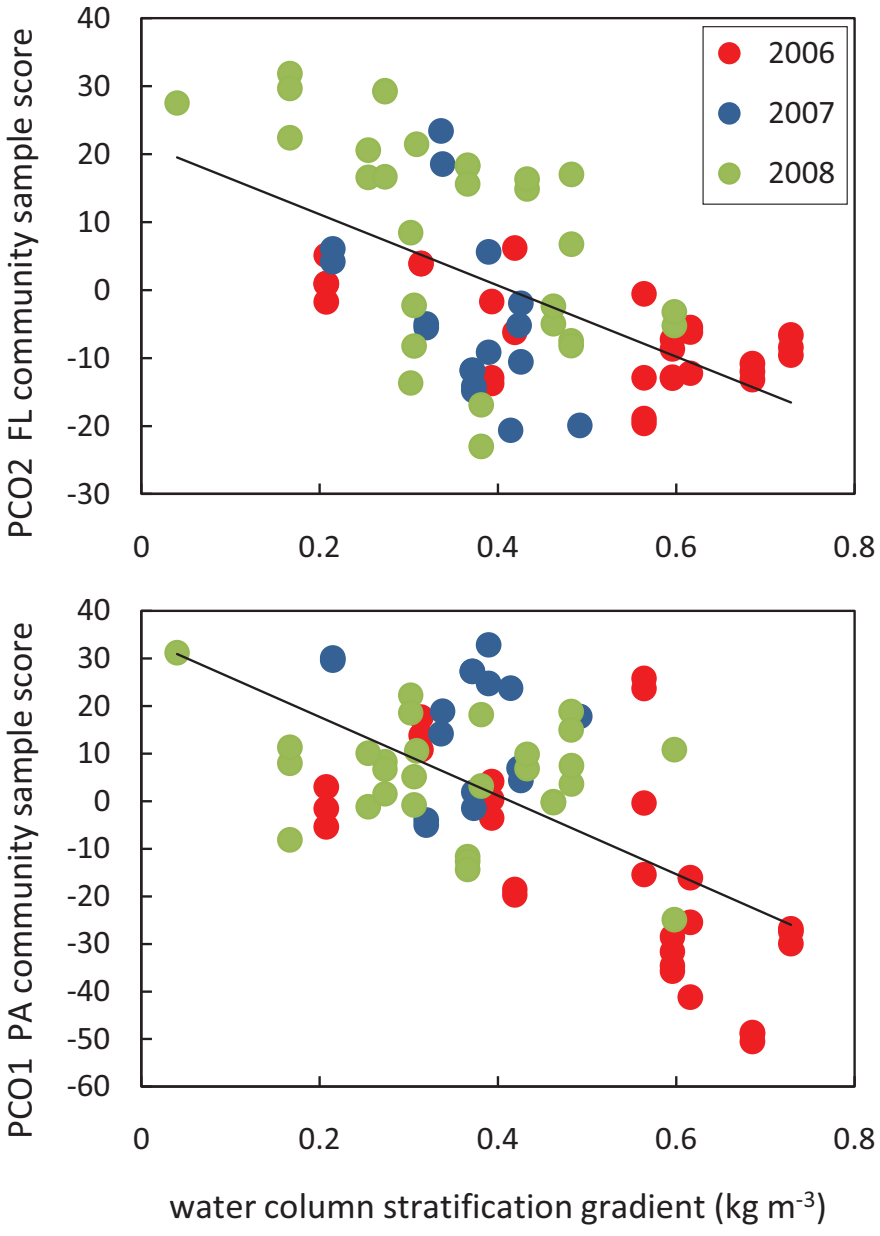

To make sure that this pattern was not influenced by inter-correlations with spatial or temporal variables, we performed redundancy analyses and partitioned the explained variation using several proxies for the degree of water column stratification. Each proxy highlights a specific feature of the structure of the water column, such as the steepness of the pycnocline and the MLD. For each campaign dataset (except 2007) as well as for the multi-annual bacterial community dataset, variables related to water column stratification contributed significantly to the variation in bacterial communities (table 4). Stormy weather during the 2007 campaign disrupted the stratification and may have led to transient conditions, shown by the higher degree of scatter in biogeochemical variables (such as pCO_2 and O_2) in 2007 compared to 2006 and 2008 (Suykens et al 2010). In 2007, the concentration of dSi which may have been re-injected into the upper mixed layer by mixing, explained a greater share of the variation in bacterial community structure than stratification-related variables. However, in a separate redundancy analysis, using only stratification-related variables, the stratification degree of the water column explained 9.8% of the variation in the PA community (not shown). This suggests that water column stratification can indeed shape the bacterial community structure, even at the shorter temporal scale of the order of weeks, rather than on seasonal timescales (Fuhrman *et al.*, 2006; Lami *et al.*, 2009; Treusch *et al.*, 2009).

Several spatial variables explained part of the variation in bacterial community structure in the multi-annual as well as the separate datasets of each campaign (table 4). This is in contrast with the findings in chapter 3 (Van Oostende *et al.*, *in prep. c*), where horizontal variation in bacterial community was not related to spatial variables and this relationship was obscured by the depth gradient in community structure (surface to 150 m depth). The low values of spatial unpartitioned explained variance in the multi-annual dataset suggest the specific areas sampled during our campaigns did not display stable and characteristic environmental features that may have influenced the bacterial community structure (table 4). By contrast, the often high values of spatial unpartitioned explained variance encountered in analyses of separate campaigns (except PA bacterial community in 2008), suggests there were pronounced spatial gradients of environmental conditions within each campaign (table 4). In this respect, Harlay *et al.* (2010; 2011) suggested that water masses gradually warm up and stratify during advection of a colder water mass from the slope of the continental margin over the shelf following the northwards residual surface currents (cf.

portion of variation explained by 'distance to slope' and latitude) (see also chapter 2, fig. 1). However, this general scenario may be influenced by weather conditions such as strong winds enhancing mixing of the water column (e.g. in 2007) and reduced irradiance slowing down the heat accumulation of the surface layer (see also chapter 2, (Van Oostende *et al.*, *in prep. a*)).

Conclusions

The FL and PA bacterial communities shared most bacterial phylotypes, but were dominated by different taxa (see also chapter 3, (Van Oostende *et al.*, *in prep. c*)). Here we showed that while both FL and PA communities are generally speaking influenced by the same environmental variables and phytoplankton groups, they differ in the strength of the impact of these variables, and especially for the PA communities where a larger part of the observed variation remained unexplained. However, the unique contribution of phytoplankton to explaining the variation in bacterial community structure was less than half (FL) or comparable (PA) to the unique contribution of the environmental variables, suggesting phytoplankton composition has an influence on the bacterial community structure in general and that PA bacteria can be closely associated to the algal cells. The amount of variation in bacterial community structure that can be accounted for by spatial, temporal and environmental variables and phytoplankton groups also differ up to threefold between campaign years. This suggests that changes in bacterial community structure were also affected by stochastic, unknown or unmeasured factors (such as grazing, lysis or positive or negative interactions between bacterial species), or that the observed patterns did not show a linear relationship with the predictor variables and hence could not be captured with the methods used. However, using the combined data of bacterial communities sampled during the three consecutive campaigns, we found that the bacterial community dynamics of both FL and PA bacteria closely matched the degree of stratification of the water column even at the shorter temporal scale of the order of weeks, rather than on seasonal timescales (Fuhrman *et al.*, 2006; Lami *et al.*, 2009; Treusch *et al.*, 2009). This substantiates the notion of a certain predictability of bacterial assemblages (Fuhrman *et al.*, 2006) in the same way size structure and succession patterns of phytoplankton functional groups can be linked with particular environmental settings (Margalef, 1978; Hood *et al.*, 2006; Leblanc *et al.*, 2009). The annual recurrence of similar phylotypes and the often strong associations between

particular phylotypes, and between the relative abundance of specific phylotypes and particular environmental conditions support the existence of a "microbial niche space" consisting of multiple ecological interactions as proposed by Fuhrman and Steele (2008).

Acknowledgements

The authors sincerely thank the officers and crew members of the R.V. Belgica for their logistic support during the campaigns. J. Backers, J.-P. De Blauw, and G. Deschepper of the Unit of the North Sea Mathematical Models (Brussels/Ostend, Belgium) are acknowledged for their support in data acquisition during the field campaigns. S. Groom is acknowledged for providing remote sensing images. We are grateful to C. Souffreau, A. De Wever, B. Vanelslander, and D. De Bock for their assistance during sample collection. We thank T. Verstraete and S. D'Hondt for performing most of the molecular analyses, and J. Goris at Applied Maths for database building support. Finally, we are grateful to all members of the PEACE network for their support during the campaigns. This study was financed by Belgian Federal Science Policy Office in the framework of the PEACE project (contract numbers SD/CS/03A and SD/CS/03B). N. Van Oostende received a PhD grant from the agency for Innovation by Science and Technology (IWT-Flanders).

Supplementary tables

Table SP1. Overview of physical variables characterising the stations visited during the three campaigns. The first numeral of the station code denotes the last digit of the year of the respective campaign (2006, 2007, 2008), followed by the station number during each campaign. Station codes followed by a "b" indicate the station was revisited during the second leg of the campaign. Stations located at the slope of the continental margin are denoted by an asterisk. Distance to slope where offshore slope stations have negative values (dist. to slope).

station	date	area	lat. (°N)	lon. (°W)	SST (°C)	strat. deg. (kg m^{-3})	pycno. steep.	MLD (m)	dist. to slope (km)
6-1	31/05/2006	La Chapelle	47.75	7.00	13.00	0.31	0.23	32	17
6-2*	1/06/2006	La Chapelle	47.53	7.17	12.78	0.21	0.16	40	-4
6-3*	1/06/2006	La Chapelle	47.42	7.27	13.85	0.42	0.27	21	-18
6-4	2/06/2006	Meriadzek	48.10	7.50	13.15	0.39	0.20	34	16
6-8	6/06/2006	Meriadzek	48.50	8.90	14.47	0.73	0.22	19	15
6-6*	7/06/2006	Meriadzek	47.69	8.21	14.91	0.60	0.39	16	-39
6-7	7/06/2006	Meriadzek	48.40	8.10	14.51	0.69	0.24	20	17
6-4b	8/06/2006	Meriadzek	48.10	7.50	14.27	0.62	0.21	23	16
6-1b	9/06/2006	La Chapelle	47.75	7.00	14.23	0.56	0.23	22	17
7-2	10/05/2007	La Chapelle	47.79	6.90	13.36	0.27	0.34	42	24
7-5	12/05/2007	Meriadzek	48.20	7.62	12.96	0.24	0.35	39	21
7-8	13/05/2007	Meriadzek	48.50	8.50	13.19	0.27	0.35	39	28
7-9	14/05/2007	Goban	49.20	9.49	12.95	0.33	0.31	43	58
7-10	15/05/2007	Goban	49.50	10.51	12.73	0.32	0.34	36	38
7-11	16/05/2007	Goban	51.34	10.50	12.28	0.39	0.47	39	50
7-8b	21/05/2007	Meriadzek	48.50	8.50	13.13	0.29	0.26	43	28
7-5b	22/05/2007	Meriadzek	48.22	7.59	13.30	0.31	0.54	36	24
7-4*	23/05/2007	La Chapelle	47.42	7.27	13.29	0.11	0.16	54	-18
7-7*	23/05/2007	Meriadzek	47.68	8.20	13.39	0.24	0.18	36	-40
7-2b	24/05/2007	La Chapelle	47.80	6.89	13.40	0.22	0.29	28	25
8-1	7/05/2008	Armorican	48.50	6.00	12.71	0.17	0.28	40	114
8-3	7/05/2008	La Chapelle	47.53	7.16	12.49	0.30	0.14	13	-4
8-2	8/05/2008	La Chapelle	47.80	6.90	12.80	0.25	0.22	15	25
8-6	9/05/2008	Meriadzek	47.90	7.91	12.16	0.04	0.13	100	-10
8-5	10/05/2008	Meriadzek	48.20	7.59	12.91	0.27	0.21	25	22
8-8	11/05/2008	Meriadzek	48.50	8.50	12.95	0.31	0.23	18	28
8-9	12/05/2008	Goban	49.20	9.50	13.12	0.38	0.31	15	57
8-10	13/05/2008	Goban	49.50	10.50	13.09	0.43	0.34	22	38
8-11	14/05/2008	Goban	50.50	10.50	12.70	0.31	0.24	14	20
8-12	19/05/2008	Goban	51.00	10.00	13.63	0.60	0.29	19	73
8-13	20/05/2008	Goban	50.00	10.34	13.40	0.46	0.43	34	41
8-9b	21/05/2008	Goban	49.20	9.50	13.61	0.48	0.40	23	57
8-5b	22/05/2008	Meriadzek	48.20	7.60	13.52	0.37	0.23	39	22
8-4	23/05/2008	La Chapelle	47.42	7.27	14.23	0.48	0.20	20	-18

Table SP2. Average values for biogeochemical variables in the upper mixed layer for each station. Abbreviations as in Materials and Methods section.

station	nitra. depth (m)	NOx (µmol l^{-1})	dSi (µmol l^{-1})	PO_4 (µmol l^{-1})	$\%O_2$	TA anomaly (µmol kg^{-1})	TEP (µg X eq. l^{-1})	POC (µmol l^{-1})	PN (µmol l^{-1})
6-1	23	0.70	0.98	0.05	109	-7	155	10.39	1.32
6-2*	0	2.20	1.67	0.15	107	-6	1587	11.94	1.48
6-3*	0	1.83	0.86	0.16	109	-8	434		
6-4	27	0.47	0.50	0.07	108	-18	149	13.61	1.37
6-8	32	0.12	1.66	0.05	110	-20	208	10.38	1.58
6-6*	11	0.56	0.49	0.05	115	-13	1283		
6-7	30	0.13	0.46	0.01	110	-17	439	14.55	1.42
6-4b	38	0.08	0.52	0.04	108	-19	619	7.81	0.99
6-1b	30	0.02	0.29	0.03	111	-7	1552	11.26	0.85
7-2	0	1.19	1.16	0.09	104	-28	12	8.25	1.34
7-5	17	0.80	0.26	0.09	104	-14	16	12.99	2.50
7-8	25	0.89	0.14	0.06	106	-7	19	15.96	3.79
7-9	37	0.68	0.50	0.07	101	-20	23	10.85	1.44
7-10	0	1.21	0.18	0.07	103	-6	10	6.13	0.84
7-11	41	0.49	0.76	0.06	106	-9	32	16.40	2.53
7-8b	43	0.49	0.11	0.07	106	-5	26	13.11	1.70
7-5b	23	0.38	0.17	0.10	105	-13	16		
7-4*	0	2.19	1.20	0.15	105	-13	26	14.90	2.82
7-7*	27	0.51	0.18	0.10	113	-9	249	21.02	3.51
7-2b	0	1.47	1.95	0.06	106	-18	51	14.82	1.89
8-1	11	0.22	1.00	0.07	106	2	2	15.78	2.25
8-3	0	2.48	1.08	0.20	97	-13	15		
8-2	24	0.15	0.75	0.06	104	0	51	8.78	1.45
8-6	0	4.23	1.30	0.32	94	-2	23	5.09	1.10
8-5	33	0.27	0.27	0.06	101	-4	39	8.90	1.26
8-8	23	0.23	0.08	0.07	100	-8	29	6.39	1.03
8-9	28	0.23	0.10	0.01	107	0	57	4.73	0.72
8-10	29	0.26	0.11	0.05	103	-11	111	8.16	1.73
8-11	13	0.27	0.16	0.02	103	-8	81	4.25	0.67
8-12	41	0.21	0.28	0.05	102	-14	44	6.81	1.64
8-13	48	0.16	0.08	0.04	102	-16	66	14.75	3.03
8-9b	41	0.22	0.01	0.04	100	-25	40	10.14	2.21
8-5b	15	1.69	0.72	0.14	100	-2	77	14.39	3.08
8-4	28	0.24	0.04	0.07	104	-8	76	12.53	2.67

Table SP3. Average concentrations of total Chla and phytoplankton groups (in µg Chla l^{-1}) in the upper mixed layer at each station. Phytoplankton groups are abbreviated as follows: diatoms (diat), dinoflagellates (dino), coccolithophores (cocco), chrysophytes (chryso), prasinophytes (pras), cryptophytes (crypto), *Synechoccocus* spp. (Syn).

station	Chla	diat	dino	cocco	chryso	pras	crypto	Syn
6-1	1.27	0.41	0.03	0.51	0.11	0.19	0.01	0.01
6-2*	1.96	0.23	0.08	1.21	0.12	0.25	0.03	0.03
6-3*	1.23	0.00	0.14	0.85	0.09	0.11	0.01	0.04
6-4	1.13	0.49	0.03	0.10	0.05	0.26	0.21	0.00
6-8	0.52	0.03	0.09	0.13	0.04	0.11	0.11	0.01
6-6*	1.12	0.11	0.23	0.53	0.09	0.08	0.05	0.02
6-7	0.91	0.51	0.03	0.04	0.08	0.13	0.13	0.00
6-4b	1.14	0.72	0.02	0.09	0.07	0.15	0.09	0.00
6-1b	0.45	0.16	0.03	0.14	0.05	0.04	0.01	0.00
7-2	0.63	0.08	0.05	0.29	0.02	0.02	0.11	0.05
7-5	0.43	0.37	0.02	0.02	0.01	0.01	0.00	0.00
7-8	0.34	0.30	0.01	0.02	0.01	0.00	0.00	0.00
7-9	0.37	0.02	0.01	0.20	0.02	0.07	0.01	0.05
7-10	0.34	0.01	0.03	0.13	0.01	0.14	0.02	0.00
7-11	1.00	0.14	0.05	0.29	0.06	0.23	0.18	0.06
7-8b	0.38	0.28	0.00	0.01	0.01	0.00	0.01	0.07
7-5b	0.48	0.27	0.07	0.05	0.03	0.00	0.00	0.07
7-4*	0.59	0.00	0.03	0.15	0.10	0.06	0.17	0.07
7-7*	0.59	0.09	0.02	0.32	0.04	0.04	0.01	0.06
7-2b	0.51	0.04	0.09	0.05	0.01	0.13	0.18	0.00
8-1	1.20	0.28	0.00	0.10	0.03	0.06	0.72	0.01
8-3	0.25	0.09	0.03	0.06	0.02	0.02	0.02	0.01
8-2	0.21	0.07	0.02	0.03	0.02	0.05	0.02	0.01
8-6	0.39	0.14	0.04	0.08	0.03	0.04	0.05	0.01
8-5	0.53	0.03	0.07	0.15	0.06	0.04	0.17	0.00
8-8	0.40	0.03	0.11	0.09	0.02	0.05	0.10	0.01
8-9	0.40	0.32	0.02	0.00	0.00	0.00	0.04	0.01
8-10	0.62	0.31	0.07	0.12	0.03	0.02	0.06	0.01
8-11	0.25	0.04	0.04	0.11	0.02	0.02	0.02	0.00
8-12	0.46	0.00	0.02	0.12	0.08	0.05	0.18	0.01
8-13	1.00	0.08	0.07	0.49	0.14	0.08	0.12	0.01
8-9b	1.34	0.05	0.23	0.76	0.08	0.12	0.09	0.01
8-5b	1.56	0.19	0.12	0.71	0.10	0.23	0.21	0.01
8-4	0.54	0.14	0.05	0.26	0.03	0.01	0.03	0.02

Table SP4. Results of two-way crossed PERMANOVA analysis testing the effect of bacterial life-mode (FL-PA) and campaign year on the bacterial community structure of the upper mixed layer (BC UML).

Factors		**BC UML**
FL-PA	df	1
	MS	22687
	pseudo-F	17.71
	p	0.0001
year	df	2
	MS	17925
	pseudo-F	13.99
	p	0.0001
FL-PA x year	df	2
	MS	3034
	pseudo-F	2.37
	p	0.0022
Res	df	142
	MS	1281

5

Phytoplankton cell lysis and grazing mortality rates, and dimethylsulphonioproprionate dynamics during coccolithophorid blooms

Nicolas Van Oostende[1], Caroline De Bodt[2], Caroline Souffreau[1],
Wim Vyverman[1], Lei Chou[2], and Koen Sabbe[1]

[1] Laboratory for Protistology and Aquatic Ecology, Biology Department, Ghent University, Krijgslaan 281 – S8, B-9000 Gent, Belgium.

[2] Laboratoire d'Océanography Chimique et Géochimie des Eaux, Université Libre de Bruxelles, Campus de la Plaine, CP208, boulevard du Triomphe, B-1050 Brussels, Belgium.

Authors' contributions

NVO, CDB, LC, and KS conceived and designed the study. CDB performed the cell lysis rate measurements. NVO, CS, and KS performed the seawater dilution experiments for assessment of phytoplankton growth and mortality rate. LC measured the DMS and DMSP concentration. NVO and CDB analysed the data and NVO wrote the manuscript. KS, CS, WV, and LC revised the manuscript.

Abstract

Processes regulating the formation and termination of phytoplankton blooms are important parameters of the biological carbon pump. Phytoplankton cell lysis, caused by viral infection, senescence, nutrient depletion or other stress factors, has been shown to be an important loss process in addition to grazing and sedimentation. Coccolithophores are considered to be a key phytoplankton group in the marine carbon and sulphur cycle, through the production of calcite and their high intracellular dimethylsulphoniopropionate (DMSP) content. To assess the importance of group-specific phytoplankton stocks, grazing mortality rates, the cell lysis rate of the phytoplankton community, and their relationship with DMSP dynamics, we conducted biogeochemical field surveys during late spring (June 2006, May 2007 and May 2008) in the northern Bay of Biscay, when frequent coccolithophorid blooms are observed. We determined cell lysis rates, using the esterase activity method, together with DMSP and DMS concentrations in surface water. In addition, phytoplankton growth and mortality rates were determined using the seawater dilution method combined with HPLC pigments analysis. Our results confirm that both cell lysis and microzooplankton grazing can be important loss factors for phytoplankton in the northern Bay of Biscay, with lysis rates ranging from 0.04 d^{-1} to 1.96 d^{-1}. Average nutrient-corrected growth and mortality rates for total phytoplankton biomass (Chla) were respectively 0.97 ± 0.50 d^{-1} and 0.76 ± 0.49 d^{-1}. Average nutrient-corrected growth for coccolithophores (HFx) and diatoms (Fx) were respectively 1.08 ± 0.73 d^{-1} and 0.88 ± 0.70 d^{-1}, and mortality rates respectively 0.98 ± 0.65 d^{-1} and 0.89 ± 0.61 d^{-1}. The positive correlation between growth and mortality rates suggests a strong coupling between phytoplankton production and loss processes. In general, we found a positive correlation between cell lysis rates and Chla-based mortality rates, suggesting that cell lysis, and loss of phytoplankton by microzooplankton grazing co-occurred. However, phytoplankton cell lysis rates were sometimes independent of high coccolithophorid mortality rates indicating that microzooplankton grazing can acts as another origin of group-specific phytoplankton loss in this region. Phytoplankton grazing mortality increased along a water column stratification gradient representing the bloom development while cell lysis rate did not display such a linear relationship. Finally, coccolithophores constituted an important source of particulate DMSP, and cell lysis enhanced the release of dissolved DMSP, emphasizing the role of coccolithophore blooms and their termination in the oceanic cycling of DMSP.

Introduction

Coccolithophores are one of the most productive calcifying phytoplanktonic groups (Westbroek *et al.*, 1993). Massive coccolithophore blooms can be observed in temperate and sub-polar oceans; these are visible by satellite imagery as high reflectance (HR) patches caused by detached calcite scales termed coccoliths (Balch *et al.*, 1991; Holligan and Balch, 1991; Holligan *et al.*, 1993). Several studies have shown that blooms of *Emiliania huxleyi*, an abundant coccolithophore representative, occur in highly stratified waters (Balch *et al.*, 1991; Nanninga and Tyrrell, 1996; Ziveri *et al.*, 2000) under high surface irradiance levels (Ziveri and Thunell, 2000) and low nutrient conditions (Holligan *et al.*, 1993; Lampert *et al.*, 2002; Leblanc *et al.*, 2009).

The fate of photosynthetic carbon production in marine ecosystems is a key parameter of the biological carbon pump. Only a fraction of this carbon is exported from the surface layer and ultimately sequestered in the ocean floor. The efficiency by which newly fixed carbon is transferred to depth is dependent on the amount of organic carbon respired along the way down. Cell lysis releases labile dissolved organic matter that can be respired by bacteria, channelling it into the microbial loop, while microzooplankton grazing transfers phytoplankton biomass to higher trophic levels, which eventually may repackage it into faster sinking faecal pellets. Complementarily, new organic matter may be released extracellularly and be exported through coagulation into transparent exopolymer particles (TEP) and aggregation into particles (Engel *et al.*, 2004a). Phytoplankton cell lysis has been shown to constitute an important loss factor contributing to the decline of a bloom (Brussaard *et al.*, 1995), releasing labile dissolved organic carbon (DOC) into the water column (van Boekel *et al.*, 1992; Agusti *et al.*, 1998; Berges and Falkowski, 1998; Agusti and Duarte, 2002; Riegman and Winter, 2003). Cell lysis has been found to be an important loss factor for phytoplankton in the termination of *Phaeocystis* blooms in the North Sea (van Boekel *et al.*, 1992; Brussaard *et al.*, 1995), during mesocosm experiments (Brussaard *et al.*, 2005a; Brussaard *et al.*, 2005b), and in phytoplankton blooms in the northwestern Mediterranean (Agusti *et al.*, 1998; Agusti and Duarte, 2002). Phytoplankton cell lysis is often associated with viral activity, nutrient depletion or extreme light or temperature conditions. In this respect, cell lysis rates are expected to increase towards the decaying

phase of the bloom and may be associated with enhanced microbial activity and export of particulate matter to the seafloor (van Boekel *et al.*, 1992; Brussaard *et al.*, 1995; Riegman and Winter, 2003). To our knowledge cell lysis rates have never been measured during natural coccolithophorid blooms.

Grazing on *E. huxleyi* and production of faecal pellets by mesozooplankon has been shown to be important for the export of particulate material (Harris, 1994). Nonetheless, Holligan *et al.* (1993), using the seawater dilution technique, reported that microzooplankton as well can be major grazers on *E. huxleyi* in the North Atlantic Ocean. Microzooplankton, the <200 µm size fraction of pelagic heterotrophs, are dominated by phagotrophic protists and are the primary grazers of phytoplankton in the open ocean (Sherr and Sherr, 2002; Landry and Calbet, 2004). Low grazing pressure can promote the formation of *E. huxleyi* blooms and their temporary persistence, as has been reported during extensive blooms in the southeast Bering Sea (Olson and Strom, 2002), during coastal blooms in the Celtic Sea (Fileman *et al.*, 2002) and during mesocosm experiments (Suffrian *et al.*, 2008). While microzooplankton grazing appears to be a moderate loss factor for *E. huxleyi*, viral lysis by *E. huxleyi* viruses (*EhV*) has been shown to be responsible for bloom termination during different mesocosm experiments (Castberg *et al.*, 2001; Jacquet *et al.*, 2002; Delille *et al.*, 2005) and natural blooms (Bratbak *et al.*, 1996).

Coccolithophores are also major producers of dimethylsulphoniopropionate (DMSP) which is the main precursor of dimethyl sulphide (DMS), an important natural cloud-forming sulphur aerosol (Stefels *et al.*, 2007). Through its oxidation products, DMS affects the number and size distribution of tropospheric cloud condensation nuclei, thus potentially affecting cloud albedo and heat balance (Simó, 2001). High DMSP and DMS concentrations in the surface waters of the North Atlantic are often associated with blooms of coccolithophores, especially *E. huxleyi* (Holligan *et al.*, 1993). Dissolved DMSP is released in seawater by active exudation and by cell lysis due to senescence or viral infection and zooplankton grazing (Stefels *et al.*, 2007). DMSP and DMS can act as a foraging cue for both macro- and microorganisms, and form substrates for marine bacterial growth (Vila *et al.*, 2004; Neufeld *et al.*, 2008; Seymour *et al.*, 2010). Because of the microbial cycling and the ecological function of DMSP in the ocean, a potentially large and direct influence of the marine biosphere on climate is ultimately mediated by microbial interactions (Seymour *et al.*, 2010).

We conducted biogeochemical field studies (2006-2008) during late spring in the northern Bay of Biscay, where frequent and recurrent coccolithophorid blooms are observed. The dynamics of these blooms in relation to their physical and biogeochemical environment are described in chapter 2 (Van Oostende *et al.*, *in prep. a*). In the present study, we focus on the phytoplankton loss factors such as cell lysis and microzooplankton grazing, which are key determinants of the fate of photosynthetic carbon production. Cell lysis rates were measured using the improved esterase activity method of Riegman and Winter (2003). Phytoplankton group-specific growth rates and mortality rates resulting from grazing were determined using the seawater dilution method of Landry and Hassett (1982). The levels of DMS, and particulate and dissolved DMSP are reported in relation to coccolithophore and diatom biomass. Finally, we integrate these data to analyse (1) the relationship between the rates of cell lysis and phytoplankton mortality, (2) the relationship between the rates of cell lysis along a water column stratification gradient representing bloom development, and (3) the role of cell lysis as a source of dissolved DMSP.

Materials and Methods

Study site and field sampling

Field investigations, supported by remote sensing data, were conducted onboard the Research Vessel *Belgica* in June 2006 (29 May - 10 June), May 2007 (7 - 24 May) and May 2008 (5 - 23 May) along the shelf break in the northern Bay of Biscay (fig.1). Each campaign was carried out in two legs. Three areas were investigated during the campaigns: La Chapelle Bank (47°N, 8°W), Meriadzek Terrace (48°N, 9°W) and Goban Spur (50°N, 10°W). The northeast Atlantic margin in the northern Bay of Biscay is characterised by a broad continental shelf (the Celtic Sea), delimited westward by a steep slope down to 4000 m depth. Internal tides along the continental margin of the northern Bay of Biscay significantly enhance vertical mixing of water masses at the shelf edge (Pingree and Mardell, 1981; Pingree and New, 1995).

Measurement of cell lysis rates and dilution experiments to estimate growth and grazing mortality rates of microphytoplankton were performed in surface waters only (see below). These processes were measured together with the concentration of DMS, dissolved and particulate DMSP at several stations (tables 1 and 2) along the continental margin, which

were determined by tracking the phytoplanktonbloom using near real-time satellite images (fig. 1). In June 2006, cell lysis rates were measured in the vicinity of La Chapelle Bank and Meriadzek Terrace, at stations 6-2, 6-4, 6-8, 6-7 and 6-1b (fig. 1a). Station 6-1b corresponds to station 6-1 revisited during the second leg of this campaign. During the May 2007 campaign, cell lysis measurements were carried out at 3 stations (stations 7-5, 7-8 and 7-8b; fig. 1b). In May 2008, we determined cell lysis rates at 5 shelf stations (stations 8-2, 8-5 and 8-5b near La Chapelle Bank; stations 8-11, 8-12 and 8-13 near Goban Spur; fig. 1c).

Dilution experiments were performed to estimate growth and mortality rates of microphytoplankton in surface waters during 2007, at stations 7-5, 7-5b, and 7-8b, and during 2008 at stations 8-5, 8-5b, 8-9, 8-9b, and 8-12.

Measurements of DMS and DMSP were performed at water depths of 5, 10, 20, 40, 60, and 80 m during 2006 at stations 6-2, 6-7, and 6-8, and in 2008 at stations 8-5, 8-5b, 8-9, 8-9b, 8-12, and 8-13. During 2007 only DMSPp was measured at stations 7-2, 7-5, 7-5b, 7-8, 7-10, and 7-11, at the same depths as the other years.

Satellite images indicate the occurrence of cold water masses at the shelf break which is related to local upwelling of nutrient-rich deep water inducing enhanced primary production (Pingree and Mardell, 1981; Sharples *et al.*, 2009; Harlay *et al.*, 2010). Stratification starts in late April or early May and is well established in early June, after which the upper mixed layer deepens until September. Diatoms and coccolithophores are the two major phytoplankton groups during the spring bloom in the Bay of Biscay but other phytoplankton like dinoflagellates are present (Joint *et al.*, 2001; Neufeld *et al.*, 2008). In general, blooms of coccolithophores follow those of diatoms in waters that have been recently depleted in inorganic nutrients and are becoming more stable and stratified (Leblanc *et al.*, 2009). Yet, during the late spring in the Bay of Biscay, diatom and coccolithophore-dominated blooms can occur alternatively depending on the dissolved silicic acid to nitrate ratio (see chapter 2) (Van Oostende *et al.*, *in prep. a*).

Fig. 1. Location of the stations along the 200 m and the 2000 m isobath superimposed on reflectance satellite images taken during the three field campaigns in the northern Bay of Biscay (a) on 1 June 2006, (b) composite 20-22 May 2007 and (c) composite 18-20 May 2008 (Courtesy of S. Groom, PML). The position of the sampling stations for the measurement of cell lysis rates in surface waters is represented by red symbols, those where grazing rate measurements were also made are in bold italic type.

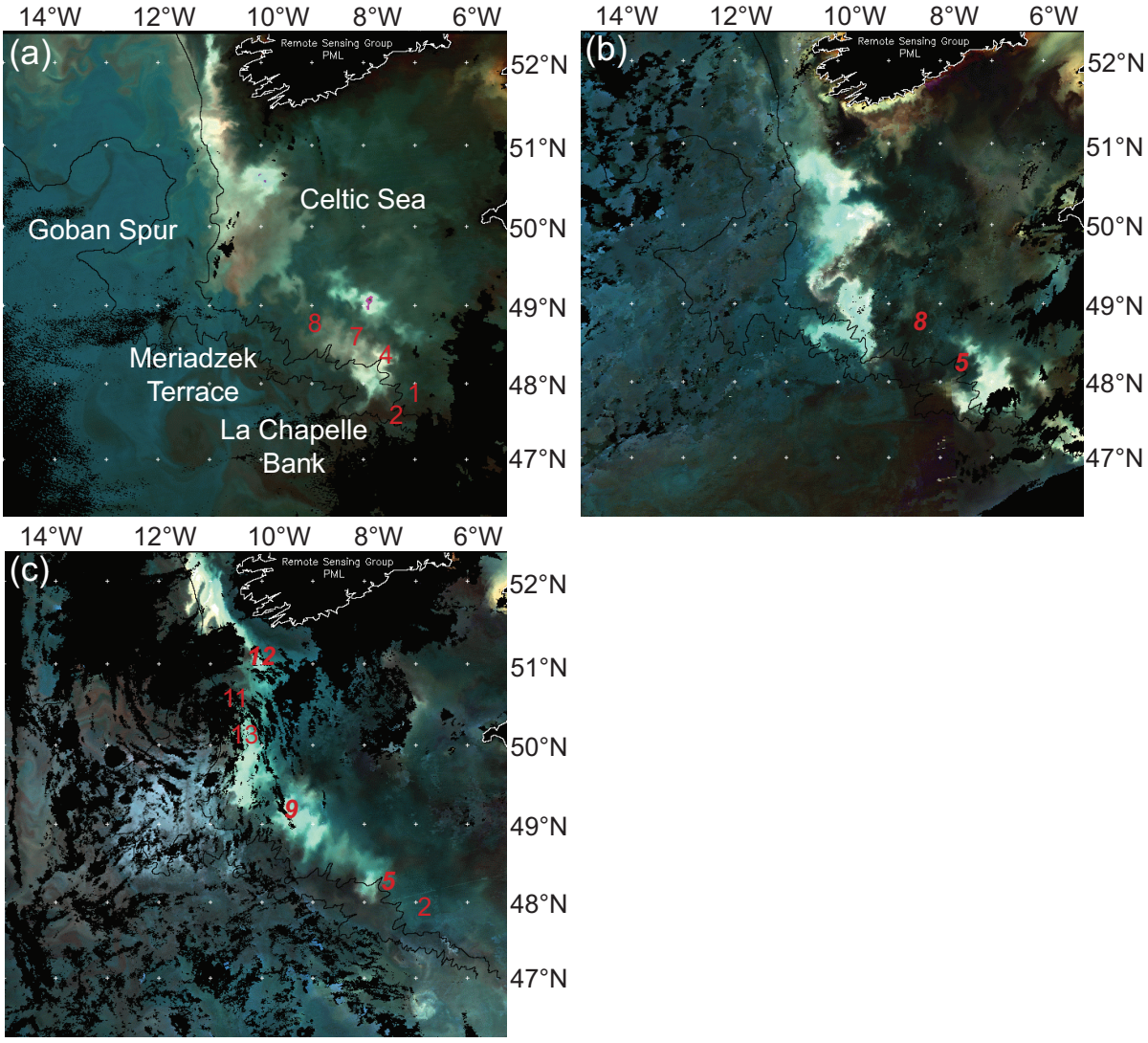

A Seabird Conductivity-Temperature-Depth system (SBE21), equipped with a 12 Niskin bottles (10 l) rosette sampler, was used to determine depth profiles of temperature and salinity and to sample seawater for chemical and biological analyses. At each station, water was collected in the morning at different depths spanning the water column from the surface layer to above and below the thermocline. We collected samples for the analysis of algal pigments, dissolved nutrients, and DMS and DMSP at various depths from the surface to below the thermocline. Water from different casts was used to determine the cell lysis

rates and the dilution experiments. All samples were processed onboard immediately after sampling. Vertical profiles of *in situ* photosynthetic active radiation (PAR) were acquired around noon for each station with a Seabird SBE19 equipped with a LiCor Li-192-SA PAR sensor. The photic depths reported in this study correspond to 1% of the incoming PAR (table 1).

Analytical methods

Algal pigment analysis

Between 0.5 and 3.5 l of seawater were filtered through glass fibre filters (Whatman GF/F) using a low vacuum pressure (< 200 mbar). Chlorophyll *a* (Chla) concentration of the samples used for the determination of cell lysis rates was quantified fluorimetrically following Yentsch and Menzel (1963) after extraction of the particulate material retained on glass fibre filters (Whatman GF/F) in 90% aqueous acetone overnight at 4°C in the dark. During the dilution experiments, samples used for the determination of algal pigment concentrations were stored immediately in liquid nitrogen until analysis by high performance liquid chromatography (HPLC). Separation of the algal pigments was performed using a HPLC method based on that of Wright and Jeffrey (1997), as described in chapter 2 (Van Oostende *et al.*, *in prep. a*). Standard pigment mixtures were run together with the samples to allow identification and quantification of the detected pigment peaks in the chromatogram.

Nutrients

Samples for the measurement of phosphate (PO_4), nitrate and nitrite (NO_x) and dissolved silicate (dSi) were filtered onto 0.4 µm Nuclepore filters (∅ = 47 mm). PO_4 and dSi concentrations were measured onboard, with the colorimetric molybdate blue method of Grasshoff *et al.* (1983). NO_x samples were stored frozen and NOx concentration was determined spectrophotometrically with a "Skalar" Autoanalyzer system using the method of Grasshoff *et al.* (1983).

DMSP and DMS

For the 2006 and 2007 campaigns, the total concentrations of DMS and DMSP (i.e. dissolved (DMSPd) plus particulate DMSP (DMSPp)) were determined on unfiltered water samples; the dissolved forms ([DMS+DMSPd] and DMS) were determined on the filtrates of GF/F filtered

samples. A 10 ml aliquot of filtered or unfiltered seawater was transferred to a glass tube designed for dissolved gas sampling, and 200 µl of 5N NaOH was added. The addition of the base allowed the conversion of DMSP to DMS, allowing calculation of the DMSPd concentration from the concentration of the dissolved species. The tubes were closed immediately with aluminium caps with Teflon-lined septa. Samples were stored at 4°C until analysis. Another 10 ml aliquot of filtered seawater was acidified with 20 µl 4.5N H_2SO_4 and stored frozen at -20°C for the DMS analysis (Smith *et al.*, 1999). For the 2008 campaign, a 10 ml aliquot of the filtrate of the GF/F filtered sample was additionally collected and bubbled with nitrogen during 20 minutes to eliminate the DMS. Two hundred µl of 5N NaOH was then added to the degassed sample, closed with an aluminium cap with Teflon-lined septa and stored at 4°C until analysis of the DMSPd. Protocols for sampling and sample preparation for the analyses of DMS and DMSP were based on the personal communications of L. Chou with both J. Stefels (University of Groningen, NL) and M. Steinke (University of Essex, UK). For the analyses carried out at the Glaciology laboratory (ULB), two needles were placed in the septa, one was bubbling nitrogen through the sample for 30 minutes at a flow rate of 25 ml min^{-1} and the other was collecting the flushed gases that were cryotrapped with liquid nitrogen in a 0.16 mm diameter FEP-Teflon loop. The trap was then heated at 100°C and its content was immediately injected into a TRACE gas chromatograph (GC) INTERSCIENCE device equipped with a Flame Photometric Detector (FPD). DMS was calibrated from DMS standards (Merck) prepared in the laboratory.

Measurement of lysis rates

Estimation of the lysis rates was based on the detection of intracellular esterase released in seawater after cell lysis (van Boekel *et al.*, 1992; Riegman *et al.*, 2002; Riegman and Winter, 2003). During the assay, release of esterases following cell lysis results in hydrolysis of fluorescein diacetate (FDA), a nonfluorescent compound which is added as a substrate, causing the release of fluorescein (F), a fluorescent compound.

The esterase activity (EA in nmol F l^{-1} h^{-1}) was measured fluorimetrically in triplicate. The total esterase activity (TEA) was determined on untreated samples, the dissolved esterase activity (DEA) was analysed on 0.2 µm filtrate. Because FDA is not stable in seawater and its decay rate is dependent on its concentration, temperature, salinity, pH, and alkalinity of the

sample (Riegman *et al.*, 2002), we measured the non-enzymatic esterase activity (NEEA) on samples filtered through 10 kDa molecular weight cut-off filters to remove esterases.

To determine the specific cell lysis rate of a natural phytoplankton community, four components have to be measured: (1) the total esterase activity (TEA) in untreated samples, (2) the amount of extracellular dissolved esterase activity (DEA), (3) the NEEA to calculate the dissolved esterase activity corrected for non-enzymatic hydrolysis of FDA (DEA_c), where DEA_c = DEA - NEEA, and (4) the decay rate of DEA_c in the sample (expressed as $t_{1/2}$, i.e., the half-life of EA in seawater). The rate of EA decrease was calculated from the temporal changes in DEA_c by fitting the exponential decay equation. The amount of intracellular EA in phytoplankton (PEA) was calculated as PEA = TEA – DEA. The amount of DEA produced enzymatically (DEA_{prod}) was calculated taking the decay rate of DEA_c into account:

$$DEA_{prod} = 0.5\ (DEA_c / t_{1/2}) \quad (1)$$

The cell lysis rate (μ_L) is defined here as the ratio of the dissolved esterase activity produced (DEA_{prod}) to particulate esterase activity (PEA) in a natural assemblage on an hourly basis and expressed as per day (d^{-1}):

$$\mu_L = 24\ (DEA_{prod} / PEA) \quad (2)$$

All measurements of EA were made according to the following procedure. 100 µl of Tris-EDTA buffer (pH = 8, final concentration 0.5 mmol l^{-1}) were added to 1.9 ml sample, followed by the addition of 20 µl of 2 mmol l^{-1} FDA (in acetone, final concentration 20 µmol l^{-1}). The increase in fluorescence at 520 nm was measured after incubation of the samples at 25°C during 1 hour in the dark. Fluorescence was converted into fluorescein concentration using an internal standard (Fluorescein, final concentration 5 nmol l^{-1}). The half-life (in hours) of DEAc was by linear regression of the decay of DEA and NEEA measured between t = 0 and 24 h of incubation at *in situ* temperature in the dark. It is assumed that DEA predominantly originates from phytoplankton rather than heterotrophic organisms (van Boekel *et al.*, 1992; Brussaard *et al.*, 1996; Agusti *et al.*, 1998), and the rate of DEA_{prod} represents the rate of dissolved esterase released by phytoplankton. These assumptions imply that this technique should be considered as a semi-quantitative method.

Phytoplankton growth and mortality rates

The seawater dilution method (Landry and Hassett, 1982) was designed to simultaneously determine the phytoplankton growth and grazing mortality rates. Because phytoplankton prey and microzooplankton predators are often in the same size range they cannot easily be physically separated. By diluting whole seawater with particle-free seawater, we minimize the encounter rate between prey and their predators. It is presumed that prey growth is density independent, whereas predator growth is dependent on the density of the prey. Our experimental set-up was largely based upon that of Olson and Strom (2002) and included HPLC pigment analysis allowing determination of growth and mortality of specific phytoplankton groups. Only Chla, fucoxanthin (Fx) and 19'-hexanoyloxyfucoxanthin (HFx) marker pigments were present in sufficiently high concentrations to be analyzed. The HFx has been used as a biomarker for prymnesiophytes on several occasions, while Fx is an indicator of diatom biomass (Barlow *et al.*, 1993; Wright and Jeffrey, 1997; Joint *et al.*, 2001; Leblanc *et al.*, 2009).

Sample water was obtained from a depth where light attenuation reached 50% of the surface light intensity (depth between 5 to 10 m) and particle-free seawater (PFW) for the dilution experiments was prepared by draining the Niskin bottles into a carboy and this *in situ* seawater was further filtered gravitationally through a Millipore capsule with a large area pleated filter (0.2 µm pore size). PFW and whole seawater (WSW) were gently pre-screened through a 200 µm mesh size Nitex filter to remove macro- and mesozooplankton. Prior to the experiment all carboys, bottles, silicone tubing and capsule filters were soaked in an aqueous HCl solution (0.1 N) and thoroughly rinsed with deionised water and PFW. For the experiment, WSW was siphoned, avoiding bubble formation, into 2.3 l polycarbonate bottles containing premeasured volumes of PFW to achieve targeted dilutions (in duplicate) of whole seawater: 0.1, 0.2, 0.35, 0.6, and 1.0 WSW. In order to satisfy the assumption that phytoplankton growth is unaffected by dilution, and to prevent biased mortality estimates from nutrient regeneration within dilution treatments (Andersen *et al.*, 1991), dissolved inorganic nutrients were added to all incubation bottles to supplement *in situ* levels by 0.5 µM PO_4 (added as KH_2PO_4) and 5 µM NO_3 (added as KNO_3). Two additional bottles of 1.0 WSW were incubated without added inorganic nutrients and served as controls for nutrient enrichment effects. Incubation bottles, enclosed in one layer of neutral density screen to

simulate 50% surface irradiance, were incubated for 24 h in an on-deck incubator supplied with a continuous flow of surface seawater to ensure a stable temperature.

Initial pigment samples (1500 - 2000 ml) from pre-screened WSW from the Niskin bottles were filtered through GF/F filters (Ø = 47 mm) at low vacuum pressure. The filters were folded, dipped dry with absorbing paper, packed in aluminium foil, placed in cryovials, and frozen in liquid nitrogen until processing. Pigment samples of the dilution series were obtained and stored in the same way as described above.

Phytoplankton growth and mortality rates were determined from measurements of changes in the phytoplankton concentration (i.e. the net or observed growth rate) over the course of the incubation which were made assuming the exponential growth equation of Landry & Hassett (1982):

$$P_t = P_0 \ e^{t\,(\mu-m)} \qquad (3)$$

where the net growth rate (r) for a time interval (t) is the difference between instantaneous rates of phytoplankton growth (μ) and mortality (m), and P_0 and P_t are, respectively, measured initial and final concentrations of Chla (or other biomarker pigments):

$$r = \ln (P_t/P_0)/t = \mu - m \qquad (4)$$

The rates of phytoplankton growth and mortality were estimated by linear regression of the net growth rate versus the fraction of undiluted seawater (i.e. microzooplankton grazer density). The ordinate intercept of the regression is the instantaneous rate of phytoplankton growth in the absence of grazing (μ), and the negative slope of the regression corresponds to the rate of mortality (m). To correct the estimated growth rate for potential effects of nutrient addition, the nutrient-corrected instantaneous growth rate (μ_c) was calculated following (Olson and Strom, 2002):

$$\mu_c = r_c + m \qquad (5)$$

where r_c is the net growth rate in unenriched 1.0 WSW bottles and m the estimated rate of phytoplankton mortality from the corresponding enriched dilution series. The proportion of initial pigment standing stock (P_i) potentially turned over, as % d^{-1}, by microzooplankton was calculated following Stelfox-Widdicombe *et al.* (2000), according to:

$P_i = (1 - e^{-m}) \times 100$ (6)

We did not quantify the microzooplankton during the dilution experiments to account for possible grazer cell loss during incubation.

Statistical treatment of data

Averages are reported as their arithmetic mean followed by their standard deviation. We used Pearson's product-moment correlations to assess the degree and significance of linear relationships between two variables. We used Student's t-test to test the null hypothesis of no difference between the ratio of μ to μ_c and 1. Linear regression was used to estimate the slope of the relation between pigment concentrations and the dilution level in the dilution experiments. Values were checked for normal distribution and homoscedacity (where applicable) before performing these tests using the Statistica 7.0 (StatSoft, Inc.) program.

Results

Environmental setting and phytoplankton community composition

During the June 2006 campaign sea surface temperature (SST) ranged from 13.0 to 14.5 °C, while the SST was slightly lower in 2007 and 2008 (12.7 to 13.5 °C) (table 1). Surface Chla concentration was always < 2.0 µg l^{-1}, with the highest values measured in 2006 and the lowest in 2008 (table 1). Phytoplankton growth in surface waters led to the depletion of inorganic nutrients down to 40-60 m depth (see chapter 2) (Van Oostende *et al.*, *in prep. a*). PO_4 concentrations exhibited similar yearly vertical profiles with concentrations close to 0 (< 0.1 µmol l^{-1} at surface) in surface waters and around 0.5 µmol l^{-1} below the photic zone. As for PO_4, NO_x levels were depleted at surface, ranging from 0 to 1.0 µmol l^{-1} in June 2006, from 0.4 to 0.9 µmol l^{-1}in May 2007, and below 0.3 µmol l^{-1} at 3 m depth in May 2008. Surface PO_4 and NO_x concentrations measured during our campaigns yielded NO_x:PO_4 ratios below the Redfield ratio of 16 ($3.92 < NO_x:PO_4 < 14.52$) (table 1).

Table 1. Physical and biochemical characteristics of the surface waters at the stations where the rate of cell lysis (μ_L) and/or phytoplankton mortality were determined. The cell lysis rate (μ_L) was determined as a function of dissolved esterase activity corrected for non-enzymatic hydrolysis (DEAc) and particulate esterase activity (PEA). The produced dissolved esterase activity (DEA_{prod}) was computed from the half-life ($t_{1/2}$) and DEA_c in ambient seawater. Station codes are presented together with their geographic position (lat.: latitude; lon.: longitude), time of sampling, photic depth, stratification degree of the water column (strat. deg.), sea surface temperature (SST), nutrient ratio (NO_x:PO_4), and chlorophyll *a* (Chla) concentration.

Stations	**date**	**lat.** (°N)	**lon.** (°W)	**photic depth** (m)	**strat. deg.** (kg m^{-3})	**SST** (°C)	**NO_x:PO_4**	**Chla** ($\mu g\ l^{-1}$)	**DEA_c** (nmol F l^{-1} h^{-1})	**PEA** (nmol F l^{-1} h^{-1})	**$t_{½}$** (h)	**DEA_{prod}** (nmol F l^{-1} h^{-1})	**μ_L** (d^{-1})
6-2	01/06/2006	47.53	7.17	31	0.21	12.99	12.63	1.76	2.84	33.06	12.03	0.12	0.09
6-4	02/06/2006	48.10	7.50	26	0.39	13.29	4.25	1.27	5.38	39.44	5.58	0.48	0.29
6-8	06/06/2006	48.50	8.90	34	0.73	14.47	3.00	0.80	2.33	33.25	3.04	0.38	0.28
6-7	07/06/2006	48.40	8.10	26	0.69	14.51	12.00	0.96	0.50	45.89	3.12	0.08	0.04
6-1b	09/06/2006	47.75	7.00	37	0.56	14.32	2.33	0.39	6.03	13.30	3.98	0.76	1.37
7-5	12/05/2007	48.20	7.62	45	0.24	12.97	9.36	1.03	3.26	11.76	3.84	0.42	0.87
7-8	13/05/2007	48.50	8.50	37	0.27	13.21	14.52	1.39	2.71	6.72	6.80	0.20	0.71
7-8b	21/05/2007	48.50	8.50	27	0.29	13.27	6.92	1.25	6.95	17.27	4.62	0.75	1.05
7-5b	22/05/2007	48.22	7.59	33	0.31	13.30	3.91	0.52					
8-2	08/05/2008	47.80	6.90	40	0.25	12.75	3.92	0.78	2.37	8.23	8.89	0.13	0.39
8-5	10/05/2008	48.20	7.59	42	0.27	12.91	4.00	0.34	1.38	6.15	5.50	0.13	0.49
8-9	12/05/2008	49.20	9.50	38	0.38	12.91	22.80	0.13					
8-11	14/05/2008	50.50	10.50	36	0.31	12.70	11.78	0.27	1.25	15.10	2.22	0.28	0.45
8-12	19/05/2008	51.00	10.00	25	0.60	13.61	4.88	0.24	1.67	5.21	1.96	0.43	1.96
8-13	20/05/2008	50.00	10.34	24	0.46	13.42	4.80	0.63	5.64	26.44	4.13	0.68	0.62
8-9b	21/05/2008	49.20	9.50	23	0.48	13.62	7.18	0.81					
8-5b	22/05/2008	48.20	7.60	25	0.37	13.53	3.96	0.94	2.60	22.23	2.96	0.44	0.47

dSi was less depleted with concentrations close to 1.0 µmol l^{-1} during the June 2006 campaign. Nevertheless, a decrease in dSi at surface was observed between the two legs and values below 1.0 µmol l^{-1} were observed at stations 6-7 and 6-1b. In May 2007, surface waters exhibited a stronger depletion in dSi with concentrations close to 0 µmol l^{-1}, indicating its consumption by diatoms. Surface waters were heavily depleted in dSi during May 2008 with concentrations below 1.0 µmol l^{-1}.

Based on the seasonal evolution of remotely sensed Chla concentration in the area of study, during each campaign year (fig. 2), the 2006 campaign was carried out during the decline phase of coccolithophorid blooms, while the 2007 and 2008 campaigns were carried out at the end of the diatom bloom and corresponded to the growth phase of the coccolithophorid bloom. .The first peak in Chla is ascribed to diatoms and the second one, of lower amplitude, to coccolithophore-dominated blooms (Leblanc *et al.*, 2009). We observed several high reflectance (HR) patches distributed inshore of the 200 m isobath during each campaign, indicating the presence of coccolithophores (fig. 1). In June 2006, the northern part of the investigated area exhibited HR patches (fig. 1a, stations 6-4, 6-5, 6-7 and 6-8). In May 2007, HR patches were observed at the La Chapelle Bank (stations 7-2 and 7-4) and at the Goban Spur (stations 7-9, 7-10 and 7-11) (fig. 1b), while in May 2008 HR patches were observed at the Meriadzek Terrace (stations 8-5 and 8-6) and in Goban Spur (stations 8-9 to 8-13) (fig. 1c).

In this study, the coccolithophore *E. huxleyi* was the main representative of the prymnesiophytes as indicated by microscope observations (see chapter 2, fig. 3). Using phytoplankton biomarker pigment concentrations and a CHEMTAX routine (see chapter 2), we partitioned the Chla between the dominant groups of the phytoplankton community (fig. 5). During 2006 the phytoplankton community was dominated by coccolithophores at stations 6-2 and 6-1b and by diatoms at stations 6- 7 and 6-4. During the 2007 campaign, diatoms were the dominant species at all stations where lysis rates were measured (stations 7-5 and 7-8), while in 2008 coccolithophores were the dominant species at all stations except stations 8-2, 8-5, and 8-9.

Fig. 2. Time-series of remotely sensed, weekly Chla concentrations (µg l^{-1}) at Meriadzek Terrace (lat. [48.0°N; 48.5°N], lon. [8°W; 8.5°W]), from January to September in 2006, 2007, and 2008. The vertical dotted lines delimit the period during which the campaigns took place (red lines for 2006, blue lines for 2007, and green lines for 2008). Chla are Level-3 Sea viewing Wide Field-of-view Sensor data (http://reason.gsfc.nasa.gov/OPS/Giovanni/).

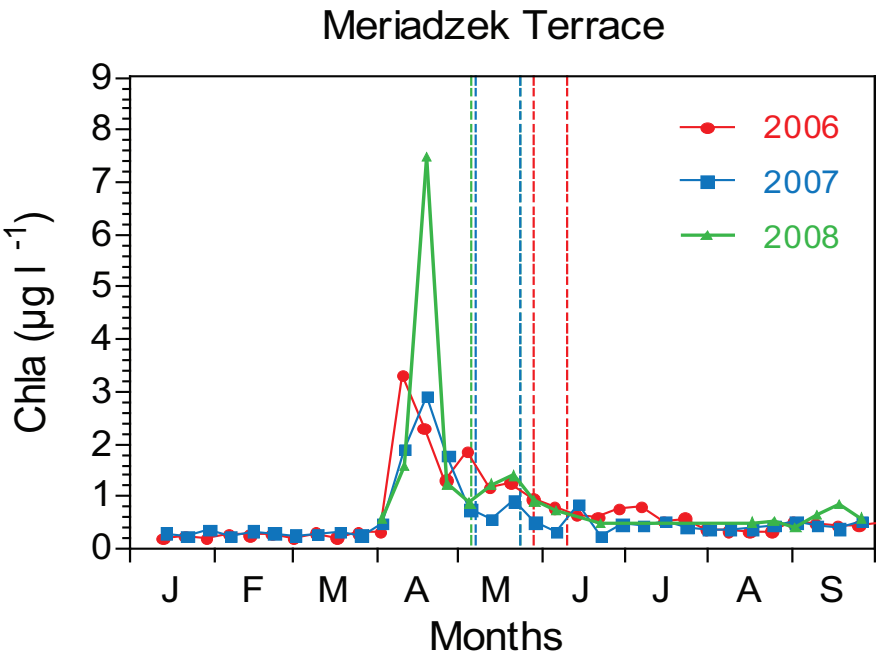

DMS and DMSP concentration

In general, the concentrations of DMS, DMSPd, and DMSPp were highest in the upper 40 m of the water column (fig. SP1). At the stations where cell lysis rates were determined, the concentrations of DMS, DMSPd, and DMSPp ranged between 11-39 nmol l^{-1}, 3-58 nmol l^{-1}, and 24-98 nmol l^{-1}, respectively (table 2). Unfortunately, the DMS and DMSPd concentrations from the 2007 samples could not be measured due to sample conservation issues. At the stations where cell lysis rates were determined, DMSPp levels were generally higher than DMSPd, except at station 8-12 (table 2), where an elevated cell lysis rate was determined (table 1). Moreover, we observed high DMSPp concentrations associated with the presence of coccolithophores (stations 6-2, 6-8, 8-13, and 8-5b), while we did not find a linear relationship between DMSPp levels and diatom biomass (fig. 3).

Table 2. Surface concentration of DMS, DMSPd, and DMSPp, and the ratio of dissolved and particulate DMSP levels measured at stations where cell lysis rates were determined.

Station	DMS (nmol l^{-1})	DMSPd (nmol l^{-1})	DMSPp (nmol l^{-1})	DMSPd/DMSPp
6-2	15	48	98	0.49
6-8	24	41	65	0.64
6-7	11	3	31	0.10
7-5			34	
7-8			27	
8-5	14	18	24	0.76
8-12	12	30	25	1.18
8-13	39	25	64	0.40
8-5b	15	58	88	0.65

Fig. 3. Relation between the DMSPp concentration and the Chla concentration assigned to coccolithophores (a) and diatoms (b) (using a CHEMTAX routine, see chapter 2), measured in the upper 20 m of the water column during the three consecutive campaigns (2006, 2007, and 2008). The trendlines represent the linear regressions of DMSPp versus coccolithophorid Chla ($y = 54.6\ x + 29.1$; $r^2 = 0.59$; $p<0.01$) and DMSPp versus diatom Chla ($y= -26.3\ x + 53.8$; $r^2 = 0.05$; $p>0.05$).

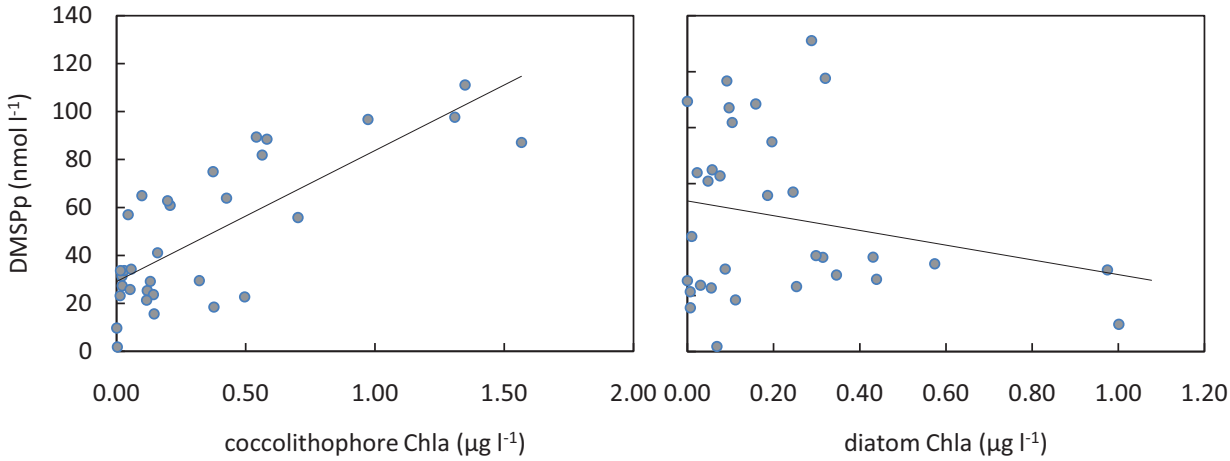

Phytoplankton cell lysis in the northern Bay of Biscay

Phytoplankton cell lysis rates ranged from 0.04 d^{-1} (station 6-7) to 1.96 d^{-1} (station 8-12) (table 1), with an average rate of 0.65 ± 0.52 d^{-1} (n=14) during our campaigns. In June 2006, the highest lysis rate was observed at station 6-1b (1.37 d^{-1}). Stations 6-2, 6-4, 6-8 and 6-7 presented below average levels of cell lysis rates (table 1). In May 2007, lysis rates exhibited

a minimum value of 0.71 d^{-1} at station 7-8 and a maximum value of 1.05 d^{-1} at station 7-8b. An increase in cell lysis rate was observed between the two legs at station 7-8 (from 0.71d^{-1} to 1.05 d^{-1}, table 1). These lysis rates were within the range of those determined in the same area in June 2006. In May 2008, the minimum lysis rate was observed at station 8-2 (0.39 d^{-1}) and the maximum at station 8-12 (1.96 d^{-1}). A slight decrease was observed at the revisited station 8-5, 12 days later (from 0.49 to 0.47 d^{-1}, table 1). Stations 8-12 and 8-13, located in the Goban Spur area exhibited higher lysis rates than more southerly stations.

Non-enzymatic hydrolysis of FDA in our samples ranged from 8 % (station 6-8) to 59 % (station 7-8) of the TEA with an average of 28 % ± 17 %. DEA_c ranged from 0.50 nmol F l^{-1} h^{-1} (station 6-7) to 6.95 nmol F l^{-1} h^{-1} (station 7-8b), with an average of 3.21 ± 1.99 nmol F l^{-1} h^{-1}. The half-live of natural esterases ($t_{1/2}$) varied between 2 h and 12 h. For samples collected at stations on the shelf during the 2006 campaign, we determined a PEA:Chla ratio of 32.73 nmol F µg Chla $^{-1}$ h^{-1} by linear regression, while did not find a significant linear relationship between PEA and Chla using the entire dataset (fig. 4).

Fig. 4. PEA as a function of Chla concentration during 2006 (red dots; full dots represent the stations on the continental shelf, while the empty dot represents the station on the slope of the shelf edge), 2007 (blue diamonds), and 2008 (green triangles). The trend lines represent the linear regression of PEA versus Chla for all data points (full line: y = 16.19 x + 5.26, r^2 = 0.28, p >0.05), and only the shelf stations sampled in 2006 (dashed line: y = 32.73 x + 4.99, r^2 = 0.72, p <0.05).

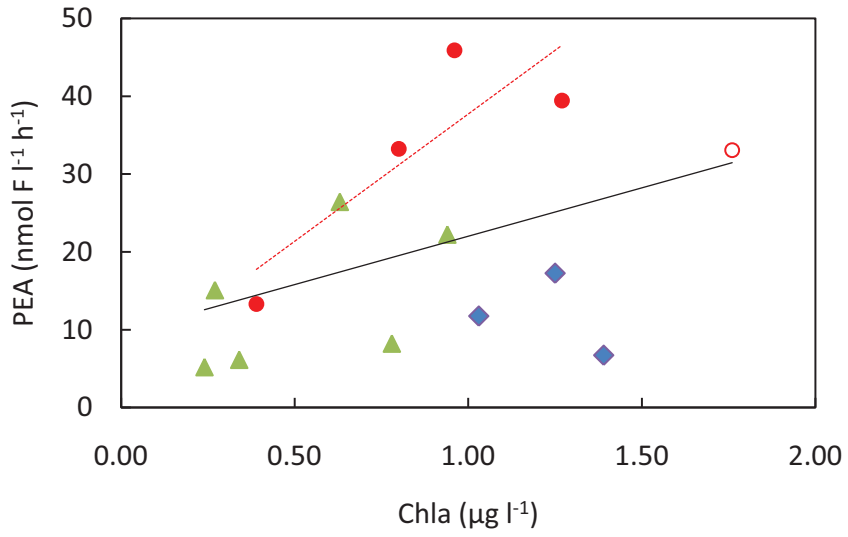

Fig. 5. Cell lysis rate expressed as a function of Chla concentration (a) and the stratification degree of the water column (b) during the 2006 (red dots), 2007 (bue diamonds), and 2008 campaign (green triangles). Phytoplankton mortality rate as a function of the stratification degree of the water column (c) during the 2007 (bue diamonds) and 2008 campaign (green triangles). The trendlines represent the linear regressions of lysis rate versus Chla ($y = -0.51 x + 1.09$, $r^2 = 0.20$, $p>0.05$), of the lysis rate versus the stratification degree for the values of 2008 ($y = 4.05 x – 0.79$, $r^2 = 0.77$, $p<0.05$), and of the phytoplankton mortality rates versus the stratification degree for the values of both years ($y = 2.85 x – 0.28$, $r^2 = 0.50$, $p=0.05$).

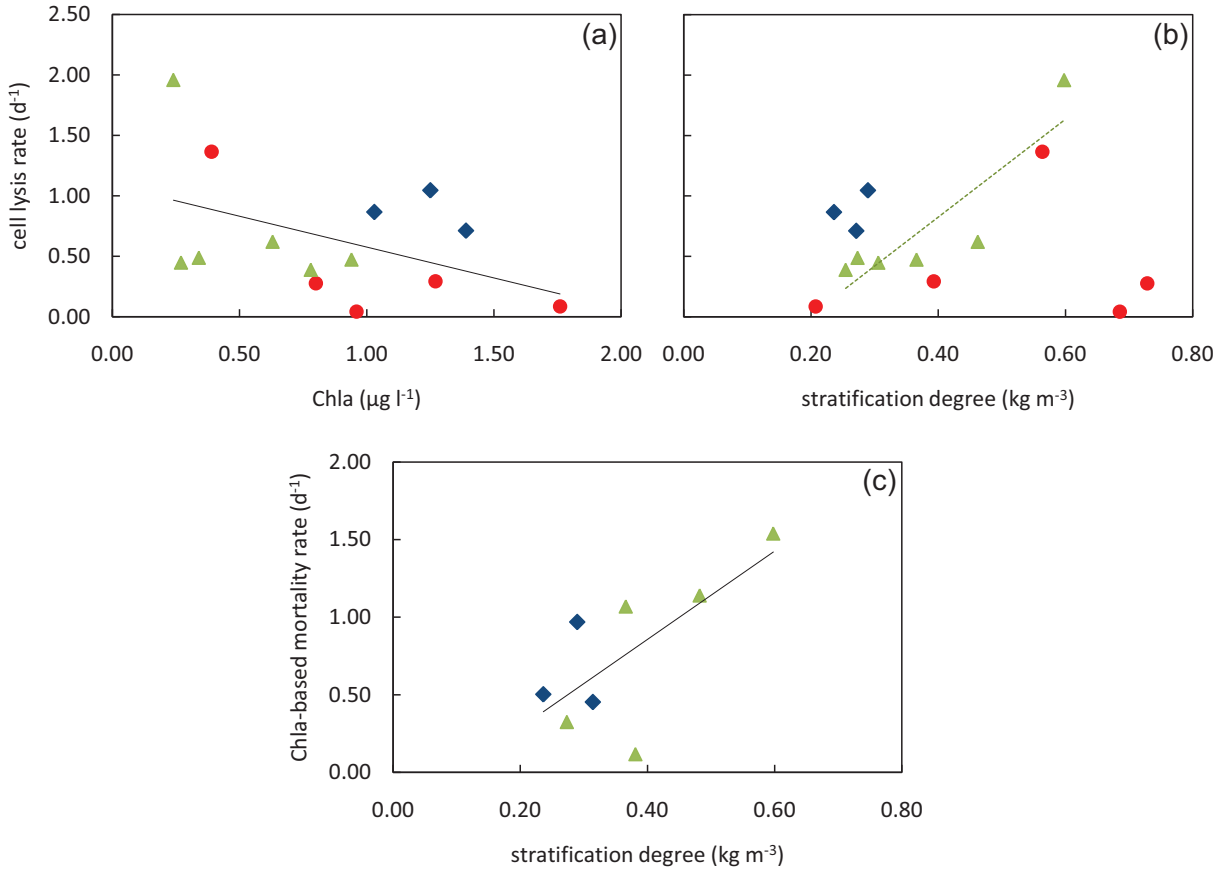

Fig. 7. The ratio of DMSPd and DMPSp concentrations as a function of cell lysis rate for the measurements of 2006 (red dots) and 2008 (green triangles). The trendline represents the linear regression of DMSPd/DMSPp ratio versus cell lysis rate for all the represented values ($y = 0.42\ x + 0.36$; $r^2 = 0.68$; $p=0.02$).

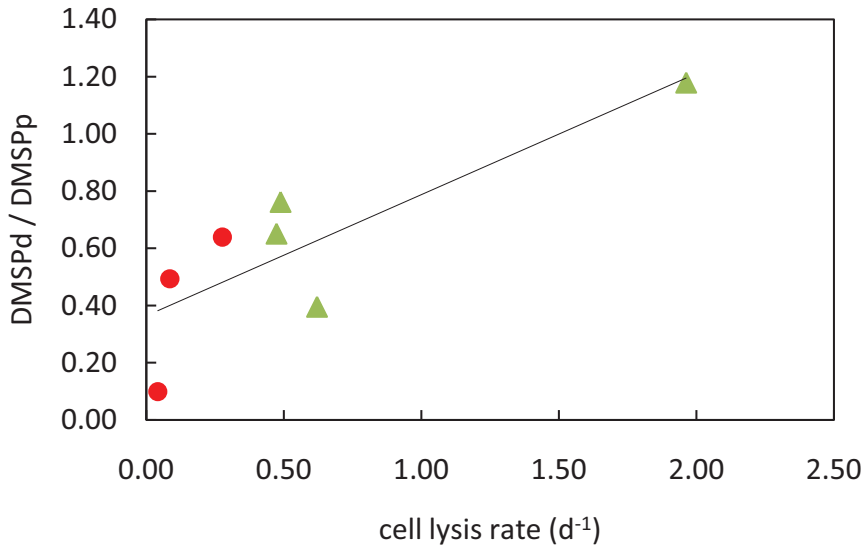

Phytoplankton growth and grazing mortality determined by the dilution technique

Dilution experiments were performed at eight stations (table 3); for five of these lysis rates were also measured (at stations 7-5, 7-8b, 8-5, 8-5b, and 8-12). Table 3 summarizes the estimates of phytoplankton growth and mortality rates from dilution experiments for 3 marker pigments (Chla, HFx, and Fx). Nutrient-corrected phytoplankton growth rates and mortality rates varied widely across experiments and pigments. Average nutrient-corrected growth and mortality rates for total phytoplankton biomass (Chla) were respectively 0.97 ± 0.50 d^{-1} and 0.76 ± 0.49 d^{-1}. For prymnesiophytes (HFx) and diatoms (Fx) these were respectively 1.08 ± 0.73 d^{-1} and 0.88 ± 0.70 d^{-1}, and 0.98 ± 0.65 d^{-1} and 0.89 ± 0.61 d^{-1}. In general, instantaneous nutrient-enhanced growth rates were higher than the nutrient-corrected growth rates, which indicates a general state of nutrient limited growth among phytoplankton cells (t-test of ratio $\mu:\mu_c > 1$: $t=2.4$, $df=14$, $p<0.05$). Irrespective of the size of the phytoplankton standing stocks, a strong coupling between algal growth (μ_c) and microzooplankton grazing was apparent, as indicated by the strong positive correlation between these two processes (Chla: $r=0.88$, $n=8$, $p<0.01$; HFx: $r=0.98$, $n=7$, $p<0.01$; Fx: $r=0.90$, $n=6$, $p<0.01$).

Fig. 6. Cell lysis rate versus grazing mortality rate. The mortality rate is estimated from Chla concentrations (a), from HFx concentrations (b), and from Fx concentrations (c). Blue diamonds represent results obtained in 2007 and green triangles represent results obtained during the 2008 campaign. The station code is indicated next to its respective symbol. Black lines represent the linear regressions for all results (n=5) and r^2 is the regression coefficient. The dotted lines represent the linear regressions for results of 2008 only and r^2 is the regression coefficient. Asterisk denote significant regression results at $p<0.05$.

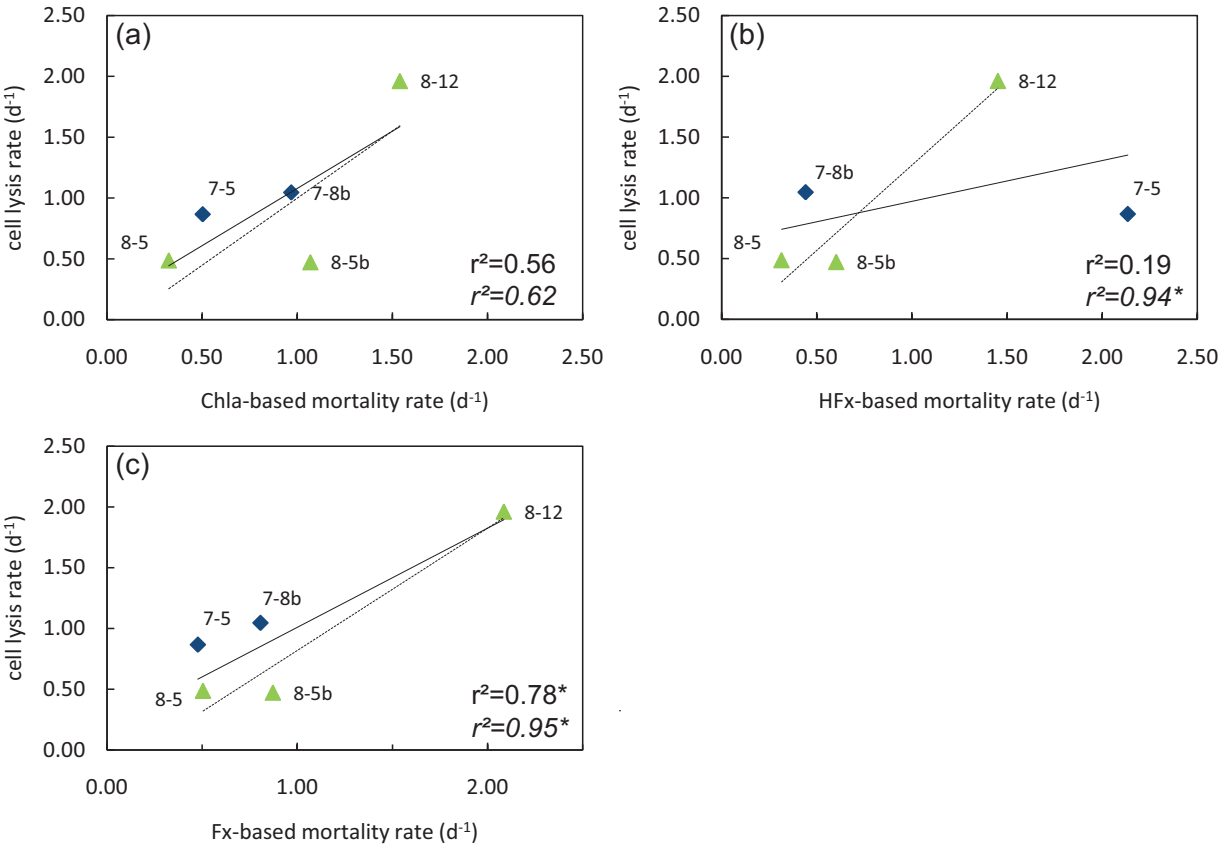

Table 3. Instantaneous growth rates (μ), nutrient-corrected growth rates (μ_c), rates of mortality (m), and the proportion of pigment standing stock grazed daily derived from linear regressions of Chla, 19'-hexanoyloxyfucoxanthin (HFx), and fucoxanthin (Fx) data of dilution experiments performed during May 2007 and 2008. r is the correlation coefficient of linear regression between observed, net phytoplankton growth rate and dilution factor, (*p < 0.05, **p < 0.01). Values represented by "-" could not be determined due to low pigment concentrations.

Station	Growth μ (d^{-1})			Nutrient corrected growth μ_c (d^{-1})			mortality m (d^{-1})			Proporion of stock grazed (% d^{-1})			r		
	Chla	HFx	Fx	Chla	HFx	Fx	Chla	HFx	Fx	Chla	HFx	Fx	Chla	HFx	Fx
7-5	1.14	3.36	1.01	0.94	2.44	1.03	0.50	2.13	0.48	40	88	38	0.78**	0.77*	0.80**
7-5b	0.82	0.58	0.71	0.74	0.50	0.71	0.45	0.23	0.56	36	20	43	0.73**	0.71**	0.78**
7-8b	0.92	0.80	0.67	0.88	0.76	0.57	0.97	0.44	0.81	62	36	55	0.76*	0.44	0.70*
8-5	0.38	0.45	0.81	0.17	0.32	0.36	0.32	0.32	0.50	28	27	40	0.95**	0.84**	0.84**
8-5b	1.95	1.47	2.02	1.34	0.84	1.01	1.07	0.60	0.87	66	45	58	0.75*	0.84*	0.82*
8-9	0.81	-	-	0.65	-	-	0.12	-	-	11	-	-	0.06	-	-
8-9b	1.44	1.34	-	1.19	1.10	-	1.14	1.02	-	68	64	-	0.97**	0.90**	-
8-12	2.16	1.94	2.44	1.87	1.61	2.19	1.54	1.45	2.09	79	77	88	0.97**	0.98**	0.97**

Discussion

The esterase activity method

Although lysis rate measurements have been published on several occasions since the first study of van Boekel *et al.* (1992), these investigations used different methods to measure the lysis rate. Riegman *et al.* (2002) indicated that, due to various artefacts in the methods, some previous estimations of the lysis rate had been biased. There are principally two factors that cause the discrepancy between the methods. The first important drawback of the studies of Agusti *et al.* (Agusti *et al.*, 1998; Agusti and Duarte, 2000, 2002) or the earlier study of van Boekel *et al.* (1992) is the lack of correction for the non-enzymatic hydrolysis of FDA (Riegman *et al.*, 2002). A second source of error is that the authors did not deduce the PEA directly from the measurements but instead calculated it from the Chla concentrations using a ratio of PEA to Chla derived from phytoplankton cultures (Riegman *et al.*, 2002). We therefore applied the method described in Riegman and Winter (2003).

The broad range in non-enzymatic hydrolysis of FDA emphasizes the usefulness of such a correction. The average DEAc concentration of 3.21 $\pm$ 1.99 nmol F l^{-1} h^{-1} is comparable to the 3.2 nmol F l^{-1} h^{-1} reported by Riegman *et al.* (2002) in the southern North Sea. The half-live of natural esterases ($t_{1/2}$) varied between 2 h and 12 h, which is shorter than reported in the literature: from 14 to 40 h in Agusti and Duarte (2000) for oligotrophic Mediterranean waters or 49 $\pm$ 6 h in Riegman *et al.* (2002) for the southern North Sea. In June 2006 and May 2008, the rates of decay of DEA_c (expressed as $t_{1/2}$), measured during incubations carried out at *in situ* temperature, were higher at lower temperatures during the first leg of 2006 campaign (stations 6-2 and 6-4) and the first leg of 2008 campaign (stations 8-2 and 8-5). Such a temperature dependence of DEA was also observed by Agusti and Duarte (2000).

The PEA:Chla ratio, using the PEA concentrations of only the 2006 shelf stations, was 32.73 nmol F µg Chla $^{-1}$ h^{-1}, one order of magnitude higher than those in the southern North Sea 2.48 nmol F µg Chla $^{-1}$ h^{-1} (Riegman *et al.*, 2002). The determination of this factor in a batch culture of *E. huxleyi* using the same procedure showed a ratio of 11.78 nmol F µg Chla $^{-1}$ h^{-1} (De Bodt, unpublished data), which is in the same range as those of van Boekel *et al.* (1992), who reported a ratio of 9.2 nmol F µg Chla $^{-1}$ h^{-1} for *E. huxleyi*. Different PEA:Chla ratios were

thus obtained for different natural phytoplankton assemblages at different field locations and laboratory cultures. Our results underline the need to measure the PEA in the natural assemblages instead of deducing it from phytoplankton cultures.

Nevertheless, in the natural sample, a fraction of the PEA results from non-phytoplankton species. According to Riegman *et al.* (2002), when phototrophs and heterotrophs are in equal biomasses, the contribution of heterotrophic PEA to the total PEA is approximately 10-20%. A comparable fraction of DEA will also originate from non-phytoplankton sources. The results of different laboratory studies indicate however that the DEA of heterotrophs is negligible (van Boekel *et al.*, 1992; Agusti *et al.*, 1998; Agusti and Duarte, 2002). Since we do not know the contribution of heterotrophs to the total biomass during our surveys and the fraction of DEA or PEA originating from heterotrophs rather than phototrophs remains uncertain, our results should be regarded as semi-quantitative.

Cell lysis rate and phytoplankton bloom state

Blooms of coccolithophore have been reported to occur after the main diatom spring blooms (Head *et al.*, 1998) or co-occurring with diatoms (Lampert *et al.*, 2002; Van Oostende *et al.*, *in prep. a*) (see also chapter 2), because *E. huxleyi* does not require dSi to grow and is able to form blooms at low or depleted PO_4 concentrations (Egge and Heimdal, 1994; Riegman *et al.*, 2000). During our field studies, nutrients were largely depleted and massive coccolithophorid blooms occurred as evidenced by microscopy, pigment analysis, and remote sensing (fig. 1) (see also chapter 2, fig. 3). Patches of high reflectance in this area, which are characteristic of the declining stage of *E. huxleyi* blooms, were observed by remote sensing after the main spring bloom and caused by the accumulation of suspended coccoliths in the surface water layer (Balch *et al.*, 1991; Harlay *et al.*, 2009). Such patches of high cellular density, are prone the virus infection or grazing, ultimately leading to bloom collapse (Brussaard *et al.*, 1996; Castberg *et al.*, 2001; Jacquet *et al.*, 2002). The average level of cell lysis rate in this study (0.65 ± 0.52 d^{-1}) is higher than previous studies (Brussaard *et al.*, 1995; Brussaard *et al.*, 1996; Riegman and Winter, 2003) where lysis rates were close to 0.3 d^{-1} during *Phaeocystis* (prymnesiophyte) blooms in the North Sea. The highest rates of cell lysis of 1.37 d^{-1} and 1.96 d^{-1} were measured at respectively station 6-1b and station 8-12. Station 6-1b is thought to be in the decay phase of a coccolithophorid bloom (Harlay *et al.*, 2009) and exhibited a low Chla concentration during this campaign (0.39 µg l^{-1}, table 1). The

high lysis rates measured at station 8-12 corroborate the scenario where cell lysis may be an important factor in the termination of *E. huxleyi* blooms. This station was located in a HR patch (fig. 1) where we detected high densities of coccoliths together with *E. huxleyi* coccospheres (see also chapter 2, fig. 3d), indicative for declining *E. huxleyi* blooms. Although these cell lysis values are significantly higher than the other estimates in this study, they agree with those reported for a stratified oligotrophic Mediterranean Bay (Agusti and Duarte, 2000, 2002). Measurements of Agusti *et al.* (1998) showed lowest cell lysis rates at maximum Chla concentration. This would be expected when high cell lysis rates due to e.g. viral infection effectively reduce phytoplankton biomass. However, we did not find a significant linear relationship between Chla concentration and the rate of cell lysis (fig. 5). Because the lack of relationship may be due to the difference in bloom stage of the different stations, which is not reflected by Chla levels, we plotted the cell lysis rates along a water column stratification gradient which serves as a proxy of bloom development in this area (fig. 5) (Suykens *et al.*, 2010; Harlay *et al.*, 2011; Van Oostende *et al.*, *in prep. a*). We found a positive relationship between stratification of the water column and the rate of cell lysis in 2008, however this was not the case in 2006. Cell lysis rates at station 6-7 and 6-8 were low but the water column was already highly stratified, which may suggest these stations were in a post-lysis stage compared to other stations of this campaign. The lack of linear relationship may be due to the unimodal nature of the cell lysis rates versus the stratification degree, as we suggested for the phytoplankton bloom development in chapter 2, although more data is needed to confirm this observation.

Phytoplankton growth and grazing mortality

Average phytoplankton growth and mortality rates (0.97 ± 0.50 d^{-1} and 0.76 ± 0.49 d^{-1}, respectively) in this study are higher than those compiled by Calbet and Landry (2004) for the total phytoplankton community in open ocean environment (0.59 d^{-1} and 0.39 d^{-1}, respectively for growth and mortality rates). However, growth and mortality rates for the total phytoplankton biomass are quite variable, ranging from 0.01 to 1.71 d^{-1} in the North Atlantic Ocean (Calbet and Landry, 2004, and references therein). The higher end values for the growth and mortality rates measured in our study (i.e. above 2 d^{-1}) are generally not encountered in any oceanic environment, but similar rates up to 2.69 d^{-1} (Strom *et al.*, 2001) have been found in several coastal studies (Landry *et al.*, 1998; Huang *et al.*, 2008; Chen *et*

al., 2009). Although growth rate values above 3 d^{-1} have been reported in an estuarine study (Ruiz *et al.*, 1998), they are probably an artefact that may be due to possible grazer mortality in the dilute treatments, nutrient effects, or an increase in cellular pigment content, which were not accounted for here (Dolan *et al.*, 2000; Liu *et al.*, 2009).

Differences in growth and mortality rates between the two pigment-based phytoplankton groups, diatoms and coccolithophores, point to differential control of these populations by microzooplankton (table 3). Selective grazing by microzoplankton such as ciliates and dinoflagellates has been reported before and phytoplankton prey palatability may even be enhanced by its degree of viral infection (Hamels *et al.*, 2004; Evans and Wilson, 2008). Furthermore, our results from the revisited stations indicate strong temporal (and/or spatial, if we consider water mass advection) variation in phytoplankton dynamics. In 2007 diatoms often dominated the phytoplankton assemblage, possibly due to the stormy weather condition conditions during this campaign (fig. SP2) (see also chapter 2) (Van Oostende *et al.*, *in prep. a*). This is substantiated by the high diatom and low coccolithophore biomarker concentrations measured (average Fx:HFx = 9.18 ± 5.72). Total phytoplankton growth rate decreased while the grazing rate increased from station 7-5 to 7-5b, suggesting a stronger control exerted on phytoplankton by microzooplankton grazing. In 2008 on the other hand, different stages of a coccolithophorid bloom were sampled. At station 8-5, low growth and grazing rates were measured together with intermediate HFx concentrations, suggesting the very beginning of an *E. huxleyi* bloom (fig. 5). At station 8-5b, the onset of the bloom was marked by a higher growth than grazing rate, accompanied by a high *E. huxleyi* biomass (fig. SP2 and fig. 3 in chapter 2). Finally, at station 8-12 the prevalence of coccoliths and the lower HFx concentration as compared to station 8-5b together with the high proportion of standing stock grazed daily, strongly suggest the demise of the bloom (chapter 2, fig. 3).

The strong correlation we measured between growth and mortality rates suggests a strong coupling between phytoplankton production and loss processes. Comparison with the data on growth and mortality rates for studies in temperate oceanic North Atlantic environments we compiled from Calbet and Landry (2004), showed that strong correlation between both processes is typical ($r= 0.71$, $n=62$, $p<0.01$).

Co-occurrence of phytoplankton grazing mortality and cell lysis rates

The sometimes high lysis and grazing mortality rates (measured by independent techniques) indicate phytoplankton biomass proliferation was often under tight control in our area of study. We did not find a significant relationship between the cell lysis rate and the phytoplankton mortality rates (Chla-based) determined during both 2007 and 2008 campaigns (fig. 6a). This indicates that phytoplankton grazing mortality did not always co-occur with cell lysis. The lack of correlation when using the coccolithophorid marker pigment HFx indicates that, at least at station 7-5, cell lysis and grazing mortality are independent of each other (fig. 6b, solid line). Nonetheless, a positive relation was found in 2008 between lysis and HFx-based mortality rate (fig. 6b, dotted line). Finally, a significant correlation was observed again when using the marker pigment Fx (fig. 6c), indicating that diatom grazing mortality co-occurred with cell lysis in our study. During our seawater dilution experiments we only determined the rate of grazing mortality of the phytoplankton, since we did not perform additional incubations to exclude viral particles from our dilution experiments (as was done by e.g. Kimmance *et al.* (Kimmance *et al.*, 2007) and Evans *et al.* (Evans *et al.*, 2003)). Thus, no gradient of viral lysis pressure was created as only the phytoplankton host cells were diluted (Kimmance and Brussaard, 2010). In the present study, we did not measure the abundance of free viri and we can thus only speculate on the cause of phytoplankton cell lysis.

Microzooplankton, and more specifically phagotrophic protists, are important consumers of phytoplankton (Sherr and Sherr, 2002) and their grazing activity contributes significantly to the respiration of carbon and the functioning of the microbial loop (Landry and Calbet, 2004). Yet in contrast to macrozooplankton, generation of labile DOM by so-called “sloppy” feeding tends to be minor during microzooplankton grazing, as suggested by a review of different studies made by Bronk (Bronk, 2002). According to Bronk (Bronk, 2002), 9 % ± 5 % of the nitrogen ingested by a number of microzooplankton species was released as dissolved amino acids. However, several bacterivory studies did find more enhanced release of intracellular material upon grazing by flagellates or ciliates (Ferrier-Pages *et al.*, 1998; Alonso *et al.*, 2000). On the other hand, laboratory experiments showed that grazing by copepods or by heterotrophic dinoflagellates did not stimulate EA release (van Boekel *et al.*, 1992), and

thus would not contribute to the rate of cell lysis measured by the method used in this study.

DMSP release as a function of the rate of cell lysis

E. huxleyi is an important DMSP and DMS producer and can therefore contribute to the release of DMS to the atmosphere through direct excretion or mediated by bacterial catabolism of DMSP released after cell lysis (Stefels *et al.*, 2007). In our study we found a positive relationship between the biomass of coccolithophores and DMSPp concentrations, supporting the importance of coccolithophore as DMSP producers (fig. 3). DMSPd is an important intermediate product in the production of DMS through enzymatic cleavage. Pathways through which particulate DMSP is released into the dissolved phase are active exudation, cell lysis due to senescence or viral attack and grazing by zooplankton (Stefels *et al.*, 2007). Our DMS values agree with those reported by Uher *et al.* (Uher *et al.*, 2000) who measured DMS concentrations in the surface waters of the Celtic Sea in July 1995 ranging from 2.9 nmol l^{-1} to 38.5 nmol l^{-1}. Our DMSPp values (table 2, and fig. SP1) also fall within the range of those reported in studies devoted to the DMS biogeochemistry in coccolithophorid blooms, where DMSPp concentrations of up to 100 nmol l^{-1} and 175 nmol l^{-1} were reported by Archer *et al.* (2002) and Matrai and Keller (1993), respectively. Using a conversion factor for the amount of Chla per *E. huxleyi* cell of 110 fg $cell^{-1}$ (Muggli and Harrison, 1996a) and the linear relationship between DMSPp concentrations and coccolithophore Chla of this study (DMSPp (nM) = 54.64 x µg Chla + 29.07, r^2=0.59, $p<0.05$) (fig. 3), the DMSPp cell content of *E. huxleyi* was estimated at 0.8 pg $cell^{-1}$. This value compares with 0.75-1.90 pg $cell^{-1}$ measured by Keller *et al.* (1989) in laboratory cultures, but is lower than the value determined by Archer *et al.* (2002), which may have been biased due to the presence of other DMSP-containing phytoplankton species than *E. huxleyi* in their study. Although Archer *et al.* (2001) observed significant production of DMS+DMSPd due to microzooplankton grazing, we could not ascertain such a relation due to lack of sufficient data. However, we did find a positive relation between the ratio of dissolved to particulate DMSP and the rate of cell lysis (fig. 7), suggesting that cell lysis is source of DMSPd, when DMSP-rich phytoplankton cells are present. Although DMSPd is considered to be a source of DMS, we did not find a significant correlation between their concentrations (upper 20 m: r^2=-0.04, n=22, $p>0.05$). However, we observed only a positive correlation between the ratio of DMS

to DMSPp and the rate of cell lysis (r^2=0.68, n=7, p=0.02), emphasizing that cell lysis may be a direct source of DMS. Nonetheless, other processes such as bacterial consumption may modulate its release into the environment (Vila *et al.*, 2004; Stefels *et al.*, 2007; Reisch *et al.*, 2011).

Conclusions

This paper reports on the first measurements of phytoplankton cell lysis rates during late spring blooms of coccolithophores in the northern Bay of Biscay during three consecutive years from 2006 to 2008. While the first campaign took place in June 2006 at the end of the coccolithophorid bloom, the May 2007 and May 2008 campaigns were conducted mainly during its growth phase. The levels of cell lysis rates determined during this study indicate that cell lysis can be a main phytoplankton loss factor. High phytoplankton mortality rates determined by the dilution technique were sometimes independent of high cell lysis rates pointing at microzooplankton grazing as another key source of phytoplankton loss. Phytoplankton grazing mortality increased along a water column stratification gradient representing bloom development while cell lysis rate did not display such a linear relationship. In addition, the relation between the dissolved to particulate DMSP ratio and cell lysis rates together with the positive correlation between coccolithophore biomass and DMSPp levels substantiate the important role of coccolithophore blooms and their termination in the oceanic cycling of DMSP. Finally, high phytoplankton loss rates caused by microzooplankton grazing and possibly virally induced cell lysis during phytoplankton blooms in stratifying water conditions would both sequester more carbon in the particulate form, making it available to higher trophic levels, and stimulate the microbial loop functioning by releasing labile dissolved organic matter (such as DMSP), thereby modulating strength of the biological carbon pump.

Acknowledgements

The authors sincerely thank the officers and crew members of the R.V. Belgica for their logistic support during the campaigns. J. Backers, J.-P. De Blauw and G. Deschepper of the Unit of the North Sea Mathematical Models (Brussels/Ostend, Belgium) are acknowledged for their support in data acquisition during the field campaigns. S. Groom is acknowledged for providing remote sensing images. C. Brussaard is acknowledged for the protocol of lysis rates measurement and advices. J. Harlay is acknowledged for helpful discussions about cell lysis. We would like to thank N. Roevros for her technical assistance before and after the surveys and for helpful discussions concerning DMS analysis. J. Stefels and M. Steinke kindly provided their advices on DMS and DMSP sampling and sample treatment. Many thanks to A. De Wever, B. Vanelslander, and D. De Bock for their assistance in performing the dilution experiments and to N. Breine for the microscopic analyses. We are grateful to all members of the PEACE network for their support during the campaigns. This study was financed by Belgian Federal Science Policy Office in the framework of the PEACE project (contract numbers SD/CS/03A and SD/CS/03B). C. De Bodt was supported by a PhD grant from the EU FP6 IP CarboOcean project (contract no. 511176–2). N. Van Oostende received a PhD grant from the Institute for the Promotion of Innovation through Science and Technology in Flanders (IWT-Vlaanderen).

Supplementary figures

Fig. SP1. Distribution of DMS, DMSPd, and DMSPp concentrations along depth profiles of stations sampled in 2006, 2007 and 2008. Concentrations of DMS are represented by grey dots, DMSPd by empty dots, and DMSPp by black dots.

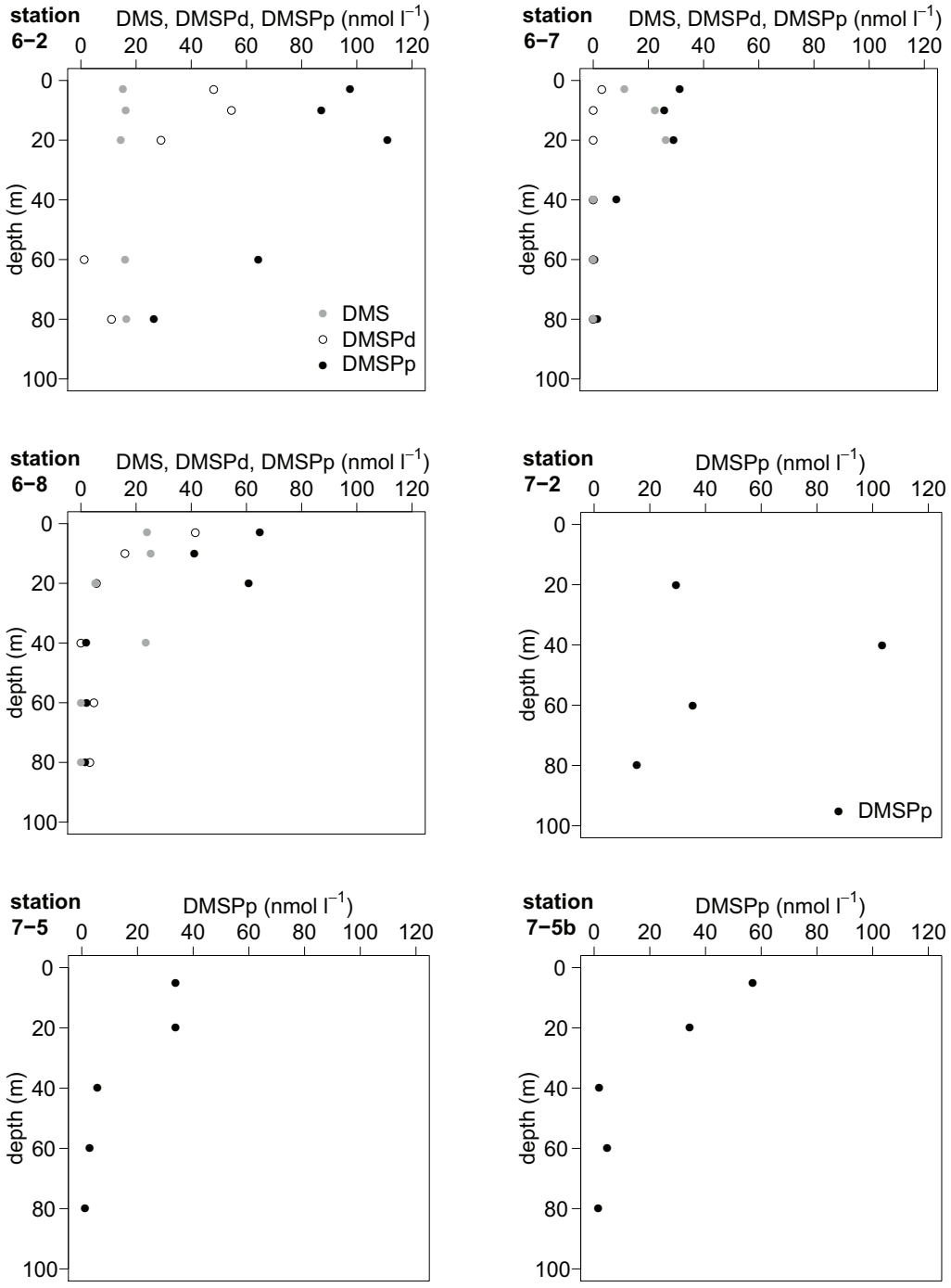

Fig. SP1. Continued

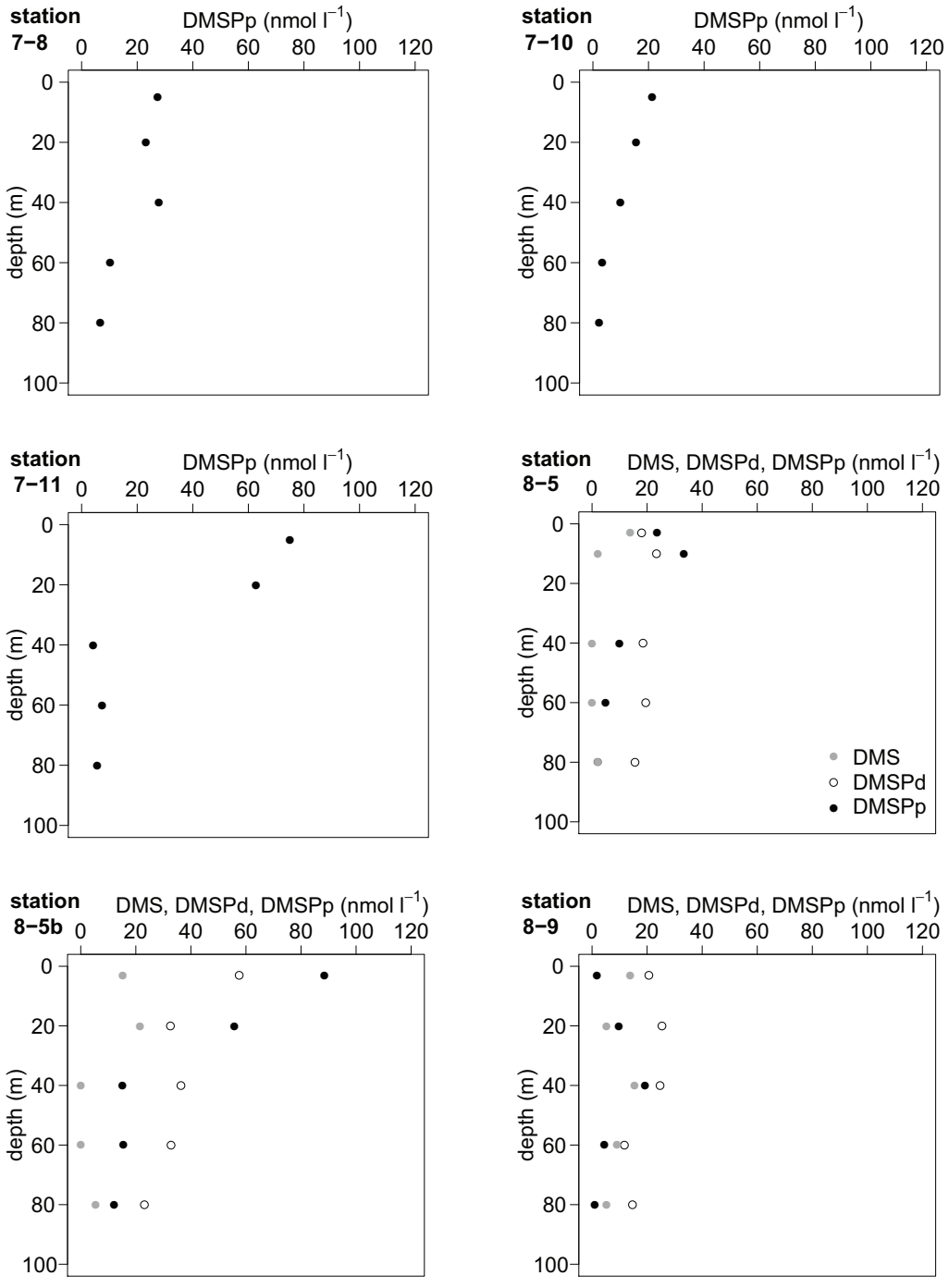

Fig. SP1. Continued

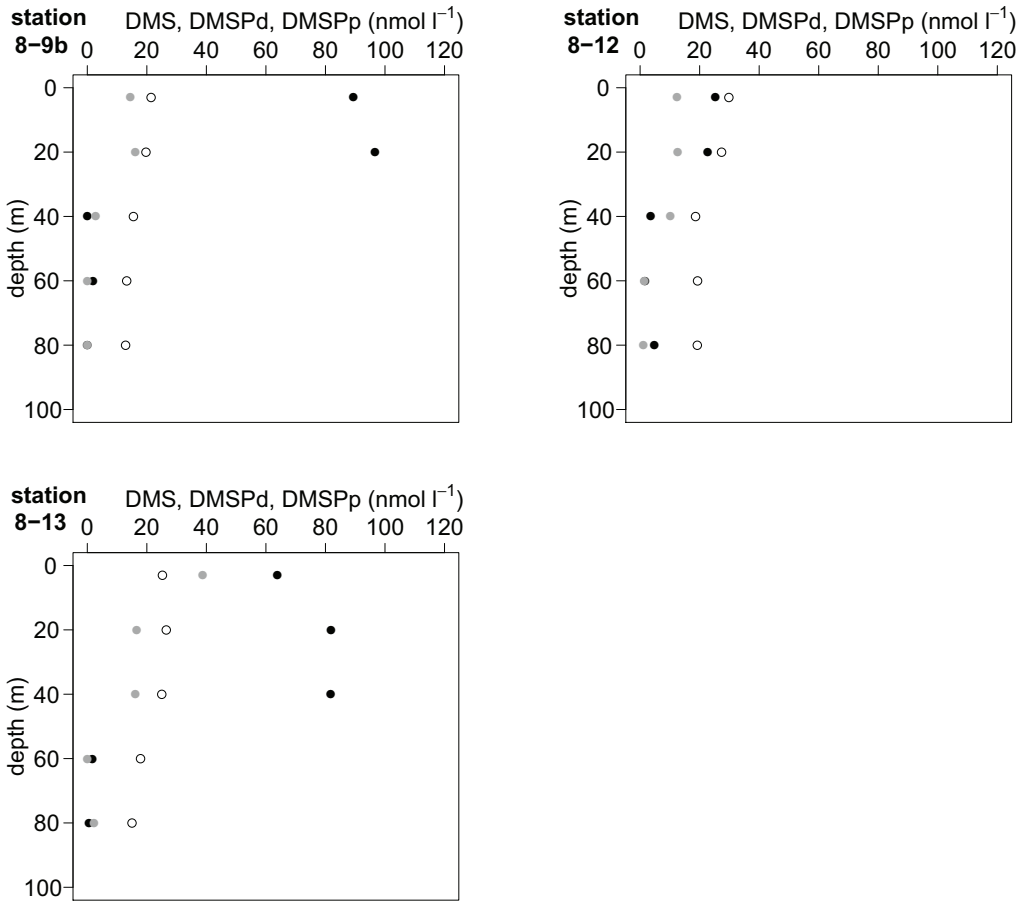

Fig. SP2. Areal Chla concentrations partitioned over the dominant chemotaxonomic phytoplankton groups for the stations visited in 2006, 2007, and 2008.

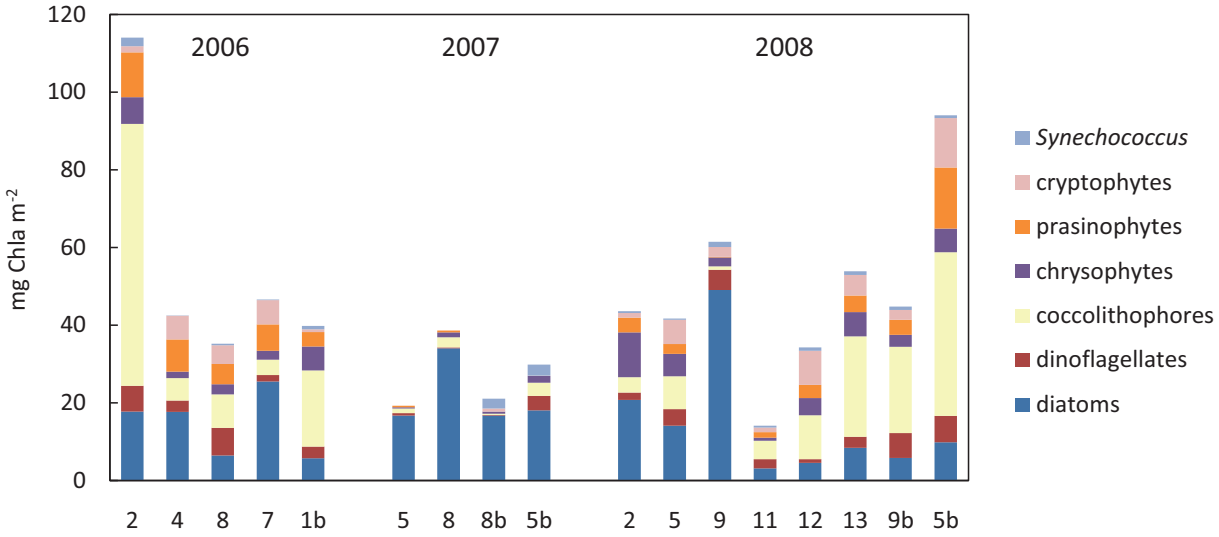

6

Dynamics of dissolved carbohydrates and transparent exopolymer particles in axenic and non-axenic *Emiliania huxleyi* cultures: assessment of extracellular release using compound-specific isotope analysis

Nicolas Van Oostende[1], Tanja C.W. Moerdijk-Poortvliet[2], Wim Vyverman[1], Henricus T.S. Boschker[2], Koen Sabbe[1]

[1] Laboratory for Protistology and Aquatic Ecology, Biology Department, Ghent University, Krijgslaan 281 – S8, B-9000 Gent, Belgium.

[2] Netherlands Institute of Ecology (NIOO-KNAW), Centre for Estuarine and Marine Ecology, P.O. Box 140, 4400 AC Yerseke, The Netherlands.

Authors' contributions

NVO and KS conceived and designed the study. NVO performed the culturing experiments and stable isotope probing experiment. TCWMP performed the LC/IRMS analyses of carbohydrates. HTSB and NVO performed the PLFA analyses. NVO analysed the data and wrote the manuscript. TCWMP, KS, WV, and HTSB revised the manuscript.

Abstract

Exudation of carbohydrates by phytoplankton is an important pathway in primary production, fuelling the microbial loop and acting as a source of labile to recalcitrant compounds to the huge dissolved organic carbon (DOC) reservoir of oceans. To assess the influence of bacterial activity and life cycle stage of *Emiliania huxleyi* on the dynamics of dissolved carbohydrates and transparent exopolymer particles (TEP) we measured their production and composition during the stationary growth phase of batch cultures. Additionally, we traced the fate of photosynthetically fixed carbon by stable isotope probing in non-axenic calcifying *E. huxleyi* cultures using liquid chromatographic separation of neutral aldoses (NAld) combined with isotope ratio mass spectrometry (LC/IRMS).

Unbalanced growth caused an accumulation of organic carbon in non-calcifying haploid, and calcifying axenic and non-axenic, diploid *E. huxleyi* cultures, which was independent of biomass accumulation. We found a marked build-up of extracellular particulate organic carbon (POC) in calcifying *E. huxleyi* cultures, while there was a more pronounced accumulation of dissolved carbohydrates in the haploid *E. huxleyi* cultures. Bacteria favoured the accumulation of polysaccharides and the formation of TEP containing high densities of stainable moieties, enhancing their aggregation in calcifying *E. huxleyi* cultures. Furthermore, bacteria preferentially assimilated newly produced organic matter and altered the composition of dissolved high molecular weight (HMW) NAld, which changed during the course of the experiment, with a proportional increase of rha+ara. Based on the similar NAld composition of coccoliths polysaccharides and HMW NAld and the positive relationship between newly produced particulate inorganic carbon (PIC) and HMW NAld, we propose that the production of coccoliths is the main source of HMW NAld in our non-axenic calcifying *E. huxleyi* cultures.

Extracellular release of carbon in the dissolved and the particulate pools reached up to 76 % of total primary production during the stationary growth phase of *E. huxleyi*. The accumulation of extracellular POC together with coccolith production and enhanced TEP formation and aggregation suggest that *E. huxleyi* blooms could have a positive impact on the efficiency of export production in the ocean.

Introduction

Exudation of dissolved organic matter (DOM) by phytoplankton transfers the products of primary production confined into cellular particulate material to seawater (Baines and Pace, 1991; Norrman *et al.*, 1995; Aluwihare and Repeta, 1999). Whereas exudation of DOM by phytoplankton has been considered to divert primary production from contributing to vertical flux of particle in the ocean, polysaccharide aggregation constitutes an effective pathway to channel dissolved matter into the particulate pool (Engel *et al.*, 2004a). Carbohydrates make up an important share (13% - 46%) of the dissolved organic carbon (DOC) in the ocean (Pakulski and Benner, 1994) while polysaccharides make-up an even higher fraction (25% - 50%) of the high molecular weight (HMW) colloidal fraction of marine DOM (Benner *et al.*, 1992; Biddanda and Benner, 1997). Although HMW DOM forms a minor (25-30%) part of DOM compared to LMW DOM it is the most bioreactive part of the dissolved carbon pool as shown by higher bacterial growth and respiration in the presence of HMW DOM than for LMW dissolved material (Amon and Benner, 1994; Aluwihare and Repeta, 1999). Moreover, phytoplankton has been reported to produce substantial amounts of HMW DOM (Lancelot, 1984; Biddanda and Benner, 1997), even though the physiological mechanisms of phytoplankton exudation are still poorly understood. Passive diffusion through the cell membrane or active exudation of DOM when nutrient and light availability become uncoupled has been hypothesized (Bjørnsen, 1988; Wood and Van Valen, 1990; Van den Meersche *et al.*, 2004).

Emiliania huxleyi, a cosmopolitan coccolithophore, is one of the most abundant phytoplankton species in the ocean, playing an important role in the biogeochemical carbon and sulphur cycle through calcification and dimethylsulphoniopropionate (DMSP) production (Stefels *et al.*, 2007). The production of dense calcite particles, such as coccoliths, together with the formation of particles having high aggregation potential, such as transparent exopolymer particles (TEP),is thought to greatly increase the efficiency of the biological carbon pump through the scavenging of coccoliths by aggregates, increasing their sinking velocities (De La Rocha and Passow, 2007). *E. huxleyi* exhibits a haplo-diplontic life cycle, alternating between calcified, non-motile, diploid cells and non-calcified, motile, haploid cells, with both phases being capable of asexual cell division (Green *et al.*, 1996; von Dassow *et al.*, 2009).

During blooms of diploid *E. huxleyi* cells, a cell proliferation phase is followed by a calcification phase which is typically induced by inorganic phosphorus limitation (Shiraiwa, 2003). During conditions of depleted inorganic phosphorus levels, calcifying *E. huxleyi* cells have been shown to switch their carbon fixation flow from neutral storage polysaccharides to acidic coccolith polysaccharides (Kayano and Shiraiwa, 2009). These water soluble polysaccharides are thought to mediate the production of coccoliths, and are released upon exocytosis of coccoliths to form an external coating (de Jong *et al.*, 1979; Godoi *et al.*, 2009). The extracellular release of acidic polysaccharides by calcifying cells (Nanninga *et al.*, 1996) is thought to function as a precursor step for the formation of TEP (Passow, 2002b; Engel *et al.*, 2004b; Harlay *et al.*, 2009). Although both coccolith polysaccharides and TEP contain an acidic polysaccharide having galacturonic acid and sulphate groups, neutral aldoses are one of their main constituents (Fichtinger-Schepman *et al.*, 1979; Skoog *et al.*, 2008). Yet, little information is available about the production and loss of dissolved carbohydrates and TEP, especially during the stationary growth phase when their production and formation by coagulation are favoured (Engel *et al.*, 2004b; Schartau *et al.*, 2007).

Bacterial activity has been shown to influence both the composition and the concentration of dissolved carbohydrates and TEP through degradation and production processes and through ecological interactions with algal cells (Stoderegger and Herndl, 1998; Grossart and Simon, 2007; Gärdes *et al.*, 2010; Rochelle-Newall *et al.*, 2010). Changes in the composition of HMW dissolved carbohydrates could influence the surface-active properties of these TEP precursors and thus affect particle aggregation (Giroldo *et al.*, 2003; Gogou and Repeta, 2010). However, the influence of bacterial activity on dissolved carbohydrate and TEP dynamics during *E. huxleyi* blooms has not yet been investigated.

Recent technological advances have made it possible to combine stable isotope labelling experiments with compound-specific isotope analysis (CSIA) of carbohydrates, allowing assessment of the dynamics of individual monosaccharides (Bellinger *et al.*, 2009; Oakes *et al.*, 2010). We performed a ^{13}C labelling experiment which together with a phospholipid-derived fatty acid (PLFA) biomarker approach, to quantify the microbial biomass pool, allowed us to assess the fate of carbon exuded by calcifying *E. huxleyi* cells in non-axenic cultures. Furthermore, we analysed the production and composition of dissolved carbohydrate and TEP during the stationary growth phase of haploid (S +bact) and calcifying

E. huxleyi cultures, and assessed the influence of bacteria on these processes by comparing them in axenic (C axenic) and non-axenic calcifying cultures (C +bact). We used liquid chromatographic separation combined with isotope ratio mass spectrometry (LC/IRMS) of dissolved HMW neutral aldoses to assess the effect of the culture treatments on this important and dynamic subset of the carbohydrate pool, together with spectrophotometric measurements of bulk dissolved carbohydrates. Finally, changes in the concentration, composition, and aggregation of TEP were assessed by combining the size frequency distribution and the dye-binding capacity of these functional particles. The different fractions of organic matter we sampled during this study are listed in table 1.

Materials & Methods

Emiliania huxleyi cultures

The culture vessels consisted of 20 l polycarbonate bottles closed with a screw cap which was fitted with three-way valves connecting two air-venting filters, one of which was connected to a sterile air inflow, and allowing access to a glass sampling tube inside the bottle. The bottles were filled with 16 l (± 0.05 l) of 0.2 µm filtered oligotrophic oceanic water from the northern Bay of Biscay, and autoclaved to ensure a sterile culture environment. The water in the culture vessels was allowed to equilibrate with the atmosphere and ambient temperature for 2 days before we inoculated them with 30 ml of exponentially growing culture of *E. huxleyi* strain BG10-5 (isolated by Ian Probert at Roscoff Culture Collection (strain number RCC1266); collection site in the Celtic Sea: 10°30'W 49°30'N; collection date: August 2007). *E. huxleyi* cells and nutrients were added to the culture vessels using sterile syringes at an initial concentration of 500 cells l^{-1}, 1 µmol l^{-1} of PO_4^{3-} and 32 µmol l^{-1} of NO_3^-. This nutrient ratio was chosen to cause the depletion of phosphate prior to that of nitrate. The experiment was set up in a climate room with the following light and temperature conditions: 14h/10h light/dark diel cycle, irradiance flux density of 60 µmol photon m^{-2} s^{-1}, at 16°C. In order to homogenise the content of the bottles they were shaken daily in a swirling motion during 30 seconds. The bacterial community in the *E. huxleyi* inoculates originated from natural communities collected during coccolithophorid blooms in the Celtic Sea. These bacterial communities were sampled during an oceanographic campaign in May 2008 from stations 8-5b, 8-9b, 8-10, 8-12, and 8-13 (Van

Oostende *et al.*, *in prep. c*) (see also chapter 3) by concentration onto membrane filters, and cryopreserved in liquid nitrogen, in a 20% glycerol solution. Co-cultures of calcifying *E. huxleyi* cells and bacteria were used as inocula for the "C +bact" culture experiment. Some of the *E. huxleyi* inoculates changed from the calcifying to the motile, non-calcifying life cycle phase. These cells were used to inoculate the "S +bact" culture experiment. Calcifying *E. huxleyi* inoculates were made axenic using a sequential treatment of a bacterial cell wall synthesis inhibitor (penicillin G, 100 mg l^{-1}, 24 h) and a protein synthesis inhibitor (streptomycine, 50 mg l^{-1}, 24 h), followed by dilution in antibiotics-free culture medium (K/2) (Ietswaart *et al.*, 1994; Guillard, 2005). Once algal cell growth was observed we incubated a subsample in sterile culture medium containing 0.05 % (w/v) yeast extract at 20 °C during three days, to stimulate potential bacterial cell growth. The absence of bacterial cells was checked using epifluorescence microscopy after staining with DAPI, for which the detection limit for bacterial cells was 1.54 10^5 cells l^{-1} (Porter and Feig, 1980). These axenic *E. huxleyi* inoculates were used to seed the culture vessels in the "C axenic" experiment.

During the C +bact culture experiment we also traced the fate of photosynthetically fixed carbon using a pulse of isotopically labelled bicarbonate ($NaH^{13}CO_3$, 99% ^{13}C, Cambridge Isotope Laboratories Inc.). The isotopic tracer was added to the cultures at the start of the light phase, nine days after the inoculation of the cultures. Each of the culture treatments was sampled for dissolved carbohydrates, TEP, and HMW NAld at midday on days 9, 13, and 19 following culture inoculation (see below for description). The same variables and PLFA's were sampled in the C +bact cultures on day 9 (= t0), 14 hours, 24 hours (day 10), 96 hours (day 13), and 240 hours (day 19) following the isotopic tracer pulse.

During the culture experiments algal and bacterial cell concentrations were measured every second day by epifluorescence microscopy (Porter and Feig, 1980). At least 600 *E. huxleyi* cells were counted in 25 fields of view, and at least 25 fields of view were screened for enumeration of bacterial cells.

Growth rates were estimated from the slopes of linear regressions using the natural logarithm of the cell concentrations during the exponential growth phase.

Table 1. Abbreviations of the organic carbon and carbohydrate fractions measured by different analytical methods. For further details we refer to the 'Materials and Methods' section.

abbreviation	fraction	method
POC	particulate organic carbon	elemental analysis (- IRMS)
DOC	dissolved organic carbon	wet oxidation - IRMS
TCHO	total dissolved carbohydrates	spectrophotometry, TPTZ
MCHO	dissolved mono- and oligosaccharides	spectrophotometry, TPTZ
HMW NAld	HMW dissolved neutral aldoses (>10 kDa)	LC/IRMS
TEP-C	particulate (ESD: 0.6 - 50 µm)	light microscopy, alcian blue
TEPcolor	particulate (> 0.4 µm)	spectrophotometry, alcian blue

Nutrient concentration

The concentration of nitrate and phosphate in filtrates of the cultures (GF/F, Whatman) was measured on a two-daily basis using standard semi-automated colorimetric techniques (Grasshoff *et al.*, 1983) and the spectrophotometric method of (Koroleff, 1983) respectively. The detection limit was 0.1 µmol l^{-1} for nitrate and 0.02 µmol l^{-1} for phosphate.

Transparent exopolymer particle concentration and carbon content

TEP concentrations were measured according to the dye-binding assay technique (TEPcolor) (Passow and Alldredge, 1995) and by microscopic determination of their size-frequency distribution (TEPmicro) (Passow and Alldredge, 1994) as outlined in (Engel, 2009).

In brief, culture medium samples (0.5 – 1 ml) were gently filtered (<130 mbar) onto 0.4 µm pore-size polycarbonate filters (nuclepore, Whatman). Particles on the filter were stained for approximately 4 s with 1000 µL of a 0.02% aqueous solution of alcian blue (8GX, Sigma) in 0.06% acetic acid (0.2 µm filtered, pH=2.5). Stained filters were gently rinsed with 2 ml deionized low carbon water to remove excess dye and then transferred either into scintillation vials for the dye-binding assay or onto microscopy slides treated to avoid diffraction patterns due to light penetration through the filter pores, and stored at -20 °C (Cytoclear, Poretics corp.) (Logan *et al.*, 1994).

For the dye-binding assay, 6 ml of 80% aqueous H_2SO_4 were added to the filters in the scintillation vials and soaked for 6 h, in order to release the alcian blue bound to the TEP. The absorption maximum of the solution at 787 nm was measured in a 1 cm cuvette against

deionized low carbon water as a reference. The adsorption of alcian blue on TEP is considered to be related to the concentration of acidic and sulphated moieties of their polysaccharide content (Ramus, 1977). A concentration equivalent for the alcian blue adsorption is given by standardization with the acidic polysaccharide gum xanthan (TEPcolor in µg X eq. l^{-1}).

The microscopic measurement of the size-frequency distribution of TEPmicro was performed by analysis of 30 colour images along a horizontal and vertical cross section of the filter area at 100 and at 200 times magnification (Axiocam HRc camera, Zeiss) as described in (Harlay *et al.*, 2009). TEP with an area larger than 0.3 µm² were enumerated and sized using the WCIF ImageJ software (a public domain program developed at the US National Institute of Health — http://www.uhnresearch. ca/facilities/wcif/fdownload.html — courtesy of Wayne Rasband, National Institute of Mental Health,Bethesda, MD, USA). The equivalent spherical diameter (ESD) was calculated for individual particles from area measurements, leading to a range of 0.6 – 50 µm (ESD). TEP were classified according to their ESD into 20 logarithmic size classes (Mari and Burd, 1998). TEP size distributions were described using a power-law of the type $dN/d(d_p) = kd_p^{\delta}$, where dN is the number of particles per unit volume in the size range d_p to $[d_p + d(d_p)]$. The parameter k, depending on the concentration of particles and the spectral slope, δ (with δ<0), describing the size distribution, were derived from linear regressions of log $[dN/d(d_p)]$ versus log $[d_p]$. The volume concentration is defined here as the mean volume of the particles that belong to a size class in the sample. δ is related to the slope of the cumulative size distribution $N=ad_p^{\beta}$ by $\delta = \beta+1$. Spectral slopes were used to describe the TEP size distribution, an increase in $|\delta|$ being due to an increase of the fraction of large TEP (Harlay *et al.*, 2009), thus changes of this quantity indicate some changes in the dynamics of particles due to aggregation or disaggregation processes.

TEP carbon content

The carbon content of TEPmicro (TEP-C) was assessed by the microscopic approach assuming that the volume of TEP is proportional to r^D, where r is the equivalent spherical radius in µm and D the fractal dimension associated with the size distribution of particles. As such, TEP-C was determined from TEP size spectra according to (Mari, 1999). For each sample, D was deduced from the spectral slope, δ, according to the semi-empirical relationship (Burd and Jackson, unpublished data, as referred to in Mari and Burd, 1998):

$$D = (64-\delta)/26.2 \quad (1)$$

Subsequently, TEP-C was derived from the size frequency distribution described above, according to:

$$\text{TEP-C} = a/12\ \Sigma_i\ n_i r_i^D \quad (2)$$

where n_i is the concentration of TEP in the size class i and r_i the mean equivalent spherical radius of this size class. The constant, a = 0.25 10^6 µg C, was determined by Mari (1999).

Dissolved carbohydrate concentration

Spectrophotometric measurement of free dissolved (MCHO) carbohydrates (mono- and oligosaccharides) and total dissolved carbohydrates concentrations (TCHO) (i.e. free and combined carbohydrates) in the filtrate of the culture medium (GF/F, Whatman) were performed according to the TPTZ (2,4,6-tripyridyl-*s*-triazine) method of Myklestad *et al.* (1997). This method uses the reducing properties of monosaccharides dissolved in water samples, which are subjected to an oxidation reaction at alkaline pH, during which ferricyanide (Fe^{3+}) is reduced to ferrocyanide (Fe^{2+}). The Fe^{2+} is then determined colorimetrically after condensation with the cromogen TPTZ to give the strongly violet coloured $Fe(TPTZ)_2^{2+}$ complex. The absorption maximum of the solution at 595 nm was measured in a 1 cm cuvette against deionized low carbon water as a reference, and calibrated against a D-glucose solution as in Myklestad *et al.*(1997). Polysaccharides were made reducing by hydrolysis of the glycosidic bonds in 0.1 mol l^{-1} HCl at 150°C for 1 h and analyzed as above. The hydrolysis procedure allowed determination of TCHO concentrations. Each sample was measured in triplicate and the standard error for glucose at a concentration of 8.48 µmol C l^{-1} was 9%. Polysaccharide concentration (PCHO) was determined by the difference between MCHO and TCHO. The carbon content of mono- and polysaccharides was calculated assuming a conversion of 30 µg glucose μmol^{-1} C.

HMW DOM ultrafiltration

We used a cross-flow ultrafiltration and continuous diafiltration method based on Zhang and Santschi (2009) to concentrate and desalt dissolved carbohydrate in the HMW fraction of DOM before processing for further HPLC analysis. In brief, between 1500 and 2000 ml of culture medium were filtered in aliquots of 400 to 500 ml through glassfibre filters (GF/F, Ø

47 mm, Whatman) using low vacuum pressure (< 200 mbar). Tests using fluorescent nucleic acid detection in the filtrate (Veldhuis *et al.*, 2001) indicated there was no loss of intracellular material using this filtration procedure. The filtrate was concentrated to approximately 70 ml using two Minimate catridges (Pall) fitted with a 10kDa pore size Omega membrane, set-up in parallel. This concentrated dissolved carbohydrate sample was then desalted by continuous diafiltration using 10 volumes of low carbon deionized water, further concentrated to 50 ml, and partially retrieved without emptying the system completely. The cartridges were subsequently soaked for 1 hour with an additional 20 ml of low carbon deionized water before recirculation and retrieval of the added water. The system was then rinsed again by recirculation of another 25 ml of low carbon deionized water. The rinsing water and concentrated and desalted dissolved carbohydrate samples were pooled and freeze-dried before further processing.

Neutral aldose extraction and analysis

In order to analyse the concentration and carbon isotopic composition of the high molecular weight neutral aldoses (HMW NAld) the freeze-dried HMW DOM samples were hydrolysed by adding 5 ml of H_2SO_4 (1.1 *M*) and incubated for 1 h at 120°C. The samples were cooled in crushed ice to stop the hydrolysis, and the hydrolysates were transferred to centrifuge tubes, neutralised to pH 5.5-6.0 by adding $SrCO_3$ (0.4 g/ml), and centrifuged (15 min, 4000 x g). The supernatant liquid was collected into micro centrifuge tubes and frozen overnight to further precipitate $SrSO_4$, which was then removed from thawed samples by centrifugation (15 min, 4000 x g). The supernatant liquid containing the carbohydrates was finally filtered through a 0.22 µm pore size syringe filter (Millex-GV4, Millipore) into HPLC vials and stored at -20 °C until analysis via LC/IRMS.

Concentrations and carbon isotope ratios of carbohydrates were determined using the method of Boschker et al. (2008). Analysis of carbohydrates was achieved using an LC system interfaced with a Delta V Advantage IRMS via an LC Isolink interface (LC/IRMS). Carbohydrates were separated on a CarboPac PA-20 analytical column (3 x 150 mm; Dionex Benelux) and were eluted isocratically with 1 mmol l^{-1} degassed NaOH at 300 µl min^{-1}. Neutral aldose standards (fucose (fuc), rhamnose (rha), glucose (glc), galactose (gal), xylose (xyl), ribose (rib), mannose (man), fructose (fru)) were injected at concentrations between 100 and 4000 µmol l^{-1} to check for consistency of isotope ratios (within < 0.5‰ standard

deviation) and for linearity of peak areas with carbohydrate concentrations (R^2 = 0.96) (Boschker *et al.*, 2008). Ribose, fructose, amino sugars, methyl sugars, and 3-deoxy sugars were not detected in our study. Rhamnose and arabinose (ara) could not be distinguished because they had similar retention times, and are further reported as rha+ara. The number of carbon atoms in rhamnose was used to convert from the concentration of rha+ara to carbon concentrations.

Biomarker extraction and analysis

We filtered 1.00 l of culture medium through combusted glassfibre filters (GF/F, Whatman) to collect algal and bacterial cells for measurement of PLFA concentration and isotopic composition on day 9 (= t0), 14 hours, 24 hours (day 10), 96 hours (day 13), and 240 hours (day 19) following the isotopic tracer pulse. In brief, PLFAs were extracted according to the method of Boschker *et al.* (1999) and Middelburg *et al.* (2000) and concentrations were measured using gas chromatography (GC) (Thermo Trace GC Ultra) with flame ionization detection. Incorporation of ^{13}C in phytoplankton and bacterial biomass was quantified by carbon isotope analysis of specific PLFA using GC coupled with a Thermo Delta V Plus isotope ratio mass spectrometer (IRMS) via a Thermo Conflo III interface (Boschker and Middelburg, 2002). A polar 60-m BPX-70 column (0.32 mm i.d., 0.25 µm film thickness, SGE Analytical Science) was used with helium as a carrier gas.

Algal (*E. huxleyi*) and bacterial organic carbon concentrations were calculated from PLFA concentrations as described in Middelburg *et al.* (2000). Using the concentration of specific bacterial PLFAs (i14:0, i15:0, ai15:0, and cy17:0), total bacterial carbon concentration was calculated as:

$$C_{bact} = \Sigma (PLFA_{bact} / a) = \Sigma (PLFA_{bact,\ spec} / a \times b) \quad (3)$$

where a is the average PLFA concentration in bacteria (0.073 g of carbon $PLFA_{bact}$ per gram of carbon biomass for aerobic environments, Brinch-Iversen and King (1990)) and b = 0.21 g Bacteria-specific biomarker PLFAbact, spec (i14:0, i15:0, ai15:0, and cy17:0) per gram of bacterial PLFA content (calculation adapted from Moodley *et al*. (2000) based on the average proportion of cy17:0 to total $PLFA_{bact,\ spec}$ concentration). Algal carbon concentration was calculated from the difference between total PLFA and bacterial PLFA as:

$$C_{E.\ huxleyi} = (\Sigma\ PLFA - \Sigma\ PLFA_{bact,\ spec}) / c \quad (4)$$

Where *c*, the average concentration of PLFA in *E. huxleyi*, was estimated from the organic carbon and PLFA content of axenic *E. huxleyi* cultures in the exponential growth phase (*c* = 0.112 g C $PLFA_{E.\ huxleyi}$ g C_{org}^{-1}). The value of this conversion factor is comparable to that of Dijkman and Kromkamp (2006) which was 0.129 g C $PLFA_{E.\ huxleyi}$ g C_{org}^{-1}.

Particulate matter analysis

Total nitrogen and carbon, and following acidification (by HCl vapour exposition for 24 h), organic carbon content of suspended particulate matter (retentate of 500 ml culture medium filtered through GF/F glassfibre filters, Whatman) were determined using an elemental analyzer (Thermo Scientific Flash 2000 Organic Elemental Analyzer for isotopically unlabelled cultures, and Thermo Finnigan Flash EA 112 for labelled cultures). Delta ^{13}C of total and organic particulate carbon (POC) was determined using a Thermo Finnigan Flash EA 112 interfaced via a Thermo Conflo III with a Thermo Delta V Plus IRMS.

Dissolved carbon analysis

Samples for dissolved organic carbon concentration (DOC) and $\delta^{13}C$ of DOC were filtered through combusted glassfibre filtres (GF/F, Whatman), 20 ml of filtrate was preserved in glass vials with Teflon-coated screw caps, by addition of 200 µl of HCl (10 %). DOC and $\delta^{13}C$ of DOC were measured using a wet chemical oxidation organic carbon analyzer (Thermo HiPerTOC TIC/TOC analyzer) coupled to Thermo Delta Plus XL IRMS via a Conflo III interface, according to Bouillon *et al.* (2006) and Osburn and St-Jean (2007). Unfortunately, DOC samples of S +bact and C axenic culture experiments were lost due to machine failure.

Samples for dissolved inorganic carbon (DIC) and $\delta^{13}C$ of DIC were filtered through combusted glassfibre filters (GF/F, Whatman), collected in headspace vials (20 ml) and stored upside down at 4 °C for maximally three weeks, until analysis. In the laboratory, a He headspace was created, and the concentration and isotopic composition of carbon dioxide in the headspace were measured using an elemental analyzer coupled to a Finnigan Delta XL IRMS (Moodley *et al.*, 2002).

Isotopic data treatment

Stable carbon isotope data are expressed in the delta notation relative to Vienna Pee Dee Belemnite (VPDB). Delta ^{13}C values of *E. huxleyi* and bacterial biomass were calculated using the weighed sum (by mol C %) of the $\delta^{13}C$ of individual PLFA's. Excess ^{13}C in a particular carbon pool or compound (compared to background levels) was derived by calculating the atom % ^{13}C in enriched samples and subtracting the atom % ^{13}C in the unlabelled carbon pool or compound, giving the atom % excess ^{13}C (APE, in %), which was multiplied by the concentration of the pool (Middelburg *et al.*, 2000; Veuger *et al.*, 2006). The concentration of newly produced NAld was calculated as the ratio of excess ^{13}C concentration to time-averaged APE of DIC. Production rates of POC, *E. huxleyi* and bacterial biomass, DOC, and NAld were calculated according to Hama and Yanagi (2001):

$$(\text{excess } ^{13}C \text{ compound}/ APE_{DIC}) \times t^{-1} \quad (5)$$

where APE_{DIC} is the time-averaged APE of DIC on time t after label addition. Bacterial respiration (BR) rate was calculated using PLFA-based bacterial biomass production (Bact NP) and a bacterial growth efficiency (BGE) coefficient of 0.2 (del Giorgio and Cole, 1998):

$$BR = \text{Bact NP}/BGE - \text{Bact NP} \quad (6)$$

Statistical treatment of data

Average values of the replicates cultures are given as the arithmetic mean and its standard deviation. The effect of a treatment on the values of a variable was tested using analysis of variance (ANOVA). If there was a treatment effect, a Tukey HSD post hoc test was used to determine which culture treatment caused the difference between the mean values of the variables. A two-tailed Student's t-test was used to test for the difference between the mean values of two treatments. Values were checked for normal distribution and homoscedacity before performing these tests using the Statistica 7.0 (StatSoft, Inc.) program. Temporal change in a variable's values was calculated as the slope of linear regression between this variable and time. Linear correlation between pairs of observations is given as Pearson's product-moment correlation coefficient R. Ordination of the NAld composition of HMW DOM during the progression of the stationary growth phase of the different culture treatments was performed using redundancy analysis (RDA). Culture treatments and time

after inoculation were used as categorical variables. RDA was performed using Canoco 4.5 for Windows. Probability threshold of all statistical tests was set at $p<0.05$.

Results

Culture development

Culture growth, nutrient consumption, and particulate matter accumulation followed typical logistic growth curves, with a sequence of lag, exponential, and stationary phases (fig. 1 and 2). Phosphate became depleted (i.e. below detection limit) after seven days, marking the transition from the exponential to the stationary phase in the non-axenic cultures (fig.1), and by day 9 in the axenic culture. Although the axenic culture displayed a longer lag phase, growth rates of *E. huxleyi* in the calcifying non-axenic and axenic cultures was similar (C+bact: 0.76 ± 0.01 d^{-1}; C+axenic: 0.75 ± 0.03 d^{-1}), while that of the non-calcifying *E. huxleyi* cells was higher (0.98 ± 0.05 d^{-1}). Nitrate levels were low from day 11 onwards in the non-axenic cultures (0.84 ± 0.27 µmol l^{-1}; 0.25 ± 0.23 µmol l^{-1}), but only on day 19 in the C axenic culture. Average algal cell density in the stationary phase was similar in the calcifying cultures but a third lower in the non-calcifying S +bact culture, where apparent cell loss occurred during the last three days (table 2 and fig. 1). Microscopic counting of cells in the S +bact cultures was sometimes hampered due to the formation of *E. huxleyi* cell aggregates during the last 4 days of the experiment. Bacterial cell concentration was almost twice as high in the S +bact culture compared to the C +bact culture, and remained below 1.56 10^5 cells l^{-1} in the C axenic culture (table 2).

Table 2. Average cell concentration during the stationary growth phase of the non-axenic haploid (S +bact), non-axenic calcifying (C +bact), and axenic calcifying (C axenic) *E. huxleyi* cultures.

culture	stationary growth phase	*E. huxleyi* (10^8 cells l^{-1})		bacteria (10^9 cells l^{-1})	
S +bact	day 9-19	2.10	± 0.41	2.41	± 0.29
C +bact	day 9-19	3.28	± 0.15	1.33	± 0.12
C axenic	day 11-19	3.07	± 0.25	≈ 0	

Fig. 1. Change in average algal (a) and bacterial cell concentration (b) and phosphate (c) and nitrate concentration (d) during the development of non-calcifying non-axenic (triangles), calcifying non-axenic (empty circles), and calcifying axenic cultures (black dots). Error bars denote standard deviations of the means.

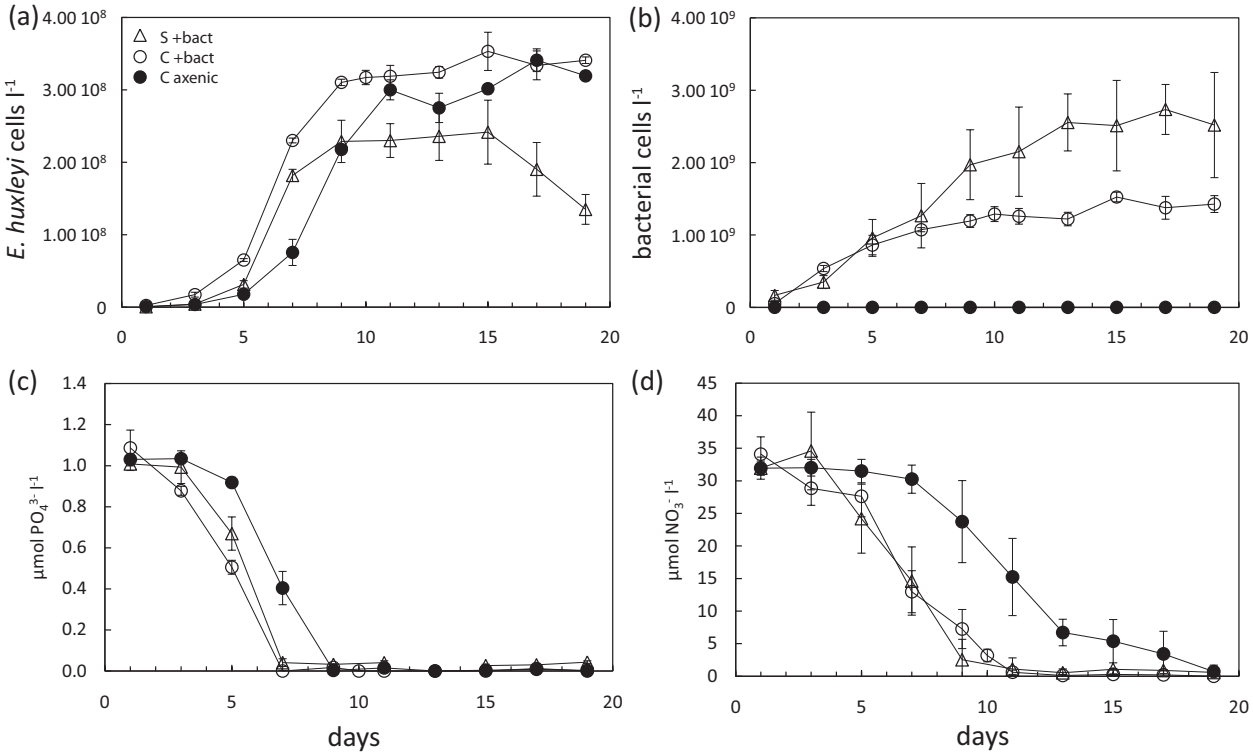

Particulate carbon and nitrogen accumulation

In all three culture treatments, POC levels significantly increased during the stationary phase while PN remained stable, reflecting minor changes in biomass during this growth phase (figs. 2a and b), resulting in a significant increase in the POC:PN ratio (table 3). Particulate inorganic carbon concentration significantly increased (by during the stationary phase in the calcifying cultures (fig. 2c).

Table 3. Average concentration of particulate organic and inorganic carbon (POC and PIC) and particulate nitrogen (PN) and their molar ratios on day 9 and 19 after inoculation of the non-axenic haploid (S +bact), non-axenic calcifying (C +bact), and axenic calcifying (C axenic) *E. huxleyi* cultures.

culture	day	POC (µmol l^{-1})	PIC (µmol l^{-1})	PN (µmol l^{-1})	POC : PN	PIC : POC
S +bact	9	244 ± 16	0 ± 0	37 ± 1	6.5 ± 0.4	na
	19	342 ± 34	0 ± 0	35 ± 1	9.9 ± 1.0	na
C +bact	9	304 ± 18	273 ± 30	33 ± 1	9.1 ± 0.3	0.9 ± 0.1
	19	700 ± 141	858 ± 98	45 ± 6	15.6 ± 1.8	1.2 ± 0.2
C axenic	9	224 ± 11	140 ± 11	36 ± 1	6.2 ± 0.2	0.6 ± 0.0
	19	535 ± 28	683 ± 29	45 ± 3	11.9 ± 1.3	1.3 ± 0.0

Fig. 2. Change in average particulate organic carbon (POC), inorganic carbon (PIC), and nitrogen (PN) concentration during the stationary growth phase of non-calcifying non-axenic (triangles), calcifying non-axenic (empty circles), and calcifying axenic cultures (black dots). Error bars denote standard deviations of the means.

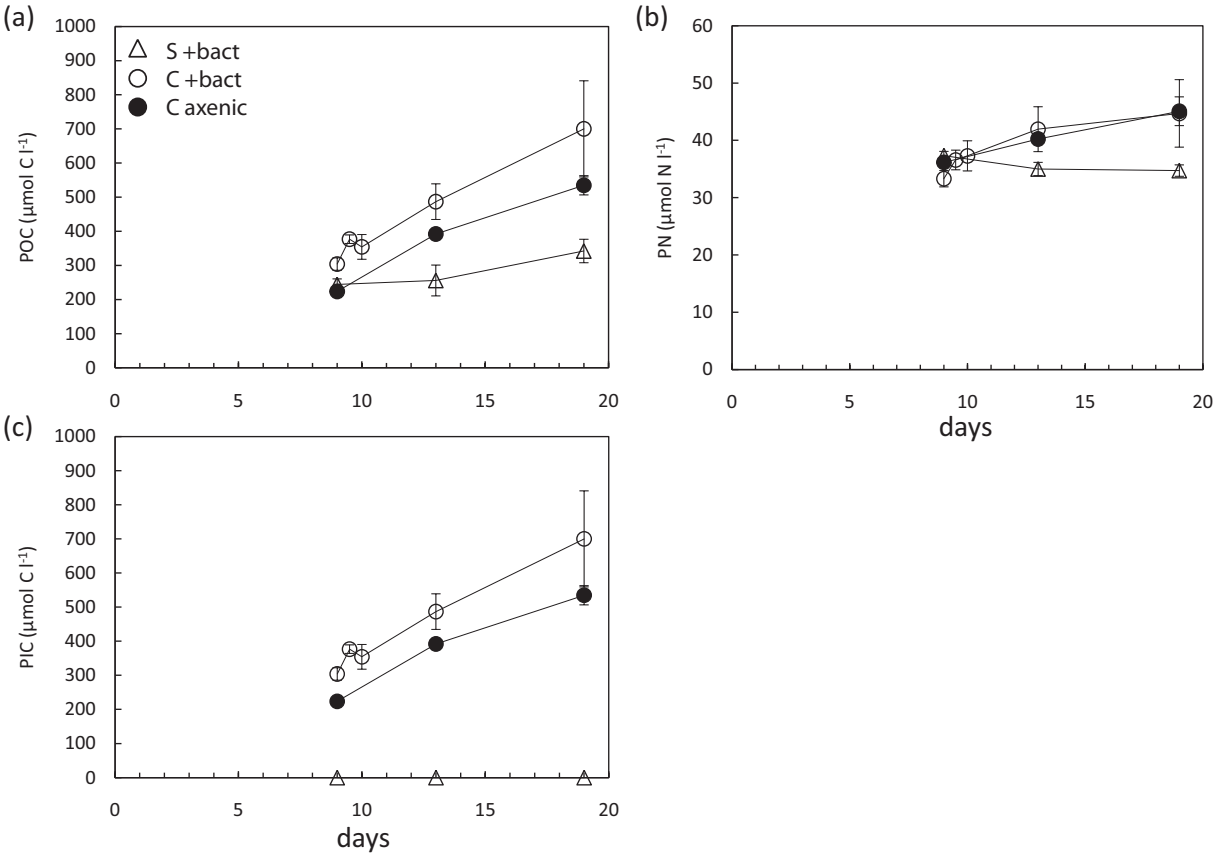

TEP dynamics

As part of the particulate carbon pool, the microscopically determined TEP-C concentration also increased during the stationary phase in all cultures (table 4 and fig. 3a). Although *E. huxleyi* cell concentration-normalised TEP-C levels did not significantly differ between culture treatments at the start of the stationary growth phase (day 9) (ANOVA: $F=1.19$, $df=2$, $p=0.37$), the cultures differed from each other for this variable at the end of the experiment (day 19) (ANOVA: $F=37.92$, $df=2$, $p<0.001$), when the S+bact cultures had the highest levels of TEP-C per cell (Tukey post hoc test, $df=6$, both $p<0.005$). The *E. huxleyi* cell-normalised TEP-C concentration was higher on day 19 in the C +bact than in the C axenic culture (t-test: $t=-4.19$, $df=4$, $p<0.02$).

The concentration of alcian blue adsorbed to particles, TEPcolor, showed a temporal increase also exhibited by TEP-C (fig. 3 b). However the differences in TEPcolor concentration between the culture treatments were more pronounced (table 4) (ANOVA *E. huxleyi* cell-normalised TEPcolor on day 19: $F=95.86$, $df=2$, $p<0.001$). The concentration of TEPcolor per *E. huxleyi* cell was markedly lower in the non-calcifying S +bact culture compared to the calcifying cultures C +bact and C axenic, despite the apparent decrease in cell concentration on day 19 in the former (fig. 1 a) (t-test day 19: S +bact-C axenic: $t=5.96$, $df=4$; S +bact-C +bact: $t=-11.33$, $df=4$, all $p<0.005$). Moreover, TEPcolor per *E. huxleyi* cell was higher in the C+bact than in the C axenic cultures (t-test day 19 C +bact-C axenic: $t=-8.90$, $df=4$, $p<0.001$).

Proportional differences between TEP-C, derived from particle size and abundance, and TEPcolor indicate a change in density of stainable moieties in TEP, which increased during the stationary growth phase (fig. 4a). This increase was most pronounced in the C +bact cultures, which differed significantly from the S +bact cultures (ANOVA slopes of linear regression: $F=10.99$, $df=2$, $p<0.01$; Tukey post hoc test: $df=6$, S +bact-C +bact: $p<0.01$, C axenic-C +bact: $p=0.07$). Moreover, changes in the spectral slope δ between day 9 and day 19 were only significant in the C +bact cultures, indicating aggregation of TEP during the stationary growth phase (table 4 and fig. 4b) (t-test slope δ C +bact: $t=4.98$, $df=4$, $p<0.01$).

Table 4. Average concentration of TEP-C, TEPcolor and their values normalised to *E. huxleyi* cell concentration, and the spectral slope δ of the TEP size frequency distribution during the stationary growth phase of the non-axenic haploid (S +bact), non-axenic calcifying (C +bact), and axenic calcifying (C axenic) *E. huxleyi* cultures**.**

culture	day	TEP-C (µmol C l^{-1})	pmol TEP-C $cell^{-1}$	slope δ	TEPcolor (µg X eq. l^{-1})	pg X eq. $cell^{-1}$
S +bact						
	9	63 ± 2	0.28 ± 0.03	-3.30 ± 0.07	1363 ± 109	6.05 ± 1.13
	13	126 ± 8	0.55 ± 0.11	-3.06 ± 0.18	1958 ± 179	8.35 ± 0.46
	19	144 ± 11	1.09 ± 0.18	-3.03 ± 0.11	2832 ± 106	21.27 ± 2.85
C +bact						
	9	86 ± 8	0.29 ± 0.03	-2.85 ± 0.19	5790 ± 192	19.23 ± 1.33
	10	79 ± 6	0.25 ± 0.02	-3.35 ± 0.18	7660 ± 543	24.14 ± 1.35
	13	115 ± 8	0.36 ± 0.03	-3.55 ± 0.1	11685 ± 168	36.03 ± 0.47
	19	175 ± 21	0.51 ± 0.07	-3.48 ± 0.12	19823 ± 1488	58.17 ± 4.87
C axenic						
	9	55 ± 5	0.25 ± 0.03	-3.20 ± 0.05	3686 ± 410	16.98 ± 2.34
	13	86 ± 12	0.28 ± 0.04	-3.20 ± 0.18	7562 ± 302	25.09 ± 1.00
	19	108 ± 9	0.34 ± 0.03	-3.24 ± 0.1	10280 ± 535	32.18 ± 1.38

Fig. 3. Average TEP-C concentration per Ehux cell (a) and average TEPcolor concentration per Ehux cell (b) during the stationary growth phase of cultures of non-calcifying non-axenic (triangles), calcifying non-axenic (empty circles), and calcifying axenic cultures (black dots). Error bars denote the standard deviation of the means.

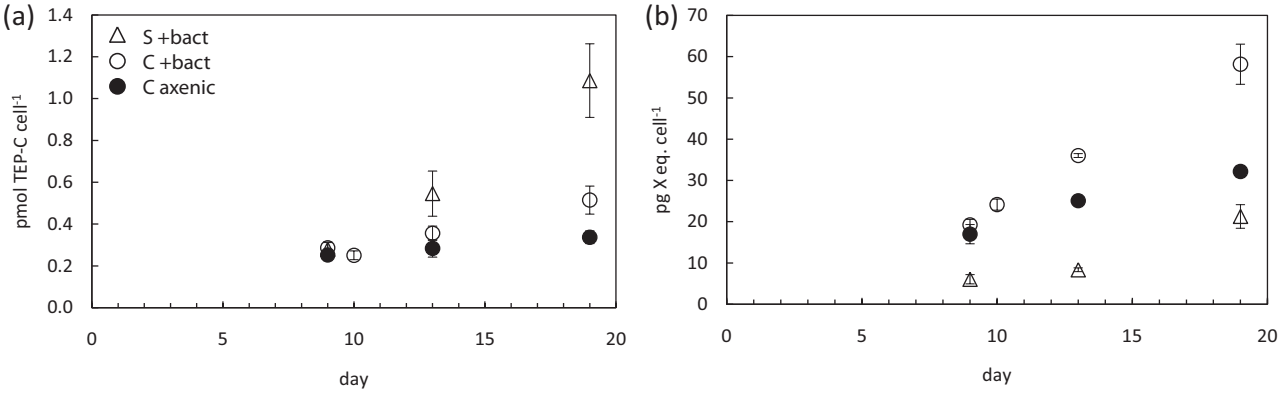

Fig. 4. Relationship between average TEP-C (µmol C l^{-1}) and TEPcolor concentration (µg X eq. l^{-1}) during the stationary growth phase of cultures of non-calcifying non-axenic (triangles), calcifying non-axenic (empty circles), and calcifying axenic cultures (black dots) (a). Change in the average spectral slope δ of the TEP size frequency distribution during the stationary phase of the above mentioned cultures (b). Error bars denote the standard deviation of the means.

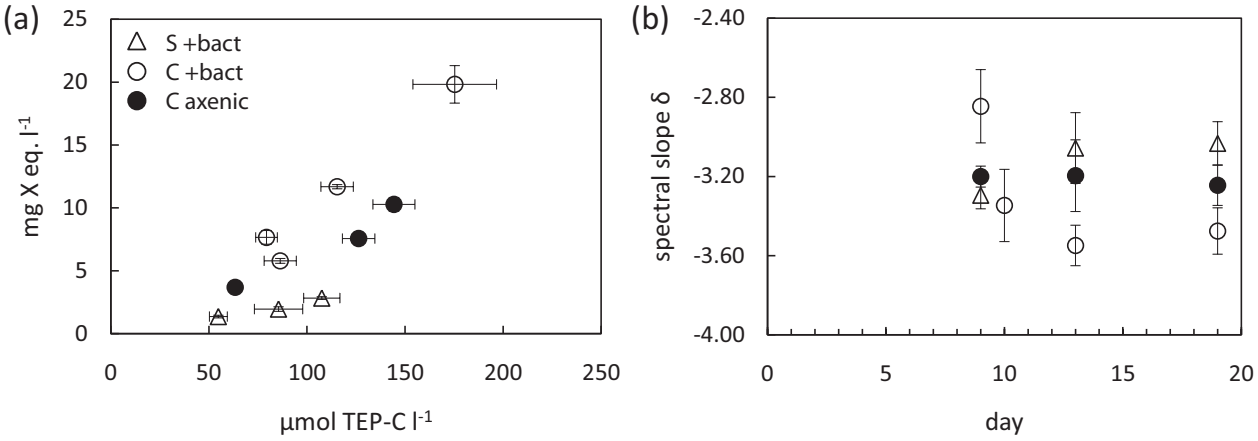

Dissolved carbohydrates dynamics

Total (TCHO) and free (MCHO) dissolved carbohydrates accumulated during the stationary growth phase in all cultures, and mainly consisted of polysaccharides at the end of the experiment, except in the C axenic cultures where half of the dissolved carbohydrates were in the MCHO pool (table 5 and figs. 5a and b). While the concentration of dissolved carbohydrates was similar on day 9 in the different cultures (ANOVA TCHO: F=0.97, df=2, p=0.43; ANOVA MCHO: F=2.57, df=2, p=0.16), the S +bact cultures had significantly higher levels of dissolved carbohydrates on day 19 compared to the calcifying cultures (ANOVA TCHO: F=47.03, df=2, p<0.001; Tukey post hoc test TCHO: df=6, both p<0.005; ANOVA MCHO: F=26.31, df=2, p<0.005; Tukey post hoc test TCHO: df=6, both p<0.01). The concentration of TCHO and their polysaccharide content in the C +bact cultures on day 19 were significantly higher than in the C axenic cultures (t-test TCHO: t=-4.37, df=4, p<0.02; t-test %polysaccharide: t=-3.95, df=4, p<0.02). Measurements on HMW DOM from the C +bact cultures on day 19 showed that the TCHO concentration in the dissolved HMW fraction (12.9 ± 1.9 µmol C l^{-1}) made up a significant part of the total dissolved carbohydrate pool (43 ± 10%). Polysaccharides almost entirely made up the dissolved carbohydrates in this HMW fraction (98% ± 0.1%).

Table 5. Average concentrations of total dissolved carbohydrates (TCHO), free dissolved carbohydrates (MCHO), and the proportion of polysaccharides in TCHO (%) during the stationary growth phase.

culture	day	TCHO	MCHO	% polysaccharide
S +bact				
	9	12.9 ± 5.7	6.0 ± 0.7	46.1 ± 26.4
	13	36.0 ± 8.8	9.0 ± 0.8	74.3 ± 4.8
	19	69.1 ± 10.5	13.1 ± 0.9	80.9 ± 1.7
C +bact				
	9	12.3 ± 1.2	3.6 ± 1.9	69.4 ± 18.5
	10	14.4 ± 1.3	4.1 ± 0.6	71.2 ± 3.0
	13	18.5 ± 0.5	4.6 ± 0.9	75.3 ± 4.6
	19	30.6 ± 2.9	6.1 ± 1.1	80.2 ± 2.7
C axenic				
	9	9.1 ± 2.3	4.7 ± 0.7	45.8 ± 19.3
	13	11.1 ± 0.6	5.1 ± 0.9	54.7 ± 5.6
	19	19.6 ± 3.2	8.8 ± 1.5	54.2 ± 11.0

Dissolved HMW neutral aldose composition

Total neutral aldoses (ΣNAld) concentration in HMW DOM (>10kDa) increased during the stationary growth phase in each treatment (table 6). The ΣNAld yield did not differ between C +bact and C axenic cultures but were much higher in the S +bact treatment on day 19 (ANOVA: $F=13.65$, $df=2$, $p<0.01$; Tukey post hoc test: $df=5$, both $p<0.015$). Changes in the proportions of individual monosaccharides with respect to bloom development (days) and treatment are visualized using RDA (fig. 6). The temporal change in the relative composition of individual sugars was responsible for the main gradient of variation in the RDA plot, while the differences in sugar composition between the calcifying (C +bact and C axenic) and non-calcifying (S +bact) treatments related to the second axis. At the end of the experiment, rha+ara made up the highest share of the ΣNAld yield in each culture treatment. The contribution of rha+ara to the yield of ΣNAld significantly increased during the development of each culture while that of glucose decreased (linear regressions: S +bact $df=1$, rha: $F=11.41$, $p<0.03$, glc: $F=10.66$-24.73, $p<0.03$; C +bact $df=1$, rha: $F=84.00$, $p<0.001$, glc: $F=113.62$, $p<0.001$; C axenic $df=1$, rha: $F=9.47$, $p<0.02$, glc: $F=48.39$, $p<0.001$). The contribution of galactose only decreased during the development of the calcifying cultures while the contribution of mannose respectively decreased or increased in the S +bact and C

axenic treatments (linear regressions: S+bact df=1, man: F=8.68, p<0.05; C+bact df=1, gal: F=36.49, p<0.001; C+axenic df=1, man: F=127.31, p<0.001).

Fig. 5. Average concentration of dissolved carbohydrates as total carbohydrates (TCHO) (a) and free carbohydrates (MCHO) (b) during the stationary growth phase of non-calcifying non-axenic (triangles), calcifying non-axenic (empty circles), and calcifying axenic cultures (black dots). Average concentration of DOC (c) during the stationary growth phase of calcifying non-axenic cultures. Error bars denote standard deviations of the means.

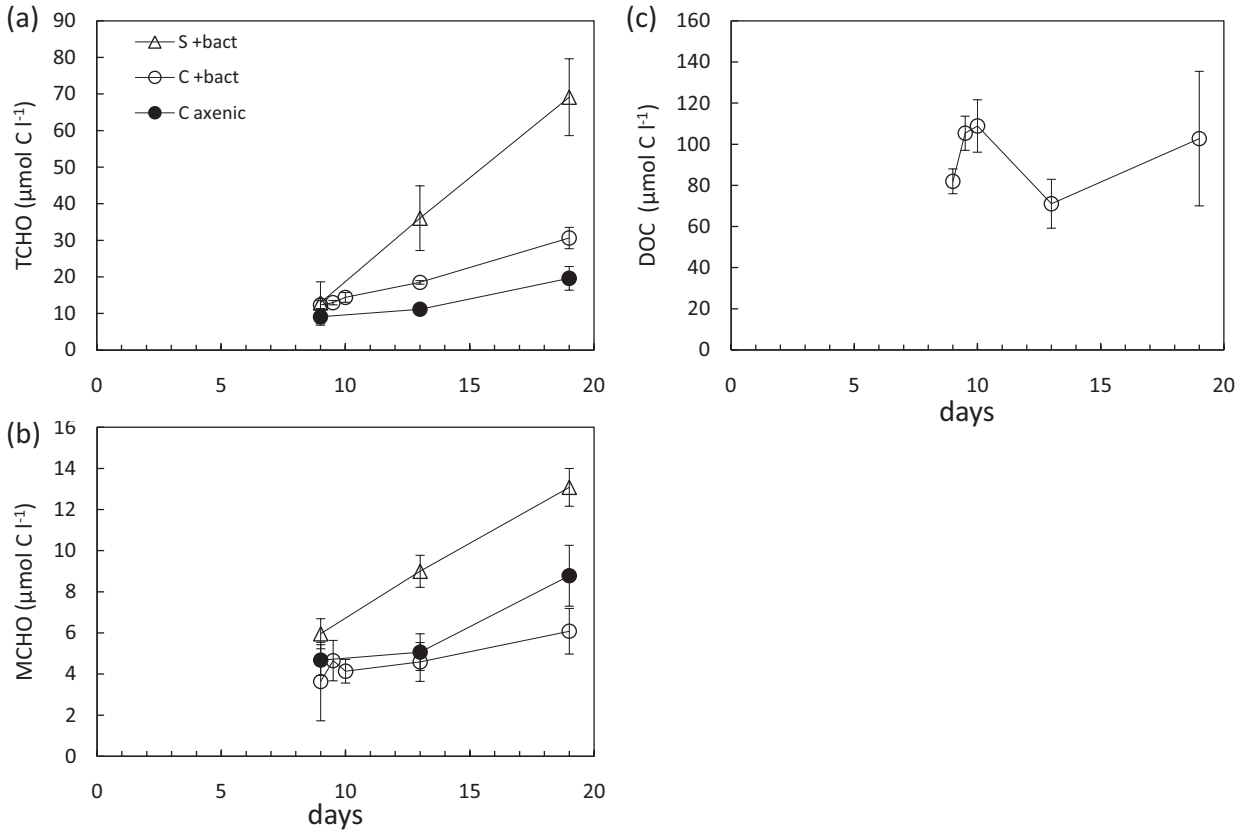

Finally, we found differences in the proportion of each individual monosaccharide in the HMW DOM between different culture treatments which depended on the day of sampling. There was a significant difference in the proportions of rha+ara, glucose, and mannose between the C +bact and C axenic cultures on day 9 (t-test day 9, df= 4, $t_{rha+ara}$=5.68; t_{glc}=-8.28; t_{man}=-2.78, all p<0.05), while they were not significantly different between the C +bact and C axenic cultures on day 19 (t-test day 19, df=4, all monosaccharides p>0.05). The relative contribution of rha+ara, galactose, and glucose differed significantly between the C +bact and S +bact *E. huxleyi* cultures on day 9 (t-test day 9, df=3, $t_{rha+ara}$=-6.76; t_{gal}=-4.17; t_{glc}=16.12, all p<0.05) while that of galactose, xylose, and mannose differed significantly on day 19 (t-test day 19, df=3, t_{gal}=-23.97; t_{xyl}=3.89; t_{man}=12.71, all p<0.05).

Table 6. Relative neutral aldose composition of HMW DOM and total concentration of the measured monosaccharides (Σ NAld) in µmol C l^{-1} in different *E. huxleyi* culture treatments. The number of days after inoculation of the culture, when samples were taken, is indicated in the first column. Arrows indicate significant temporal increases (up) or decreases (down) in the proportion of individual monosaccharides.

day	fuc	rha+ara	rha	ara	gal	glc	xyl	man	Σ NAld
Ehux C axenic (this study)		↗			↘	↘		↗	
9	13	34			22	11	10	10	0.5
13	11	38			19	7	11	13	1.5
19	10	40			16	5	12	16	3.5
Ehux C +bact (this study)		↗			↘	↘			
9	12	15			25	17	14	18	0.7
9.5	14	18			24	15	12	17	1.0
10	12	18			24	14	14	18	1.3
13	10	30			22	9	15	14	2.1
19	11	39			15	5	12	17	4.0
Ehux S +bact (this study)		↗				↘		↘	
9	10	33			33	7	8	10	4.7
13	7	39			34	4	8	7	31.0
19	8	40			34	4	9	6	28.3
Ehux + bact (Biersmith & Benner 1998)									
14	12	13	2	10	24	15	22	14	13
Ehux + bact (Aluwihare & Repeta 1999)									
22	5	39	9	30	24	9	12	9	17

Biomass labelling

The transfer of DIC to *E. huxleyi* cells, photosynthetic and calcification products (POC, DOC, HMW NAld, and PIC) and bacteria was followed after addition of inorganic ^{13}C carbon as a tracer to the C +bact cultures, at the onset of the light phase at the beginning of the stationary growth phase (day 9) (fig. 7). After addition of ^{13}C-DIC, the $\delta^{13}C$ of DIC increased to 5535‰ ± 759‰, which is equivalent to an APE of 6.84 ± 0.74. Delta ^{13}C-DIC decreased linearly to 1650‰ ± 66‰ ten days after labelling, which corresponded to an APE of ^{13}C of 1.78 ± 0.07 (fig. 7). Incorporation of ^{13}C label into the algal and bacterial cells was apparent 14 h after the pulse of labelled bicarbonate to the cultures (figs. 7c and d). The initial rapid build-up of ^{13}C label in algal and bacterial biomass levelled off as measured 4 days after labelling (fig. 7c and d). Ten days after labelling, both the *E. huxleyi* and bacterial biomass were highly labelled, exhibiting a $\delta^{13}C$ value of respectively 2023‰ ± 73‰ and 1809‰ ± 59

‰ (table 7). *E. huxleyi* biomass based on PLFA concentrations was estimated at 276.3 ± 16.8 µmol C l^{-1} 4 days after labelling. Net production rate of *E. huxleyi* biomass was estimated to be 48.8 ± 7.6 µmol C l^{-1} d^{-1} one day after labelling and gradually decreased during the remainder of the experiment (table 7).

Fig. 6. Redundancy analysis plot of the proportions of individual monosaccharides in samples of non-calcifying non-axenic (triangles), calcifying non-axenic (empty circles), and calcifying axenic *E. huxleyi* cultures (black dots) on different time points following culture inoculation (in days, next to the symbols). Symbols represent the centroids of the samples while arrows indicate the the direction of increase of individual monosaccharides, their size is relative to their correlation to the axes.

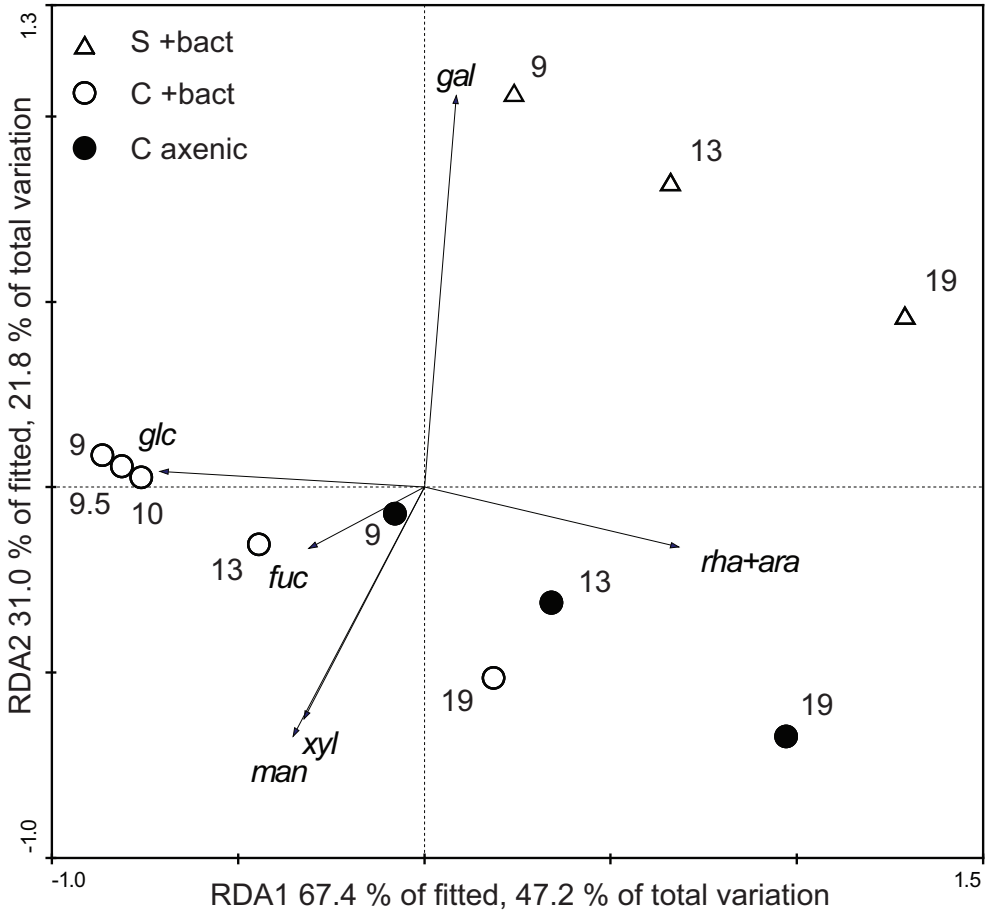

Bacterial biomass based on PLFA concentrations was estimated at 1.6 ± 0.4 µmol C l^{-1} 4 days after labelling. The low levels of label incorporated into bacterial biomass are caused by their low biomass compared to the algal biomass, not by their lack of uptake of newly fixed carbon, as indicated by the high $\delta^{13}C$ of bacterial biomass. We estimated the secondary

bacterial production rate to be around 152 ± 30 nmol C l^{-1} d^{-1} one day after label addition (table 7), which would amount to a rate of bacterial respiration of 606 ± 122 nmol C l^{-1} d^{-1}.

Fig. 7. Average change in excess ^{13}C incorporation into POC, PIC, bacterial and *E. huxleyi* biomass, originating from the pool of DI^{13}C (expressed in atom percent excess ^{13}C of DIC), during the stationary growth phase of calcifying, non-axenic *E. huxleyi* cultures. Error bars denote the standard deviations of the means of the replicate cultures.

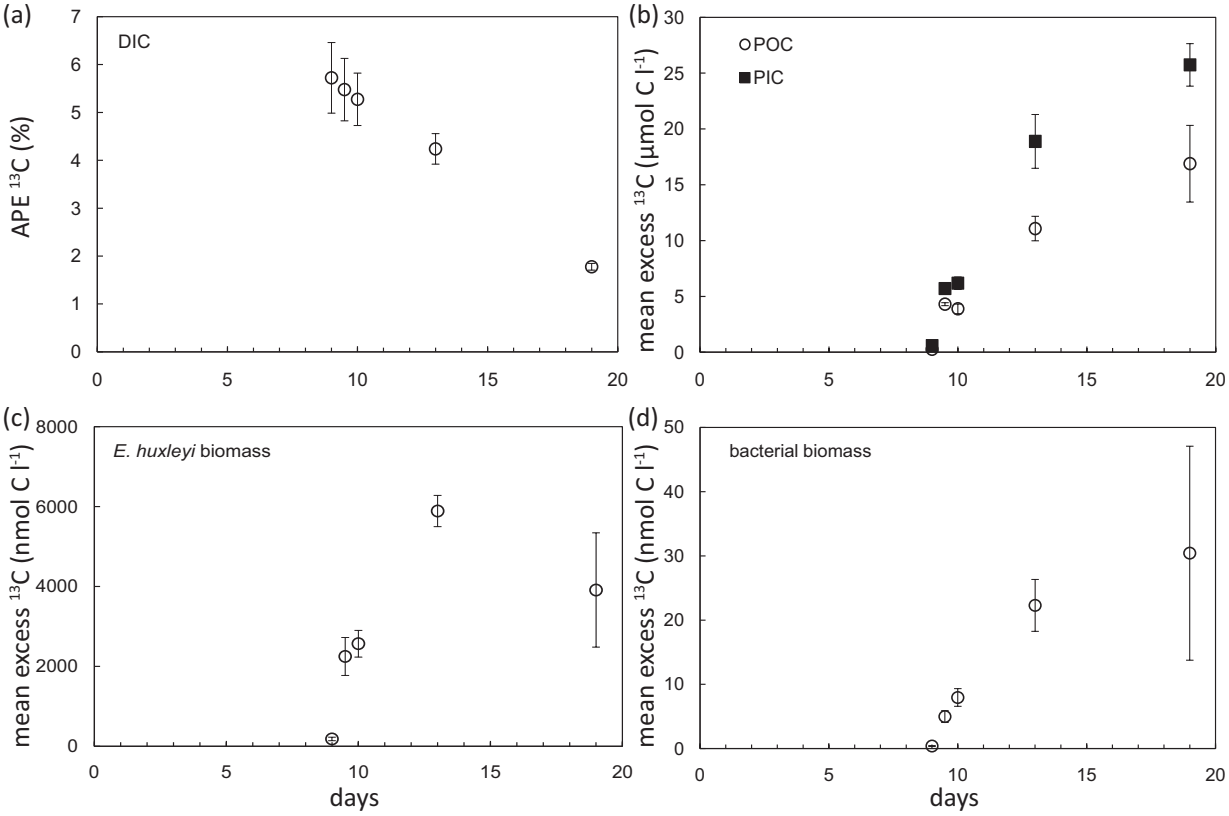

Table 7. Average $\delta^{13}C$ values (‰) of DIC, *E. huxleyi* biomass ($Ehux_{PLFA}$), bacterial biomass ($Bact_{PLFA}$), PIC, POC, DOC, and total HMW NAld (ΣNAld), during the stationary growth phase of non-axenic, calcifying *E. huxleyi* cultures (C +bact).

time after labelling	$\delta^{13}C$ DIC	$\delta^{13}C$ $Ehux_{PLFA}$	$\delta^{13}C$ $Bact_{PLFA}$	$\delta^{13}C$ POC	$\delta^{13}C$ PIC	$\delta^{13}C$ DOC	$\delta^{13}C$ NAld
14 h	5282 ± 668	984 ± 68	500 ± 37	1027 ± 66	1465 ± 196	-21 ± 2	179 ± 81
1 d	5076 ± 558	1015 ± 66	626 ± 110	985 ± 65	1542 ± 145	-17 ± 1	308 ± 137
4 d	4035 ± 317	1964 ± 106	1751 ± 159	2097 ± 122	2845 ± 251	84 ± 12	1572 ± 233
10 d	1650 ± 66	2023 ± 73	1809 ± 59	2225 ± 57	2796 ± 122	275 ± 78	2223 ± 111

Extracellular release and label transfer

The sustained production of coccoliths was reflected in the accumulation of excess ^{13}C into PIC during the stationary growth phase, which occurred at a rate of 117.2 ± 9.5 µmol C l^{-1} d^{-1} 24 h after labelling (fig. 7b and table 8). Newly fixed, ^{13}C-enriched, carbon diluted the POC pool and as such increased the $\delta^{13}C$ of POC from natural background values to 2225 ± 57‰ ten days after labelling (table 7). New POC, produced at a rate of 73.8 ± 10.0 µmol C l^{-1} d^{-1} 24 h after labelling, encompasses both the organic carbon present in cells and the organic carbon particles released extracellularly. Once cellular biomass has been taken into account, this represents a particulate organic extracellular release of 33.7 ± 1.2% 24 h after label addition (day 10). This percentage of organic particulate extracellular release further increased to 73.8 ± 13.7% ten days after label addition (table 9). The production rate of this particulate extracellular organic carbon (POCxc) was estimated to amount to 24.9 ± 2.5 µmol C l^{-1} d^{-1} 24 h after labelling and further increased during the experiment (table 8).

Table 8. Average production rates of *E. huxleyi* biomass (Ehux NP), bacterial biomass (Bact NP), PIC, POC, extracellular POC (POCxc), and DOC during the stationary growth phase of non-axenic, calcifying *E. huxleyi* cultures (C +bact).

time after labelling	**Ehux NP** (µmol C l^{-1} d^{-1})	**Bact NP** (nmol C l^{-1} d^{-1})	**PIC** (µmol C l^{-1} d^{-1})	**POC** (µmol C l^{-1} d^{-1})	**POCxc** (µmol C l^{-1} d^{-1})	**DOC** (nmol C l^{-1} d^{-1})
14 h	83.2 ± 18.9	184 ± 31	211.1 ± 10.1	159.0 ± 6.2	75.6 ± 15.1	329 ± 76
1 d	48.8 ± 7.6	152 ± 30	117.2 ± 9.5	73.8 ± 10.0	24.9 ± 2.5	260 ± 42
4 d	30.1 ± 2.7	114 ± 25	96.9 ± 16.8	56.7 ± 7.4	26.5 ± 4.6	447 ± 79
10 d	10.5 ± 3.7	82 ± 44	69.3 ± 5.7	45.5 ± 9.6	34.9 ± 13.3	886 ± 60

Table 9. Average percentage extracellular release of particulate (PERp) and dissolved (PERd) organic carbon during the stationary growth phase of non-axenic, calcifying *E. huxleyi* cultures (C +bact), expressed in % of total primary production (particulate + dissolved).

time after labelling	**PERp (%)**	**PERd (%)**
14 h	47.6 ± 10.3	0.2 ± 0.1
1 d	33.7 ± 1.2	0.4 ± 0.1
4 d	46.1 ± 2.2	0.8 ± 0.2
10 d	73.8 ± 13.7	1.7 ± 0.1

Labelling of DOC and dissolved HMW NAld was apparent 14 h after label addition and attained $\delta^{13}C$ values of respectively 274 ± 78‰ and 2223 ± 111‰ ten days after labelling (table 7). Production of newly fixed DOC and HMW NAld proceeded steadily throughout the stationary phase as indicated by the accumulation of excess ^{13}C into these pools (figs. 8a and b). The production rate of DOC increased during the stationary phase (table 7) although there was no trend in concentration change during the stationary phase (day 9 to 19: 94 ± 17 µmol C l^{-1}) (fig. 5c), indicating the measured DOC represents a transient stock in a highly dynamical carbon pool. This was reflected in the low but increasing dissolved extracellular release of organic carbon with time (table 9). The higher production rate of the DOC, POC, POCxc, PIC, and *E. huxleyi* biomass pools at 14 h compared to 24 h after labelling indicates the light-dependency of these processes (table 8).

The amount of newly fixed dissolved carbon in the HMW NAld was approximately a third of the newly fixed carbon retrieved in DOC (maximum four days after labelling: 39 ± 8%) (figs. 8a and b). Production of these monosaccharides by *E. huxleyi* cells was corroborated by an increase of excess ^{13}C incorporated into each individual monosaccharide during the culture development (figs. 8c to h). Concomitantly, the production rates of neutral aldoses increased during the stationary growth phase (table 10). The production rate of rha+ara was the most important, contributing to almost half of the ΣNAld production in HMW DOM. Galactose, mannose and xylose had intermediate production rates compared to rhamnose, while that of fucose and glucose were least important. High $\delta^{13}C$ values of rha+ara, gal, xyl, and man, comparable to that of *E. huxleyi* biomass indicate that they were directly excreted by *E. huxleyi* cells (24 h after labelling $\delta^{13}C$ of rha+ara: 771 ± 203‰; gal: 315 ± 172‰; xyl: 272 ± 162‰; man: 243 ± 107‰) (compare with table 7).

Table 10. Average production rates (nmol C l^{-1} d^{-1}) of neutral aldoses in HMW dissolved organic matter during stationary growth phase of non-axenic, calcifying *E. huxleyi* cultures (C +bact). ΣNAld is the sum of the production rates of individual neutral aldoses.

time after labelling	fuc	rha+ara	gal	glc	xyl	man	ΣNAld
14 h	5 ± 0	37 ± 0	17 ± 0	2 ± 0	10 ± 0	12 ± 0	83 ± 0
1 d	4 ± 4	39 ± 17	20 ± 10	1 ± 2	9 ± 4	11 ± 7	85 ± 39
4 d	8 ± 2	86 ± 25	28 ± 11	3 ± 1	23 ± 6	32 ± 9	179 ± 51
10 d	9 ± 2	121 ± 28	31 ± 11	5 ± 1	32 ± 12	48 ± 16	247 ± 66

Fig. 8. Average change in excess ^{13}C incorporation into DOC, total dissolved HMW NAld, and individual monosaccharides of HMW DOM: fucose, rhamnose, galactose, glucose, xylose, and mannose, during the stationary growth phase of calcifying, non-axenic *E. huxleyi* cultures. Error bars denote standard deviations of the means of replicate cultures.

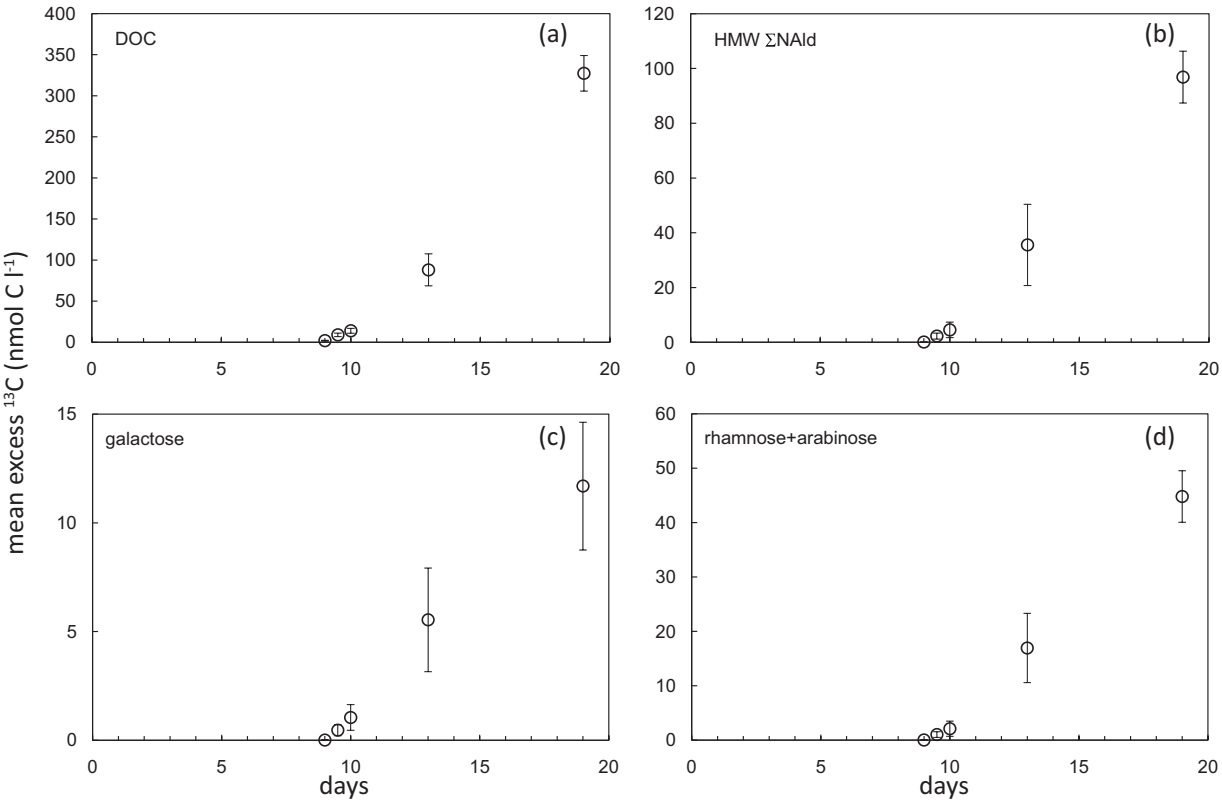

Fig. 8. Continued.

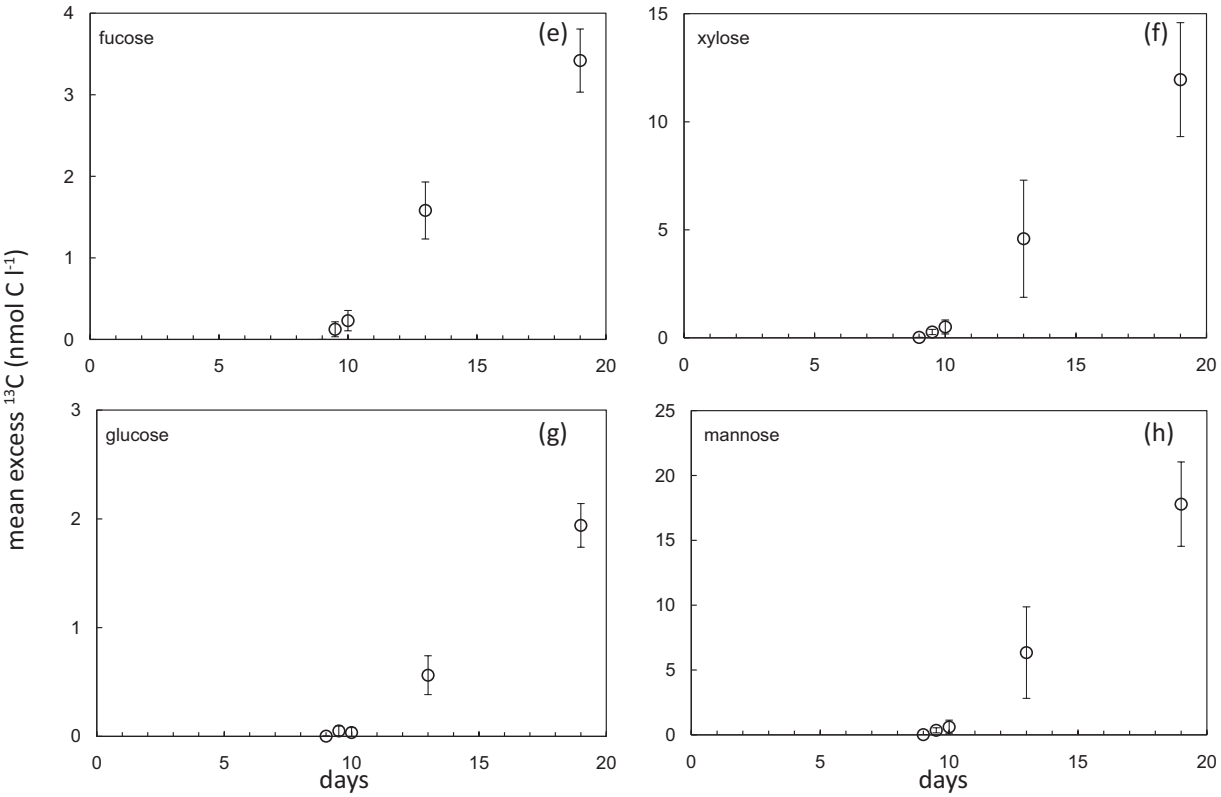

Discussion

Unbalanced growth

During the stationary growth phase of each treatment we observed a decoupling of the carbon and nitrogen metabolism of the cells, as indicated by rising POC to PN ratios. This typically occurs when nutrients (N, P) essential for the production of proteins or nucleic acids, and consequently cell proliferation, become limiting, while carbon metabolism is sustained (i.e. unbalanced growth). This carbon overconsumption often results in the exudation of carbon rich material, such as carbohydrates, which can aggregate to form TEP-rich POC (Passow, 2002a; Van den Meersche *et al.*, 2004).

Extracellular release and TEP production are thought to be influenced by nutrient limitation and growth rate of phytoplankton cells (Lancelot, 1983; Obernosterer and Herndl, 1995; Passow, 2002b). The longer lag phase in the C axenic cultures compared to the non-axenic cultures together with the absence of bacterial nutrient consumption (mainly nitrate) are responsible for the delay in nutrient depletion in the C axenic cultures (fig. 1). Although non-

limiting nitrate concentrations were still measured during the stationary growth phase of the axenic cultures we do not expect this to confound comparison between axenic and non-axenic culture treatments, because of similar algal growth rates during the exponential and stationary phase of the calcifying cultures and the complete exhaustion of dissolved inorganic phosphate were found in all treatments.

After the pulse of ^{13}C labelled bicarbonate, we measured its rapid incorporation into the algal and bacterial cells using PLFA biomarkers (fig. 7c and d). The close agreement between the $\delta^{13}C$ values of algal and bacterial biomass (table 7) point to the close coupling between bacteria and *E. huxleyi*. The low production rates calculated for *E. huxleyi* and bacteria (table 8) are in accordance with the stable cell numbers during the stationary growth phase. We used a low value for the coefficient of bacterial growth efficiency, typically encountered in oligothrophic oceanic environments (del Giorgio and Cole, 1998), to estimate bacterial carbon consumption, because of the high share of carbohydrate in DOM, and thus high C:N ratio, which has been shown to affect the bacterial growth efficiency (Kroer, 1993). The bacterial production rates we calculated were lower than the one estimated by Van den Meersche *et al.* (2004) in nutrient limited conditions (11.3 µmol C l^{-1} d^{-1}), even though the bacterial biomass during their study was approximately 13 times higher than in our study. The presence of grazers during their incubation, a potential source of labile DOC, may provide a possible explanation for this discrepancy. Thus, although the organic material in the cultures probably was of low nutritional quality, which together with nutrient limitation caused the low bacterial production rates that we determined, bacterial cells were metabolically active and respired approximately 3% of the extracellular organic carbon (i.e. POCxc+DOC) on the first day after isotopic label addition.

Production of dissolved carbohydrates and dissolved HMW neutral aldoses

Carbohydrates often form an important constituent of DOM released by healthy microalgal cells (Myklestad, 2000). We measured direct release of DOC and more specifically dissolved HMW NAld by *E. huxleyi* cells using a pulse of isotopically labelled DIC and by subsequently following its incorporation into these pools. Excretion of neutral aldoses by microalgae has been reported before, through measurements of isotopically labelled monosaccharides in benthic communities of intertidal and subtidal sediment (Bellinger *et al.*, 2009; Oakes *et al.*, 2010) or by determining the concentration build-up of monosaccharides in batch cultures of

E. huxleyi (Biersmith and Benner, 1998; Aluwihare and Repeta, 1999; Kayano and Shiraiwa, 2009). Yet, to our knowledge, this is the first demonstration of direct excretion of NAld by planktonic microalgae into HMW DOM using compound specific isotope analysis of carbohydrates. Carbohydrates in HMW DOM, and polysaccharides in particular, form a substantial part of the total dissolved carbohydrate pool as indicated by measurements during the stationary growth phase of non-axenic, probably calcifying, *E. huxleyi* cultures in other studies (Biddanda and Benner, 1997; Biersmith and Benner, 1998). In our study, we measured sizeable concentrations of TCHO (>9.1 ± 2.3 µmol C l^{-1}) at the beginning of the stationary growth phase which indicates prior release and accumulation of carbohydrates by exponentially growing *E. huxleyi* cells in balanced conditions (POC:PN<10). This was also demonstrated in axenic *E. huxleyi* cultures, thereby excluding bacterial origin of at least a major part of this dissolved carbon pool (table 5). Similar to our results, Biddanda and Benner (1997) observed an increase in carbohydrate content of DOC (23% - 70%) and an increase of the share of polysaccharides in TCHO (78% - 87%) during non-axenic E. huxleyi culture development. However, Grossart *et al.* (2007b) did not observe such an increase in polysaccharide proportion of TCHO during culture development of Phaeocystis sp. and diatoms during mesocosm experiments, nor did Biddanda and Benner (1997) in their *Skeletonema* cultures, where polysaccharide content of TCHO remained uniform (85%) throughout phytoplankton growth, suggesting species-specific patterns of exudation.

The heterogeneous distribution of monosaccharides in the HMW DOM suggests that heteropolysaccharides make up the carbohydrates of this fraction in the present study (table 6). Rhamnose+arabinose and galactose were the most abundant neutral aldoses, while glucose was the least abundant in HMW DOM. We substantiated the direct production and release of the most abundant neutral aldoses of HMW DOM by *E. huxleyi* using a stable isotope tracer approach. Although some studies reported glucose and galactose to be the most abundant aldoses in HMW DOM of natural seawater (Skoog and Benner, 1997; Hama and Yanagi, 2001; Skoog *et al.*, 2008), the high proportions of rha+ara in the HMW DOM of our culture experiments were comparable to those reported by Aluwihare and Repeta (1999) but higher than those of Biersmith and Benner (1998) from their E. huxleyi culture experiments (table 6).

Neutral aldoses comprise the largest identified carbohydrate fraction in HMW DOM, ranging from 6 % to 20 % in natural seawater (McCarthy *et al.*, 1996; Skoog and Benner, 1997; Skoog *et al.*, 2008). An estimate of TCHO content of HMW DOM on the last day of the experiment in the C +bact cultures showed that approximately one third (32 ± 6%) of the carbohydrates in this fraction were neutral aldoses. This prompts the question what the remaining two thirds of carbohydrates are made of. As discussed by Skoog and Benner (1997), the term "neutral aldoses" refers to uncharged carbohydrates with an aldehyde end group (in contrast to amino sugars which are charged aldoses). Several naturally occurring classes of carbohydrates, i.e. polyhydroxy aldehydes or ketones and their derivatives, were not detected (e.g. sugar alcohols and amino sugars) or could not be quantified with the HPLC method used in the present study (e.g. uronic acids). Nuclear magnetic resonance spectroscopy of HMW DOM confirmed the importance a structurally well-defined class of acylated polysaccharides (APS) and other structural carbohydrates such as methyl sugars and 3-deoxysugars which were not detected by our HPLC method (Aluwihare *et al.*, 1997; Panagiotopoulos *et al.*, 2007). However, acidic sugars such as uronic acids probably comprised an important part of the dissolved polysaccharide pool as indicated by elevated levels of TEPcolor, probably formed by dissolved precursors during our experiments.

Influence of bacterial activity on the dynamics of dissolved carbohydrates and HMW neutral aldoses

Higher concentrations of TCHO and higher shares of polysaccharides in TCHO in non-axenic compared to axenic *E. huxleyi* cultures suggests bacterial activity influenced the formation of dissolved carbohydrates as well as the molecular size spectrum of this pool (table 5). The latter is counterintuitive as bacterial exoenzymatic activity would tend to decrease the molecular size spectrum of DOM. The resulting mono- and oligosaccharides may then have been consumed by bacterial cells.

During the development of calcifying cultures the proportion of rha+ara increased while that of glucose and galactose decreased (table 6 and fig. 5). Compositional changes in HMW DOM can be caused by a temporal change in production rate of certain sugars, by preferential degradation of certain sugars by bacterial activity, or by the preferential coagulation of colloids containing higher fractions of certain sugars, moving them up in the size spectrum of organic matter. The production rate of galactose, estimated from label incorporation in the

HMW NAld from non-axenic calcifying cultures, decreased compared to the total NAld production rate during culture development (table 9). This suggests either a physiological change of the *E. huxleyi* cells or loss of galactose from the HMW pool due to preferential degradation or aggregation processes. Changes in the content of rhamnose and glucose in organic matter have been reported during degradation experiments (Meon and Kirchman, 2001; Giroldo *et al.*, 2003; Panagiotopoulos and Sempere, 2007), between different organic matter size-fractions (Skoog *et al.*, 2008), and along depth-profiles in the ocean (Amon and Benner, 2003), and have been interpreted as diagenetic changes along a bioreactivity gradient. In general, the aforementioned authors observed an enrichment of glucose and deoxysugars (fucose and rhamnose), and a decrease in galactose, arabinose, and other neutral aldoses. In the present study, bacteria preferentially assimilated newly produced organic carbon as indicated by their high $\delta^{13}C$ values compared to DOC (Norrman *et al.*, 1995). We measured a significant effect of bacterial activity on the neutral aldose composition on day 9 in calcifying *E. huxleyi* cultures (table 5), and even when taking into account the apparent two-day lag period in growth of the C axenic cultures compared to C +bact cultures, the difference in neutral aldose composition remained significant (t-test between day 10 C +bact and day 13 C axenic: df= 4, $t_{rha+ara}$=-9.34; t_{gal}=3.92; t_{glc}=9.23, all $p<0.02$). Compositional changes measured during progression of the stationary growth phase partly corroborate this diagenetic hypothesis, except for the share of glucose which decreased in our study. Degradation experiments using DOM from axenic *E. huxleyi* cultures (Van Oostende, unpublished results) or DOM containing coccolith polysaccharides (Nanninga *et al.*, 1996) did not show a decrease in concentration of HMW NAld or coccolith polysaccharides after 2 weeks of incubation in nutrient replete conditions, demonstrating the recalcitrant nature of HMW polysaccharides produced by *E. huxleyi*.

Influence of life cycle stage on the dynamics of dissolved carbohydrates and

HMW neutral aldoses

We measured higher concentrations of dissolved carbohydrates (TCHO and HMW NAld) in S +bact cultures compared to calcifying cultures (table 4 and 5). However, the influence of the algal life cycle stage is obscured by higher bacterial cell concentrations in the S +bact compared to the C +bact cultures which may be partly responsible for the higher dissolved carbohydrates as mentioned earlier. Nonetheless, higher concentrations of dissolved

carbohydrates together with lower POC and TEPcolor concentrations suggest reduced coagulation potential of the dissolved polysaccharides which would then remain in the dissolved phase instead of being transferred to the particulate pool (Engel *et al.*, 2004a). Unfortunately, due to loss of DOC samples for this treatment, we could not make a carbon balance between the particulate and dissolved pool to verify this hypothesis. Calcification was associated with a shift in neutral aldose composition brought about by changes in the proportions of galactose and mannose, and stable higher proportions of xylose (fig. 6 and table 6). A switch from cellular proliferation to calcification upon phosphate depletion is typical for diploid E. huxleyi cells. Kayano and Shiraiwa (2009) showed that both calcification and the associated production of coccolith polysaccharides were stimulated under inorganic phosphate deficiency, as the cells switched from the production of storage glucan (neutral polysaccharide) to coccolith polysaccharide (acidic polysaccharides), composed of mannose, galacturonic acid, xylose, and rhamnose. This coccolith polysaccharide is a macromolecule with a weight-average molar mass of 88600 ± 3200 g mol^{-1}, made up of different neutral saccharides (galactose, rhamnose, mannose, xylose), methyl-sugars and galacturonic acid, which is released in the surrounding medium when coccoliths are extruded to the cell surface (de Jong *et al.*, 1979; Fichtinger-Schepman *et al.*, 1979; Borman *et al.*, 1986; Borman *et al.*, 1987). In another study, the calcifying *E. huxleyi* strain 92D (PML) had high levels of rhamnose and galactose, and a low arabinose concentration, even though the composition of coccolith-associated polysaccharide showed some strain specificity, such as higher molar ratios of rhamnose and galactose, absence of ribose, and only traces of methylated sugars in strain 92D compared to two other strains (Borman *et al.* 1987). The resemblance in composition between the HMW NAld in our study and the coccolith polysaccharides in previous studies suggests that coccolith polysaccharides are main the source of the dissolved HMW NAld here.

Although very little physiological and ecological information is available about the haploid (motile, non-calcifying) life cycle stage of *E. huxleyi*, these cells have been shown to produce non-calcified scales covering their cells but lack the coccoliths-forming apparatus present in non-calcifying diploid cells (Green *et al.*, 1996; Billard and Inouye, 2004). Based on the presence of similar transcripts of the biomineralization protein (glutamic acid-proline-alanine or GPA) in both diploid calcifying and haploid *E. huxleyi* cells, von Dassow *et al.*

(2009) suggested that this glycoprotein may play a structural role in the formation of organic scales in haploid *E. huxleyi* cells. These elliptical scales, with dimensions of 0.4 µm to 0.6 µm and carrying a pattern of radiating fibrils, are much smaller than coccoliths (Green *et al.*, 1996) and could thus theoretically pass through glassfibre filters used in this study (nominal pore-size of 0.7 µm), especially if prior bacterial degradation of these scales had occurred. Supposing the production of these scales by motile cells proceeds in a similar continuous fashion as coccoliths in diploid cells, which shed surplus coccoliths into the surrounding medium, the internal process leading to the formation of these organic scales could represent a source of HMW NAld in our experiment. However, this hypothesis requires further experimental confirmation.

Influence of life cycle stage and bacterial activity on TEP dynamics

Accumulation of TEP during the stationary growth phase was probably caused by nutrient limitation which triggered the release of polysaccharides by algal cells and reduced the synthesis of hydrolytic enzymes by heterotrophic bacteria (cf. Engel *et al.*, 2004b). We compared the production of TEP between haploid and diploid, calcifying *E. huxleyi* cultures during the stationary growth phase and found a pronounced effect of life cycle stage on the composition of TEP. Cultures of haploid *E. huxleyi* cells produced at least 44% to 68% less cell-normalized TEPcolor than axenic and non-axenic calcifying cultures, respectively. Although we did not find any literature data on the TEPcolor production in haploid *E. huxleyi* cultures, Passow *et al.* (2002b) reported a value of 1 pg X eq. per cell during the stationary phase of a culture of non-calcifying diploid *E. huxleyi* cells. This is indeed a fraction of the range of TEPcolor concentration per cell for calcifying *E. huxleyi* cells (2.3 – 4.4 pg X eq. per cell) determined during mesocosm experiments by Engel *et al.* (2004b). Although our TEPcolor values are generally higher (table 4), the proportional difference between cell-normalized TEPcolor concentration of calcifying and non-calcifying cell cultures is similar to the aforementioned comparison. This difference in stainability of TEP per cell together with the high rhamnose and acidic sugar content, and the high molecular weight of coccolith polysaccharides (Fichtinger-Schepman *et al.*, 1979; Borman *et al.*, 1986) suggest that calcification may be an important source of TEP precursors (see below).

Interactions between algae and bacteria have been shown to influence the production and the aggregation of TEP, depending on the species and growth conditions (Grossart *et al.*,

2006a; Gärdes *et al.*, 2010; Bruckner *et al.*, 2011). We measured higher levels of TEP-C and TEPcolor in non-axenic compared to axenic calcifying *E. huxleyi* cultures (table 4), and a stronger decrease in the spectral slope of particle size distribution indicating enhanced TEP aggregation in the treatment with bacteria. Bacterial cells may alter the composition of TEP precursors by preferential consumption of certain components (Panagiotopoulos and Sempere, 2007), they can produce TEP themselves by excretion of capsular material (Stoderegger and Herndl, 1998; Passow, 2002b), or probably even influence the excretion of certain compounds by algal cells through as yet undetermined mechanisms (Gärdes *et al.*, 2010; Bruckner *et al.*, 2011). The differences in cell-normalized TEPcolor concentrations between the axenic and non-axenic cultures were too great to have been caused solely by the mere presence of bacterial cells. If we assume that the total bacterial biomass ($1.33\ 10^{9}$ cells l^{-1} x $20\ 10^{-15}$ g C $cell^{-1}$ = 2.22 µmol C l^{-1}) is TEP material, it would contribute only a minute fraction of the measured TEP pool (251 on 19823 µg X eq. l^{-1}). Although the slower nitrate consumption in the axenic cultures may have altered the exudation pattern compared to the non-axenic cultures, complete phosphate depletion led to very low inorganic N:P ratios in both cases. Therefore, we suggest that the changes in TEP composition and aggregation were caused by bacterial activity, through enhanced accumulation of polysaccharides in TCHO (table 5) and probable concentration increases in acidic polysaccharides precursors, ultimately stained in the determination of TEPcolor concentration.

Calcification as a source of extracellular particulate organic carbon?

An important part of newly fixed organic carbon in the labelled non-axenic calcifying *E. huxleyi* cultures was released into the surrounding culture medium and mainly retrieved in extracellular particulate material, while the percentage extracellular release of DOC stayed low during the stationary growth phase (table 9). Similar observations on the accumulation of extracellular particulate organic material have been made by Engel *et al.* (2004b) using cell-corrected TEP production. They concluded that the amount of organic carbon released by *E. huxleyi* in the form of polysaccharides can be very important to organic carbon cycling (Engel *et al.*, 2004a) and may even exceed POC production by cell growth under nutrient depleted conditions. Using a stable isotope probing, we showed that there is a tight coupling between the exudation of dissolved HMW NAld and the particulate carbon pool (table 7 and figs. 7 and 8). The increase in production rates of those sugars in HMW DOM (table 10)

together with the positive correlation between excess ^{13}C incorporated into PIC and HMW ΣNAld (from day 10 to 19: R = 0.77, n=9, $p<0.05$) suggests that coccolith polysaccharides may be the source of newly produced HMW DOM in our experiments. However, the negative correlation between PIC and ΣNAld production rates (from day 10 to 19: R = -0.81, n=9, $p<0.05$) during the progress of the stationary growth phase suggests a decoupling from the amount of carbon incorporated into calcite coccoliths and the production of dissolved HMW heteropolysaccharides. Bacterial consumption or, more likely, coagulation processes may have prevented accumulation of newly produced dissolved HMW NAld and thus may be responsible for this apparent decoupling. Moreover, low production rates and concentrations of dissolved organic carbon and HMW NAld compared to those estimated for extracellular POC suggests either direct release of particulate organic material, such as polysaccharides coating coccoliths (Godoi *et al.*, 2009), or very efficient coagulation of the released polysaccharides. The dry thickness of an organic coating on coccoliths of *E. huxleyi* cells ranged between 280 and 350 nm and could thus easily be retrieved in the particulate pool, due to its close association to coccoliths and its high aggregation potential (Godoi *et al.*, 2009). A data-assimilative modelling exercise by Schartau *et al.* (2007) indirectly determined that the vast majority of exuded carbon can become subject to coagulation and can thus be transformed into extracellular POC. Our findings corroborate this hypothesis. Moreover, results from two studies (de Jong *et al.*, 1979; Nanninga *et al.*, 1996) using non-calcifying diploid *E. huxleyi* strains further suggest that coccolith formation vesicles may play a role in the transfer of released polysaccharides from the dissolved to the particulate carbon pool. These studies observed the release of acidic polysaccharides, resembling the coccolith-associated macromolecule, by non-calcifying *E. huxleyi* cells in the dissolved phase of their cultures, using isotope labelling and immunochemical quantification. Labelling experiments using non-calcifying diploid mutant or differentially calcifying strains of *E. huxleyi* would allow further testing of this hypothesis.

Conclusions

Unbalanced growth caused an accumulation of carbon in non-calcifying haploid (S-cells), and calcifying axenic and non-axenic *E. huxleyi* batch cultures (C-cells), which was independent of biomass accumulation. The pattern of carbon accumulation into the different particulate -

POC, PIC, and TEP - and dissolved pools – mono-, and polysaccharides and HMW NAld – was influenced by the life cycle stage of *E. huxleyi* cells and bacterial activity in experimental cultures. Using stable isotope probing and PLFA biomarkers to allocate newly produced organic carbon to cellular biomass and to extracellular pools, we showed that extracellular POC production amounted to 51 % of organic carbon production allocated to algal cells at the start of the stationary growth phase of calcifying non-axenic *E. huxleyi* cultures.

Bacteria favoured the accumulation of polysaccharides and the formation of TEP containing high densities of stainable moieties, enhancing their aggregation in calcifying *E. huxleyi* cultures. Although bacterial activity in the calcifying cultures was low, probably caused by the low nutritional quality of available organic matter and by inorganic nutrient limitation, they preferentially assimilated newly produced organic matter and altered the composition of HMW NAld, at least at the beginning of the stationary growth phase. In the non-calcifying haploid cultures on the other hand, accumulation of dissolved carbohydrates and HMW NAld was enhanced while POC accumulation and the stainability of TEP was reduced compared to calcifying *E. huxleyi* cultures. In all three culture treatments, we observed a temporal change in the composition of HMW NAld, with a proportional increase of rha+ara.

Based on the similar NAld composition and the positive relation between newly produced PIC and HMW NAld we propose that the production of coccoliths is the main source of HMW NAld in our non-axenic calcifying *E. huxleyi* cultures. Moreover, calcification by *E. huxleyi* probably facilitates the transfer of released polysaccharides from the dissolved to the particulate pool, due to the acidic nature of coccolith polysaccharides, explaining the high levels of extracellular POC and TEPcolor.

Thus, extracellular release of organic carbon reached up to 76 % of total primary production during the stationary growth phase of *E. huxleyi*, and was retrieved for at least 97 % in the particulate pool. This process could have a significant impact on the efficiency of export production during coccolithophorid blooms in the ocean, especially in conjunction with nutrient-limited bacterial activity and biomineral ballasting of aggregates.

Acknowledgements

We are grateful to Prof. Jack Middelburg for fruitful discussions about the culturing experiments and to Prof. Steven Bouillon for letting us perform the $DO^{13}C$ analyses at his laboratory. We thank Ilse Daveloose who carried out the spectrophotometric determination of dissolved saccharides and Ann-Eline Debeer for helping with CN analyses at UGent. Thank you Caroline Souffreau and Aaike De Wever for helping out with the sampling of the cultures.

7

General Discussion

The edge of the European continental shelf in the NE Atlantic is characterised by annually recurrent, extensive phytoplankton blooms, which play a pivotal role in carbon cycling through photosynthetic fixation of inorganic carbon, but also through calcification and the formation of DMSP (Archer *et al.*, 2001; Joint *et al.*, 2001; Reisch *et al.*, 2011). In the northern Bay of Biscay, the study area of the PEACE project (see chapter 1), these blooms are generally characterised by a succession of diatoms to coccolithophores from early to late spring (Leblanc *et al.*, 2009). In late spring, when nutrient levels in the surface ocean are largely depleted, the blooms are initiated by intermittent nutrient injection in surface waters as a result of internal tide breaking at the shelf edge (Sharples *et al.*, 2009). It has been hypothesised that stratification of this water mass as it is advected onto the shelf, warming up along the way, then drive the wax and wane of these blooms (see chapter 1) (Suykens *et al.*, 2010; Harlay *et al.*, 2011). In the present study, we focused on these late spring, coccolithophore-dominated blooms.

In our study area stratification of the water column is thermally induced by the strength of surface heating by the sun (which is strongly seasonal) and the air temperature. A water mass is stratified when a body of less dense water sits above denser water. Stratification is a key control on shelf sea marine ecosystems, because the interface between the surface and deeper layers acts as an efficient barrier to the vertical exchange of water and any dissolved substance (e.g. nutrients, DOC) or passive particle (e.g. phytoplankton, TEP) in the water will be affected by this reduced capacity for transfer between the surface and deeper waters (Sharples *et al.*, 2010). Predictions for the end of this century suggest that thermal stratification will begin typically 1 week earlier than at present, and end 5 – 10 days later, and the strength of the stratification over the whole NW European shelf seas is projected to increase in response to changes in the seasonal heating cycle (Sharples *et al.*, 2010). Analyses of global trends in ocean primary productivity based on a remote sensing decadal ocean colour dataset have indicated an inverse linear relationship between phytoplankton productivity and stratification of the water column (Behrenfeld *et al.*, 2006). Such changes in the ocean carbon fixation would alter the magnitude and distribution of global ocean net air-

sea CO_2 exchange, fisheries yields, and dominant basin-scale biological regimes (Behrenfeld *et al.*, 2006, and references therein). Seawater temperature and nutrient concentration (N, P, Si, Fe) are the main environmental control factors that have been identified to influence the distribution of the functional phytoplankton groups (such as diatoms, coccolithophores, picocyanobacteria and N_2 fixers) considered by Boyd *et al.* (2010). Higher sea surface temperatures together with increased duration and strength of stratification may shift the relative temporal dominance of functional groups such as diatoms and coccolithophores in our study area by reducing the nutrient replenishment of surface waters by mixing with deeper, nutrient-rich water layers (see chapter 1, fig. 3). The change in community dominance between diatoms and coccolithophores can be attributed to their physiological differences. Diatoms are generally more successful in turbulent systems due to their ability to store excess nutrients into vacuoles (luxury uptake) which they can rely on to attain high growth rates for several generations, while denying other phytoplankton groups access to the limiting nutrients (Tozzi *et al.*, 2004; Cermeño *et al.*, 2011). In contrast, coccolithophores are better adapted to nutrient-depleted waters, due to their lower half-saturation constants for nutrient uptake and small intracellular quotas (Tozzi *et al.*, 2004; Cermeño *et al.*, 2011). In concert with the phytoplankton community, the structure of surface heterotrophic bacterial communities, which ultimately depend on primary production for organic matter supply, have been shown to change seasonally concurrent with seasonal mixing, surface warming, and stratification (Treusch *et al.*, 2009).

In order to predict how future changes in global atmospheric CO_2 concentrations and temperature will affect the role coccolithophore blooms play in biological carbon cycling in the world's oceans, we need to obtain a better understanding of the factors driving their occurrence, composition and production, and how interactions with other components of the microbial food web, such as bacteria and microzooplankton, affect their impact on biogeochemical cycles (Fuhrman, 2009; Boyd *et al.*, 2010). However, to date surprisingly little information is available on the dynamics of phytoplankton groups and bacteria associated with coccolithophore blooms, and how bacterial activity, cell lysis and microzooplankton grazing affect their functioning (Lampert *et al.*, 2002; Olson and Strom, 2002; Riemann and Middelboe, 2002). In addition, little is known on how interactions between bacteria and *E. huxleyi* affect organic carbon production and export. This

information is needed, as the importance of the structure of the phytoplankton community to the functioning of the biological pump is still poorly understood (Smythe-Wright *et al.*, 2010, and references therein); changes in the community composition (such as diatoms versus coccolithophores) are expected to impact primary and export production, and as such food web structure and dynamics, as well the biogeochemical cycling of carbon and bio-limiting elements in the sea (Guidi *et al.*, 2009; Riebesell *et al.*, 2009; Finkel *et al.*, 2010).

In this study, we used a combination of *in situ* biological and biogeochemical studies and onboard and laboratory experiments to (1) document the diversity and dynamics of the phytoplankton and bacterial communities associated with blooms of *E. huxleyi*, the most important coccolithophore in our study area, and identify the main abiotic and biotic environmental processes and factors structuring these communities; (2) assess the importance of cell lysis and microzooplankton grazing for phytoplankton loss processes; (3) assess the impact of bacteria on the nature and the production of carbohydrates and TEP during haploid and diploid *E. huxleyi* blooms.

In the framework of the PEACE project, three consecutive oceanographic campaigns were carried out along the continental margin of the northern Bay of Biscay during late spring of 2006, 2007 and 2008. A suite of physical (e.g. temperature and water column stratification) and biogeochemical variables (e.g. inorganic nutrients, TEP, and DMSP) were measured on 34 separate occasions in order to relate them to changes in phytoplankton and bacterial community structure. Microzooplankton grazing mortality and cell lysis rates were measured onboard using dilution experiments and the esterase activity method at a selection of stations, and were related to the cycling of DMSP in relation to bloom development. In order to assess the effect of bacterial activity and *E. huxleyi* life cycle stages on the dynamics and composition of carbohydrates and TEP during the stationary growth phase, we performed culture experiments (contrasting axenic and non-axenic treatments) using an *E. huxleyi* strain (RCC1266) isolated during the 2007 campaign. In the non-axenic calcifying *E. huxleyi* culture treatment, we used an isotope labelling approach to track the fate of newly fixed carbon in the cellular and extracellular pools, using compound specific isotope analysis of dissolved carbohydrates and phospholipid-derived fatty acids, a proxy for cellular biomass.

Late spring coccolithophorid blooms are characterized by complex phytoplankton dynamics

Rather surprisingly, only few studies have described the structure and the spatial and temporal dynamics of phytoplankton communities during coccolithophore blooms along the western European continental margin (Head *et al.*, 1998; Joint *et al.*, 2001; Lampert *et al.*, 2002). In chapter 2 we described these dynamics for the main phytoplankton groups (using CHEMTAX analysis of HPLC pigment signatures) in relation to biogeochemical and physical variables. Chla standing stocks varied substantially in space and time, both between and during the campaigns (63.8 ± 26.5, 27.9 ± 8.4 and 41.3 ± 21.8 mg Chla m^{-2} in June 2006, May 2007 and May 2008 respectively), probably owing to enhanced mixing of the water column at the slope stations compared to the shelf stations, and to different weather conditions (wind and irradiance) and sea surface temperature during and between campaigns. Although coccolithophores, mainly *E. huxleyi*, and diatoms were the dominant phytoplankton groups (up to 72% and 89% of the total Chla respectively), prasinophytes, dinoflagellates, and chrysophytes often co-occurred during the blooms. Diatom biomass fluctuated independently of the other groups. As evidenced by diatom blooms forming on top of deeper coccolith patches, diatom and coccolithophorid bloom domination could alternate in late spring, and were attributed to changes in nutrient stoichiometry (N:P and dSi:N). Our results are in general agreement with other studies investigating the conditions conducive to coccolithophore bloom development, such as low dSi:N ratio, shallow mixed layer depth, and increased irradiances (Brown and Yoder, 1994; Painter *et al.*, 2010b). The mostly depleted PO_4 levels during our campaigns probably favoured the growth of nanophytoplankton such as *E. huxleyi*. Several studies have indeed shown that this species has an unusually high affinity for PO_4 and has the ability to take up dissolved organic phosphorus as well, using alkaline phosphatase (Palenik and Henson, 1997; Riegman *et al.*, 2000; Benner and Passow, 2010). Diatom blooms observed during our campaigns did not reach the high biomass levels of the main spring diatom bloom in April, probably owing to dSi and NOx depletion following the April blooms. The low surface NOx levels at many stations may explain the presence of diatom species which harbour diazotrophic symbionts, such as *Rhizosolenia* spp. and *Chaetoceros* spp. (Gomez *et al.*, 2005; Bar Zeev *et al.*, 2008), in which case their growth would have been limited by low PO_4 and dSi concentrations rather than NOx. Thus, our data shows that on the one hand late spring phytoplankton communities in this area are complex and diverse, and on the other hand that the generally

accepted diatom-to-coccolithophore succession scenario (Joint *et al.*, 1986; Leblanc *et al.*, 2009) is too simplistic, and that diatom and coccolithophore growth can alternate in the same area in response to changing nutrient ratios through vertical mixing (this study), horizontal movements of water masses (Smythe-Wright et al. 2010) and differential nutrient depletion by specific phytoplankton groups. Moreover, biomass of the phytoplankton groups during the sampling period was not linearly related to water column stratification, but, at least in the case of coccolithophores and diatoms, displayed a unimodal-like relation with this parameter: highest biomass values were encountered at intermediate stratification, consistent with the conceptual frame for phytoplankton bloom development and decline at the continental margin proposed by Harlay *et al.* (2011) for 2006.

Bacterial succession: the phytoplankton connection

Seasonal sea surface warming and thermocline development have been shown to impact both phytoplankton bloom succession and bacterial community composition (Fuhrman *et al.*, 2006; Treusch *et al.*, 2009; Behrenfeld, 2010), while changes in bacterial community structure and activity of their members has also been shown to occur on shorter timescales in response to phytoplankton blooms (Fandino *et al.*, 2001; Alderkamp *et al.*, 2006; Lamy *et al.*, 2009).

Although the variation in bacterial community structure during the different campaigns could be related to multiple, sometimes intercorrelated variables such as nutrient and TEP concentration, anomaly of total alkalinity (reflecting the calcification/dissolution history of a water mass), temperature, phytoplankton bloom composition and intensity, or the distance of stations to the continental slope, water column stratification could be used as a unifying proxy for describing the turnover in bacterial communities in our study area (chapter 4). Moreover, the same bacterial phylotypes were present each year even though bacterial community structure was variable between different stations (chapter 3). These findings corroborate the existence of distinct ecological niche spaces for bacteria (Pommier *et al.*, 2007; Gilbert *et al.*, 2010), and substantiate the notion of certain predictability of bacterial assemblages (Fuhrman *et al.*, 2006), in the same way as size structure and succession patterns of phytoplankton functional groups can be related to particular environmental settings (Margalef, 1978; Hood *et al.*, 2006; Leblanc *et al.*, 2009). If we assume that these environmental settings indeed reflect the developmental stages of phytoplankton blooms,

as described by the unimodal relation between phytoplankton group biomass and stratification (chapter 2), the change in bacterial community structure may be considered to mirror the succession of dominant phytoplankton species during bloom progression.

Close interactions between phytoplankton and bacterial species are known to influence bacterial community composition (Grossart *et al.*, 2005; Hasegawa *et al.*, 2007; Sapp *et al.*, 2007b). However, the importance of specific interactions in the field are often difficult to disentangle because physicochemical factors structuring the bacterioplankton community are the same as, or correlate with those that shape the phytoplankton assemblage. We used ordination methods and variation partitioning of physical (e.g. water column stratification), biogeochemical (e.g. nutrients and transparent exopolymer particles (TEP), anomaly of total alkalinity) and phytoplankton variables (chemotaxonomic groups) to untangle their respective influences on bacterial community structure (chapter 4). The structure of the multi-annual bacterial communities was significantly correlated to the abundance of specific phytoplankton groups (diatoms, coccolithophores, prasinophytes, dinoflagellates, and cryptophytes), which uniquely explained 4.3% and 7.4% of the total variation in the FL and PA community structure (i.e. after partialing out the effect of the other variables). This overall moderate influence of phytoplankton on the bacterial community structure may be due to the high degree of intercorrelation with environmental, spatial and temporal factors overlapping with phytoplankton distribution, water mass biogeochemical history and trophic interactions, which obscured the often tight bacteria-phytoplankton species associations observed in experimental settings.

Interestingly, we found that bacterial genera active during our culture experiments, displayed a close match with *Marinobacter* (EF150753), *Alteromonas* (HQ836407), *Rhodospirillales* (JF292454) and *Sulfitobacter* (HQ908665) and were also represented in independent *E. huxleyi* culture experiments performed by C. De Bodt (De Bodt, 2010). Some of these genera were also repesented *in situ* in coccolithophorid blooms during our oceanographic campaigns (e.g. *Alteromonadales* EU394576, *Rhodospirillales* EU394547, see table 2 chapter 3). This observation supports the notion of highly specific associations and commensalistic interactions between specific bacteria and coccolithophores like those described by Amin *et al.* (2009).

Community composition of FL and PA bacteria: two sides of the same coin

Despite their key role in biogeochemical cycling and carbon export, very little is known about the composition and dynamics of bacterial communities associated with diatom and coccolithophore-dominated phytoplankton blooms, especially in the Bay of Biscay. Bacterial communities are often operationally differentiated on the basis of their free-living (FL, planktonic) or particle-associated (PA, sessile) growth form, which can have distinct compositions (Simon *et al.*, 2002; Hodges *et al.*, 2005). These differences are also reflected in the production of different ectoenzymes and the higher metabolic activity of PA communities compared to FL ones (Martinez *et al.*, 1996; Fandino *et al.*, 2001; Grossart *et al.*, 2007b), which can affect the efficiency of the microbial loop and export production. In chapter 3, we performed detailed PCR-based DGGE fingerprinting analyses of FL and PA bacterial communities in the upper 150 m of the water column in the study area for the three campaign years. Bacterial phylotypes were identified by sequencing of partial 16S rDNA (DGGE bands) and near complete 16S rDNA (clone libraries). Bacterial communities were dominated by *Gammaproteobacteria* and *Bacteroidetes*, and also by *Alphaproteobacteria*. Members of the *Flavobacteriaceae*, *Polaribacter* sp., and *Pseudoalteromonas* sp. were typical representatives of the PA communities, while phylotypes belonging to the *Rhodobacteriaceae*, the SAR11 group and the *Gammaproteobacteria* characterised the FL community. Nevertheless, ordination and non-parametric permutational analyses revealed a considerable overlap in the composition of both communities despite differences in community structure. These results are in line with the findings of other studies (Hollibaugh *et al.*, 2000; Ghiglione *et al.*, 2009), suggesting a continuum in lifestyles or phenotypic transitions between them (Malfatti and Azam, 2009; Slightom and Buchan, 2009; Grossart, 2010). Using variation partitioning analyses of the upper mixed layer samples (chapter 4), we found that variation in the FL and PA community structure during the whole study period was largely related to same spatial, temporal, environmental and phytoplankton variables which together explained 43.8% and 37.7% of variation in the FL and PA fractions respectively (with 16.8% and 13.5% overlap between all variables). However, the total amount of variation in bacterial community structure explained by these variables differed greatly between campaigns, possibly reflecting non-linear bottom-up or top-down controls which were not taken into account. Also, we found that the proportion of explained variation in community structure during each campaign was

consistently lower for PA than for FL bacteria, and differed more than threefold between and also within years, suggesting that some factors differentially regulate both communities.

Although we observed only a moderate depth gradient in community structure, the PA bacterial community showed a more pronounced depth gradient (surface - 150 m) compared to the FL community, suggesting more frequent exchange between surface and deeper water layers in the latter. In addition, turbulent mixing at the stations located on the shelf edge caused a stronger exchange between FL bacterial communities from the deeper and the surface water layers compared to stations located over the shelf. Using a simple prokaryotic metacommunity model in which two generalist ecotypes compete for two resources (POC and DOC), Miki and co-workers (2009) have shown that vertical mixing leads to net upward flux of the POC ecotype to the surface layer. This exchange would accelerate the shifts in the community composition during the phytoplankton bloom, contributing to a higher efficiency in POC remineralisation at the surface layer and reducing the carbon flux to the deep layer. In this respect, turbulent mixing at the shelf edge could "seed" the surface layer with PA bacterial community members and accelerate the response of the bacterial community to OM input, although this would need further *in situ* testing.

Cell lysis and microzooplankton grazing regulate phytoplankton growth and influence DMSP cycling during coccolithophorid blooms

Phytoplankton cell lysis has been shown to constitute an important loss factor contributing to the decline of phytoplankton and coccolithophorid blooms (Brussaard *et al.*, 1995; Bratbak *et al.*, 1996), releasing labile dissolved organic carbon (DOC) into the water column (Berges and Falkowski, 1998; Agusti and Duarte, 2000; Riegman and Winter, 2003) and as such influencing the biological carbon pump in terms of export production. To our knowledge, our cell lysis rate measurements using the esterase activity method are the first of its kind for coccolithophorid blooms (chapter 5). Our results suggest that cell lysis can indeed be an important loss factor for phytoplankton in the northern Bay of Biscay, with lysis rates ranging from 0.04 d^{-1} to 1.96 d^{-1}. We complemented these measurements with estimates for phytoplankton growth and mortality rates using the seawater dilution method combined with HPLC pigments analysis. Average nutrient-corrected growth and mortality rates for total phytoplankton biomass (Chla) were respectively 0.97 ± 0.50 d^{-1} and 0.76 ± 0.49 d^{-1}, with rates amounting to 1.08 ± 0.73 d^{-1} and 0.88 ± 0.70 d^{-1} for coccolithophores and

0.98 ± 0.65 d^{-1} and 0.89 ± 0.61 d^{-1} for diatoms. The high positive correlation between growth and mortality rates suggests a strong coupling between phytoplankton production and loss processes. High coccolithophore mortality rates were sometimes independent of high lysis rates indicating that microzooplankton grazing can act as an independent source of group-specific phytoplankton loss in this region. However, diatom grazing mortality co-occurred with cell lysis in our study.

We found a positive relationship between the dissolved to particulate DMSP ratio and cell lysis rates, indicating cell lysis influenced the release of dissolved DMSP, an important intermediate compound of the climatically active volatile compound DMS (Stefels *et al.*, 2007; Seymour *et al.*, 2010) and a substrate for bacterial growth (Vila *et al.*, 2004; Neufeld *et al.*, 2008; Reisch *et al.*, 2011). Dimethylsulphoniopropionate (DMSP) accounts for up to 10% of carbon fixed by marine phytoplankton in ocean surface waters (Archer *et al.*, 2002; Simó *et al.*, 2002), 80% to 90% of which is processed by marine bacteria through the demethylation/demethiolation pathway. This pathway produces methanethiol instead of DMS, which enables them to assimilate this reduced sulphur directly into methionine (Kiene *et al.*, 2000; Reisch *et al.*, 2011). The gene that encodes for the key DMSP demethylating enzyme, dmdA, was only recently discovered in the genomes of *Silicibacter pomeroyi* and *Candidatus Pelagibacter ubique*, and it appears to be prevalent in members of the numerically important *Roseobacter* and SAR11 clades and recently also reported in members of the *Flavobacteriaceae* group (Sievert *et al.*, 2007; Howard *et al.*, 2011). During our campaigns we found that the abundance of specific phylotypes related to an unclassified Gammaproteobacteria (Gam_4) and the *Polaribacter* genus (Flavo_5) showed a positive correlation with DMSPd (see chapter 4). Together with the positive correlation between coccolithophore biomass and DMSPp levels, these results underscore the importance of coccolithophore blooms and role of bacteria in oceanic cycling of DMSP.

Bacterial activity and coccolith production enhance TEP formation

Whereas exudation of DOM by phytoplankton has been considered to divert primary production from contributing to the vertical flux of particle in the ocean, polysaccharide aggregation constitutes an effective pathway to channel dissolved matter into the particulate pool which is more efficiently exported to depth (Engel *et al.*, 2004a). To assess the influence of bacterial activity and life cycle stage of *E. huxleyi* on the dynamics of

dissolved carbohydrates and TEP we measured their production and composition during the stationary growth phase of *E. huxleyi* batch cultures, reflecting the nutrient-limited conditions during later stages of algal blooms (chapter 6 and 2). Unbalanced growth during our culture experiments caused an accumulation of carbon in non-calcifying haploid, and diploid calcifying axenic and non-axenic *E. huxleyi* cultures, independent of biomass accumulation. We found a marked build-up of extracellular POC in calcifying *E. huxleyi* cultures, while there was a more pronounced accumulation of dissolved carbohydrates in the haploid *E. huxleyi* cultures. Bacteria stimulated the accumulation of polysaccharides and the formation of TEP containing high densities of stainable moieties, enhancing their aggregation in calcifying *E. huxleyi* cultures. Indeed, in other studies bacterial activity has been shown to influence both the composition and the concentration of dissolved carbohydrates and TEP through degradation and production processes and through ecological interactions with algal cells mediated by chemical factors such as extracellular polymeric substances and amino acid monomers (Stoderegger and Herndl, 1998; Grossart and Simon, 2007; Gärdes *et al.*, 2010; Rochelle-Newall *et al.*, 2010; Bruckner *et al.*, 2011).

Using a pulse of isotopically labelled bicarbonate (^{13}C) we traced the fate of photosynthetically fixed carbon into algal and bacterial biomass (PLFA biomarkers) and into neutral aldoses (NAld) (LC/IRMS) in non-axenic diploid calcifying cultures. We found that an important part of newly fixed organic carbon in these cultures was released into the surrounding culture medium and mainly retrieved in extracellular particulate carbon (such as TEP). Similar observations on the accumulation of extracellular particulate organic material have been made by Engel *et al.* (2004b), based on measurements of cell-corrected TEP production, while high TEP concentration were measured in stratified, coccolithophore-rich surface waters during our 2006 field campaign (chapter 2). Moreover, based on the similar NAld composition between coccolith polysaccharides reported in literature and the HMW DOM in our experiments, and the positive relation between newly produced PIC and HMW NAld we propose that the production of coccoliths is the main source of HMW NAld in our non-axenic, calcifying cultures. In addition, calcification probably facilitates the transfer of released polysaccharides from the dissolved to the particulate pool, due to the acidic nature of coccoliths polysaccharides, explaining the high levels of extracellular POC and TEP. Thus, extracellular release of carbon in the dissolved as well as the particulate phase during the

stationary growth phase of *E. huxleyi* forms an important part (up to 76%) of its primary production in the stationary growth phase. This has also been suggested by Harlay *et al.* (2011) and Suykens *et al.* (2010) by pointing out the importance of extracellular production in sustaining the bacterial carbon demand in the photic and aphotic layers and in impacting the fluxes of dissolved inorganic carbon in coccolithophorid blooms.

Terminus tout le monde descend

Once phytoplankton blooms, concentrated in the shallow mixed layer of a highly stratified water mass over the shelf, have depleted nutrients, it is the end of the line. As shown in chapter 5, cell lysis rates tended to increase with increasing water column stratification, suggesting a convergence of bottom-up (by nutrient limitation) and cell density dependent top-down control (e.g. viral lysis) on further phytoplankton biomass accumulation in more stratified conditions. Virally induced coccolithophorid bloom termination has already been documented several times (Castberg *et al.*, 2001; Jacquet *et al.*, 2002), although we could not confirm the cause of cell lysis during our studies. High cell lysis rates measured at stratified stations located in remote sensing high reflectance patches where high densities of coccoliths and together with *E. huxleyi* coccospheres were detected (see also fig. 3d in chapter 2) corroborate the scenario of bloom termination by viral infection during the declining phase of the bloom. The lack of linear relationship between cell lysis rate and stratification degree in 2006 however may be explained by the unimodal and plurispecific nature of phytoplankton bloom development, as we suggested in chapter 2. These late bloom, stratified water conditions also harboured a particular bacterial community structure, where e.g. the relative abundance of a specific phylotype in the PA community, affiliated to the genus *Pseudoalteromonas* (PsAlt_2), was related to higher dinoflagellate abundance and TA anomaly, characteristic of low turbulence water masses where calcification had occurred and that had not recently been mixed (see chapter 1 fig. 3 and chapter 4 fig. 2). Furthermore, the relative abundance of several phylotypes affiliated to the *Rhodobacteraceae* (Rhodo), the SAR11 (Pelagi) and the SAR86 cluster (SAR86_4), and to the *Flavobacteriaceae* (Flavo_3), were positively related to the concentration of TEP, which was typically high in nutrient-depleted, coccolithophore-rich water masses (chapter 2). Thus, on the one hand high mortality rates caused by virally induced cell lysis could stimulate the functioning of the microbial loop by releasing labile DOM, which is incorporated into

bacterial biomass, and on the other hand, enhanced formation of sticky TEP and extracellular POC by bacterial activity and coccolith production (chapter 6) could facilitate the disappearance of the bloom and enhance the production export through aggregation and ballasting mechanisms (De La Rocha and Passow, 2007). As such, carbon export efficiency is not only affected by the cell size distribution but also by the structure and composition of bacterial and phytoplankton communities, as well as by biotic interactions.

Future Perspectives

The continental margin along the northern Bay of Biscay, where field campaigns described in this work were conducted (chapters 2, 3, 4, and 5), combine high spatial variability in hydrography, community composition, water column mixing and water mass advection. Therefore, observations at fixed locations, like the Eulerian approach adopted during the campaigns, can be confounded by decoupled temporal scales of processes relevant for community composition or by spatial heterogeneity in water masses and communities. While the rationale of reconstructing bloom sequence using a water column stratification index was, to some extent, successful for biogeochemical data (Suykens *et al.*, 2010; Harlay *et al.*, 2011) including bacterial (chapter 4) and phytoplanktonic community structure and dynamics, the latter of which showed a more unimodal relationship to the stratification index (chapter 2), using a Langrangian or drifter approach with drifting sediment traps would allow a more accurate direct evaluation of the bloom sequence and the export fluxes of particulate matter.

It is clear that our understanding of the microbial community dynamics, processes, interactions and their role in the functioning of biogeochemical cycles is still very limited. One of the key questions that need to be addressed is the elucidation of the role of specific microorganisms concerning specific biogeochemical functions and determination of the regulatory factors of those organisms (Höfle *et al.*, 2008). Our approach involved the use of DNA-based community fingerprinting complemented with clone libraries and pigment-based chemotaxonomy to identify the most prominent members of the bacterial community and the abundance of the phytoplankton groups, respectively. These techniques are suitable for analysis of many samples in parallel and even allow direct identification of the community members in temporally and spatially diverse samples, but they typically lack phylogenetic depth and resolution. Also, we used an indirect, inferential approach using correlations

between the occurrence of bacterial phylotypes, phytoplankton, and environmental variables to elucidate the link between community structure and ecological function. While we identified the most abundant members of the community, ideally we would only target the most active part of the community, which does not always match with the community members contributing most to the rDNA pool (cf. Moeseneder *et al.* (2001), but see Lami *et al.* (2009)).

A potential improvement to our approach would be to use rRNA-based community fingerprinting methods, targeting the most active part of the community. Also, we could specifically assess the dynamics of specific genes encoding for e.g. hydrolytic enzymes involved in the degradation of polymeric carbon sources (such as TEP precursors) (Bauer *et al.*, 2006) together with the abundance of a particular bacterial group (e.g. *Flavobacteria*) and couple their occurrence to respiration and aggregation processes. Moreover, thanks to the recent development of increasingly powerful and cheaper next generation sequencing techniques (e.g. pyrosequencing and Illumina sequencing), microbial oceanography has entered into the genomic era. This allows massive sequencing of not only particular genes (relating to identity or function) but also of whole genomes or metagenomes, as they are called when this DNA is retrieved from environmental community samples. This "meta-approach" diversified beyond the mere collection of DNA fragments constituting genes, to several "omics" research areas such as metatranscriptomics, metaproteomics, and metametabolomics. Already, the first studies using combinations of these meta-omics approaches are yielding promising insights into the relation between the diversity and functional potential of ecosystems (Gilbert *et al.*, 2010). Ideally, we would want to link microbial diversity, which can be seen as taxonomic entities responsive to environmental change and carrying out biogeochemical functions, to its metabolic capacity.

Another recent development includes the use of stable isotope probing (SIP) (Wagner *et al.*, 2006) and multiple-isotope imaging mass spectrometry (MIMS), a new generation of secondary ion mass spectrometry (SIMS) (Ploug *et al.*, 2010), to study structure-function relationships in microbial communities. In this work we used a form of SIP by analysing the amount of isotopic label (^{13}C) incorporated into the bacterial and algal biomass through PLFA extraction (Boschker and Middelburg, 2002) (see chapter 6). This approach has a high sensitivity but is constrained by the low phylogenetic resolution associated with the

composition of the PLFA pool. Another SIP approach is to retrieve the isotopic label from DNA or RNA which have much higher phylogenetic resolution. However, using SIP technology in oligotrophic pelagic environments is still considered to be difficult, because the needed substrate concentrations and incubation times may change the *in situ* processes and bacterial community too much (Höfle *et al.*, 2008). For a review of the methods available to microbial ecologists for linking environmental processes to microbial taxa we refer to Gutierrez-Zamora and Manefield (2010).

It important to emphasize that the previous paragraphs need not to be restricted to the Prokaryote realm and that these techniques are also largely applicable to the protists, unicellular Eukaryotes. Indeed, there is increasing evidence that this group, comprising phytoplankton and heterothrophic nanoflagellates, is taxonomically and functionally very diverse (Cuvelier *et al.*, 2010; Worden and Allen, 2010). In this work (chapter 2) we used a crude approach to partition the photosynthetic biomass (Chla) between the different dominant phytoplankton groups (including cyanobacteria). Ideally, we would like to know which taxa actually contribute to the fixation of inorganic carbon, as certain groups may influence the biogeochemical cycles differently than others (cf. Si cycling by diatoms and $CaCO_3$ by coccolithophores). Combinations of the above techniques or *in situ* (i.e. by means of incubations) application of PLFA-based SIP together with Chla-partitioning would allow group-specific primary production measurements (Dijkman and Kromkamp, 2006; de Kluijver *et al.*, 2010), which could help assigning elemental fluxes to particular taxa.

Major uncertainties exist as to which phytoplankton will either benefit or lose out from climate change, and the phenotypic plasticity and genetic diversity of algal populations may become important factors to consider (Boyd *et al.*, 2010). We currently don't know how phytoplankton groups or particular strains will acclimatise and subsequently adapt to future altered ocean conditions (Langer *et al.*, 2009). Not only are coccolithophorid blooms not monospecific (see chapter 2), which can strongly affect ecosystem functioning due to inter- and intraspecific variability in ecology and ecophysiology (e.g. calcification – (Langer *et al.*, 2009) and N-metabolism – (Strom and Bright, 2009)), but what we consider to be 'species' are often species complexes, hiding considerable morphological, genetic and ecophysiological variation (the so-called (semi)cryptic species problem, which has also been reported for *E. huxleyi* (cf. Medlin *et al.*, 1996; Iglesias-Rodriguez *et al.*, 2002a)). In addition,

as recent evidence suggests, populations of single cryptic phytoplankton entities within communities are also characterized by high genetic diversity (Iglesias-Rodriguez *et al.*, 2006; Casteleyn *et al.*, 2009; Casteleyn *et al.*, 2010), even during bloom events that were hitherto considered to be largely the result of clonal growth. The population genetic and community structure of phytoplankton will therefore determine how populations and communities will react to climate change phenomena. It would thus be relevant to determine the population structure of *in situ* blooms or in climate change (e.g. pCO_2 and T) experiments using multiple species or strains in combination with population genetic techniques (e.g. microsatellite analysis, cf. Iglesias-Rodriguez *et al.* (2006), and/or variations in the GPA gene, (Martinez *et al.*, 2007)). Moreover, there is still a great lack of knowledge about the ecophysiology of the haploid life cycle stage of *E. huxleyi*, or about the occurrence and role of the haploid phase during and between blooms. These motile, noncalcifying cells are likely to have a different ecological niche than their diploid counterparts (Houdan *et al.*, 2006; von Dassow *et al.*, 2009) and are probably going to be affected differently by environmental change (Fiorini *et al.*, subm.).

8

Summary

Marine microbial organisms are the main drivers of globally important processes such as the marine carbon and sulphur biogeochemical cycles. Thus, a better knowledge of the functioning of microbial communities, their diversity and distribution, their interactions, and the factors controlling them is needed if we want to address how global changes in temperature and ocean acidification will affect ecosystem functioning in the future. The composition of bacterial and phytoplankton communities during phytoplankton blooms, and their interactions, are important properties of the microbial food web, which can potentially have a strong impact on the fate of organic matter and hence carbon cycling in the world's oceans. However, to date, little is known about the environmental factors (both abiotic and biotic) which drive the spatial heterogeneity and temporal fluctuations of microbiota in phytoplankton blooms, and how these patterns are related to organic matter production by these blooms.

The main aim of this thesis is to contribute to a better knowledge of the composition and dynamics of bacterial and phytoplankton assemblages in relation to the abiotic and biotic environment during blooms of coccolithophores. In addition, we aim at gaining a better insight into the role of these organisms in the carbon cycle through a better understanding of phytoplankton loss factors (such as microzooplankton grazing and cell lysis) and the impact of bacterial communities on the release and composition of organic matter by the coccolithophore *Emiliania huxleyi*.

During three oceanographic campaigns (2006-2008) along the NE Atlantic continental margin in the northern Bay of Biscay, we studied relationship between the composition and dynamics of phytoplankton and bacterioplankton communities during late spring phytoplankton blooms and the prevailing physicochemical and biotic constraints. These *in situ* studies were complemented by with laboratory experiments using an *E. huxleyi* strain and natural bacterial communities isolated during our campaigns, in order to investigate the influence of bacteria on the release and composition of carbohydrates by *E. huxleyi* and the formation of TEP.

In **chapter 2** we described the spatial and temporal dynamics of the main phytoplankton groups in relation to biogeochemical and physical variables. Our study area is characterised by important spring phytoplankton blooms that often initiate along the steep continental slope, where deeper nutrient-rich water is intermittently injected due to breaking of internal tidal waves at the shelf edge. These phytoplankton blooms can then be advected onto the shelf, where they find themselves in increasingly stratified waters. During our oceanographic campaigns (2006-2008) we found that Chla standing stocks varied substantially in space and time, both between and during the campaigns, probably owing to enhanced mixing of the water column at the slope stations compared to the shelf stations, and to different weather conditions (wind and irradiance) and sea surface temperature. Diatoms and coccolithophores generally dominated the phytoplankton blooms, but prasinophytes, dinoflagellates, and chrysophytes often co-occurred during coccolithophorid blooms. Moreover, diatom biomass fluctuated independently of the other groups. Alternation of diatom and coccolithophorid blooms were attributed to changes in nutrient stoichiometry (N:P and dSi:N). Our results are in general agreement with other studies investigating the conditions conducive to coccolithophore bloom development, such as low dSi:N ratio, shallow mixed layer depth, and increased irradiances. In contrast to the generally accepted phytoplankton bloom succession scenario, we found that diatom blooms (albeit less intense than the main spring bloom ones) could succeed coccolithophorid blooms in late spring. Moreover, coccolithophore and diatom biomass displayed a unimodal-like relationship with the degree of water column stratification, with highest biomass values are encountered at intermediate stratification, consistent with the conceptual frame for phytoplankton bloom development and decline at the continental margin. During conditions of high stratification we measured the highest concentration of TEP, associated to coccolithophorid blooms that probably had reached the stationary growth phase.

Despite their key role in biogeochemical cycling and carbon export, very little is known about the composition and dynamics of bacterial communities associated with diatom and coccolithophore-dominated phytoplankton blooms in the Bay of Biscay. Bacterial communities are often operationally differentiated on the basis of their free-living (FL, planktonic) or particle-associated (PA, sessile) growth form, which can have distinct compositions, and different ectoenzyme production rates which affect the efficiency of the

microbial loop and export production. In order to link the bacterial community structure with their ecological function and to describe the natural history of these microbes, we used an indirect approach by examining the statistical relationships among organisms and environmental parameters, as addressed in **chapters 3 and 4**. To this end we used rRNA-based whole community molecular profiling technique (DGGE), to rapidly characterise the microbial community composition and the overall diversity of a large number of samples, together with multivariate analysis to better identify patterns in the bacterial community.

Bacterial communities were dominated by *Gammaproteobacteria* and *Bacteroidetes*, and to a lesser degree also by *Alphaproteobacteria*. Members of the *Flavobacteriaceae*, *Polaribacter* sp., and *Pseudoalteromonas* sp. were typical representatives of the PA communities, while phylotypes belonging to the *Rhodobacteriaceae*, the SAR11 group and the *Gammaproteobacteria* characterised the FL community. Nevertheless, we found a considerable overlap in the composition of both communities. These results suggest a continuum in lifestyles or phenotypic transitions between them. Interestingly, the same bacterial phylotypes were present each year even though bacterial community structure was variable between different stations, as described in **chapter 3**. Furthermore, we observed only a moderate depth gradient in community structure, and the PA bacterial communities showed a more pronounced depth zonation (surface-150 m) compared to the FL communities, suggesting more frequent exchange between surface and deeper water layers in the latter.

In **chapter 4**, we used ordination methods and variation partitioning to relate bacterial community structure to changes in physical (e.g. water column stratification), biogeochemical (e.g. nutrients and TEP, anomaly of total alkalinity), and phytoplankton variables (chemotaxonomic groups). The proportion of explained variation in community structure during each campaign was consistently lower for PA compared to FL bacteria and differed more than threefold between years and also within years, suggesting that different factors regulate both communities. Although the variation in bacterial community structure during the different campaigns could be related to multiple, sometimes intercorrelated variables such as the concentration of nutrients, TEP, anomaly of the total alkalinity (reflecting the calcification/dissolution history of a water mass), water temperature, phytoplankton bloom composition and intensity, or the distance of stations to the

continental slope, we found that water column stratification could be taken as a unifying proxy for describing the turnover in bacterial communities in our study area.

The structure of the multi-annual communities was significantly correlated to the abundance of phytoplankton groups (diatoms, coccolithophores, prasinophytes, dinoflagellates, and cryptophytes). Interestingly, we found that bacterial genera repesented during our oceanographic campaigns were also active during our culture experiments, supporting the notion of highly specific associations and commensalistic interactions between phytoplankton and bacteria.

The findings in **chapter 3 and 4** corroborate the existence of ecological niche space for bacteria, and substantiate the notion of certain predictability of bacterial assemblages the same way size structure and succession patterns of phytoplankton functional groups can be related to particular environmental settings.

Phytoplankton growth is often under tight control of microzooplankton grazing and viral cell lysis, two important loss processes that regulate the formation and termination of phytoplankton blooms, and important parameters of the biological carbon pump in terms of export production. In **chapter 5** we provide the first estimates of cell lysis rates, using the esterase activity method, during coccolithophorid blooms. Our results suggest that cell lysis can indeed be an important loss factor for phytoplankton in the northern Bay of Biscay. We complemented these measurements with estimates for phytoplankton growth and mortality rates using the seawater dilution method combined with HPLC pigments analysis, which indicated that high phytoplankton mortality rates were sometimes independent of high cell lysis rates pointing at microzooplankton grazing as another key source of phytoplankton group-specific loss. Both processes tended to increase with increasing water column stratification, suggesting a convergence of bottom-up (by nutrient limitation) and cell density dependent top-down control (e.g. viral lysis) on further phytoplankton biomass accumulation in more stratified conditions. Moreover, the strong correlation we measured between growth and mortality rates suggests a strong coupling between phytoplankton production and loss processes.

Coccolithophores are considered to be a key phytoplankton group in the marine sulphur cycle, through the production of high intracellular concentrations of DMSP, the precursor of

DMS, a climate active volatile compound. We observed a positive relation between the dissolved to particulate DMSP ratio and cell lysis rates underscoring the important role of coccolithophore blooms and their termination in the oceanic cycling of DMSP. Thus, high phytoplankton loss rates caused by microzooplankton grazing and possibly viral-induced cell lysis during phytoplankton blooms in stratifying water conditions would both sequester more carbon in the particulate form, making it available to higher trophic levels, and stimulate the microbial loop functioning by releasing labile dissolved organic matter, thereby modulating strength of the biological carbon pump.

In **chapter 6**, the influence of bacterial activity and life cycle stage of *E. huxleyi* on the dynamics of dissolved carbohydrates and TEP was assessed by measuring their production and composition during the stationary growth phase of *E. huxleyi* batch cultures, reflecting the nutrient-limited conditions during later stages of blooms (chapter 2). We found a marked build-up of extracellular particulate organic carbon (POC) in calcifying *E. huxleyi* cultures, while there was a more pronounced accumulation of dissolved carbohydrates in the haploid *E. huxleyi* cultures. Bacteria stimulated the accumulation of polysaccharides and the formation of TEP containing high densities of stainable moieties, enhancing their aggregation in calcifying *E. huxleyi* cultures. Using a pulse of isotopically labelled bicarbonate (^{13}C) we traced the fate of photosynthetically fixed carbon into algal and bacterial biomass (PLFA biomarkers) and into HMW dissolved neutral aldoses (NAld) (using LC/IRMS) in non-axenic calcifying cultures. We propose that the production of coccoliths is the main source of HMW NAld in our non-axenic calcifying *E. huxleyi* cultures. Additionally, calcification by *E. huxleyi* probably facilitates the transfer of released polysaccharides from the dissolved to the particulate pool, due to the acidic nature of coccoliths polysaccharides, explaining the high levels of extracellular POC. We found that up to 76% of newly fixed organic carbon was released into the surrounding culture medium during the stationary growth phase of *E. huxleyi* and mainly retrieved in extracellular particulate carbon. This process could have a significant impact on the efficiency of export production during coccolithophorid blooms in the ocean, especially in conjunction with low, nutrient-limited bacterial activity and biomineral ballasting of aggregates.

In **chapter 7**, we related several aspects of phytoplankton bloom development to the conceptual framework in which a nutrient-rich water mass, produced by enhanced vertical

mixing at the continental slope, is advected onto the shelf, stratifying along the way. This physical framework is useful - at least in our area of study - to assemble the different pieces of the biogeochemical jigsaw, consisting of phytoplankton bloom development, bloom termination by cell lysis and grazing, release of dissolved DMSP, carbohydrate and TEP production, and the bacterial community succession.

Our results emphasize the advantages of a multi-annual, multidisciplinary approach to study often interrelated, complex biological processes which respond to a suite of environmental factors which vary over time and space. Moreover, by complementing field studies with controlled experiments we could identify the function of some bacteria and confirm that coccolith production can be responsible for the generation of high levels of TEP and extracellular carbon, as encountered in the field.

8

Samenvatting

Mariene microbiële organismen zijn de belangrijkste drijvers van wereldwijd belangrijke processen zoals de mariene biogeochemische koolstof en zwavel cycli. Dus een betere kennis over de functie van microbiële gemeenschappen, hun diversiteit en verspreiding, hun interacties, en de factoren die hen beïnvloeden is noodzakelijk is indien men wil bepalen hoe globale veranderingen in temperatuur en de verzuring van de oceanen hun ecosysteemfunctie in de toekomst zal beïnvloeden. De samenstelling van bacteriële en fytoplankton gemeenschappen tijdens fytoplanktonbloei, en hun interacties, zijn belangrijke eigenschappen van de microbiële voedselweb, die mogelijk kan een sterke invloed kan uitoefenen op het lot van organisch materiaal en dus de koolstofcyclus in de oceanen. Tot op heden is er echter weinig bekend over de omgevingsfactoren (zowel abiotische en biotische), die de ruimtelijke heterogeniteit en temporele schommelingen van de microbiota in fytoplanktonbloei drijven, en hoe deze patronen gerelateerd zijn aan de productie van organisch materiaal door deze bloeien.

Het belangrijkste doel van dit proefschrift is dan ook om bij te dragen tot een betere kennis van de samenstelling en dynamiek van bacteriële en fytoplankton assemblages in relatie tot het abiotische en biotische milieu, tijdens de bloei van coccolithoforen. Daarnaast richten we ons op het verkrijgen van een beter inzicht in de rol van deze organismen in de koolstofcyclus door een beter begrip van fytoplankton verliesfactoren (zoals microzooplankton begrazing en cellysis) en de impact van bacteriële gemeenschappen op de productie en de samenstelling van organisch materiaal door de coccolithofoor *Emiliania huxleyi*.

Tijdens drie oceanografische campagnes (2006-2008) langs de NE Atlantische continentale rand in het noordelijke deel van de Golf van Biskaje, bestudeerden we de samenstelling en dynamiek van fytoplankton en bacterioplankton gemeenschappen in fytoplanktonbloeien tijdens de late lente en relateerden deze aan de heersende fysisch-chemische en biotische factoren om hun functie na te gaan. Deze *in situ* studies werden aangevuld door laboratoriumexperimenten met behulp van een *E. huxleyi* stam en natuurlijke bacteriële

gemeenschappen geïsoleerd tijdens onze campagnes, met het oog op onderzoek van de invloed van bacteriën op de vrijstelling en de samenstelling van koolhydraten door *E. huxleyi* en de vorming van TEP.

In **hoofdstuk 2** hebben we de ruimtelijke en temporele dynamiek van de belangrijkste fytoplanktongroepen beschreven in relatie tot biogeochemische en fysische variabelen. Ons studiegebied wordt gekenmerkt door belangrijke voorjaarsfytoplanktonbloeien die vaak langs de steile continentale helling ontstaan, waar dieper voedselrijk water regelmatig aan de oppervalkte geïnjecteerd wordt door het breken van de interne getijdengolven op de continentale shelf rand. Deze fytoplanktonbloeien kunnen vervolgens door advectie boven de shelf getransporteerd worden, terwijl de stratificatie van de waterkolom toeneemt. Tijdens onze oceanografische campagnes (2006-2008) vonden we dat de Chla concentraties aanzienlijk konden variëren in ruimte en tijd, zowel tussen als tijdens de campagnes, waarschijnlijk als gevolg van verbeterde menging van de waterkolom op de helling stations ten opzichte van de shelf stations, en verschillende weersomstandigheden (wind en lichtintensiteit) en temperatuur van het zeewateroppervlakte. Diatomeeën en coccolithoforen vormden over het algemeen de dominante groepen tijdens de bloeien, maar prasinophytes, dinoflagellaten en chrysophyten traden vaak samen op tijdens de bloei van coccolithoforen. Bovendien, schommelde de diatomeeën biomassa onafhankelijk van die van andere groepen. Afwisseling van diatomeeën en van coccolithoforenbloeien werden toegeschreven aan veranderingen in de nutriënten stoichiometrie (N:P en dSi:N). Onze resultaten komen in het algemeen overeen met die van andere studies die de gunstige voorwaarden voor coccolithoforenbloei ontwikkeling bestudeerden, zoals een lage dSi:N-verhouding, een ondiepe gemengde oppervlaktelaag, en verhoogde lichtintensiteit. In tegenstelling tot de algemeen aanvaarde scenario voor algenbloei opeenvolging, vonden we dat diatomeeën bloeien (zij het minder intens dan tijdens de eerste voorjaarsbloei) coccolithoforen bloeien kunnen opvolgen, in het late voorjaar. Bovendien vertoonde coccolithoforen en diatomeeën biomassa een min of meer unimodale relatie met de mate van waterkolom stratificatie, met de hoogste biomassa waarden aangetroffen tijdens middelmatige stratificatie, in overeenstemming met het conceptueel kader voor de ontwikkeling en neergang van algenbloeien aan de continentale rand. Tijdens omstandigheden van hoge stratificatie maten we de hoogste concentratie van TEP,

gekoppeld aan de bloei van coccolithoforen, die waarschijnlijk de stationaire groeifase had bereikt.

Ondanks hun belangrijke rol in de biogeochemische cyclering en export van koolstof, is er heel weinig gekend over de samenstelling en dynamiek van bacteriële gemeenschappen geassocieerd met diatomeeën en coccolithoforen-gedomineerde fytoplanktonbloeien in de Golf van Biskaje. Bacteriële gemeenschappen zijn vaak operationeel gedifferentieerd op basis van hun vrij levende (FL) of partikel-geassocieerde (PA) groeivorm, die een verschillende soortensamenstelling kunnen hebben, en verschillende ectoenzymatische productiesnelheden vertonen die de efficiëntie van de microbiële lus en de productie van exportproducten beïnvloeden. Met het oog op het verband te leggen tussen de bacteriële gemeenschapsstructuur en hun ecologische functie, en om de ecologische niche van deze microben te beschrijven, hebben we gebruik gemaakt van een indirecte benadering door het onderzoek van de statistische relaties tussen organismen en milieu-parameters, zoals beschreven in de **hoofdstukken 3 en 4**. Daartoe gebruikten we een rRNA-gebaseerde moleculaire profilering techniek (DGGE), om snel de microbiële gemeenschapssamenstelling en de totale diversiteit van een groot aantal monsters te karakteriseren, gekoppeld aan multivariate analyses om beter patronen te identificeren in de bacteriële gemeenschap.

De bacteriële gemeenschappen werden gedomineerd door *Gammaproteobacteria* en *Bacteroidetes*, en ook door *Alphaproteobacteria*. Leden van de *Flavobacteriaceae*, *Polaribacter* sp. en *Pseudoalteromonas* sp. waren typische vertegenwoordigers van de PA gemeenschappen, terwijl phylotypes behorende tot de *Rhodobacteriaceae*, de SAR11 groep en de *Gammaproteobacteria* kenmerkend waren voor de FL-gemeenschappen. Toch vonden we een aanzienlijk overlap in de samenstelling van beide gemeenschappen, hetgeen duidt op een continuüm in levensstijl of fenotypische overgangen tussen beide gemeenschappen. Opmerkelijk is dat dezelfde bacteriële phylotypes elk jaar aanwezig waren, hoewel de bacteriële gemeenschapsstructuur variabel was tussen de verschillende stations, zoals beschreven in **hoofdstuk 3**. Verder zagen we slechts een matige diepte verloop in de gemeenschapsstructuur en de PA bacteriële gemeenschappen vertoonden een meer uitgesproken diepte zonering (oppervlakte-150 m) ten opzichte van de FL gemeenschappen, wat een frequentere uitwisseling tussen het oppervlak en dieper water lagen in de laatste group suggereert.

In **hoofdstuk 4**, gebruikten we de ordinatie methoden en variatie partitionering om de variatie in bacteriële gemeenschapsstructuur te relateren tot veranderingen in fysische (bv. waterkolom stratificatie), biogeochemische (bv. nutriënten en TEP, anomalie van de totale alkaliteit) en fytoplankton variabelen (chemotaxonomische groepen). Het aandeel aan verklaarde variatie in gemeenschapsstructuur tijdens elke campagne was steeds lager voor de PA ten opzichte van FL bacteriën en verschilden tot meer dan drievoudig tussen jaren en ook binnen enkele jaren, wat suggereert dat beide gemeenschappen door verschillende factoren worden gereguleerd. Hoewel de variatie in de bacteriële gemeenschapsstructuur tijdens de verschillende campagnes gerelateerd kan worden tot meerdere, soms met elkaar gecorreleerde variabelen zoals de concentratie van nutriënten, TEP, anomalie van de totale alkaliteit (als gevolg van de calcificatie/ dissolutie geschiedenis van een water-massa), watertemperatuur, algenbloei samenstelling en intensiteit, of de afstand van de stations aan de continentale helling, vonden we dat stratificatie van de waterkolom als een verenigend substituut genomen kon worden voor het beschrijven van de bacteriële gemeenschapssuccessie in ons studiegebied. De structuur van de meerjarige gemeenschappen was significant gecorreleerd de abundantie van fytoplanktongroepen (diatomeeën, coccolithoforen, prasinophytes, dinoflagellaten en cryptophytes). Verder, vonden we dat sommige bacteriële genera die tijdens onze oceanografische campagnes dominant waren ook actief waren tijdens onze cultuur experimenten, wat de notie van zeer specifieke associaties en commensale interacties tussen fytoplankton en bacteriën ondersteunt. De bevindingen in **hoofdstukken 3 en 4** bevestigen het bestaan van ecologische niche ruimte voor bacteriën, en ondersteunen het bestaan van een zekere voorspelbaarheid van bacteriële assemblages, op dezelfde manier dat de opeenvolging van functionele groepen en de grootteverdeling van fytoplankton gerelateerd kunnen worden aan bepaalde milieucondities.

Fytoplankton groei is vaak onder strikte controle van microzooplankton begrazing en virale lysis, twee belangrijke processen die de vorming en de beëindiging van fytoplanktonbloeien reguleren en belangrijke parameters van de biologische koolstofpomp vormen, in termen van de productie van exportproducten. In **hoofdstuk 5** geven we de eerste metingen van de cellysis snelheden tijdens bloeien van coccolithoforen, gemeten met behulp van de esterase activiteit methode. Onze resultaten suggereren dat cellysis inderdaad een belangrijke factor

vormt voor het verlies fytoplankton in de Golf van Biskaje. We vulden deze metingen aan met schattingen voor fytoplankton groei en begrazingssterfte met behulp van het zeewater verdunningsmethode gecombineerd met HPLC pigmentenanalyse, waaruit bleek dat hoge fytoplankton sterfte soms onafhankelijk waren van hoge cellysis snelheden. Dit wijst erop dat microzooplankton begrazing soms als een belangrijk groepspecifieke bron van fytoplankton verlies kon optreden. Beide processen de hadden de neiging toe te nemen met toenemende waterkolom stratificatie, hetgeen duidt op een convergentie van de bottom-up (door nutriëntenlimitatie) en de celconcentratie afhankelijkheid van top-down controle (bv. virale lysis) op de verdere fytoplankton biomassa accumulatie in meer gestratifieerde omstandigheden. Bovendien suggereert de sterke correlatie tussen groei en sterfte een sterke koppeling tussen de fytoplanktonproductie en verliesprocessen.

Coccolithoforen worden beschouwd als een belangrijke fytoplankton groep in het mariene zwavel cyclus, door de productie van hoge intracellulaire concentraties van DMSP, de voorloper van DMS, een vluchtige verbinding met een klimaat-actieve rol. De positieve relatie tussen de verhouding van opgeloste en particulaire DMSP en cellysis die we vonden onderstreept de belangrijke rol van coccolithoforenbloeien en hun beëindiging in de oceanische cyclus van DMSP. Dus, de hoge sterfte veroorzaakt door waarschijnlijk viraal geïnduceerde cellysis tijdens fytoplanktonbloeien in gestratifiëerd water kunnen de werking van de microbiële lus stimuleren door het vrijgeven van labiele DOM (zoals DMSP), dat opgenomen kan worden in de bacteriële biomassa.

In **hoofdstuk 6** werd de invloed van bacteriële activiteit en levenscyclus fase van de *E. huxleyi* op de dynamiek van opgeloste koolhydraten en TEP beoordeeld door het meten van hun productie en de samenstelling tijdens de stationaire groeifase van *E. huxleyi* batch culturen, die als de nutriënten gelimiteerde condities tijdens de latere stadia van natuurlijke bloeien reflecteren (hoofdstuk 2). We vonden een duidelijke opbouw van extracellulair particulair organisch koolstof (POC) in calcificerende *E. huxleyi* culturen, terwijl er een meer uitgesproken accumulatie plaatsvond van opgeloste koolhydraten in het haploïde *E. huxleyi* culturen. Bacteriën stimuleerden de accumulatie van polysacchariden en de vorming van TEP met hoge dichtheden van zure groepen, wat hun aggregatie in calcificerende *E. huxleyi* culturen bevorderde. Met behulp van een puls van isotopisch gelabelde bicarbonaat (^{13}C) volgden we het lot van fotosynthetisch gefixeerde koolstof in algen- en bacteriële biomassa

(PLFA biomerkers) en in de HMW opgeloste neutrale aldosen (NAld) (met behulp van LC/IRMS) in niet-axenische calcificerende culturen. Wij stellen voor dat de productie van coccolieten de belangrijkste bron vormt van HMW NAld in onze niet-axenische calcificerende *E. huxleyi* culturen. Bovendien, faciliteert de calcificatie door *E. huxleyi* waarschijnlijk de overdracht van de vrijgekomen polysacchariden van de opgeloste naar de particulaire pool, als gevolg van de zure groepen van coccolieten polysacchariden, wat de hoge concentratie aan extracellulaire POC zou verklaren. We vonden dat tot 76% van de nieuw gefixeerde organische koolstof tijdens de stationaire groeifase van *E. huxleyi* culturen voornamelijk vrijgesteld werd in het cultuur medium onder de vorm van extracellulair particulair koolstof. Dit proces kan een aanzienlijke impact hebben op de efficiëntie van de productie van exportproducten tijdens coccolithoforenbloien in de oceaan, vooral in combinatie met een lage, nutriënten gelimiteerde bacteriële activiteit en de biominerale ballasting van aggregaten.

In **hoofdstuk 7** hebben we verschillende aspecten van de ontwikkeling van algenbloeien in verband gebracht met het conceptuele kader waarin een nutriënten rijke water massa, geproduceerd door de sterkere verticale menging op de continentale helling, boven de shelf geadvecteerd wordt en onderweg in toenemende mate stratificeert. Dit conceptueel kader is nuttig gebleken - althans in ons studiegebied – voor de integratie van de verschillende stukjes van de biogeochemische puzzel, bestaande uit de ontwikkeling van algenbloeien, bloei neergang door cellysis en begrazing, het vrijkomen van opgelost DMSP, koolhydraten en de productie van TEP, en de bacteriële gemeenschapssuccessie.

Onze resultaten benadrukken ook de voordelen van een meerjarige, multidisciplinaire aanpak om de vaak onderling verbonden, complexe biologische processen te bestuderen die beantwoorden aan een reeks van omgevingsfactoren die variëren in de tijd en ruimte. Bovendien, door de aanvulling van veldstudies met gecontroleerde experimenten konden we de functionele niche van sommige bacteriën identificeren en bevestigen we dat productie van coccolieten verantwoordelijk kan zijn voor het genereren van hoge concentraties aan TEP en extracellulair koolstof, zoals die op zee zijn waargenomen.

Bibliography

Acinas, S. G., Anton, J., and Rodriguez-Valera, F., 1999. Diversity of free-living and attached bacteria in offshore western Mediterranean waters as depicted by analysis of genes encoding 16S rRNA. Appl. Environ. Microbiol., 65, 514-522

Acinas, S. G., Klepac-Ceraj, V., Hunt, D. E., Pharino, C., Ceraj, I., Distel, D. L., and Polz, M. F., 2004. Fine-scale phylogenetic architecture of a complex bacterial community. Nature, 430, 551-554

Adl, S. M., Simpson, A. G. B., Farmer, M. A., Andersen, R. A., Anderson, O. R., Barta, J. R., Bowser, S. S., Brugerolle, G., Fensome, R. A., Fredericq, S., James, T. Y., Karpov, S., Kugrens, P., Krug, J., Lane, C. E., Lewis, L. A., Lodge, J., Lynn, D. H., Mann, D. G., McCourt, R. M., Mendoza, L., Moestrup, O., Mozley-Standridge, S. E., Nerad, T. A., Shearer, C. A., Smirnov, A. V., Spiegel, F. W., and Taylor, M., 2005. The new higher level classification of eukaryotes with emphasis on the taxonomy of protists. J. Eukaryot. Microbiol., 52, 399-451

Agusti, S., and Duarte, C. M., 2000. Strong seasonality in phytoplankton cell lysis in the NW Mediterranean littoral. Limnol. Oceanogr., 45, 940-947

Agusti, S., and Duarte, C. M., 2002. Addressing uncertainties in the assessment of phytoplankton lysis rates in the sea - Comment. Limnol. Oceanogr., 47, 921-924

Agusti, S., Satta, M. P., Mura, M. P., and Benavent, E., 1998. Dissolved esterase activity as a tracer of phytoplankton lysis: Evidence of high phytoplankton lysis rates in the northwestern Mediterranean. Limnol. Oceanogr., 43, 1836-1849

Alderkamp, A. C., Sintes, E., and Herndl, G. J., 2006. Abundance and activity of major groups of prokaryotic plankton in the coastal North Sea during spring and summer. Aquat. Microb. Ecol., 45, 237-246

Alldredge, A. L., Passow, U., and Logan, B. E., 1993. The abundance and significance of a class of large, transparent organic particles in the ocean. Deep-Sea Res. Part I-Oceanogr. Res. Pap., 40, 1131-1140

Alonso-Gutierrez, J., Lekunberri, I., Teira, E., Gasol, J. M., Figueras, A., and Novoa, B., 2009. Bacterioplankton composition of the coastal upwelling system of 'Ria de Vigo', NW Spain. FEMS Microbiol. Ecol., 70, 493-505

Alonso-Saez, L., Aristegui, J., Pinhassi, J., Gomez-Consarnau, L., Gonzalez, J. M., Vaque, D., Agusti, S., and Gasol, J. M., 2007. Bacterial assemblage structure and carbon metabolism along a productivity gradient in the NE Atlantic Ocean. Aquat. Microb. Ecol., 46, 43-53

Alonso, C., Warnecke, F., Amann, R., and Pernthaler, J., 2007. High local and global diversity of Flavobacteria in marine plankton. Environmental Microbiology, 9, 1253-1266

Alonso, M. C., Rodriguez, V., Rodriguez, J., and Borrego, J. J., 2000. Role of ciliates, flagellates and bacteriophages on the mortality of marine bacteria and on dissolved-DNA concentration in laboratory experimental systems. J. Exp. Mar. Biol. Ecol., 244, 239-252

Aluwihare, L. I., and Repeta, D. J., 1999. A comparison of the chemical characteristics of oceanic DOM and extracellular DOM produced by marine algae. Mar. Ecol.-Prog. Ser., 186, 105-117

Aluwihare, L. I., Repeta, D. J., and Chen, R. F., 1997. A major biopolymeric component to dissolved organic carbon in surface sea water. Nature, 387, 166-169

Alvain, S., Moulin, C., Dandonneau, Y., and Loisel, H., 2008. Seasonal distribution and succession of dominant phytoplankton groups in the global ocean: A satellite view. Glob. Biogeochem. Cycle, 22, 15

Amin, S. A., Green, D. H., Hart, M. C., Kupper, F. C., Sunda, W. G., and Carrano, C. J., 2009. Photolysis of iron-siderophore chelates promotes bacterial-algal mutualism. Proceedings of the National Academy of Sciences of the United States of America, 106, 17071-17076

Amon, R. M. W., and Benner, R., 1994. Rapid-cycling of high-molecular-weight dissolved organic-matter in the ocean. Nature, 369, 549-552

Amon, R. M. W., and Benner, R., 2003. Combined neutral sugars as indicators of the diagenetic state of dissolved organic matter in the Arctic Ocean. Deep-Sea Res. Part I-Oceanogr. Res. Pap., 50, 151-169

Andersen, R. A., Bidigare, R. R., Keller*, M. D., and Latasa, M., 1996. A comparison of HPLC pigment signatures and electron microscopic observations for oligotrophic waters of the North Atlantic and Pacific Oceans. Deep Sea Research Part II: Topical Studies in Oceanography, 43, 517-537

Andersen, T., Schartau, A. K. L., and Paasche, E., 1991. Quantifying external and internal nitrogen and phosphorus pools, as well as nitrogen and phosphorus supplied through remineralization, in coastal marine plankton by means of a dilution technique.Mar. Ecol.-Prog. Ser., 69, 67-80

Anderson, M. J., Gorley, R. N., and Clarke, K. R.: PERMANOVA+ for PRIMER: Guide to Software and Statistical Methods, in, PRIMER-E: Plymouth, UK, 2008.

Archer, S. D., Stelfox-Widdicombe, C. E., Burkill, P. H., and Malin, G., 2001. A dilution approach to quantify the production of dissolved dimethylsulphoniopropionate and dimethyl sulphide due to microzooplankton herbivory. Aquat. Microb. Ecol., 23, 131-145

Archer, S. D., Smith, G. C., Nightingale, P. D., Widdicombe, C. E., Tarran, G. A., Rees, A. P., and Burkill, P. H., 2002. Dynamics of particulate dimethylsulphoniopropionate during a Lagrangian experiment in the northern North Sea. Deep-Sea Research Part Ii-Topical Studies in Oceanography, 49, 2979-2999

Aristegui, J., Gasol, J. M., Duarte, C. M., and Herndl, G. J., 2009. Microbial oceanography of the dark ocean's pelagic realm. Limnol. Oceanogr., 54, 1501-1529

Armstrong, R. A., Lee, C., Hedges, J. I., Honjo, S., and Wakeham, S. G., 2002. A new, mechanistic model for organic carbon fluxes in the ocean based on the quantitative association of POC with ballast minerals. Deep-Sea Research Part Ii-Topical Studies in Oceanography, 49, 219-236

Arnosti, C., 2004. Speed bumps and barricades in the carbon cycle: substrate structural effects on carbon cycling. Marine Chemistry, 92, 263-273

Artigas, L. F., 1998. Seasonal variability in microplanktonic biomasses in the Gironde dilution plume (Bay of Biscay): relative importance of bacteria. Oceanol. Acta, 21, 563-580

Azam, F., Fenchel, T., Field, J. G., Gray, J. S., Meyerreil, L. A., and Thingstad, F., 1983. The ecological role of water-column microbes in the sea. Mar. Ecol.-Prog. Ser., 10, 257-263

Baines, S. B., and Pace, M. L., 1991. The production of dissolved organic-matter by phytoplankton and its importance to bacteria - patterns across marine and freshwater systems. Limnol. Oceanogr., 36, 1078-1090

Balch, W. M. 2004. Re-evaluation of the physiological ecology of coccolithophores, Coccolithophores: From Molecular Processes to Global Impact, edited by: Thierstein, H. R., and Young, J. R., 165-190 pp.

Balch, W. M., Holligan, P. M., Ackleson, S. G., and Voss, K. J., 1991. Biological and optical-properties of mesoscale coccolithophore blooms in the Gulf of Maine. Limnol. Oceanogr., 36, 629-643

Bar Zeev, E., Yogev, T., Man-Aharonovich, D., Kress, N., Herut, B., Beja, O., and Berman-Frank, I., 2008. Seasonal dynamics of the endosymbiotic, nitrogen-fixing cyanobacterium Richelia intracellularis in the eastern Mediterranean Sea. Isme J., 2, 911-923

Barlow, R. G., Mantoura, R. F. C., Gough, M. A., and Fileman, T. W., 1993. Pigment signatures of the phytoplankton composition in the northeastern Atlantic during the 1990 spring bloom. Deep-Sea Research Part Ii-Topical Studies in Oceanography, 40, 459-477

Barlow, R. G., Aiken, J., Holligan, P. M., Cummings, D. G., Maritorena, S., and Hooker, S., 2002. Phytoplankton pigment and absorption characteristics along meridional transects in the Atlantic Ocean. Deep-Sea Res. Part I-Oceanogr. Res. Pap., 49, 637-660

Barquero, S., Botas, J. A., and Bode, A., 1998. Abundance and production of pelagic bacteria in the southern Bay of Biscay during summer. Sci. Mar., 62, 83-90

Bassham, J. A., Benson, A. A., and Calvin, M., 1950. The path of carbon in photosynthesis. The Journal of Biological Chemistry, 182, 781-787

Bauer, M., Kube, M., Teeling, H., Richter, M., Lombardot, T., Allers, E., Wurdemann, C. A., Quast, C., Kuhl, H., Knaust, F., Woebken, D., Bischof, K., Mussmann, M., Choudhuri, J. V., Meyer, F., Reinhardt, R., Amann, R. I., and Glockner, F. O., 2006. Whole genome analysis of the marine Bacteroidetes '*Gramella forsetii*' reveals adaptations to degradation of polymeric organic matter. Environmental Microbiology, 8, 2201-2213

Beaufort, L., and Heussner, S., 1999. Coccolithophorids on the continental slope of the Bay of Biscay - production, transport and contribution to mass fluxes. Deep-Sea Research Part Ii-Topical Studies in Oceanography, 46, 2147-2174

Behrenfeld, M. J., 2010. Abandoning Sverdrup's Critical Depth Hypothesis on phytoplankton blooms. Ecology, 91, 977-989

Behrenfeld, M. J., O'Malley, R. T., Siegel, D. A., McClain, C. R., Sarmiento, J. L., Feldman, G. C., Milligan, A. J., Falkowski, P. G., Letelier, R. M., and Boss, E. S., 2006. Climate-driven trends in contemporary ocean productivity. Nature, 444, 752-755

Bellinger, B. J., Underwood, G. J. C., Ziegler, S. E., and Gretz, M. R., 2009. Significance of diatom-derived polymers in carbon flow dynamics within estuarine biofilms determined through isotopic enrichment. Aquat. Microb. Ecol., 55, 169-187

Benner, I., and Passow, U., 2010. Utilization of organic nutrients by coccolithophores. Mar. Ecol.-Prog. Ser., 404, 21-29

Benner, R., Pakulski, J. D., McCarthy, M., Hedges, J. I., and Hatcher, P. G., 1992. Bulk chemical characteristics of dissolved organic-matter in the ocean. Science, 255, 1561-1564

Benson, B. B., and Krause, D., 1984. The concentration and isotopic fractionation of oxygen dissolved in fresh-water and seawater in equilibrium with the atmosphere. Limnol. Oceanogr., 29, 620-632

Berges, J. A., and Falkowski, P. G., 1998. Physiological stress and cell death in marine phytoplankton: Induction of proteases in response to nitrogen or light limitation. Limnol. Oceanogr., 43, 129-135

Biddanda, B., and Benner, R., 1997. Carbon, nitrogen, and carbohydrate fluxes during the production of particulate and dissolved organic matter by marine phytoplankton. Limnol. Oceanogr., 42, 506-518

Bidigare, R. R., Van Heukelem, L., and Trees, C. C. 2005. Analysis of Algal Pigments by High-Performance Liquid Chromatography, Algal Culturing Techniques, edited by: Andersen, R., Academic Press

Biersmith, A., and Benner, R., 1998. Carbohydrates in phytoplankton and freshly produced dissolved organic matter. Marine Chemistry, 63, 131-144

Billard, C., and Inouye, I. 2004. What is new in coccolithophore biology?, Coccolithophores: From Molecular Processes to Global Impact, edited by: Thierstein, H. R., and Young, J. R., Springer-Verlag Berlin, Berlin, 1-29 pp.

Bjørnsen, P. K., 1988. Phytoplankton exudation of organic-matter - why do healthy cells do it. Limnol. Oceanogr., 33, 151-154

Bollmann, J., Cortes, M. Y., Haidar, A. T., Brabec, B., Close, A., Hofmann, R., Palma, S., Tupas, L., and Thierstein, H. R., 2002. Techniques for quantitative analyses of calcareous marine phytoplankton. Marine Micropaleontology, 44, 163-185

Borman, A. H., Kok, D. J., Dejong, E. W., Westbroek, P., Varkevisser, F. A., Vantreslong, C. J. B., and Bosch, L., 1986. Molar mass determination of the polysaccharide associated with coccoliths of *Emiliania-huxleyi*. Eur. Polym. J., 22, 521-523

Borman, A. H., Dejong, E. W., Thierry, R., Westbroek, P., Bosch, L., Gruter, M., and Kamerling, J. P., 1987. Coccolith-associated polysaccharides from cells of *Emiliania-huxleyi* (*Haptophyceae*). Journal of Phycology, 23, 118-123

Boschker, H. T. S., and Middelburg, J. J., 2002. Stable isotopes and biomarkers in microbial ecology. FEMS Microbiol. Ecol., 40, 85-95

Boschker, H. T. S., de Brouwer, J. F. C., and Cappenberg, T. E., 1999. The contribution of macrophyte-derived organic matter to microbial biomass in salt-marsh sediments: Stable carbon isotope analysis of microbial biomarkers. Limnol. Oceanogr., 44, 309-319

Boschker, H. T. S., Moerdijk-Poortvliet, T. C. W., van Breugel, P., Houtekamer, M., and Middelburg, J. J., 2008. A versatile method for stable carbon isotope analysis of carbohydrates by high-performance liquid chromatography/isotope ratio mass spectrometry. Rapid Commun. Mass Spectrom., 22, 3902-3908

Boström, K. H., Simu, K., Hagstrom, A., and Riemann, L., 2004. Optimization of DNA extraction for quantitative marine bacterioplankton community analysis. Limnology and Oceanography-Methods, 2, 365-373

Bouillon, S., Korntheuer, M., Baeyens, W., and Dehairs, F., 2006. A new automated setup for stable isotope analysis of dissolved organic carbon. Limnology and Oceanography-Methods, 4, 216-226

Boyd, P. W., Strzepek, R., Fu, F. X., and Hutchins, D. A., 2010. Environmental control of open-ocean phytoplankton groups: Now and in the future. Limnol. Oceanogr., 55, 1353-1376

Bratbak, G., Wilson, W., and Heldal, M., 1996. Viral control of Emiliania huxleyi blooms? Journal of Marine Systems, 9, 75-81

Brinch-Iversen, J., and King, G. M., 1990. Effects of substrate concentration, growth-state, and oxygen availability on relationships among bacterial carbon, nitrogen and phospholipid phosphorus-content. FEMS Microbiol. Ecol., 74, 345-355

Bronk, D. A. 2002. Dynamics of DON, in: Biogeochemistry of marine dissolved organic matter, edited by: Hansell, D. A., and Carlson, C. A., Academic Press, Elsevier Science, San Diego, CA, 153-248

Brown, C. W., and Yoder, J. A., 1994. Coccolithophorid blooms in the global ocean. J. Geophys. Res.-Oceans, 99, 7467-7482

Brownlee, C., and Taylor, A. 2004. Calcification in coccolithophores: A cellular perspective, Coccolithophores: From Molecular Processes to Global Impact, edited by: Thierstein, H. R., and Young, J. R., 31-49 pp.

Bruckner, C. G. B. C. G., Rehm, C., Grossart, H. P., and Kroth, P. G., 2011. Growth and release of extracellular organic compounds by benthic diatoms depend on interactions with bacteria. Environmental Microbiology, 13, 1052-1063

Brussaard, C. P. D., 2004. Viral control of phytoplankton populations - a review. J. Eukaryot. Microbiol., 51, 125-138

Brussaard, C. P. D., Kuipers, B., and Veldhuis, M. J. W., 2005a. A mesocosm study of *Phaeocystis globosa* population dynamics - 1. Regulatory role of viruses in bloom. Harmful Algae, 4, 859-874

Brussaard, C. P. D., Gast, G. J., vanDuyl, F. C., and Riegman, R., 1996. Impact of phytoplankton bloom magnitude on a pelagic microbial food web. Mar. Ecol.-Prog. Ser., 144, 211-221

Brussaard, C. P. D., Mari, X., Van Bleijswijk, J. D. L., and Veldhuis, M. J. W., 2005b. A mesocosm study of *Phaeocystis globosa* (*Prymnesiophyceae*) population dynamics - II. Significance for the microbial community. Harmful Algae, 4, 875-893

Brussaard, C. P. D., Riegman, R., Noordeloos, A. A. M., Cadee, G. C., Witte, H., Kop, A. J., Nieuwland, G., Vanduyl, F. C., and Bak, R. P. M., 1995. Effects of grazing, sedimentation and phytoplankton cell-lysis on the structure of a coastal pelagic food-web. Mar. Ecol.-Prog. Ser., 123, 259-271

Buchan, A., Gonzalez, J. M., and Moran, M. A., 2005. Overview of the marine Roseobacter lineage. Appl. Environ. Microbiol., 71, 5665-5677

Burkill, P. H., Archer, S. D., Robinson, C., Nightingale, P. D., Groom, S. B., Tarran, G. A., and Zubkov, M. V., 2002. Dimethyl sulphide biogeochemistry within a coccolithophore bloom (DISCO): an overview. Deep-Sea Research Part Ii-Topical Studies in Oceanography, 49, 2863-2885

Calbet, A., and Landry, M. R., 2004. Phytoplankton growth, microzooplankton grazing, and carbon cycling in marine systems. Limnol. Oceanogr., 49, 51-57

Carlson, C. A. 2002. Production and Removal Processes, in: Biogeochemistry of dissolved organic matter, edited by: Hansell, D. A., and Carlson, C. A., Academic Press, 91-151

Carlson, C. A., Morris, R., Parsons, R., Treusch, A. H., Giovannoni, S. J., and Vergin, K., 2009. Seasonal dynamics of SAR11 populations in the euphotic and mesopelagic zones of the northwestern Sargasso Sea. Isme J., 3, 283-295

Castberg, T., Larsen, A., Sandaa, R. A., Brussaard, C. P. D., Egge, J. K., Heldal, M., Thyrhaug, R., van Hannen, E. J., and Bratbak, G., 2001. Microbial population dynamics and diversity

during a bloom of the marine coccolithophorid *Emiliania huxleyi* (Haptophyta). Mar. Ecol.-Prog. Ser., 221, 39-46

Casteleyn, G., Adams, N. G., Vanormelingen, P., Debeer, A. E., Sabbe, K., and Vyverman, W., 2009. Natural Hybrids in the Marine Diatom *Pseudo-nitzschia pungens* (*Bacillariophyceae*): Genetic and Morphological Evidence. Protist, 160, 343-354

Casteleyn, G., Leliaert, F., Backeljau, T., Debeer, A. E., Kotaki, Y., Rhodes, L., Lundholm, N., Sabbe, K., and Vyverman, W., 2010. Limits to gene flow in a cosmopolitan marine planktonic diatom. Proceedings of the National Academy of Sciences of the United States of America, 107, 12952-12957

Cermeño, P., Lee, J.-B., Wyman, K., Schofield, O., and Falkowski, P. G., 2011. Competitive dynamics in two species of marine phytoplankton under non-equilibrium conditions. Mar. Ecol.-Prog. Ser., 429, 19-28

Cermeño, P., Dutkiewicz, S., Harris, R. P., Follows, M., Schofield, O., and Falkowski, P. G., 2008. The role of nutricline depth in regulating the ocean carbon cycle. Proceedings of the National Academy of Sciences of the United States of America, 105, 20344-20349

Chen, B. Z., Liu, H. B., Landry, M. R., Dai, M. H., Huang, B. Q., and Sun, J., 2009. Close coupling between phytoplankton growth and microzooplankton grazing in the western South China Sea. Limnol. Oceanogr., 54, 1084-1097

Clarke, K. R., and Gorley, R. N. 2006. PRIMER v6: User manual / tutorial, PRIMER-E Ltd.

Cole, J. R., Wang, Q., Cardenas, E., Fish, J., Chai, B., Farris, R. J., Kulam-Syed-Mohideen, A. S., McGarrell, D. M., Marsh, T., Garrity, G. M., and Tiedje, J. M., 2009. The Ribosomal Database Project: improved alignments and new tools for rRNA analysis. Nucleic Acids Res., 37, D141-D145

Cottrell, M. T., and Kirchman, D. L., 2000. Community composition of marine bacterioplankton determined by 16S rRNA gene clone libraries and fluorescence in situ hybridization. Appl. Environ. Microbiol., 66, 5116-5122

Crump, B. C., Armbrust, E. V., and Baross, J. A., 1999. Phylogenetic analysis of particle-attached and free-living bacterial communities in the Columbia river, its estuary, and the adjacent coastal ocean. Appl. Environ. Microbiol., 65, 3192-3204

Cuvelier, M. L., Allen, A. E., Monier, A., McCrow, J. P., Messie, M., Tringe, S. G., Woyke, T., Welsh, R. M., Ishoey, T., Lee, J. H., Binder, B. J., DuPont, C. L., Latasa, M., Guigand, C., Buck, K. R., Hilton, J., Thiagarajan, M., Caler, E., Read, B., Lasken, R. S., Chavez, F. P., and Worden, A. Z., 2010. Targeted metagenomics and ecology of globally important uncultured eukaryotic phytoplankton. Proceedings of the National Academy of Sciences of the United States of America, 107, 14679-14684

d'Ovidio, F., De Monte, S., Alvain, S., Dandonneau, Y., and Lévy, M., 2010. Fluid dynamical niches of phytoplankton types. Proceedings of the National Academy of Sciences, 107, 18366-18370

Dandonneau, Y., Montel, Y., Blanchot, J., Giraudeau, J., and Neveux, J., 2006. Temporal variability in phytoplankton pigments, picoplankton and coccolithophores along a transect through the North Atlantic and tropical southwestern Pacific. Deep-Sea Res. Part I-Oceanogr. Res. Pap., 53, 689-712

De Bodt, C.: Pelagic calcification and the fate of carbonate production in marine systems, in, Université Libre de Bruxelles, Brussels, 2010.

de Jong, E., Vanrens, L., Westbroek, P., and Bosch, L., 1979. Bio-calcification by the marine alga *Emiliania huxleyi* (Lohmann) Kamptner. European Journal of Biochemistry, 99, 559-567

de Kluijver, A., Soetaert, K., Schulz, K. G., Riebesell, U., Bellerby, R. G. J., and Middelburg, J. J., 2010. Phytoplankton-bacteria coupling under elevated CO_2 levels: a stable isotope labelling study. Biogeosciences, 7, 3783-3797

De La Rocha, C. L., and Passow, U., 2007. Factors influencing the sinking of POC and the efficiency of the biological carbon pump. Deep-Sea Research Part Ii-Topical Studies in Oceanography, 54, 639-658

de Vargas, C., Aubry, M. P., Probert, I., and Young, J. 2007. Origin and evolution of coccolithophores: from coastal hunters to oceanic farmers, in: Evolution of Primary Producers in the Sea, edited by: Falkowski, P. G., and Knoll, A., Academic Press, 251-285

De Wever, A., Van der Gucht, K., Muylaert, K., Cousin, S., and Vyverman, W., 2008. Clone library analysis reveals an unusual composition and strong habitat partitioning of pelagic bacterial communities in Lake Tanganyika. Aquat. Microb. Ecol., 50, 113-122

De Wever, A., Muylaert, K., Van der Gucht, K., Pirlot, S., Cocquyt, C., Descy, J. P., Plisnier, P. D., and Vyverman, W., 2005. Bacterial community composition in Lake Tanganyika: Vertical and horizontal heterogeneity. Appl. Environ. Microbiol., 71, 5029-5037

del Giorgio, P. A., and Cole, J. J., 1998. Bacterial growth efficiency in natural aquatic systems. Annu. Rev. Ecol. Syst., 29, 503-541

Delille, B., Harlay, J., Zondervan, I., Jacquet, S., Chou, L., Wollast, R., Bellerby, R. G. J., Frankignoulle, M., Borges, A. V., Riebesell, U., and Gattuso, J. P., 2005. Response of primary production and calcification to changes of pCO_2 during experimental blooms of the coccolithophorid *Emiliania huxleyi*. Glob. Biogeochem. Cycle, 19

Delong, E. F., Franks, D. G., and Alldredge, A. L., 1993. Phylogenetic diversity of aggregate-attached vs free-living marine bacterial assemblages. Limnol. Oceanogr., 38, 924-934

Dijkman, N. A., and Kromkamp, J. C., 2006. Phospholipid-derived fatty acids as chemotaxonomic markers for phytoplankton: application for inferring phytoplankton composition. Mar. Ecol.-Prog. Ser., 324, 113-125

Dolan, J. R., Gallegos, C. L., and Moigis, A., 2000. Dilution effects on microzooplankton in dilution grazing experiments. Mar. Ecol.-Prog. Ser., 200, 127-139

Egge, J. K., and Aksnes, D. L., 1992. Silicate as regulating nutrient in phytoplankton competition. Mar. Ecol.-Prog. Ser., 83, 281-289

Egge, J. K., and Heimdal, B. R., 1994. Blooms of phytoplankton including *Emiliania huxleyi* (Haptophyta) - effects of nutrient supply in different N-P ratios. Sarsia, 79, 333-348

Engel, A. 2009. Marine Gel Particles, in: Practical Guidelines for the Analysis of Seawater, edited by: Wurl, O., CRC Press, Taylor & Francis Group, Boca Rayton, FL, USA,

Engel, A., Thoms, S., Riebesell, U., Rochelle-Newall, E., and Zondervan, I., 2004a. Polysaccharide aggregation as a potential sink of marine dissolved organic carbon. Nature, 428, 929-932

Engel, A., Delille, B., Jacquet, S., Riebesell, U., Rochelle-Newall, E., Terbruggen, A., and Zondervan, I., 2004b. Transparent exopolymer particles and dissolved organic carbon production by *Emiliania huxleyi* exposed to different CO_2 concentrations: a mesocosm experiment. Aquat. Microb. Ecol., 34, 93-104

Engel, A., Abramson, L., Szlosek, J., Liu, Z. F., Stewart, G., Hirschberg, D., and Lee, C., 2009. Investigating the effect of ballasting by $CaCO_3$ in *Emiliania huxleyi*, II: Decomposition

of particulate organic matter. Deep-Sea Research Part Ii-Topical Studies in Oceanography, 56, 1408-1419

Evans, C., and Wilson, W. H., 2008. Preferential grazing of *Oxyrrhis marina* on virus-infected *Emiliania huxleyi*. Limnol. Oceanogr., 53, 2035-U2012

Evans, C., Archer, S. D., Jacquet, S., and Wilson, W. H., 2003. Direct estimates of the contribution of viral lysis and microzooplankton grazing to the decline of a Micromonas spp. population. Aquat. Microb. Ecol., 30, 207-219

Falkowski, P. G., Katz, M. E., Knoll, A. H., Quigg, A., Raven, J. A., Schofield, O., and Taylor, F. J. R., 2004. The evolution of modern eukaryotic phytoplankton. Science, 305, 354-360

Fandino, L. B., Riemann, L., Steward, G. F., and Azam, F., 2005. Population dynamics of Cytophaga-Flavobacteria during marine phytoplankton blooms analyzed by real-time quantitative PCR. Aquat. Microb. Ecol., 40, 251-257

Fandino, L. B., Riemann, L., Steward, G. F., Long, R. A., and Azam, F., 2001. Variations in bacterial community structure during a dinoflagellate bloom analyzed by DGGE and 16S rDNA sequencing. Aquat. Microb. Ecol., 23, 119-130

Fasham, M. J. R., Balino, B. M., Bowles, M. C., Anderson, R., Archer, D., Bathmann, U., Boyd, P., Buesseler, K., Burkill, P., Bychkov, A., Carlson, C., Chen, C. T. A., Doney, S., Ducklow, H., Emerson, S., Feely, R., Feldman, G., Garcon, V., Hansell, D., Hanson, R., Harrison, P., Honjo, S., Jeandel, C., Karl, D., Le Borgne, R., Liu, K. K., Lochte, K., Louanchi, F., Lowry, R., Michaels, A., Monfray, P., Murray, J., Oschlies, A., Platt, T., Priddle, J., Quinones, R., Ruiz-Pino, D., Saino, T., Sakshaug, E., Shimmield, G., Smith, S., Smith, W., Takahashi, T., Treguer, P., Wallace, D., Wanninkhof, R., Watson, A., Willebrand, J., and Wong, C. S., 2001. A new vision of ocean biogeochemistry after a decade of the Joint Global Ocean Flux Study (JGOFS). Ambio, 4-31

Ferrari, V. C., and Hollibaugh, J. T., 1999. Distribution of microbial assemblages in the Central Arctic Ocean Basin studied by PCR/DGGE: analysis of a large data set. Hydrobiologia, 401, 55-68

Ferrier-Pages, C., Karner, M., and Rassoulzadegan, F., 1998. Release of dissolved amino acids by flagellates and ciliates grazing on bacteria. Oceanol. Acta, 21, 485-494

Fichtinger-Schepman, A. M. J., Kamerling, J. P., Vliegenthart, J. F. G., Dejong, E. W., Bosch, L., and Westbroek, P., 1979. Composition of a methylated, acidic polysaccharide associated with coccoliths of *Emiliania huxleyi* (Lohmann) Kamptner. Carbohydr. Res., 69, 181-189

Field, C. B., Behrenfeld, M. J., Randerson, J. T., and Falkowski, P., 1998. Primary production of the biosphere: Integrating terrestrial and oceanic components. Science, 281, 237-240

Fileman, E. S., Cummings, D. G., and Llewellyn, C. A., 2002. Microplankton community structure and the impact of microzooplankton grazing during an *Emiliania huxleyi* bloom, off the Devon coast. Journal of the Marine Biological Association of the United Kingdom, 82, 359-368

Finkel, Z. V., Beardall, J., Flynn, K. J., Quigg, A., Rees, T. A. V., and Raven, J. A., 2010. Phytoplankton in a changing world: cell size and elemental stoichiometry. J. Plankton Res., 32, 119-137

Fiorini, S., Middelburg, J. J., and Gattuso, J. P., subm. Testing the effects of elevated pCO_2 on coccolithophores (*Prymnesiophyceae*): comparison between haploid and diploid life stages.

Follows, M., and Dutkiewicz, S., 2002. Meteorological modulation of the North Atlantic spring bloom. Deep-Sea Research Part Ii-Topical Studies in Oceanography, 49, 321-344

Frette, L., Winding, A., and Kroer, N., 2010. Genetic and metabolic diversity of Arctic bacterioplankton during the post-spring phytoplankton bloom in Disko Bay, western Greenland. Aquat. Microb. Ecol., 60, 29-41

Fuhrman, J. A., 2009. Microbial community structure and its functional implications. Nature, 459, 193-199

Fuhrman, J. A., and Steele, J. A., 2008. Community structure of marine bacterioplankton: patterns, networks, and relationships to function. Aquat. Microb. Ecol., 53, 69-81

Fuhrman, J. A., and Hagström, A. 2008. Bacterial and archeal community structure and its patterns, in: Microbial Ecology of the Oceans, edited by: Kirchman, D. L., Wiley, 45-90

Fuhrman, J. A., Hewson, I., Schwalbach, M. S., Steele, J. A., Brown, M. V., and Naeem, S., 2006. Annually reoccurring bacterial communities are predictable from ocean conditions. Proceedings of the National Academy of Sciences of the United States of America, 103, 13104-13109

Garcia-Soto, C., FernÃ¡ndez, E., Pingree, R. D., and Harbour, D. S., 1995. Evolution and structure of a shelf coccolithophore bloom in the Western English Channel. J. Plankton Res., 17, 2011-2036

Gärdes, A., Iversen, M. H., Grossart, H.-P., Passow, U., and Ullrich, M. S., 2010. Diatom-associated bacteria are required for aggregation of *Thalassiosira weissflogii*. ISME J

Gasol, J. M., Pinhassi, J., Alonso-Saez, L., Ducklow, H., Herndl, G. J., Koblizek, M., Labrenz, M., Luo, Y., Moran, X. A. G., Reinthaler, T., and Simon, M., 2008. Towards a better understanding of microbial carbon flux in the sea. Aquat. Microb. Ecol., 53, 21-38

Ghiglione, J. F., Conan, P., and Pujo-Pay, M., 2009. Diversity of total and active free-living vs. particle-attached bacteria in the euphotic zone of the NW Mediterranean Sea. Fems Microbiology Letters, 299, 9-21

Ghiglione, J. F., Mevel, G., Pujo-Pay, M., Mousseau, L., Lebaron, P., and Goutx, M., 2007. Diel and seasonal variations in abundance, activity, and community structure of particle-attached and free-living bacteria in NW Mediterranean Sea. Microb. Ecol., 54, 217-231

Gibb, S. W., Cummings, D. G., Irigoien, X., Barlow, R. G., Fauzi, R., and Mantoura, C., 2001. Phytoplankton pigment chemotaxonomy of the northeastern Atlantic. Deep-Sea Research Part Ii-Topical Studies in Oceanography, 48, 795-823

Gilbert, J. A., Field, D., Swift, P., Newbold, L., Oliver, A., Smyth, T., Somerfield, P. J., Huse, S., and Joint, I., 2009. The seasonal structure of microbial communities in the Western English Channel. Environmental Microbiology, 11, 3132-3139

Gilbert, J. A., Field, D., Swift, P., Thomas, S., Cummings, D., Temperton, B., Weynberg, K., Huse, S., Hughes, M., Joint, I., Somerfield, P. J., and Muhling, M., 2010. The Taxonomic and Functional Diversity of Microbes at a Temperate Coastal Site: A 'Multi-Omic' Study of Seasonal and Diel Temporal Variation. PLoS One, 5

Giroldo, D., Vieira, A. A. H., and Paulsen, B. S., 2003. Relative increase of deoxy sugars during microbial degradation of an extracellular polysaccharide released by a tropical freshwater *Thalassiosira* sp (*Bacillariophyceae*). Journal of Phycology, 39, 1109-1115

Godoi, R. H. M., Aerts, K., Harlay, J., Kaegi, R., Ro, C. U., Chou, L., and Van Grieken, R., 2009. Organic surface coating on Coccolithophores - *Emiliania huxleyi*: Its determination and implication in the marine carbon cycle. Microchemical Journal, 91, 266-271

Gogou, A., and Repeta, D. J., 2010. Particulate-dissolved transformations as a sink for semi-labile dissolved organic matter: Chemical characterization of high molecular weight dissolved and surface-active organic matter in seawater and in diatom cultures. Marine Chemistry, 121, 215-223

Gomez-Pereira, P. R., Fuchs, B. M., Alonso, C., Oliver, M. J., van Beusekom, J. E. E., and Amann, R., 2010. Distinct flavobacterial communities in contrasting water masses of the North Atlantic Ocean. Isme J., 4, 472-487

Gomez, F., Furuya, K., and Takeda, S., 2005. Distribution of the cyanobacterium Richelia intracellularis as an epiphyte of the diatom *Chaetoceros compressus* in the western Pacific Ocean. J. Plankton Res., 27, 323-330

Gonzalez, J. M., Simo, R., Massana, R., Covert, J. S., Casamayor, E. O., Pedros-Alio, C., and Moran, M. A., 2000. Bacterial community structure associated with a dimethylsulfoniopropionate-producing North Atlantic algal bloom. Appl. Environ. Microbiol., 66, 4237-4246

Gonzalez, J. M., Fernandez-Gomez, B., Fernandez-Guerra, A., Gomez-Consarnau, L., Sanchez, O., Coll-Llado, M., del Campo, J., Escudero, L., Rodriguez-Martinez, R., Alonso-Saez, L., Latasa, M., Paulsen, I., Nedashkovskaya, O., Lekunberri, I., Pinhassi, J., and Pedros-Alio, C., 2008. Genome analysis of the proteorhodopsin-containing marine bacterium *Polaribacter* sp MED152 (*Flavobacteria*). Proceedings of the National Academy of Sciences of the United States of America, 105, 8724-8729

Grasshoff, K., Ehrhardt, M., and Kremling, K.: Methods of Seawater Analysis, in, Verlag Chemie, 1983.

Green, J. C., Course, P. A., and Tarran, G. A., 1996. The life-cycle of *Emiliania huxleyi*: A brief review and a study of relative ploidy levels analysed by flow cytometry. Journal of Marine Systems, 9, 33-44

Grossart, H. P., 2010. Ecological consequences of bacterioplankton lifestyles: changes in concepts are needed. Environ. Microbiol. Rep., 2, 706-714

Grossart, H. P., and Simon, M., 2007. Interactions of planktonic algae and bacteria: effects on algal growth and organic matter dynamics. Aquat. Microb. Ecol., 47, 163-176

Grossart, H. P., Czub, G., and Simon, M., 2006a. Algae-bacteria interactions and their effects on aggregation and organic matter flux in the sea. Environmental Microbiology, 8, 1074-1084

Grossart, H. P., Tang, K. W., Kiorboe, T., and Ploug, H., 2007a. Comparison of cell-specific activity between free-living and attached bacteria using isolates and natural assemblages. Fems Microbiology Letters, 266, 194-200

Grossart, H. P., Levold, F., Allgaier, M., Simon, M., and Brinkhoff, T., 2005. Marine diatom species harbour distinct bacterial communities. Environmental Microbiology, 7, 860-873

Grossart, H. P., Kiorboe, T., Tang, K. W., Allgaier, M., Yam, E. M., and Ploug, H., 2006b. Interactions between marine snow and heterotrophic bacteria: aggregate formation and microbial dynamics. Aquat. Microb. Ecol., 42, 19-26

Grossart, H. P., Engel, A., Arnosti, C., De La Rocha, C. L., Murray, A. E., and Passow, U., 2007b. Microbial dynamics in autotrophic and heterotrophic seawater mesocosms. III. Organic matter fluxes. Aquat. Microb. Ecol., 49, 143-156

Guidi, L., Stemmann, L., Jackson, G. A., Ibanez, F., Claustre, H., Legendre, L., Picheral, M., and Gorsky, G., 2009. Effects of phytoplankton community on production, size and export of large aggregates: A world-ocean analysis. Limnol. Oceanogr., 54, 1951-1963

Guillard, R. 2005. Purification methods for microalgae, in: Algal Culturing Techniques, edited by: Andersen, R., Elsevier Academic Press,

Gutierrez-Zamora, M. L., and Manefield, M., 2010. An appraisal of methods for linking environmental processes to specific microbial taxa. Rev. Environ. Sci. Bio-Technol., 9, 153-185

Hama, T., and Yanagi, K., 2001. Production and neutral aldose composition of dissolved carbohydrates excreted by natural marine phytoplankton populations. Limnol. Oceanogr., 46, 1945-1955

Hamels, I., Mussche, H., Sabbe, K., Muylaert, K., and Vyverman, W., 2004. Evidence for constant and highly specific active food selection by benthic ciliates in mixed diatoms assemblages. Limnol. Oceanogr., 49, 58-68

Hansell, D. A., and Carlson, C. A., 1998. Deep-ocean gradients in the concentration of dissolved organic carbon. Nature, 395, 263-266

Harlay, J. 2009. Biogeochamical study of coccolithophorid studies in the context of climate change, PhD, Département des Sciences de la Terre et de l'Environnement, ULB, Brussels

Harlay, J., De Bodt, C., Engel, A., Jansen, S., d'Hoop, Q., Piontek, J., Van Oostende, N., Groom, S., Sabbe, K., and Chou, L., 2009. Abundance and size distribution of transparent exopolymer particles (TEP) in a coccolithophorid bloom in the northern Bay of Biscay. Deep-Sea Res. Part I-Oceanogr. Res. Pap., 56, 1251-1265

Harlay, J., Chou, L., De Bodt, C., Van Oostende, N., Piontek, J., Suykens, K., Engel, A., Sabbe, K., Groom, S., Delille, B., and Borges, A. V., 2011. Biogeochemistry and carbon mass balance of a coccolithophore bloom in the northern Bay of Biscay (June 2006). Deep Sea Research Part I: Oceanographic Research Papers, 58, 111-127

Harlay, J., Borges, A. V., Van der Zee, C., Delille, B., Godoi, R. H. M., Schiettecatte, L. S., Roevros, N., Aerts, K., Lapernat, P. E., Rebreanu, L., Groom, S., Daro, M. H., Van Grieken, R., and Chou, L., 2010. Biogeochemical study of a coccolithophore bloom in the northern Bay of Biscay (NE Atlantic Ocean) in June 2004. Progress in Oceanography, 86, 317-336

Harris, R. P., 1994. Zooplankton grazing on the coccolithophore *Emiliania huxleyi* and its role in inorganic carbon flux. Marine Biology, 119, 431-439

Hasegawa, Y., Martin, J. L., Giewat, M. W., and Rooney-Varga, J. N., 2007. Microbial community diversity in the phycosphere of natural populations of the toxic alga, Alexandrium fundyense. Environmental Microbiology, 9, 3108-3121

Hasle, G. R., and Syvertsen, E. E. 1996. Marine diatoms, Identifying marine diatoms and dinoflagellates edited by: Tomas, C. R., Academic Press Inc., San Diego, 5-385 pp.

Havskum, H., Schluter, L., Scharek, R., Berdalet, E., and Jacquet, S., 2004. Routine quantification of phytoplankton groups - microscopy or pigment analyses? Mar. Ecol.-Prog. Ser., 273, 31-42

Hay, W. W. 2004. Carbonate fluxes and calcareous nannoplankton, Coccolithophores: From Molecular Processes to Global Impact, edited by: Thierstein, H. R., and Young, J. R., 509-528 pp.

Head, R. N., Crawford, D. W., Egge, J. K., Harris, R. P., Kristiansen, S., Lesley, D. J., Maranon, E., Pond, D., and Purdie, D. A., 1998. The hydrography and biology of a bloom of the coccolithophorid *Emiliania huxleyi* in the northern North Sea. Journal of Sea Research, 39, 255-266

Henson, S. A., Robinson, I., Allen, J. T., and Waniek, J. J., 2006. Effect of meteorological conditions on interannual variability in timing and magnitude of the spring bloom in the Irminger Basin, North Atlantic. Deep-Sea Res. Part I-Oceanogr. Res. Pap., 53, 1601-1615

Hewson, I., Steele, J. A., Capone, D. G., and Fuhrman, J. A., 2006. Temporal and spatial scales of variation in bacterioplankton assemblages of oligotrophic surface waters. Mar. Ecol.-Prog. Ser., 311, 67-77

Hodges, L. R., Bano, N., Hollibaugh, J. T., and Yager, P. L., 2005. Illustrating the importance of particulate organic matter to pelagic microbial abundance and community structure - an Arctic case study. Aquat. Microb. Ecol., 40, 217-227

Höfle, M. G., Kirchman, D. L., Christen, R., and Brettar, I., 2008. Molecular diversity of bacterioplankton: link to a predictive biogeochemistry of pelagic ecosystems. Aquat. Microb. Ecol., 53, 39-58

Höfle, M. G., Flavier, S., Christen, R., Botel, J., Labrenz, M., and Brettar, I., 2005. Retrieval of nearly complete 16S rRNA gene sequences from environmental DNA following 16S rRNA-based community fingerprinting. Environmental Microbiology, 7, 670-675

Hollibaugh, J. T., Wong, P. S., and Murrell, M. C., 2000. Similarity of particle-associated and free-living bacterial communities in northern San Francisco Bay, California. Aquat. Microb. Ecol., 21, 103-114

Hollibaugh, J. T., Wong, P. S., Bano, N., Pak, S. K., Prager, E. M., and Orrego, C., 2001. Stratification of microbial assemblages in Mono Lake, California, and response to a mixing event. Hydrobiologia, 466, 45-60

Holligan, P. M., and Groom, S. B., 1986. Phytoplankton distributions along the shelf break. Proceedings of the Royal Society of Edinburgh Section B-Biological Sciences, 88, 239-263

Holligan, P. M., and Balch, W. M. 1991. From the ocean to cells: coccolithophore optics and biogeochemistry, in: Particles analysis in Oceanography, edited by: Demers, S., 301-324

Holligan, P. M., Fernandez, E., Aiken, J., Balch, W. M., Boyd, P., Burkill, P. H., Finch, M., Groom, S. B., Malin, G., Muller, K., Purdie, D. A., Robinson, C., Trees, C. C., Turner, S. M., and Vanderwal, P., 1993. A biogeochemical study of the coccolithophore, *Emiliania huxleyi*, in the North-Atlantic. Glob. Biogeochem. Cycle, 7, 879-900

Honjo, S. 1996. Fluxes of particles to the interior of the open oceans, in: Particle Flux in the Oceans, edited by: Ittekkot, V., Schäfer, P., Honjo, S., and Depetris, P., Scope, Wiley, 91-154

Honjo, S., Dymond, J., Prell, W., and Ittekkot, V., 1999. Monsoon-controlled export fluxes to the interior of the Arabian Sea. Deep-Sea Research Part Ii-Topical Studies in Oceanography, 46, 1859-1902

Hood, R. R., Laws, E. A., Armstrong, R. A., Bates, N. R., Brown, C. W., Carlson, C. A., Chai, F., Doney, S. C., Falkowski, P. G., Feely, R. A., Friedrichs, M. A. M., Landry, M. R., Moore, J. K., Nelson, D. M., Richardson, T. L., Salihoglu, B., Schartau, M., Toole, D. A., and Wiggert, J. D., 2006. Pelagic functional group modeling: Progress, challenges and prospects. Deep-Sea Research Part Ii-Topical Studies in Oceanography, 53, 459-512

Houdan, A., Probert, I., Van Lenning, K., and Lefebvre, S., 2005. Comparison of photosynthetic responses in diploid and haploid life-cycle phases of *Emiliania huxleyi* (*Prymnesiophyceae*). Mar. Ecol.-Prog. Ser., 292, 139-146

Houdan, A., Probert, I., Zatylny, C., Veron, B., and Billard, C., 2006. Ecology of oceanic coccolithophores. I. Nutritional preferences of the two stages in the life cycle of *Coccolithus braarudii* and *Calcidiscus leptoporus*. Aquat. Microb. Ecol., 44, 291-301

Houdan, A., Billard, C., Marie, D., Not, F., Sáez, A. G., Young, J. R., and Probert, I., 2004. Holococcolithophore-heterococcolithophore (Haptophyta) life cycles: Flow cytometric analysis of relative ploidy levels. Systematics and Biodiversity, 1, 453-465

Howard, E. C., Sun, S. L., Reisch, C. R., del Valle, D. A., Burgmann, H., Kiene, R. P., and Moran, M. A., 2011. Changes in Dimethylsulfoniopropionate Demethylase Gene Assemblages in Response to an Induced Phytoplankton Bloom. Appl. Environ. Microbiol., 77, 524-531

Huang, B. Q., Liu, Y., Xiang, W. G., Tian, H. J., Liu, H. B., Cao, Z. R., and Hong, H. S., 2008. Grazing impact of microzooplankton on phytoplankton in the Xiamen Bay using pigment-specific dilution technique. Acta Oceanol. Sin., 27, 147-162

Huthnance, J. M., Coelho, H., Griffiths, C. R., Knight, P. J., Rees, A. P., Sinha, B., Vangriesheim, A., White, M., and Chatwin, P. G., 2001. Physical structures, advection and mixing in the region of Goban spur. Deep-Sea Research Part Ii-Topical Studies in Oceanography, 48, 2979-3021

Ietswaart, T., Schneider, P. J., and Prins, R. A., 1994. Utilization of organic nitrogen-sources by 2 phytoplankton species and a bacterial isolate in pure and mixed cultures. Appl. Environ. Microbiol., 60, 1554-1560

Iglesias-Rodriguez, M. D., Probert, I., and Batley, J., 2006. Microsatellite cross-amplification in coccolithophores: application in population diversity studies. Hereditas, 143, 99-102

Iglesias-Rodriguez, M. D., Saez, A. G., Groben, R., Edwards, K. J., Batley, J., Medlin, L. K., and Hayes, P. K., 2002a. Polymorphic microsatellite loci in global populations of the marine coccolithophorid *Emiliania huxleyi*. Mol. Ecol. Notes, 2, 495-497

Iglesias-Rodriguez, M. D., Brown, C. W., Doney, S. C., Kleypas, J., Kolber, D., Kolber, Z., Hayes, P. K., and Falkowski, P. G., 2002b. Representing key phytoplankton functional groups in ocean carbon cycle models: Coccolithophorids. Glob. Biogeochem. Cycle, 16

Irigoien, X., Meyer, B., Harris, R., and Harbour, D., 2004. Using HPLC pigment analysis to investigate phytoplankton taxonomy: the importance of knowing your species. Helgoland Mar. Res., 58, 77-82

Iversen, M. H., and Ploug, H., 2010. Ballast minerals and the sinking carbon flux in the ocean: carbon-specific respiration rates and sinking velocity of marine snow aggregates. Biogeosciences, 7, 2613-2624

Jacquet, S., Heldal, M., Iglesias-Rodriguez, D., Larsen, A., Wilson, W., and Bratbak, G., 2002. Flow cytometric analysis of an *Emiliana huxleyi* bloom terminated by viral infection. Aquat. Microb. Ecol., 27, 111-124

Jasti, S., Sieracki, M. E., Poulton, N. J., Giewat, M. W., and Rooney-Varga, J. N., 2005. Phylogenetic diversity and specificity of bacteria closely associated with *Alexandrium* spp. and other phytoplankton. Appl. Environ. Microbiol., 71, 3483-3494

Ji, R. B., Edwards, M., Mackas, D. L., Runge, J. A., and Thomas, A. C., 2010. Marine plankton phenology and life history in a changing climate: current research and future directions. J. Plankton Res., 32, 1355-1368

Johnsen, G., and Sakshaug, E., 1993. Biooptical characteristics and photoadaptive responses in the toxic and bloom-forming dinoflagellates *Gyrodinium aureolum,Gymnodinium*

galatheanum, and 2 strains on *Prorocentrum minimum*. Journal of Phycology, 29, 627-642

Joint, I., Wollast, R., Chou, L., Batten, S., Elskens, M., Edwards, E., Hirst, A., Burkill, P., Groom, S., Gibb, S., Miller, A., Hydes, D., Dehairs, F., Antia, A., Barlow, R., Rees, A., Pomroy, A., Brockmann, U., Cummings, D., Lampitt, R., Loijens, M., Mantoura, F., Miller, P., Raabe, T., Alvarez-Salgado, X., Stelfox, C., and Woolfenden, J., 2001. Pelagic production at the Celtic Sea shelf break. Deep-Sea Research Part Ii-Topical Studies in Oceanography, 48, 3049-3081

Joint, I. R., Owens, N. J. P., and Pomroy, A. J., 1986. Seasonal production of photosynthetic picoplankton and nanoplankton in the Celtic Sea. Mar. Ecol.-Prog. Ser, 28, 251-258

Jones, K. L., Mikulski, C. M., Barnhorst, A., and Doucette, G. J., 2010. Comparative analysis of bacterioplankton assemblages from *Karenia brevis* bloom and nonbloom water on the west Florida shelf (Gulf of Mexico, USA) using 16S rRNA gene clone libraries. FEMS Microbiol. Ecol., 73, 468-485

Kayano, K., and Shiraiwa, Y., 2009. Physiological Regulation of Coccolith Polysaccharide Production by Phosphate Availability in the Coccolithophorid *Emiliania huxleyi*. Plant Cell Physiol., 50, 1522-1531

Keller, M. D., Bellows, W. K., and Guillard, R. R. L., 1989. Dimethyl sulfide production in marine-phytoplankton. Acs Symposium Series, 393, 167-182

Kiene, R. P., Linn, L. J., and Bruton, J. A., 2000. New and important roles for DMSP in marine microbial communities. Journal of Sea Research, 43, 209-224

Kimmance, S. A., and Brussaard, C. P. D. 2010. Estimation of viral-induced phytoplankton mortality using the modified dilution method, in: Manual of Aquatic Viral Ecology, edited by: Wilhelm, S. W., Weinbauer, M. G., and Suttle, C. A., American Sociaty of Limnology and Oceanography, Inc., 65-73

Kimmance, S. A., Wilson, W. H., and Archer, S. D., 2007. Modified dilution technique to estimate viral versus grazing mortality of phytoplankton: limitations associated with method sensitivity in natural waters. Aquat. Microb. Ecol., 49, 207-222

Kiørboe, T. 1993. Turbulence, phytoplanlton cell size, and the structure of pelagic food webs, Advances in Marine Biology, Academic Press Limited

Koroleff, F. 1983. Determination of dissolved inorganic phosphate, in: Methods of Seawater Analysis, 2nd ed., edited by: Grasshoff, K., Kremling, K., and Ehrhardt, M., Verlag,

Kroer, N., 1993. Bacterial-growth efficiency on natural dissolved organic-matter. Limnol. Oceanogr., 38, 1282-1290

Lami, R., Ghiglione, J. F., Desdevises, Y., West, N. J., and Lebaron, P., 2009. Annual patterns of presence and activity of marine bacteria monitored by 16S rDNA-16S rRNA fingerprints in the coastal NW Mediterranean Sea. Aquat. Microb. Ecol., 54, 199-210

Lampert, L., Queguiner, B., Labasque, T., Pichon, A., and Lebreton, N., 2002. Spatial variability of phytoplankton composition and biomass on the eastern continental shelf of the Bay of Biscay (north-east Atlantic Ocean). Evidence for a bloom of *Emiliania huxleyi* (*Prymnesiophyceae*) in spring 1998. Cont. Shelf Res., 22, 1225-1247

Lamy, D., Obernosterer, I., Laghdass, M., Artigas, L. F., Breton, E., Grattepanche, J. D., Lecuyer, E., Degros, N., Lebaron, P., and Christaki, U., 2009. Temporal changes of major bacterial groups and bacterial heterotrophic activity during a Phaeocystis globosa bloom in the eastern English Channel. Aquat. Microb. Ecol., 58, 95-107

Lancelot, C., 1983. Factors affecting phytoplankton extracellular release in the southern bight of the North-Sea. Mar. Ecol.-Prog. Ser., 12, 115-121

Lancelot, C., 1984. Extracellular release of small and large molecules by phytoplankton in the southern bight of the North-Sea. Estuar. Coast. Shelf Sci., 18, 65-77

Landry, M. R., and Hassett, R. P., 1982. Estimating the grazing impact of marine micro-zooplankton. Marine Biology, 67, 283-288

Landry, M. R., and Calbet, A., 2004. Microzooplankton production in the oceans. Ices Journal of Marine Science, 61, 501-507

Landry, M. R., Brown, S. L., Campbell, L., Constantinou, J., and Liu, H. B., 1998. Spatial patterns in phytoplankton growth and microzooplankton grazing in the Arabian Sea during monsoon forcing. Deep-Sea Research Part Ii-Topical Studies in Oceanography, 45, 2353-2368

Landry, M. R., Ohman, M. D., Goericke, R., Stukel, M. R., and Tsyrklevich, K., 2009. Lagrangian studies of phytoplankton growth and grazing relationships in a coastal upwelling ecosystem off Southern California. Progress in Oceanography, 83, 208-216

Langer, G., Nehrke, G., Probert, I., Ly, J., and Ziveri, P., 2009. Strain-specific responses of Emiliania huxleyi to changing seawater carbonate chemistry. Biogeosciences, 6, 2637-2646

Latasa, M., 2007. Improving estimations of phytoplankton class abundances using CHEMTAX. Mar. Ecol.-Prog. Ser., 329, 13-21

Latasa, M., Scharek, R., Le Gall, F., and Guillou, L., 2004. Pigment suites and taxonomic groups in Prasinophyceae. Journal of Phycology, 40, 1149-1155

Lauro, F. M., McDougald, D., Thomas, T., Williams, T. J., Egan, S., Rice, S., DeMaere, M. Z., Ting, L., Ertan, H., Johnson, J., Ferriera, S., Lapidus, A., Anderson, I., Kyrpides, N., Munk, A. C., Detter, C., Han, C. S., Brown, M. V., Robb, F. T., Kjelleberg, S., and Cavicchioli, R., 2009. The genomic basis of trophic strategy in marine bacteria. Proceedings of the National Academy of Sciences of the United States of America, 106, 15527-15533

Lear, G., Anderson, M. J., Smith, J. P., Boxen, K., and Lewis, G. D., 2008. Spatial and temporal heterogeneity of the bacterial communities in stream epilithic biofilms. FEMS Microbiol. Ecol., 65, 463-473

Leblanc, K., Hare, C. E., Feng, Y., Berg, G. M., DiTullio, G. R., Neeley, A., Benner, I., Sprengel, C., Beck, A., Sanudo-Wilhelmy, S. A., Passow, U., Klinck, K., Rowe, J. M., Wilhelm, S. W., Brown, C. W., and Hutchins, D. A., 2009. Distribution of calcifying and silicifying phytoplankton in relation to environmental and biogeochemical parameters during the late stages of the 2005 North East Atlantic Spring Bloom. Biogeosciences, 6, 2155-2179

Legendre, P., and Legendre, L. 1998. Numerical Ecology, 2nd ed., Elsevier Science BV, Amsterdam, 853 pp.

Lessard, E. J., Merico, A., and Tyrrell, T., 2005. Nitrate : phosphate ratios and *Emiliania huxleyi* blooms. Limnol. Oceanogr., 50, 1020-1024

Litchman, E., Klausmeier, C. A., Schofield, O. M., and Falkowski, P. G., 2007. The role of functional traits and trade-offs in structuring phytoplankton communities: scaling from cellular to ecosystem level. Ecol. Lett., 10, 1170-1181

Liu, H. B., Bidigare, R. R., Laws, E., Landry, M. R., and Campbell, L., 1999. Cell cycle and physiological characteristics of *Synechococcus* (WH7803) in chemostat culture. Mar. Ecol.-Prog. Ser., 189, 17-25

Liu, H. B., Suzuki, K., Nishioka, J., Sohrin, R., and Nakatsuka, T., 2009. Phytoplankton growth and microzooplankton grazing in the Sea of Okhotsk during late summer of 2006. Deep-Sea Res. Part I-Oceanogr. Res. Pap., 56, 561-570

Llewellyn, C. A., and Gibb, S. W., 2000. Intra-class variability in the carbon, pigment and biomineral content of prymnesiophytes and diatoms. Mar. Ecol.-Prog. Ser., 193, 33-44

Lochte, K., Ducklow, H. W., Fasham, M. J. R., and Stienen, C., 1993. Plankton succession and carbon cycling at 47°N-20°W during the JGOFS North-Atlantic bloom experiment. Deep-Sea Research Part Ii-Topical Studies in Oceanography, 40, 91-114

Loebl, M., Cockshutt, A. M., Campbell, D. A., and Finkel, Z. V., 2010. Physiological basis for high resistance to photoinhibition under nitrogen depletion in *Emiliania huxleyi*. Limnol. Oceanogr., 55, 2150-2160

Logan, B. E., Grossart, H. P., and Simon, M., 1994. Direct observation of phytoplankton, TEP and aggregates on polycarbonate filters using brightfield microscopy. J. Plankton Res., 16, 1811-1815

Longnecker, K., Wilson, M. J., Sherr, E. B., and Sherr, B. F., 2010. Effect of top-down control on cell-specific activity and diversity of active marine bacterioplankton. Aquat. Microb. Ecol., 58, 153-165

Macián, M. C., Arahal, D. R., Garay, E., Ludwig, W., Schleifer, K. H., and Pujalte, M. J., 2005. *Thalassobacter stenotrophicus* gen. nov., sp. nov., a novel marine Alpha-proteobacterium isolated from Mediterranean sea water. Int J Syst Evol Microbiol, 55, 105-110

Mackey, M. D., Mackey, D. J., Higgins, H. W., and Wright, S. W., 1996. CHEMTAX - A program for estimating class abundances from chemical markers: Application to HPLC measurements of phytoplankton. Mar. Ecol.-Prog. Ser., 144, 265-283

Malfatti, F., and Azam, F., 2009. Atomic force microscopy reveals microscale networks and possible symbioses among pelagic marine bacteria. Aquat. Microb. Ecol., 58, 1-14

Margalef, R., 1978. Life-forms of phytoplankton as survival alternatives in an unstable environment. Oceanol. Acta, 1, 493-509

Mari, X., 1999. Carbon content and C : N ratio of transparent exopolymeric particles (TEP) produced by bubbling exudates of diatoms. Mar. Ecol.-Prog. Ser., 183, 59-71

Mari, X., and Kiorboe, T., 1996. Abundance, size distribution and bacterial colonization of transparent exopolymeric particles (TEP) during spring in the Kattegat. J. Plankton Res., 18, 969-986

Mari, X., and Burd, A., 1998. Seasonal size spectra of transparent exopolymeric particles (TEP) in a coastal sea and comparison with those predicted using coagulation theory. Mar. Ecol.-Prog. Ser., 163, 63-76

Martinez, J., Smith, D. C., Steward, G. F., and Azam, F., 1996. Variability in ectohydrolytic enzyme activities of pelagic marine bacteria and its significance for substrate processing in the sea. Aquat. Microb. Ecol., 10, 223-230

Martinez, J. M., Schroeder, D. C., Larsen, A., Bratbak, G., and Wilson, W. H., 2007. Molecular dynamics of *Emiliania huxleyi* and cooccurring viruses during two separate mesocosm studies. Appl. Environ. Microbiol., 73, 554-562

Matrai, P. A., and Keller, M. D., 1993. Dimethylsulfide in a large-scale coccolithophore bloom in the Gulf of Maine. Cont. Shelf Res., 13, 831-843

Mayali, X., and Azam, F., 2004. Algicidal bacteria in the sea and their impact on algal blooms. J. Eukaryot. Microbiol., 51, 139-144

McArdle, B. H., and Anderson, M. J., 2001. Fitting multivariate models to community data: A comment on distance-based redundancy analysis. Ecology, 82, 290-297

McCarren, J., Becker, J. W., Repeta, D. J., Shi, Y., Young, C. R., Malmstrom, R. R., Chisholm, S. W., and DeLong, E. F., 2010. Microbial community transcriptomes reveal microbes and metabolic pathways associated with dissolved organic matter turnover in the sea. Proceedings of the National Academy of Sciences, 107, 16420-16427

McCarthy, M., Hedges, J., and Benner, R., 1996. Major biochemical composition of dissolved high molecular weight organic matter in seawater. Marine Chemistry, 55, 281-297

Medlin, L. K., Barker, G. L. A., Campbell, L., Green, J. C., Hayes, P. K., Marie, D., Wrieden, S., and Vaulot, D., 1996. Genetic characterisation of *Emiliania huxleyi* (Haptophyta). Journal of Marine Systems, 9, 13-31

Meon, B., and Kirchman, D. L., 2001. Dynamics and molecular composition of dissolved organic material during experimental phytoplankton blooms. Marine Chemistry, 75, 185-199

Michaels, A. F., and Silver, M. W., 1988. Primary production, sinking fluxes and the microbial food web. Deep-Sea Research Part a-Oceanographic Research Papers, 35, 473-490

Middelburg, J. J., Barranguet, C., Boschker, H. T. S., Herman, P. M. J., Moens, T., and Heip, C. H. R., 2000. The fate of intertidal microphytobenthos carbon: An in situ C-13-labeling study. Limnol. Oceanogr., 45, 1224-1234

Miki, T., Giuggioli, L., Kobayashi, Y., Nagata, T., and Levin, S. A., 2009. Vertically structured prokaryotic community can control the efficiency of the biological pump in the oceans. Theor. Ecol., 2, 199-216

Moeseneder, M. M., Winter, C., and Herndl, G. J., 2001. Horizontal and vertical complexity of attached and free-living bacteria of the eastern Mediterranean Sea, determined by 16S rDNA and 16S rRNA fingerprints. Limnol. Oceanogr., 46, 95-107

Moodley, L., Boschker, H. T. S., Middelburg, J. J., Pel, R., Herman, P. M. J., de Deckere, E., and Heip, C. H. R., 2000. Ecological significance of benthic foraminifera: (13)C labelling experiments. Mar. Ecol.-Prog. Ser., 202, 289-295

Moodley, L., Middelburg, J. J., Boschker, H. T. S., Duineveld, G. C. A., Pel, R., Herman, P. M. J., and Heip, C. H. R., 2002. Bacteria and Foraminifera: key players in a short-term deep-sea benthic response to phytodetritus. Mar. Ecol.-Prog. Ser., 236, 23-29

Morán, X. A. G., Calvo-Diaz, A., and Ducklow, H. W., 2010. Total and phytoplankton mediated bottom-up control of bacterioplankton change with temperature in NE Atlantic shelf waters. Aquat. Microb. Ecol., 58, 229-239

Morris, R. M., Vergin, K. L., Cho, J. C., Rappe, M. S., Carlson, C. A., and Giovannoni, S. J., 2005. Temporal and spatial response of bacterioplankton lineages to annual convective overturn at the Bermuda Atlantic Time-series Study site. Limnol. Oceanogr., 50, 1687-1696

Morris, R. M., Rappe, M. S., Connon, S. A., Vergin, K. L., Siebold, W. A., Carlson, C. A., and Giovannoni, S. J., 2002. SAR11 clade dominates ocean surface bacterioplankton communities. Nature, 420, 806-810

Mou, X. Z., Sun, S. L., Edwards, R. A., Hodson, R. E., and Moran, M. A., 2008. Bacterial carbon processing by generalist species in the coastal ocean. Nature, 451, 708-U704

Muggli, D. L., and Harrison, P. J., 1996a. Effects of nitrogen source on the physiology and metal nutrition of Emiliania huxleyi grown under different iron and light conditions. Mar. Ecol.-Prog. Ser., 130, 255-267

Muggli, D. L., and Harrison, P. J., 1996b. EDTA suppresses the growth of oceanic phytoplankton from the Northeast Subarctic Pacific. J. Exp. Mar. Biol. Ecol., 205, 221-227

Muylaert, K., Van der Gucht, K., Vloemans, N., De Meester, L., Gillis, M., and Vyverman, W., 2002. Relationship between bacterial community composition and bottom-up versus top-down variables in four eutrophic shallow lakes. Appl. Environ. Microbiol., 68, 4740-4750

Myklestad, S. M., 1995. Release of Extracellular Products by Phytoplankton with Special Emphasis on Polysaccharides. Science of the Total Environment, 165, 155-164

Myklestad, S. M. 2000. Dissolved organic carbon from phytoplankton, in: Marine Chemistry, edited by: Wangersky, P., The Handbook of Environmental Chemistry, 5D, Springer-Verlag, 111-148

Myklestad, S. M., Skanoy, E., and Hestmann, S., 1997. A sensitive and rapid method for analysis of dissolved mono- and polysaccharides in seawater. Marine Chemistry, 56, 279-286

Nanninga, H. J., and Tyrrell, T., 1996. Importance of light for the formation of algal blooms by *Emiliania huxleyi*. Mar. Ecol.-Prog. Ser., 136, 195-203

Nanninga, H. J., Ringenaldus, P., and Westbroek, P., 1996. Immunological quantitation of a polysaccharide formed by *Emiliania huxleyi*. Journal of Marine Systems, 9, 67-74

Neufeld, J. D., Boden, R., Moussard, H., Schafer, H., and Murrell, J. C., 2008. Substrate-Specific Clades of Active Marine Methylotrophs Associated with a Phytoplankton Bloom in a Temperate Coastal Environment. Appl. Environ. Microbiol., 74, 7321-7328

Norrman, B., Zweifel, U. L., Hopkinson, C. S., and Fry, B., 1995. Production and utilization of dissolved organic-carbon during an experimental diatom bloom. Limnol. Oceanogr., 40, 898-907

Oakes, J. M., Eyre, B. D., Middelburg, J. J., and Boschker, H. T. S., 2010. Composition, production, and loss of carbohydrates in subtropical shallow subtidal sandy sediments: Rapid processing and long-term retention revealed by C-13-labeling. Limnol. Oceanogr., 55, 2126-2138

Obernosterer, I., and Herndl, G. J., 1995. Phytoplankton Extracellular Release and Bacterial-Growth - Dependence on the Inorganic N-P Ratio. Mar. Ecol.-Prog. Ser., 116, 247-257

Olsen, G. J., Lane, D. J., Giovannoni, S. J., Pace, N. R., and Stahl, D. A., 1986. Microbial ecology and evolution - a ribosomal-RNA approach. Annual Review of Microbiology, 40, 337-365

Olson, M. B., and Strom, S. L., 2002. Phytoplankton growth, microzooplankton herbivory and community structure in the southeast Bering Sea: insight into the formation and temporal persistence of an *Emiliania huxleyi* bloom. Deep-Sea Research Part Ii-Topical Studies in Oceanography, 49, 5969-5990

Osburn, C. L., and St-Jean, G., 2007. The use of wet chemical oxidation with high-amplification isotope ratio mass spectrometry (WCO-IRMS) to measure stable isotope values of dissolved organic carbon in seawater. Limnology and Oceanography-Methods, 5, 296-308

Paasche, E., 2002. A review of the coccolithophorid *Emiliania huxleyi* (*Prymnesiophyceae*), with particular reference to growth, coccolith formation, and calcification-photosynthesis interactions. Phycologia, 40, 503-529

Pace, N. R., Olsen, G. J., and Woese, C. R., 1986. Ribosomal-RNA phylogeny and the primary lines of evolutionary descent. Cell, 45, 325-326

Painter, S. C., Lucas, M. I., Stinchcombe, M. C., Bibby, T. S., and Poulton, A. J., 2010a. Summertime trends in pelagic biogeochemistry at the Porcupine Abyssal Plain study site in the northeast Atlantic. Deep-Sea Research Part Ii-Topical Studies in Oceanography, 57, 1313-1323

Painter, S. C., Poulton, A. J., Allen, J. T., Pidcock, R., and Balch, W. M., 2010b. The COPAS'08 expedition to the Patagonian Shelf Physical and environmental conditions during the 2008 coccolithophore bloom. Cont. Shelf Res., 30, 1907-1923

Pakulski, J. D., and Benner, R., 1994. Abundance and distribution of carbohydrates in the ocean. Limnol. Oceanogr., 39, 930-940

Palenik, B., and Henson, S. E., 1997. The use of amides and other organic nitrogen sources by the phytoplankton Emiliania huxleyi. Limnol. Oceanogr., 42, 1544-1551

Panagiotopoulos, C., and Sempere, R., 2007. Sugar dynamics in large particles during in vitro incubation experiments. Mar. Ecol.-Prog. Ser., 330, 67-74

Panagiotopoulos, C., Repeta, D. J., and Johnson, C. G., 2007. Characterization of methyl sugars, 3-deoxysugars and methyl deoxysugars in marine high molecular weight dissolved organic matter. Org. Geochem., 38, 884-896

Passow, U., 2002a. Transparent exopolymer particles (TEP) in aquatic environments. Progress in Oceanography, 55, 287-333

Passow, U., 2002b. Production of transparent exopolymer particles (TEP) by phyto- and bacterioplankton. Mar. Ecol.-Prog. Ser., 236, 1-12

Passow, U., and Alldredge, A. L., 1994. Distribution, size and bacterial-colonization of transparent exopolymer particles (TEP) in the ocean. Mar. Ecol.-Prog. Ser., 113, 185-198

Passow, U., and Alldredge, A. L., 1995. Aggregation of a Diatom Bloom in a Mesocosm - the Role of Transparent Exopolymer Particles (Tep). Deep-Sea Research Part Ii-Topical Studies in Oceanography, 42, 99-109

Passow, U., Shipe, R. F., Murray, A., Pak, D. K., Brzezinski, M. A., and Alldredge, A. L., 2001. The origin of transparent exopolymer particles (TEP) and their role in the sedimentation of particulate matter. Cont. Shelf Res., 21, 327-346

Pedrotti, M. L., Beauvais, S., Kerros, M. E., Iversen, K., and Peters, F., 2009. Bacterial colonization of transparent exopolymeric particles in mesocosms under different turbulence intensities and nutrient conditions. Aquat. Microb. Ecol., 55, 301-312

Peres-Neto, P. R., Legendre, P., Dray, S., and Borcard, D., 2006. Variation partitioning of species data matrices: Estimation and comparison of fractions. Ecology, 87, 2614-2625

Pernthaler, A., Pernthaler, J., Eilers, H., and Amann, R., 2001. Growth patterns of two marine isolates: Adaptations to substrate patchiness? Appl. Environ. Microbiol., 67, 4077-4083

Pingree, R. D., and Mardell, G. T., 1981. Slope turbulence, internal waves and phytoplankton growth at the Celtic sea shelf-break. Philosophical Transactions of the Royal Society of London Series a-Mathematical Physical and Engineering Sciences, 302, 663-&

Pingree, R. D., and Lecann, B., 1989. Celtic and Armorican slope and shelf residual currents. Progress in Oceanography, 23, 303-338

Pingree, R. D., and New, A. L., 1995. Structure, seasonal development and sunglint spatial coherence of the internal tide on the Celtic and Armorican shelves and in the Bay of Biscay. Deep-Sea Res. Part I-Oceanogr. Res. Pap., 42, 245-284

Pinhassi, J., Sala, M. M., Havskum, H., Peters, F., Guadayol, O., Malits, A., and Marrase, C. L., 2004. Changes in bacterioplankton composition under different phytoplankton regimens. Appl. Environ. Microbiol., 70, 6753-6766

Piontek, J., Händel, N., De Bodt, C., Harlay, J., Chou, L., and Engel, A., submitted. The utilization of polysaccharides by heterotrophic bacterioplankton in the Bay of Biscay (North Atlantic Ocean). Biogeosciences

Ploug, H., Musat, N., Adam, B., Moraru, C. L., Lavik, G., Vagner, T., Bergman, B., and Kuypers, M. M. M., 2010. Carbon and nitrogen fluxes associated with the cyanobacterium *Aphanizomenon* sp. in the Baltic Sea. Isme J., 4, 1215-1223

Pomeroy, L. R., 1974. Oceans food web, a changing paradigm. Bioscience, 24, 499-504

Pommier, T., Canback, B., Riemann, L., Bostrom, K. H., Simu, K., Lundberg, P., Tunlid, A., and Hagstrom, A., 2007. Global patterns of diversity and community structure in marine bacterioplankton. Mol. Ecol., 16, 867-880

Porter, K. G., and Feig, Y. S., 1980. The use of DAPI for identifying and counting aquatic microflora. Limnol. Oceanogr., 25, 943-948

Poulton, A. J., Adey, T. R., Balch, W. M., and Holligan, P. M., 2007. Relating coccolithophore calcification rates to phytoplankton community dynamics: Regional differences and implications for carbon export. Deep-Sea Research Part Ii-Topical Studies in Oceanography, 54, 538-557

Poulton, A. J., Charalampopoulou, A., Young, J. R., Tarran, G. A., Lucas, M. I., and Quartly, G. D., 2010. Coccolithophore dynamics in non-bloom conditions during late summer in the central Iceland Basin (July-August 2007). Limnol. Oceanogr., 55, 1601-1613

Raitsos, D. E., Lavender, S. J., Pradhan, Y., Tyrrell, T., Reid, P. C., and Edwards, M., 2006. Coccolithophore bloom size variation in response to the regional environment of the subarctic North Atlantic. Limnol. Oceanogr., 51, 2122-2130

Ramette, A., 2007. Multivariate analyses in microbial ecology. FEMS Microbiol. Ecol., 62, 142-160

Ramus, J., 1977. Alcian blue - quantitative aqueous assay for algal acid and sulfated polysaccharides. Journal of Phycology, 13, 345-348

Rappe, M. S., and Giovannoni, S. J., 2003. The uncultured microbial majority. Annual Review of Microbiology, 57, 369-394

Rees, A. P., Joint, I., and Donald, K. M., 1999. Early spring bloom phytoplankton-nutrient dynamics at the Celtic Sea Shelf Edge. Deep-Sea Res. Part I-Oceanogr. Res. Pap., 46, 483-510

Reisch, C. R., Stoudemayer, M. J., Varaljay, V. A., Amster, I. J., Moran, M. A., and Whitman, W. B., 2011. Novel pathway for assimilation of dimethylsulphoniopropionate widespread in marine bacteria. Nature, 473, 208-211

Richardson, T. L., and Jackson, G. A., 2007. Small phytoplankton and carbon export from the surface ocean. Science, 315, 838-840

Richardson, T. L., Ciotti, Á. M., Cullen, J. J., and Villareal, T. A., 1996. Physiological and optical properties of *Rhizosolenia formosa* (*Bacillariophyceae*) in the context of open-ocean vertical migration. Journal of Phycology, 32, 741-757

Riebesell, U., Kortzinger, A., and Oschlies, A., 2009. Sensitivities of marine carbon fluxes to ocean change. Proceedings of the National Academy of Sciences of the United States of America, 106, 20602-20609

Riegman, R., and Winter, C., 2003. Lysis of plankton in the non-stratified southern North Sea during summer and autumn 2000. Acta Oecol.-Int. J. Ecol., 24, S133-S138

Riegman, R., van Bleijswijk, J. D. L., and Brussaard, C. P. D., 2002. The use of dissolved esterase activity as a tracer of phytoplankton lysis - Comment. Limnol. Oceanogr., 47, 916-920

Riegman, R., Stolte, W., Noordeloos, A. A. M., and Slezak, D., 2000. Nutrient uptake, and alkaline phosphate (EC 3 : 1 : 3 : 1) activity of *Emiliania huxleyi* (*Prymnesiophyceae*) during growth under N and P limitation in continuous cultures. Journal of Phycology, 36, 87-96

Riemann, L., and Middelboe, M., 2002. Stability of bacterial and viral community compositions in Danish coastal waters as depicted by DNA fingerprinting techniques. Aquat. Microb. Ecol., 27, 219-232

Riemann, L., Steward, G. F., and Azam, F., 2000. Dynamics of bacterial community composition and activity during a mesocosm diatom bloom. Appl. Environ. Microbiol., 66, 578-587

Riemann, L., Steward, G. F., Fandino, L. B., Campbell, L., Landry, M. R., and Azam, F., 1999. Bacterial community composition during two consecutive NE Monsoon periods in the Arabian Sea studied by denaturing gradient gel electrophoresis (DGGE) of rRNA genes. Deep-Sea Research Part Ii-Topical Studies in Oceanography, 46, 1791-1811

Rink, B., Seeberger, S., Martens, T., Duerselen, C. D., Simon, M., and Brinkhoff, T., 2007. Effects of phytoplankton bloom in a coastal ecosystem on the composition of bacterial communities. Aquat. Microb. Ecol., 48, 47-60

Robertson, J. E., Robinson, C., Turner, D. R., Holligan, P., Watson, A. J., Boyd, P., Fernandez, E., and Finch, M., 1994. The impact of a coccolithophore bloom on oceanic carbon uptake in the northeast atlantic during summer 1991. Deep-Sea Res. Part I-Oceanogr. Res. Pap., 41, 297-&

Rochelle-Newall, E. J., Mari, X., and Pringault, O., 2010. Sticking properties of transparent exopolymeric particles (TEP) during aging and biodegradation. J. Plankton Res., 32, 1433-1442

Rodriguez, F., Varela, M., Fernandez, E., and Zapata, M., 2003. Phytoplankton and pigment distributions in an anticyclonic slope water oceanic eddy (SWODDY) in the southern Bay of Biscay. Marine Biology, 143, 995-1011

Ruiz, A., Franco, J., and Villate, F., 1998. Microzooplankton grazing in the estuary of Mundaka, Spain, and its impact on phytoplankton distribution along the salinity gradient. Aquat. Microb. Ecol., 14, 281-288

Sapp, M., Wichels, A., Wiltshire, K. H., and Gerdts, G., 2007a. Bacterial community dynamics during the winter-spring transition in the North Sea. FEMS Microbiol. Ecol., 59, 622-637

Sapp, M., Schwaderer, A. S., Wiltshire, K. H., Hoppe, H. G., Gerdts, G., and Wichels, A., 2007b. Species-specific bacterial communities in the phycosphere of microalgae? Microb. Ecol., 53, 683-699

Sarmento, H., and Gasol, J. M., subm. Use of phytoplankton-derived dissolved organic matter by bacteriolankton large phylogenetic groups.

Sarmiento, J. L., and Gruber, N. 2006. Organic Matter Production, in: Ocean Biogeochemical Dynamics, edited by: Sarmiento, J. L., and Gruber, N., Princeton University Press, Princeton, NJ, 102-172

Schartau, M., Engel, A., Schroter, J., Thoms, S., Volker, C., and Wolf-Gladrow, D., 2007. Modelling carbon overconsumption and the formation of extracellular particulate organic carbon. Biogeosciences, 4, 433-454

Schluter, L., Mohlenberg, F., Havskum, H., and Larsen, S., 2000. The use of phytoplankton pigments for identifying and quantifying phytoplankton groups in coastal areas: testing the influence of light and nutrients on pigment/chlorophyll a ratios. Mar. Ecol.-Prog. Ser., 192, 49-63

Seymour, J. R., Simo, R., Ahmed, T., and Stocker, R., 2010. Chemoattraction to Dimethylsulfoniopropionate Throughout the Marine Microbial Food Web. Science, 329, 342-345

Sharples, J., Holt, J., and Dye, S. 2010. Shelf Sea Salinity, MCCIP Annual Report Card 2010-11, Review, M. S., 6

Sharples, J., Moore, C. M., Hickman, A. E., Holligan, P. M., Tweddle, J. F., Palmer, M. R., and Simpson, J. H., 2009. Internal tidal mixing as a control on continental margin ecosystems. Geophys. Res. Lett., 36

Sharples, J., Tweddle, J. F., Green, J. A. M., Palmer, M. R., Kim, Y. N., Hickman, A. E., Holligan, P. M., Moore, C. M., Rippeth, T. P., Simpson, J. H., and Krivtsov, V., 2007. Spring-neap modulation of internal tide mixing and vertical nitrate fluxes at a shelf edge in summer. Limnol. Oceanogr., 52, 1735-1747

Sherr, B. F., and Sherr, E. B. 2000. Marine microbes: an overview, in: Microbial ecology of the oceans, edited by: Kirchman, D. L., Wiley-Liss, Inc., 13-46

Sherr, E. B., and Sherr, B. F.: Preservation and storage of samples for enumeration of heterotrophic protists, in: Handbook of methods in aquatic microbial ecology, edited by: Kemp, P. F., Sherr, E. B., Sherr, B. F., and Cole, J., Lewis Publishers (USA), 207-212, 1993.

Sherr, E. B., and Sherr, B. F., 2002. Significance of predation by protists in aquatic microbial food webs. Antonie Van Leeuwenhoek International Journal of General and Molecular Microbiology, 81, 293-308

Shiraiwa, Y., 2003. Physiological regulation of carbon fixation in the photosynthesis and calcification of coccolithophorids. Comp. Biochem. Physiol. B-Biochem. Mol. Biol., 136, 775-783

Sievert, S. M., Kiene, R. P., and Schulz-Vogt, H. N., 2007. The Sulfur Cycle. Oceanography, 20, 117-123

Simó, R., 2001. Production of atmospheric sulfur by oceanic plankton: biogeochemical, ecological and evolutionary links. Trends in Ecology & Evolution, 16, 287-294

Simó, R., Archer, S. D., Pedros-Alio, C., Gilpin, L., and Stelfox-Widdicombe, C. E., 2002. Coupled dynamics of dimethylsulfoniopropionate and dimethylsulfide cycling and the microbial food web in surface waters of the North Atlantic. Limnol. Oceanogr., 47, 53-61

Simon, M., Grossart, H. P., Schweitzer, B., and Ploug, H., 2002. Microbial ecology of organic aggregates in aquatic ecosystems. Aquat. Microb. Ecol., 28, 175-211

Simon, N., Cras, A. L., Foulon, E., and Lemée, R., 2009. Diversity and evolution of marine phytoplankton. Comptes Rendus Biologies, 332, 159-170

Six, C., Thomas, J. C., Brahamsha, B., Lemoine, Y., and Partensky, F., 2004. Photophysiology of the marine cyanobacterium *Synechococcus* sp. WH8102, a new model organism. Aquat. Microb. Ecol., 35, 17-29

Skerratt, J. H., Bowman, J. P., Hallegraeff, G., James, S., and Nichols, P. D., 2002. Algicidal bacteria associated with blooms of a toxic dinoflagellate in a temperate Australian estuary. Mar. Ecol.-Prog. Ser., 244, 1-15

Skoog, A., and Benner, R., 1997. Aldoses in various size fractions of marine organic matter: Implications for carbon cycling. Limnol. Oceanogr., 42, 1803-1813

Skoog, A., Alldredge, A., Passow, U., Dunne, J., and Murray, J., 2008. Neutral aldoses as source indicators for marine snow. Marine Chemistry, 108, 195-206

Skovhus, T. L., Holmstroem, C., Kjelleberg, S., and Dahllof, I., 2007. Molecular investigation of the distribution, abundance and diversity of the genus Pseudoalteromonas in marine samples. FEMS Microbiol. Ecol., 61, 348-361

Slightom, R. N., and Buchan, A., 2009. Surface Colonization by Marine Roseobacters: Integrating Genotype and Phenotype. Appl. Environ. Microbiol., 75, 6027-6037

Smith, G. C., Clark, T., Knutsen, L., and Barrett, E., 1999. Methodology for analyzing dimethyl sulfide and dimethyl sulfoniopropionate in seawater using deuterated internal standards. Anal. Chem., 71, 5563-5568

Smythe-Wright, D., Boswell, S., Kim, Y. N., and Kemp, A., 2010. Spatio-temporal changes in the distribution of phytopigments and phytoplanktonic groups at the Porcupine Abyssal Plain (PAP) site. Deep-Sea Research Part Ii-Topical Studies in Oceanography, 57, 1324-1335

Sogin, M. L., Morrison, H. G., Huber, J. A., Welch, D. M., Huse, S. M., Neal, P. R., Arrieta, J. M., and Herndl, G. J., 2006. Microbial diversity in the deep sea and the underexplored rare biosphere. Proceedings of the National Academy of Sciences, 103, 12115-12120

Stefels, J., 2000. Physiological aspects of the production and conversion of DMSP in marine algae and higher plants. Journal of Sea Research, 43, 183-197

Stefels, J., Steinke, M., Turner, S., Malin, G., and Belviso, S., 2007. Environmental constraints on the production and removal of the climatically active gas dimethylsulphide (DMS) and implications for ecosystem modelling. Biogeochemistry, 83, 245-275

Stelfox-Widdicombe, C. E., Edwards, E. S., Burkill, P. H., and Sleigh, M. A., 2000. Microzooplankton grazing activity in the temperate and sub-tropical NE Atlantic: summer 1996. Mar. Ecol.-Prog. Ser., 208, 1-12

Stocker, R., Seymour, J. R., Samadani, A., Hunt, D. E., and Polz, M. F., 2008. Rapid chemotactic response enables marine bacteria to exploit ephemeral microscale nutrient patches. Proceedings of the National Academy of Sciences of the United States of America, 105, 4209-4214

Stoderegger, K., and Herndl, G. J., 1998. Production and release of bacterial capsular material and its subsequent utilization by marine bacterioplankton. Limnol. Oceanogr., 43, 877-884

Stoica, E., and Herndl, G. J., 2007. Bacterioplankton community composition in nearshore waters of the NW Black Sea during consecutive diatom and coccolithophorid blooms. Aquat. Sci., 69, 413-418

Strom, S. L., and Bright, K. J., 2009. Inter-strain differences in nitrogen use by the coccolithophore *Emiliania huxleyi*, and consequences for predation by a planktonic ciliate. Harmful Algae, 8, 811-816

Strom, S. L., Brainard, M. A., Holmes, J. L., and Olson, M. B., 2001. Phytoplankton blooms are strongly impacted by microzooplankton grazing in coastal North Pacific waters. Marine Biology, 138, 355-368

Suffrian, K., Simonelli, P., Nejstgaard, J. C., Putzeys, S., Carotenuto, Y., and Antia, A. N., 2008. Microzooplankton grazing and phytoplankton growth in marine mesocosms with increased CO2 levels. Biogeosciences, 5, 1145-1156

Sunda, W. G., and Huntsman, S. A., 1995. Iron uptake and growth limitation in oceanic and coastal phytoplankton. Marine Chemistry, 50, 189-206

Suykens, K. 2010. Benthic remineralization in the northeast European continental margin (northern Bay of Biscay), PhD, ULg

Suykens, K., Delille, B., Chou, L., De Bodt, C., Harlay, J., and Borges, A. V., 2010. Dissolved inorganic carbon dynamics and air-sea carbon dioxide fluxes during coccolithophore blooms in the northwest European continental margin (northern Bay of Biscay). Glob. Biogeochem. Cycle, 24, 14

Teira, E., Martinez-Garcia, S., Calvo-Diaz, A., and Moran, X. A. G., 2010. Effects of inorganic and organic nutrient inputs on bacterioplankton community composition along a latitudinal transect in the Atlantic Ocean. Aquat. Microb. Ecol., 60, 299-313

Teira, E., Gasol, J. M., Aranguren-Gassis, M., Fernandez, A., Gonzalez, J., Lekunberri, I., and Alvarez-Salgado, X. A., 2008. Linkages between bacterioplankton community composition, heterotrophic carbon cycling and environmental conditions in a highly dynamic coastal ecosystem. Environmental Microbiology, 10, 906-917

Thomas, T., Evans, F. F., Schleheck, D., Mai-Prochnow, A., Burke, C., Penesyan, A., Dalisay, D. S., Stelzer-Braid, S., Saunders, N., Johnson, J., Ferriera, S., Kjelleberg, S., and Egan, S., 2008. Analysis of the *Pseudoalteromonas tunicata* Genome Reveals Properties of a Surface-Associated Life Style in the Marine Environment. PLoS One, 3, 11

Thyssen, M., Garcia, N., and Denis, M., 2009. Sub meso scale phytoplankton distribution in the North East Atlantic surface waters determined with an automated flow cytometer. Biogeosciences, 6, 569-583

Tozzi, S., Schofield, O., and Falkowski, P., 2004. Historical climate change and ocean turbulence as selective agents for two key phytoplankton functional groups. Mar. Ecol.-Prog. Ser., 274, 123-132

Treusch, A. H., Vergin, K. L., Finlay, L. A., Donatz, M. G., Burton, R. M., Carlson, C. A., and Giovannoni, S. J., 2009. Seasonality and vertical structure of microbial communities in an ocean gyre. Isme J., 3, 1148-1163

Tyrrell, T., and Taylor, A. H., 1996. A modelling study of *Emiliania huxleyi* in the NE Atlantic. Journal of Marine Systems, 9, 83-112

Uher, G., Schebeske, G., Barlow, R. G., Cummings, D. G., Mantoura, R. F. C., Rapsomanikis, S. R., and Andreae, M. O., 2000. Distribution and air-sea gas exchange of dimethyl sulphide at the European western continental margin. Marine Chemistry, 69, 277-300

Uitz, J., Claustre, H., Gentili, B., and Stramski, D., 2010. Phytoplankton class-specific primary production in the world's oceans: Seasonal and interannual variability from satellite observations. Glob. Biogeochem. Cycle, 24

Utermöhl, v. H., 1958. Zur Vervollkommung der quantitative Phytoplankton Methodik. Mitteilungen Internationale Vereinigung für Theoretische und Angewande Limnologie, 9, 1-38

van Boekel, W. H. M., Hansen, F. C., Riegman, R., and Bak, R. P. M., 1992. Lysis-induced decline of a *Phaeocystis* spring bloom and coupling with the microbial foodweb. Mar. Ecol.-Prog. Ser., 81, 269-276

Van den Meersche, K., Middelburg, J. J., Soetaert, K., van Rijswijk, P., Boschker, H. T. S., and Heip, C. H. R., 2004. Carbon-nitrogen coupling and algal-bacterial interactions during an experimental bloom: Modeling a C-13 tracer experiment. Limnol. Oceanogr., 49, 862-878

Van der Gucht, K., Sabbe, K., De Meester, L., Vloemans, N., Zwart, G., Gillis, M., and Vyverman, W., 2001. Contrasting bacterioplankton community composition and seasonal dynamics in two neighbouring hypertrophic freshwater lakes. Environmental Microbiology, 3, 680-690

Van der Gucht, K., Vandekerckhove, T., Vloemans, N., Cousin, S., Muylaert, K., Sabbe, K., Gillis, M., Declerk, S., De Meester, L., and Vyverman, W., 2005. Characterization of bacterial communities in four freshwater lakes differing in nutrient load and food web structure. FEMS Microbiol. Ecol., 53, 205-220

Van der Gucht, K., Cottenie, K., Muylaert, K., Vloemans, N., Cousin, S., Declerck, S., Jeppesen, E., Conde-Porcuna, J. M., Schwenk, K., Zwart, G., Degans, H., Vyverman, W., and De Meester, L., 2007. The power of species sorting: Local factors drive bacterial community composition over a wide range of spatial scales. Proceedings of the National Academy of Sciences of the United States of America, 104, 20404-20409

Van Oostende, N., Chou, L., Vyverman, W., and Sabbe, K., *in prep. c*. Community composition of free-living and particle-associated bacterial assemblages in late spring phytoplankton blooms along the NE Atlantic continental shelf break (northern Bay of Biscay, 2006-2008).

Van Oostende, N., Moerdijk-Poortvliet, T. C. W., Vyverman, W., Boschker, H. T. S., and Sabbe, K., *in prep. e*. Dynamics of dissolved carbohydrates and transparent exopolymer particles in axenic and non-axenic *Emiliania huxleyi* cultures: assessment of extracellular release using compound-specific isotope analysis.

Van Oostende, N., De Bodt, C., Souffreau, C., Vyverman, W., Chou, L., and Sabbe, K., *in prep. b*. Phytoplankton cell lysis and grazing mortality rates, and dimethylsulphoniopropionate dynamics during coccolithophorid blooms.

Van Oostende, N., Harlay, J., De Bodt, C., Vanelslander, B., Chou, L., Vyverman, W., and Sabbe, K., *in prep. a*. Phytoplankton dynamics during late spring coccolithophore blooms at the continental margin of the northern Bay of Biscay (North East Atlantic, 2006-2008).

Varela, M. M., van Aken, H. M., Sintes, E., and Herndl, G. J., 2008. Latitudinal trends of Crenarchaeota and Bacteria in the meso- and bathypelagic water masses of the Eastern North Atlantic. Environmental Microbiology, 10, 110-124

Veldhuis, M. J. W., Kraay, G. W., and Timmermans, K. R., 2001. Cell death in phytoplankton: correlation between changes in membrane permeability, photosynthetic activity, pigmentation and growth. European Journal of Phycology, 36, 167-177

Verdugo, P., Alldredge, A. L., Azam, F., Kirchman, D. L., Passow, U., and Santschi, P. H., 2004. The oceanic gel phase: a bridge in the DOM-POM continuum. Marine Chemistry, 92, 67-85

Veuger, B., van Oevelen, D., Boschker, H. T. S., and Middelburg, J. J., 2006. Fate of peptidoglycan in an intertidal sediment: An in situ C-13-labeling study. Limnol. Oceanogr., 51, 1572-1580

Vila, M., Simo, R., Kiene, R. P., Pinhassi, J., Gonzalez, J. A., Moran, M. A., and Pedros-Alio, C., 2004. Use of microautoradiography combined with fluorescence in situ hybridization to determine dimethylsulfoniopropionate incorporation by marine bacterioplankton taxa. Appl. Environ. Microbiol., 70, 4648-4657

von Dassow, P., Ogata, H., Probert, I., Wincker, P., Da Silva, C., Audic, S., Claverie, J. M., and de Vargas, C., 2009. Transcriptome analysis of functional differentiation between

haploid and diploid cells of *Emiliania huxleyi*, a globally significant photosynthetic calcifying cell. Genome Biol., 10, 33

Wagner, M., Nielsen, P. H., Loy, A., Nielsen, J. L., and Daims, H., 2006. Linking microbial community structure with function: fluorescence in situ hybridization-microautoradiography and isotope arrays. Current Opinion in Biotechnology, 17, 83-91

Weinbauer, M. G., Kerros, M. E., Motegi, C., Wilhartitz, I. C., Rassoulzadegan, F., Torreton, J. P., and Mari, X., 2010. Bacterial community composition and potential controlling mechanisms along a trophic gradient in a barrier reef system. Aquat. Microb. Ecol., 60, 15-28

Westberry, T. K., and Siegel, D. A., 2006. Spatial and temporal distribution of *Trichodesmium* blooms in the world's oceans. Glob. Biogeochem. Cycle, 20

Westbroek, P., Brown, C. W., Vanbleijswijk, J., Brownlee, C., Brummer, G. J., Conte, M., Egge, J., Fernandez, E., Jordan, R., Knappertsbusch, M., Stefels, J., Veldhuis, M., Vanderwal, P., and Young, J., 1993. A model system approach to biological climate forcing - the example of *Emiliania huxleyi*. Glob. Planet. Change, 8, 27-46

Whitman, W. B., Coleman, D. C., and Wiebe, W. J., 1998. Prokaryotes: The unseen majority. Proceedings of the National Academy of Sciences of the United States of America, 95, 6578-6583

Wietz, M., Gram, L., Jorgensen, B., and Schramm, A., 2010. Latitudinal patterns in the abundance of major marine bacterioplankton groups. Aquat. Microb. Ecol., 61, 179-189

Wollast, R., and Chou, L., 2001. The carbon cycle at the ocean margin in the northern Gulf of Biscay. Deep-Sea Research Part Ii-Topical Studies in Oceanography, 48, 3265-3293

Wood, A. M., and Van Valen, L. M., 1990. Paradox lost? On the release of energy-rich compounds by phytoplankton. Marine Microbial Food Webs, 4, 103 - 116

Worden, A. Z., and Allen, A. E., 2010. The voyage of the microbial eukaryote. Current Opinion in Microbiology, 13, 652-660

Wright, S. W., and Jeffrey, S. W. 1997. High-resolution HPLC system for chorophylls and carotenoids of marine phytoplankton, in: Phytoplankton pigments in oceanography, edited by: Jeffrey, S. W., Mantoura, F., and Wright, S. W., UNESCO publishing,

Wright, S. W., Jeffrey, S. W., Mantoura, R. F. C., Llewellyn, C. A., Bjornland, T., Repeta, D., and Welschmeyer, N., 1991. Improved HPLC method for the analysis of chlorophylls and carotenoids from marine-phytoplankton

Mar. Ecol.-Prog. Ser., 77, 183-196

Yentsch, C. S., and Menzel, D. W., 1963. A method for the determination of phytoplankton chlorophyll and phaeophytin by fluorescence. Deep-Sea Research Part a-Oceanographic Research Papers, 10, 221-231

Yokokawa, T., and Nagata, T., 2005. Growth and grazing mortality rates of phylogenetic groups of bacterioplankton in coastal marine environments. Appl. Environ. Microbiol., 71, 6799-6807

Zapata, M., and Garrido, J. L., 1991. Influence of injection conditions in reversed-phase high-performance liquid-chromatography of chlorophylls and carotenoids. Chromatographia, 31, 589-594

Zapata, M., Jeffrey, S. W., Wright, S. W., Rodriguez, F., Garrido, J. L., and Clementson, L., 2004. Photosynthetic pigments in 37 species (65 strains) of Haptophyta: implications for oceanography and chemotaxonomy. Mar. Ecol.-Prog. Ser., 270, 83-102

Zhang, R., Liu, B. Z., Lau, S. C. K., Ki, J. S., and Qian, P. Y., 2007. Particle-attached and free-living bacterial communities in a contrasting marine environment: Victoria Harbor, Hong Kong. FEMS Microbiol. Ecol., 61, 496-508

Zhang, S. J., and Santschi, P. H., 2009. Application of cross-flow ultrafiltration for isolating exopolymeric substances from a marine diatom (*Amphora* sp.). Limnology and Oceanography-Methods, 7, 419-429

Zhou, J., Mopper, K., and Passow, U., 1998. The role of surface-active carbohydrates in the formation of transparent exopolymer particles by bubble adsorption of seawater. Limnol. Oceanogr., 43, 1860-1871

Ziveri, P., and Thunell, R. C., 2000. Coccolithophore export production in Guaymas Basin, Gulf of California: response to climate forcing. Deep-Sea Research Part Ii-Topical Studies in Oceanography, 47, 2073-2100

Ziveri, P., Broerse, A. T. C., van Hinte, J. E., Westbroek, P., and Honjo, S., 2000. The fate of coccoliths at 48 degrees N 21 degrees W, northeastern Atlantic. Deep-Sea Research Part Ii-Topical Studies in Oceanography, 47, 1853-1875

Zondervan, I., 2007. The effects of light, macronutrients, trace metals and CO_2 on the production of calcium carbonate and organic carbon in coccolithophores - A review. Deep-Sea Research Part Ii-Topical Studies in Oceanography, 54, 521-537

Zubkov, M. V., Fuchs, B. M., Burkill, P. H., and Amann, R., 2001a. Comparison of cellular and biomass specific activities of dominant bacterioplankton groups in stratified waters of the Celtic Sea. Appl. Environ. Microbiol., 67, 5210-5218

Zubkov, M. V., Fuchs, B. M., Archer, S. D., Kiene, R. P., Amann, R., and Burkill, P. H., 2001b. Linking the composition of bacterioplankton to rapid turnover of dissolved dimethylsulphoniopropionate in an algal bloom in the North Sea. Environmental Microbiology, 3, 304-311

Zwart, G., Huismans, R., van Agterveld, M. P., Van de Peer, Y., De Rijk, P., Eenhoorn, H., Muyzer, G., van Hannen, E. J., Gons, H. J., and Laanbroek, H. J., 1998. Divergent members of the bacterial division Verrucomicrobiales in a temperate freshwater lake. FEMS Microbiol. Ecol., 25, 159-169

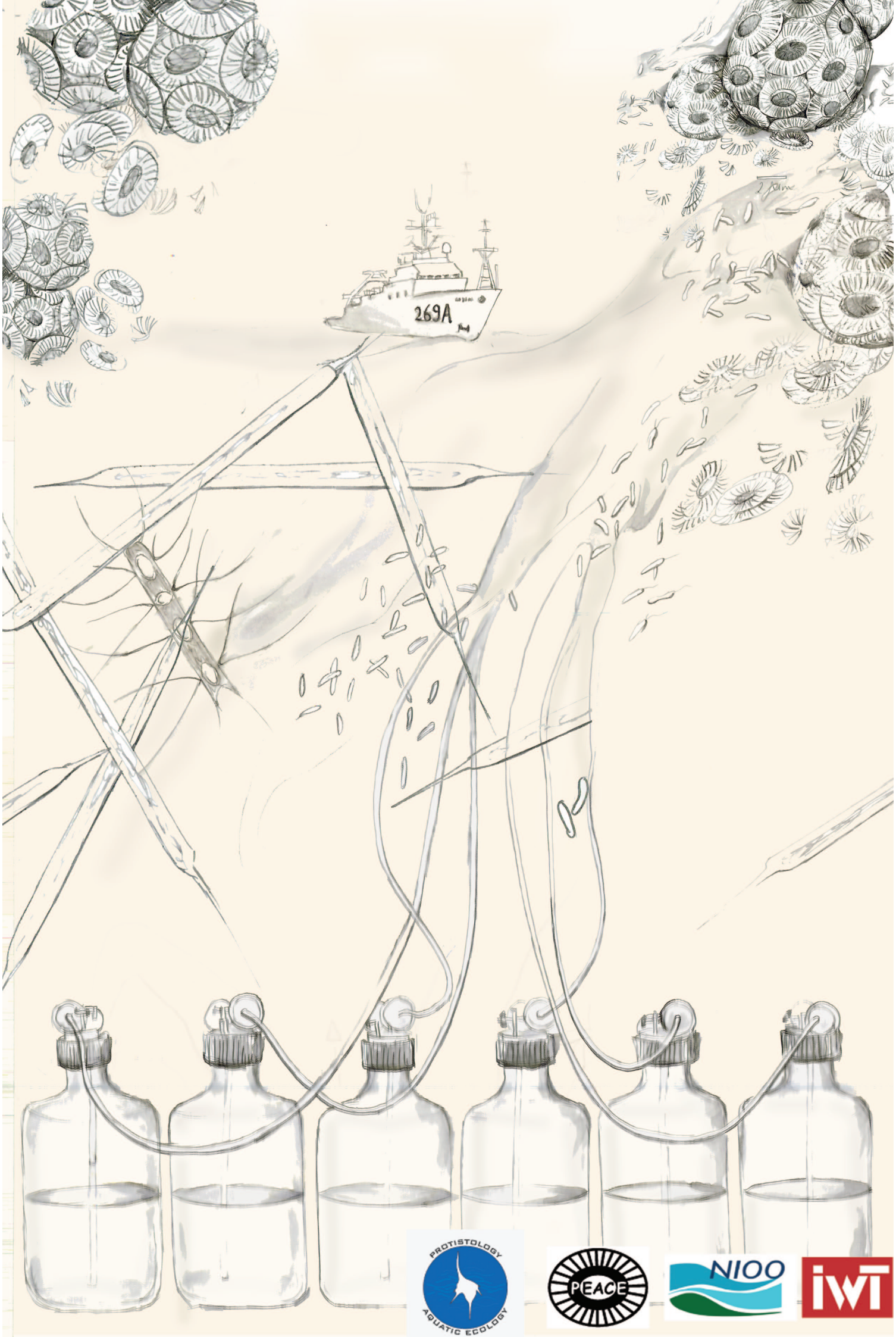
269A
PROTISTOLOGY
AQUATIC ECOLOGY
PEACE
NIOO
iwt